Biomimetic Synthesis Enables the Structural Revision of Natural Products

Tomás Mendes Gouveia Vieira de Castro

M.Sc Chemistry

Thesis submitted for the degree of Master of Philosophy

THE UNIVERSITY of ADELAIDE

April 2022

Department of Chemistry

The University of Adelaide

Table of Contents

Abstract

Chemists have managed to isolate and catalogue innumerable chemical compounds synthesized by nature. The diversity, complexity, and therapeutic potential present in some of these natural products often make them alluring targets for total synthesis. Yet, despite the evolution of analytical techniques it is still commonplace for novel molecules to be mischaracterized. The scarcity, purity, and intricate structures of some chemical compounds all contribute to the challenges an isolation chemist faces when characterizing newly discovered natural products.

A biomimetic synthesis takes into account the target molecule's biosynthetic origins and attempts to replicate chemical reactions of the compound's known or proposed biosynthesis within a laboratory setting. Recently, total synthesis, and by extension biomimetic synthesis, has been expertly employed in the structural revisions of many natural products.

This thesis will describe in detail the first biomimetic synthesis of several meroterpenoid natural products. Every compound's total synthesis features the same key step: a hetero-Diels–Alder reaction between a common *ortho*-quinone methide intermediate and caryophyllene or humulene. Furthermore, structural revisions are proposed for three of these compounds: littordial E, littordial F and drychampone B. These revisions are proposed on the basis of our biosynthetic speculation and the final structural reassignments of these compounds were carried out by means of 2D NMR spectroscopy with supporting computational studies.

This work addresses a long-standing and still present problem in natural product chemistry: the erroneous assignment of newly isolated compounds. There are many avenues leading to mischaracterization of novel natural products and this work exemplifies how total synthesis in conjunction with insightful biosynthetic speculation can be used alongside modern sprectoscopic tools to correct such misassignments.

Declaration

I certify that this work contains no material which has been accepted for the award of any other degree or diploma in my name, in any university or other tertiary institution and, to the best of my knowledge and belief, contains no material previously published or written by another person, except where due reference has been made in the text. In addition, I certify that no part of this work will, in the future, be used in a submission in my name, for any other degree or diploma in any university or other tertiary institution without the prior approval of the University of Adelaide and where applicable, any partner institution responsible for the joint-award of this degree.

I give permission for the digital version of my thesis to be made available on the web, via the University's digital research repository, the Library Search and also through web search engines, unless permission has been granted by the University to restrict access for a period of time.

Tomás Mendes Gouveia Vieira de Castro

6th of April 2022……

Date

Acknowledgements

First and foremost, I would like to thank my supervisor Prof. Jonathan George for giving me the opportunity to work in his research group. The time I spent in Adelaide was truly wonderful and I am immensely proud of what we were able to achieve during my short time here. Though I leave Australia due to the unfortunate disruption of a global pandemic, I do so with fond memories and a hope that I may return sometime in the future. I would also be remiss if I did not mention the incredible support Jonathan showed me throughout my time in his group with matters both in and out of the lab, for which I am eternally grateful. The onset of the COVID-19 pandemic left me in a very difficult position, but Jonathan's advice and unwavering support helped weather the storm and carve out a path for the completion of my studies.

Next, I would like to thank all the members of the George group that I had the pleasure of working alongside. To Aaron, Lauren, Laura, and Stefania, thank you for taking me under your wing and helping me get started in the lab. Thank you for introducing me to Australia and for putting up with me but more importantly, thank you for the great times we spent together. To Sarah, thank you for being a great neighbour and wonderful person. I wish you nothing but success during the rest of your PhD, I'm rooting for you! To Matt, thanks for always brightening up the mood in the lab, I hope you enjoy your PhD as much as your Honours project. And to Ossama, although you only officially joined the George group for your post-doc after I left Australia, thank you for the good times and for all your help with getting the work for this thesis over the finish line.

I would also like to thank the Fallon and Newton research groups. Your generosity and expertise were always greatly appreciated. I will miss our big group meetings, especially the days when I didn't have to go up on the board! A special thank you to Dr. Thomas Fallon, my co-supervisor, for your help and your contribution to the littordials project.

Lastly, I must give thanks to my wonderful, wonderful family. To my parents, Miguel and Mafalda, and to my younger brothers, Henrique and Francisco, your unconditional love and support got me through the worst of times over these past years. I only hope that I can continue to make you all proud. Obrigado por tudo.

List of Abbreviations

°C	degrees Celsius
^{13}C	carbon-13
^{1}H	hydrogen-1
$^{1}O_2$	singlet oxygen
Å	angstrom
Ac	acetyl, acetate
AcOH	acetic acid
aq.	aqueous
atm.	atmosphere
brsm	based on recovered starting material
Bn	benzyl
BnBr	benzyl bromide
br.	broad
Boc	*tert*-butoxycarbonyl
Bu	butyl
CAN	ceric ammonium nitrate
CD	circular dichroism
cm^{-1}	wavenumber
conc.	concentration
COSY	correlation spectroscopy
CSA	camphorsulfonic acid
d	days
DMF	dimethylformamide
DMP	Dess-Martin periodinane
DMSO	dimethyl sulfoxide
d.r.	diastereomeric ratio
EDDA	ethylenediamine diacetic acid
EI	electron impact
ent	enantiomer
e.r.	enantiomeric ratio
epi	epimer

equiv	equivalents
Et	ethyl
Et_3N	triethylamine
Et_2O	diethyl ether
ESI	electron spray ionisation
EtOAc	ethyl acetate
g	grams
h	hours
HFIP	hexafluoroisopropanol
HMBC	heteronuclear multiple bond correlation spectroscopy
HPLC	high performance liquid chromatography
HRMS	high resolution mass spectrometry
HSQC	heteronuclear single quantum correlation
Hz	Hertz
hν	light
i-Pr	isopropyl
IR	infrared
J	coupling constant
KHMDS	potassium hexamethyldisilazide
LDA	lithium diisopropylamide
m-CPBA	*meta*-chloroperoxybenzoic acid
Me	methyl
Mz	megahertz
min	minutes
Mp	melting point
Ms	mesyl
MS	molecular sieves
n-Bu	*n*-butyl
n-BuLi	*n*-butyllithium
nm	nanometre
NMR	nuclear magnetic resonance
NMO	N-methyl morpholine

NOESY	Nuclear Overhauser Effect Spectroscopy
Nu	nucleophile
o-QM	*ortho*-quinine methide
p-TsOH	*para*-toluenesulfonic acid
Pd/C	palladium on activated carbon
Ph	phenyl
PhMe	toluene
PIDA	phenyliodine diacetate, diacetoxy iodobenzene
PIFA	phenyliodine bis(trifluoroacetate), (Bis(trifluoroacetoxy)iodo)benzene
ppm	parts per million
PPTS	*p*-toluenesulfonate
rsm	recovered starting material
R_f	retention factor
rt	room temperature
S_N2	substitution nucleophilic bimolecular
TASF	tris(dimethylamino)sulfonium difluorotrimethylsilicate
TBAF	*tert*-butylammonium fluoride
TBS	*tert*-butyldimethylsilyl
TBDPS	*Tert*-butyldiphenylsilyl
t-BuLi	*tert*-butyllithium
TEMPO	(2,2,6,6-Tetramethylpiperidin-1-yl)oxyl
TES	triethylsilyl
TFA	trifluoroacetic acid
Tf	trifluoromethanesulfonate
THF	tetrahydrofuran
TLC	thin layer chromatography
TMS	trimethylsilyl
TMEDA	tetramethylethlyenediamine
TPAP	tetrapropylammonium perruthenate
Ts	*p*-toluenesulfonyl (tosyl)
TsCl	tosyl chloride

Chapter 1

Introduction

1.1 Total Synthesis of Natural Products

For every living organism, nature has selectively developed a myriad of complex and structurally diverse chemical compounds for all manner of functions (Figure 1.1). New molecules are discovered every day and despite the impressive effort made by chemists to isolate and characterize these compounds, we have only recorded a small fraction of Nature's ever expanding molecular library.[1]

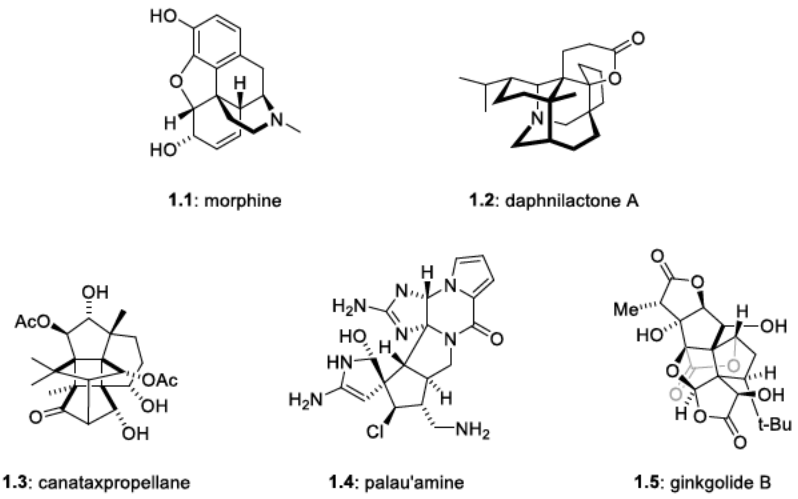

Figure 1.1: The diverse structures of different natural products.

Natural products have long been attractive targets for the synthetic chemist. Their intriguing biological properties and therapeutic potential are highly desirable for study in both academia and in industry. Indeed, novel molecules are often employed as lead compounds in drug discovery, as demonstrated by the fact that many pharmaceuticals on the market today are either natural products or natural product derivatives.[2-4] Additionally, natural product synthesis is often motivated by the desire for new chemical understanding or the development of new methodologies. One example

that illustrates this well is that of paclitaxel (sold under the brand name Taxol® by Bristol-Meyers-Squibb, **1.6**), a natural product with exceptionally potent anti-cancer activity that was originally isolated from the Pacific yew, *Taxus brevifolia*.[5] Although Taxol® is typically produced through semisynthetic methods on industrial scales, its fascinating chemical properties made it one the most contested and sought-after total synthesis targets of the 1990's. The first, though disputed, total synthesis of Taxol® was published K. C. Nicolaou in 1994.[6] Since then, several syntheses of this compound have been reported with varying strategies (Figure 1.2).[7-14] Taxol® remains a highly relevant natural product to this day, both as a target for new total synthesis strategies as well as a chemotherapeutic agent.

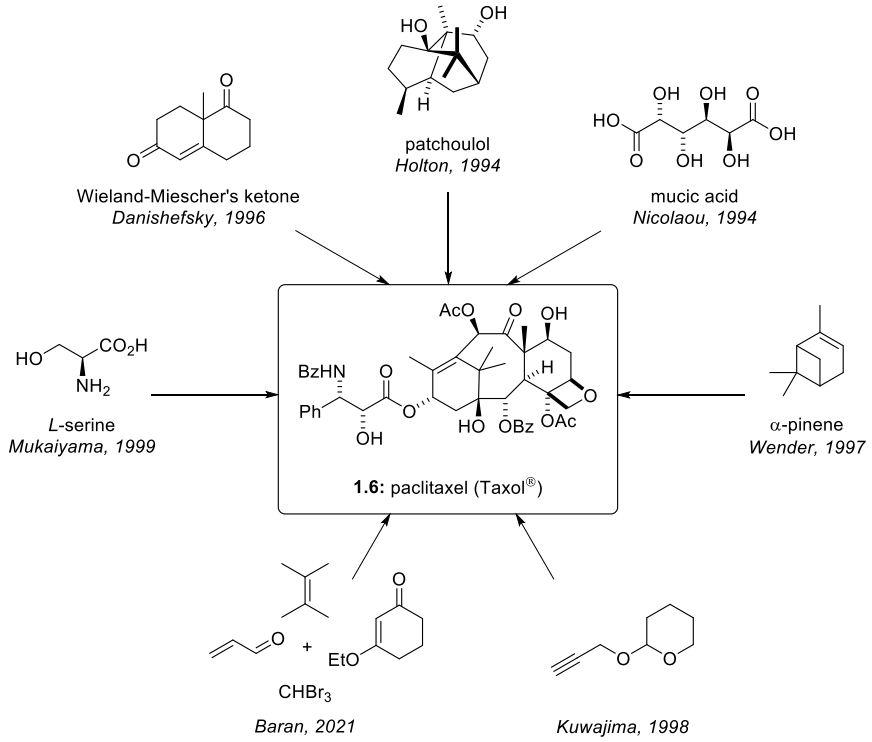

Figure 1.2: Total syntheses of Taxol® achieved from diverse starting materials.[6-14]

Despite nature's impressive ability to synthesize such complex compounds, these may only exist in scarce quantities, making their extraction and isolation difficult and low yielding. In such cases, total synthesis facilitates the production of appreciable amounts of a desired compound that would otherwise be inefficient to obtain directly from biological sources. Bryostatin 1 (**1.14**) is a marine-derived natural product that has been tested in clinical trials against Alzheimer's disease,[15] as an immunotherapeutic agent against leukemia[16,17] and HIV/AIDS eradication[18,19] but the scarcity of **1.14** has significantly impacted its use in further clinical trials. The National Cancer Institute (NCI)

possessed an original stock of 18 g of **1.14** dating back to 1991. This material was isolated from 14 tonnes of the marine organism *Bugula neritina,* a yield of 0.00014%.[20] Given the challenges present in the isolation of bryostatin 1, total synthesis presented itself as a viable alternative to generate sizeable quantities of **1.14** for further testing. The first total synthesis of bryostatin 1 was reported by Keck in 57 steps (30 steps longest linear sequence, not shown)[21] but would be improved upon by Wender et al. who achieved the synthesis of **1.14** in 29 steps. The end-game of this synthesis involves a Yamaguchi esterification/Prins cyclization sequence between compounds **1.7** and **1.8** to form macrolactone **1.9** in good yield. The final sequence of manipulations includes ozonolysis, an alkynoate-to-diene isomerization, a Horner–Wadsworth–Emmons olefination and silyl ether deprotection to afford bryostatin 1 on gram-scales, sufficient to meet global clinical needs (Scheme 1.1).[22]

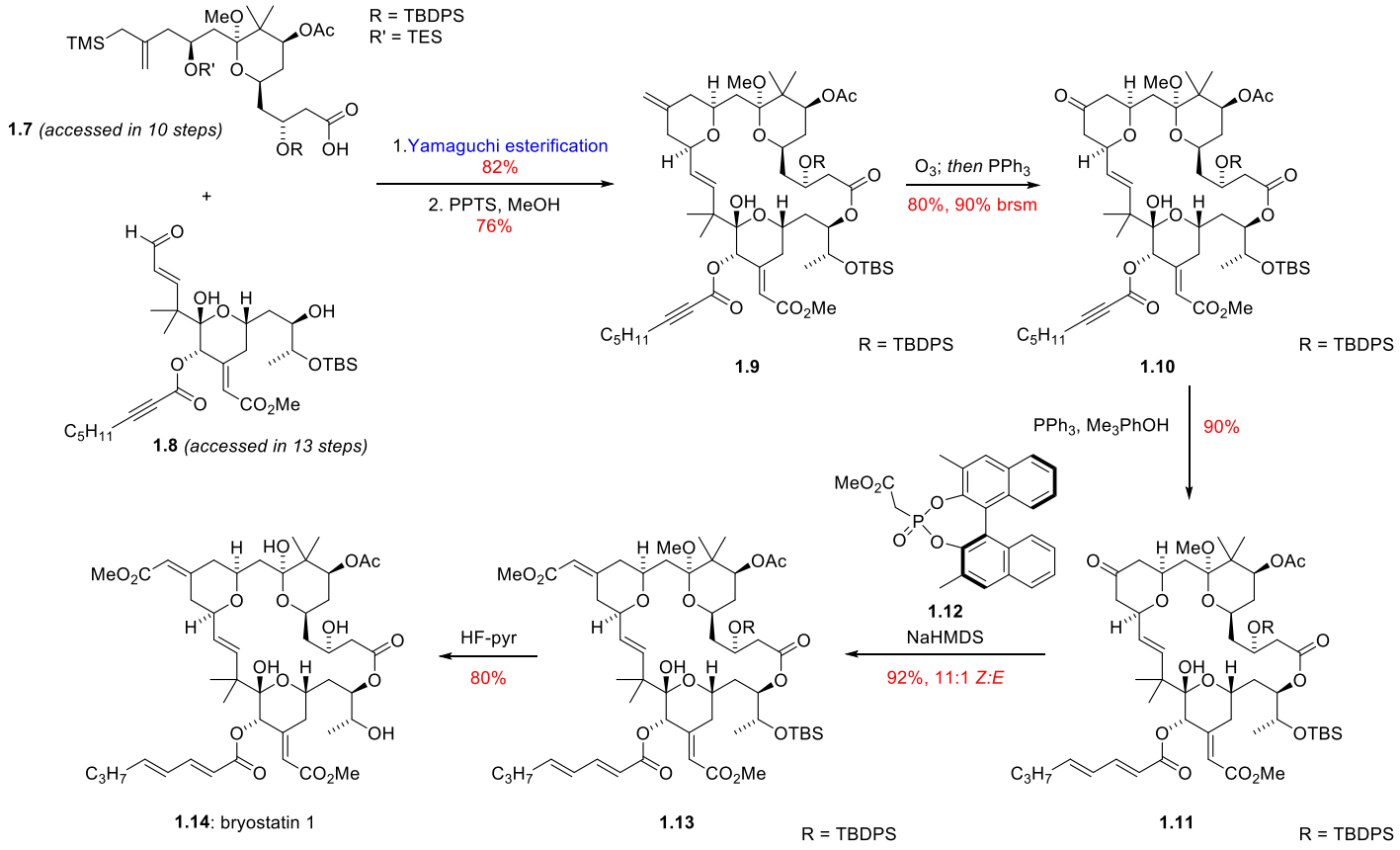

Scheme 1.1: Wender's total synthesis of bryostatin 1 (**1.14**).[22]

1.2 Biomimetic Synthesis of Natural Products

Synthesizing some of the natural products that have been presented thus far is a daunting challenge – their successful synthesis represents many years of hard work and research. Entirely new methodologies might need to be developed mid-project or novel reagents need to be designed to overcome a litany of issues a chemist may face in any given synthesis. One way in which chemists can optimize and direct their own syntheses is to take inspiration from the processes that have been engineered by nature. Biomimetic synthesis aims to recreate the chemical environments in which natural products, and any biosynthetic intermediates *en route* to these natural products, have been formed in living organisms. By design, these biomimetic syntheses tend to be concise and efficient, often employing elegant reaction cascades paralleling more complex enzymatic processes, inducing significant complexity from comparatively simple starting materials. The classical and most often cited example of a biomimetic synthesis is that of the alkaloid tropinone (**1.19**), achieved in 1917 by Sir Robert Robinson through an intramolecular "double Mannich reaction". A one-pot reaction between succinaldehyde (**1.15**), methylamine (**1.16**) and acetonedicarboxylic acid (**1.17**) generates intermediate **1.18** which undergoes immediate decarboxylation to afford tropinone in 17% yield (Scheme 1.2).[23] This work is a landmark in the field of organic synthesis, inspiring future chemists to carefully consider the biogenesis of their synthetic targets and facilitating the study of exceptionally complicated molecules.

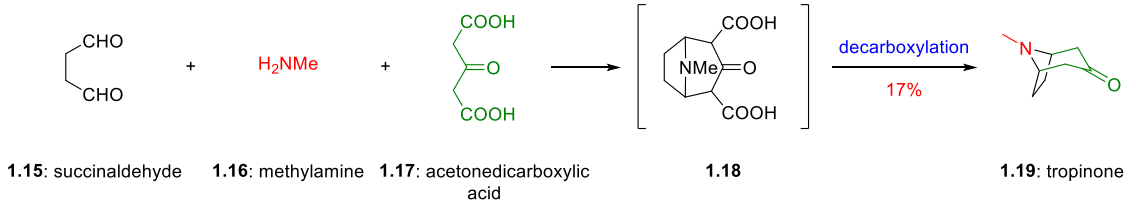

Scheme 1.2: The biomimetic synthesis of tropinone (**1.19**) by Robinson.[23]

The *Daphniphyllum* alkaloids are a series of natural products isolated from plants of the Daphniphyllaceae family. Since the discovery of daphnimacrin by Yagi in 1909[24] over 320 of these alkaloids have been identified.[25] Due to their highly intricate framework, these caged compounds have made *Daphniphyllum* alkaloids highly sought-after targets for total synthesis. Perhaps the greatest contribution to the field of *Daphniphyllum* alkaloid chemistry came from the work of Clayton Heathcock who achieved a biomimetic synthesis of *proto*-daphniphylline (**1.21**).[26] *Proto*-

daphniphylline is an important intermediate in the biosynthesis of other members of this captivating family including daphniphylline (**1.22**) and secodaphniphylline (**1.23**) (Scheme 1.3). *Proto*-daphniphylline was proposed to originate from squalene (**1.20**) in several steps, with subsequent transformations accounting for natural products **1.22** and **1.23** (Scheme 1.3, a). Key to Heathcock's biomimetic synthesis is the formation of the *E*/*Z*-aldehydes **1.24** and **1.25**, whose structures are clearly analogous to squalene. Heathcock successfully generated **1.21** in 15% yield over three simple steps from these aldehydes (Scheme 1.3, b), a true testament to the power of the biomimetic approach.

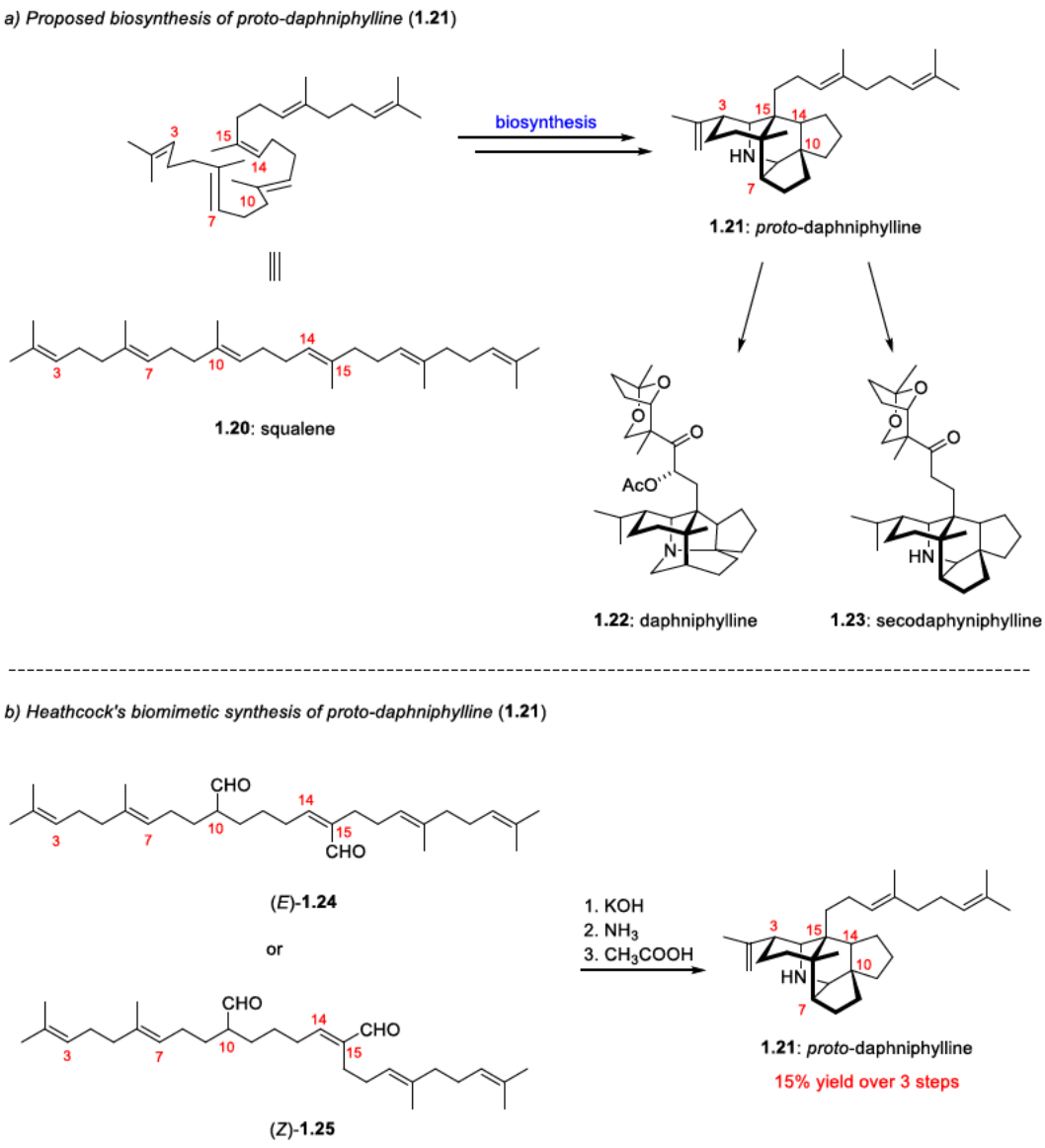

Scheme 1.3: a) A simplified scheme Heathcock's proposed biosynthesis of **1.21**, highlighting key carbon atoms in the final alkaloid skeleton. b) Heathcock's biomimetic synthesis of **1.21**.[26]

Biomimetic synthesis is the main focus of the George group and of one the best examples to demonstrate its potential is seen in garcibracteatone (**1.32**, Scheme 1.4).[27] Isolated from the bark of *Garcinia bracteata,* this polycyclic polyprenylated acylphloroglucinol's (PPAP) complex scaffold presents a significant synthetic challenge. George and co-workers proposed a biomimetic synthesis of **1.32** *via* an oxidative radical cyclization cascade. Starting from commercially available phloroglucinol (**1.26**), Friedel-Crafts acylation followed by prenylation and dearomative alkylation affords precursor **1.27** as a mixture of diastereoisomers. The free radical cyclization cascade was induced using $Mn(OAc)_3/Cu(OAc)_2$ in AcOH, affording garcibracteatone (**1.32**) and its C-5 epimer **1.33** in 14% and 8% yields respectively. The total synthesis of garcibracteatone highlights the success of employing a biomimetic approach, demonstrated by the efficiency and selectivity of the oxidative radical cascade to form this natural product's ornate architecture.

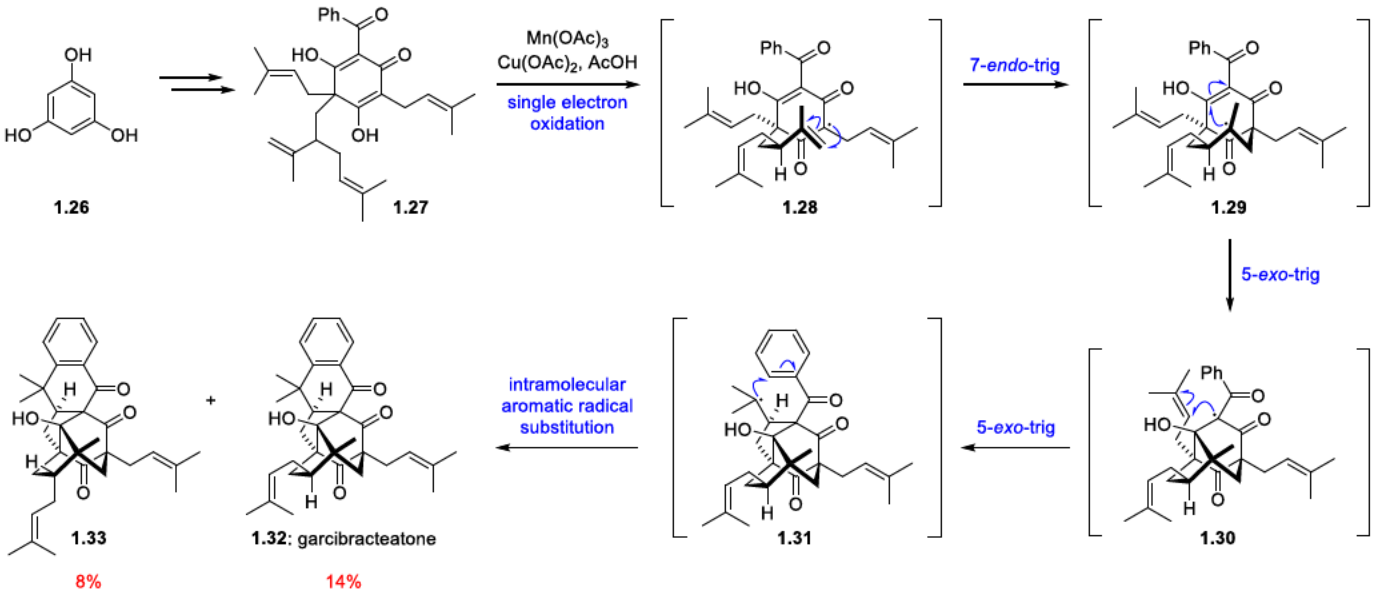

Scheme 1.4: George's biomimetic synthesis of garcibracteatone (**1.32**).[27]

From these few examples it is clear that the biomimetic approach is a powerful means by which chemists may induce significant molecular complexity in a few short steps. However, consideration of a compound's biosynthetic origin can have more benefits than simply achieving its synthesis in a concise fashion, as shall be described in the next section.

1.3 Structural Revisions of Natural Products by Biomimetic Synthesis

A total synthesis begins with the retrosynthetic analysis of the target molecule and having the correct structure for said molecule is paramount. While this may seem like an obvious statement, without a correct structure, a working forward synthesis becomes impossible. Misassigned structures for newly isolated natural products is a common problem and the result of several obstacles that isolation chemists can encounter during the characterization process. Anything from the methods used in the material isolation steps to data interpretation present opportunities for error. Ideally, an X-ray crystal structure would be obtained to provide the unambiguous assignment of the molecule. Of course, this is only possible if appropriate crystals of the compound are available and with many new natural products isolated as oils or amorphous solids, chemists are forced to adopt other analytical techniques when assigning structures. Besides X-ray crystallography, NMR spectroscopy has become the most widely used method for compound characterization and is frequently supported by other experiments such as computational studies and mass spectrometry. Despite the advances made in the field of NMR spectroscopy, structural assignments of novel compounds remain a challenging undertaking with molecules still subject to erroneous assignments.[28]

Presently, compound purity and quantity still greatly impact the quality of NMR data. Furthermore, molecules which exhibit more intricate architectures will naturally generate complex spectra, requiring more thorough examination and often leading to human error in the interpretation of this data. Outside of more conventional analytical techniques, total synthesis has proven to be an effective method for the revision of previously misassigned natural products.[29] The highly designed and controlled nature of the laboratory setting allows reaction products to predicted, isolated, and characterized during most steps of the synthesis. A biomimetic approach is even more enlightening, as structural revisions are based on plausible biosynthetic pathways. Additionally, a biomimetic synthesis often intercepts products that act as intermediates *en route* to the target compound or result in yet to be isolated products, adding further credibility to proposed revisions. The George group has a great deal of experience in the realm of natural product structure revisions, a few examples of which are highlighted further.

Siphonodictyal B (Figure 1.3) is a meroterpenoid isolated from *Aka coralliphaga* (also known as *Siphonodictyon coralliphagum*), a bright yellow marine sponge. The true structure of this natural product eluded chemists for a number of years; having been misassigned by Faulkner initially upon its isolation in 1981[30] (**1.34**) and again by Faulkner and Clardy in 1986[31] (**1.35**).

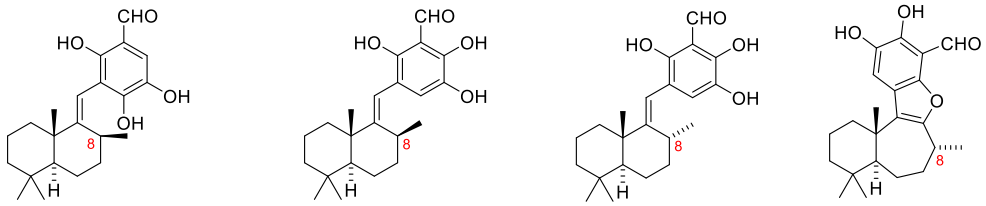

1.34: siphonodictyal B
originally proposed structure

1.35: siphonodictyal B
second proposed structure

1.36: siphonodictyal B
revised structure

1.37: liphagal

Figure 1.3: Proposed and revised structures of siphonodictyal B, and liphagal.

The George group's interest in siphonodictyal B was derived from a proposed biosynthesis of the related meroterpenoid liphagal (**1.37**), also isolated from *Aka coralliphaga*.[32] Liphagal (**1.37**) possesses an intriguing 6-7 terpene ring system fused to an electron-rich benzofuran ring that was assigned by means of 2D NMR studies. Its elaborate structure and potent, selective inhibition of phosphatidylinositol-3-kinase (PI3K) α quickly made liphagal a synthetic target for several research groups. In their original isolation work, Andersen and co-workers put forward two possible biosynthetic pathways to rationalise the construction of the liphagal framework. The first pathway hypothesized a late-stage polyene cyclization event to generate the 6-7 ring system, an approach which inspired their own total synthesis of **1.37**. This biogenesis raises some questions regarding the feasibility of the proposed cyclization reactions, an issue which Andersen and co-workers encountered in their own synthetic studies,[32] as well as the plausibility of some of the proposed intermediate structures, which had yet to be isolated in nature. The second pathway detailed that an epoxidation and subsequent ring expansion of the co-isolated siphonodictyal B could generate **1.37**. (Scheme 1.5). At the time, Andersen had put forth this hypothetical biosynthesis using Faulkner's second proposed structure of siphonodictyal B (**1.35**). Thus, to achieve correct stereochemistry in the final natural product, a late-stage C-8 epimerization was required. Considering both siphonodictyal B and liphagal were isolated from *Aka coralliphaga*, this second pathway seemed the more likely route towards **1.37**. Additionally, this theorized biosynthesis gives an indication as to a second potential misassignment of siphonodictyal B (**1.35**). Ideally, the C-8 epimer of **1.35** i.e., the revised structure **1.36** (Figure 1.3), should provide liphagal

through Andersen's second proposed pathway without the need for an extra epimerization step (Scheme 1.5). Epoxidation of revised siphonodictyal B (**1.36**) to **1.38** and subsequent acid-catalysed epoxide ring-opening should provide the *o*-QM intermediate **1.39**. Bond migration results in the desired ring expansion to cycloheptanone **1.40** which is primed to undergo the final benzofuran formation step to produce liphagal (**1.37**).

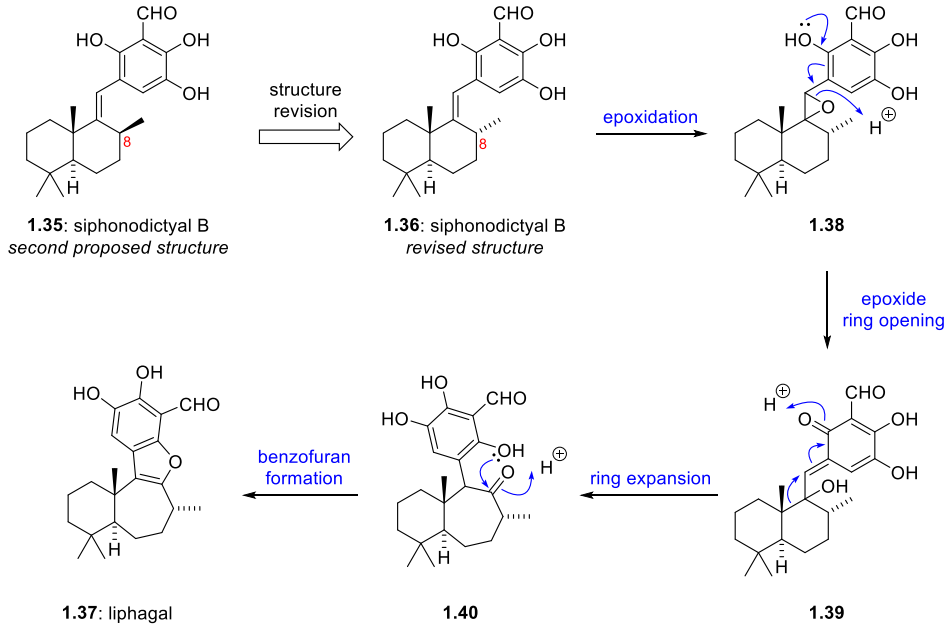

Scheme 1.5: The proposed biosynthesis of liphagal (**1.37**) starting from a structural revision of siphonodictyal B (**1.36**).

The synthesis of the revised structure of siphonodictyal B (**1.36**) begins with the conversion of (+)-sclareolide (**1.41**) to aldehyde **1.42** in six steps according to known literature procedures (Scheme 1.6). Arylation of **1.42** with the organolithium species derived from arylbromide **1.43** affords alcohol **1.44** as a single diastereomer. Dehydration of **1.44** is achieved upon treatment with $POCl_3$ giving alkene **1.45** in 54% yield. Finally, formylation to **1.46** and subsequent global deprotection yields (–)-siphonodictyal B (**1.36**) in good yield. The relative configuration of C-8 was confirmed by clearly visible NOESY correlations; Faulkner had originally assigned this configuration through observation of the coupling constants of H-8. The stage was now set to perform the final biomimetic cascade. Gratifyingly, treatment of **1.36** with *m*-CPBA followed by TFA to induce the epoxide ring-opening generated (+)-liphagal (**1.37**) in 42% yield.[33] Data for synthesized liphagal matched that of isolated material exceptionally, strongly supporting the hypothesis of revised siphonodictyal B (**1.36**) acting as the biosynthetic precursor to liphagal. To further validate this structural revision, Faulkner's second proposed structure of siphonodictyal B (**1.35**) was also

synthesized and submitted to the same biomimetic cascade conditions as **1.36**. NMR data for the product of this cascade did not match isolated **1.37** and was instead assigned as 8-*epi*-liphagal (not shown), thus confirming George's structural revision.

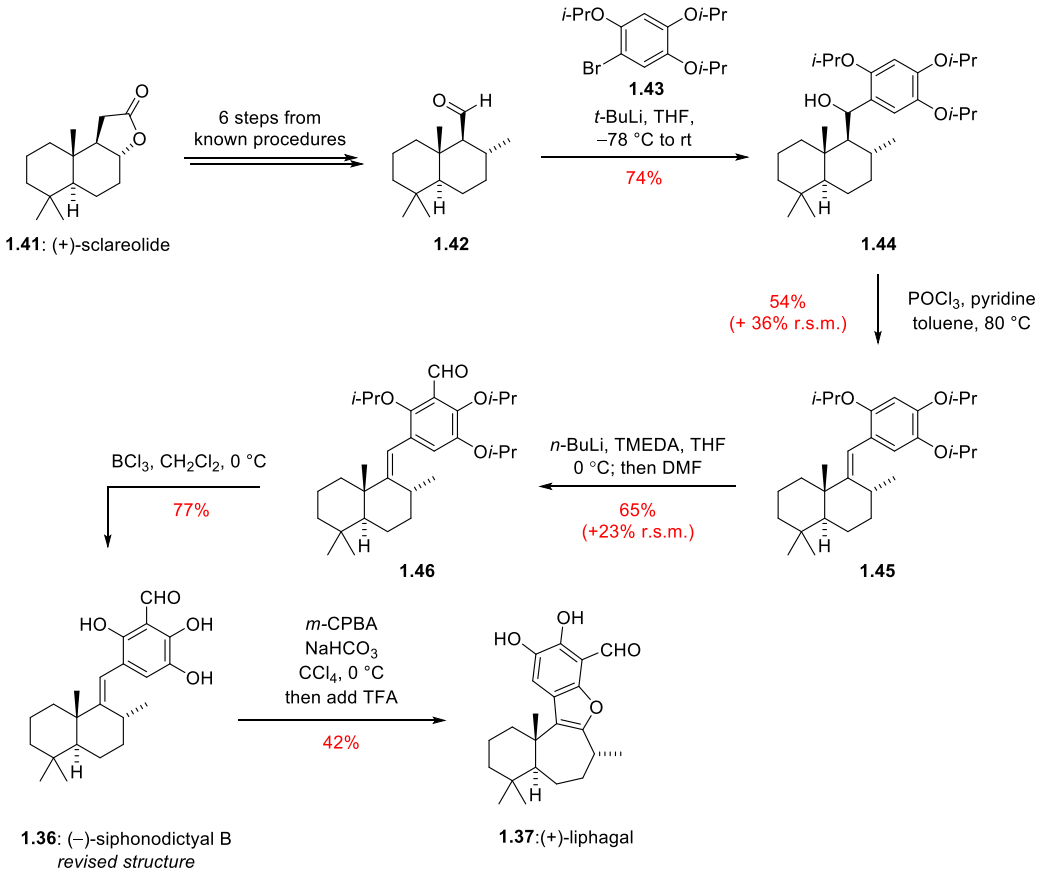

Scheme 1.6: The synthesis of the revised structure siphonodictyal (**1.36**) and its biomimetic conversion to liphagal (**1.37**).[33]

Furoerioaustralasine (**1.53**) is a pentacyclic alkaloid natural product isolated in 1993 by Waterman from *Eriostemon banksi*, a flowering plant species native to Far North Queensland.[34] The structure of furoerioaustralasine was originally proposed to have a *cis* relationship between oxygen substituents at the C-1′ and C-2′ positions (**1.54**, Scheme 1.7). In addition to furoerioaustralasine, Waterman and co-workers also isolated and characterized epoxides *cis*-erioaustralasine (**1.51**) and *trans*-erioaustralasine (**1.52**) in the same paper. These natural products could be biosynthesized from the quinolone derivative **1.47** (Scheme 1.7). Oxidation and alkene isomerization of **1.47** to **1.48** facilitates an intramolecular hetero-Diels–Alder reaction to the *cis*- and *trans*-decalins **1.49** and **1.50**. Epoxidation and *N*-Me oxidation furnishes *cis*-erioaustralasine and *trans*-erioaustralasine. Epoxide **1.51** can undergo an epoxide ring opening by nucleophilic attack of the

neighbouring carbonyl to afford the final product **1.53**. The co-isolation of *cis*-erioaustralasine (**1.51**) and *trans*-erioaustralasine (**1.52**) served as inspiration for a structural revision by the George group.[35] Mechanistically, nucleophilic attack during the epoxide ring-opening stage is only possible from the face opposite the epoxide, resulting in a *trans* relationship between oxygen functionalities (**1.53**). To confirm this hypothesis a concise biomimetic synthesis of furoerioaustralasine was achieved in 3 steps from commercially available starting materials.

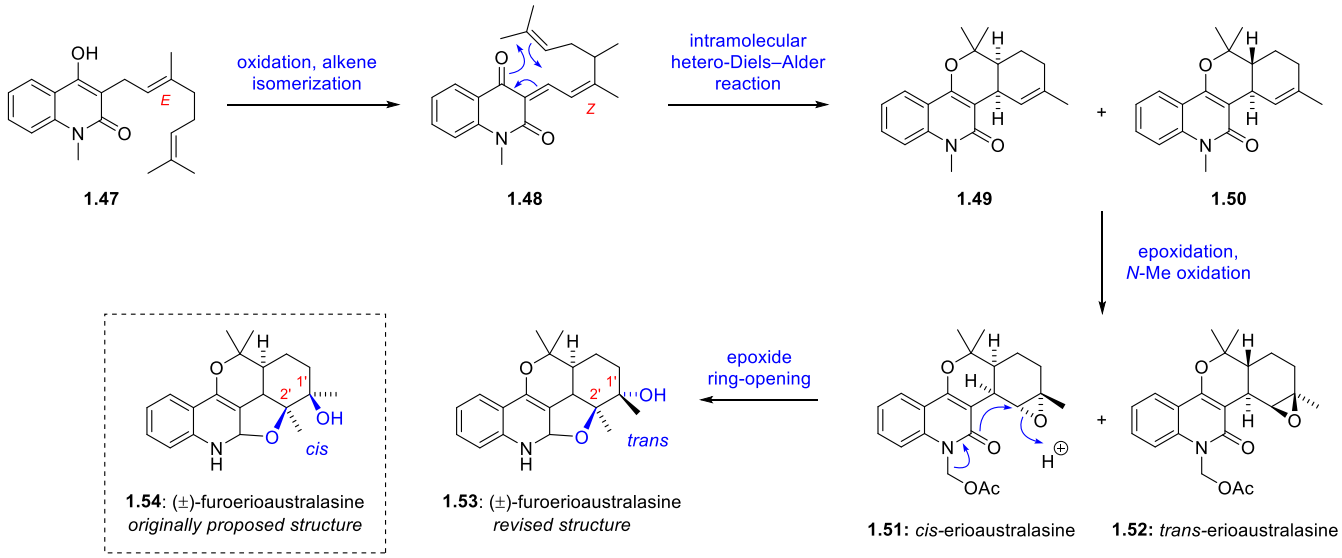

Scheme 1.7: The proposed biosynthesis of furoerioaustralasine (**1.53**).

The synthesis of **1.53** begins with a tandem Knoevenagel condensation/oxa-6π-electrocyclization between commercially available starting materials 2,4-dihyroxyquinoline (**1.55**) and citral (**1.56**) (Scheme 1.8). Treating a mixture of **1.55** and **1.56** with catalytic amounts of EDDA and refluxing in toluene affords pyranoquinoline **1.57** in 94% yield on a multigram scale (~15 g). Construction of the decalin motif was achieved by an elegant thermal rearrangement cascade based on a procedure described by Riviera.[36] Adsorption of **1.57** on silica gel and heating to 140 ºC triggers an initial retro-oxa-6π-electrocyclization. Subsequent alkene isomerization and a concomitant intramolecular hetero-Diels–Alder reaction produces a 1.3:1 mixture of *cis*-/*trans*-decalin diastereomers (**1.59** and **1.60**), separable only by recrystallization. Epoxidation of the desired *cis*-decalin **1.59** with *m*-CPBA afforded a mixture of epoxide products **1.62** and **1.61**, with moderate selectivity for epoxidation of the *exo* face of the alkene (2.2:1 ratio **1.62** to **1.61**). Finally, treatment of *exo*-epoxide **1.62** with trifluoroacetic acid initiates the crucial intramolecular S_N2 epoxide ring-opening, resulting in the sought-after stereochemical inversion at C-2′ with retention at C-1′ to

yield the revised structure of furoerioaustralasine (**1.53**) in 77% yield. This already concise synthesis was streamlined further by telescoping the final epoxidation and acid-catalysed ring-opening steps into a one-pot protocol, sacrificing moderate stereoselectivity for increased step economy. NMR data of synthetic **1.53** matched that of isolated furoerioaustralasine. Furthermore, appropriate crystals of **1.53** were grown and submitted for X-ray diffraction analysis, unambiguously confirming the revised structure of furoerioaustralasine.

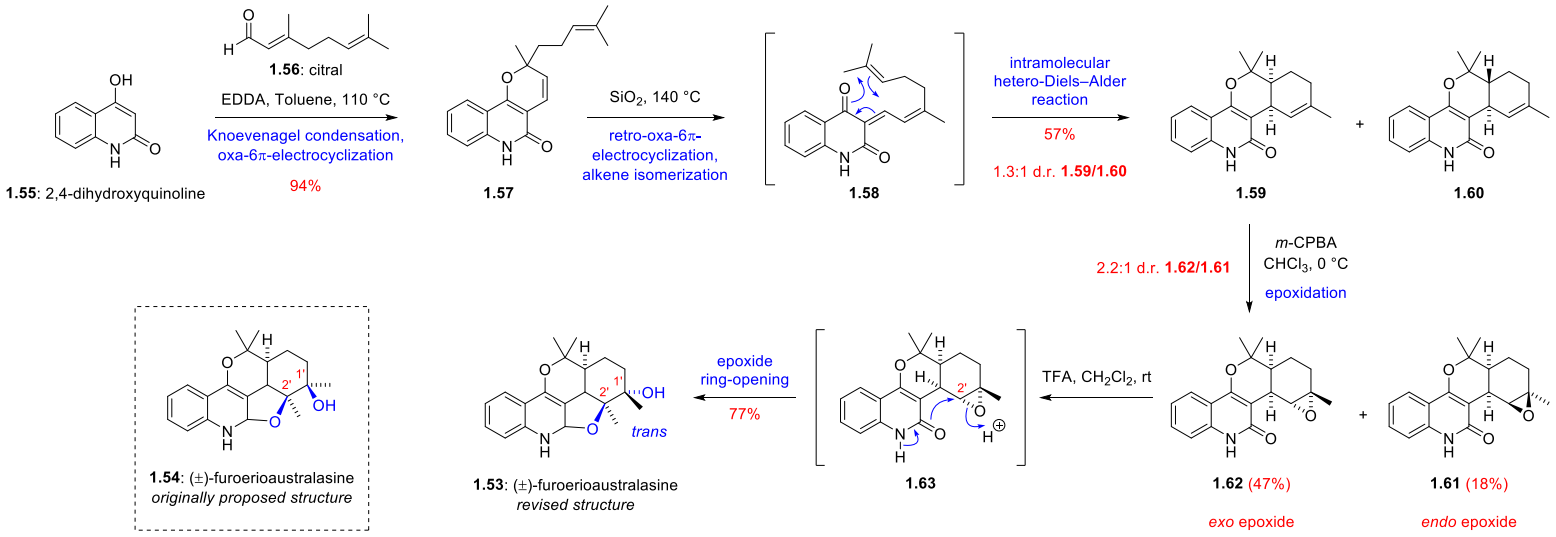

Scheme 1.8: The biomimetic synthesis of furoerioaustralasine (**1.53**).[35]

Cytosporolide A is a caryophyllene-derived meroterpenoid isolated and characterized in 2010 by Che and co-workers.[37] The most striking feature in its proposed structure is the presence of a highly strained, 9-membered peroxylactone ring (**1.64**, Figure 1.4, a). The unusual peroxide bond of **1.64** was assigned on the basis of the chemical shift at C-8 (δ_c = 87.5), which is significantly downfield in relation to C-8 (δ_c = 74.2) of a known caryophyllene-derived meroterpenoid 6-hydroxypunctaporonin (**1.66**).[38] By comparing the C-8 chemical shifts of **1.64** with NMR data of the caryophyllene-derived meroterpenoids guajadial and psidial A (not shown), synthesized by Lee and co-workers,[39] George and Spence propose a 6-membered aryl ether ring could account for the C-8 chemical shift reported for the cytosporolide natural products. Biosynthetically, the revised structure of cytosporolide A (**1.65**) could be achieved via a hetero-Diels–Alder reaction between (–)-fuscoatrol A (**1.67**) and an *ortho*-quinone methide (**1.69**) derived from the dehydration of known fungal metabolite CJ-12,373 (**1.68**) (Figure 1.4, b).

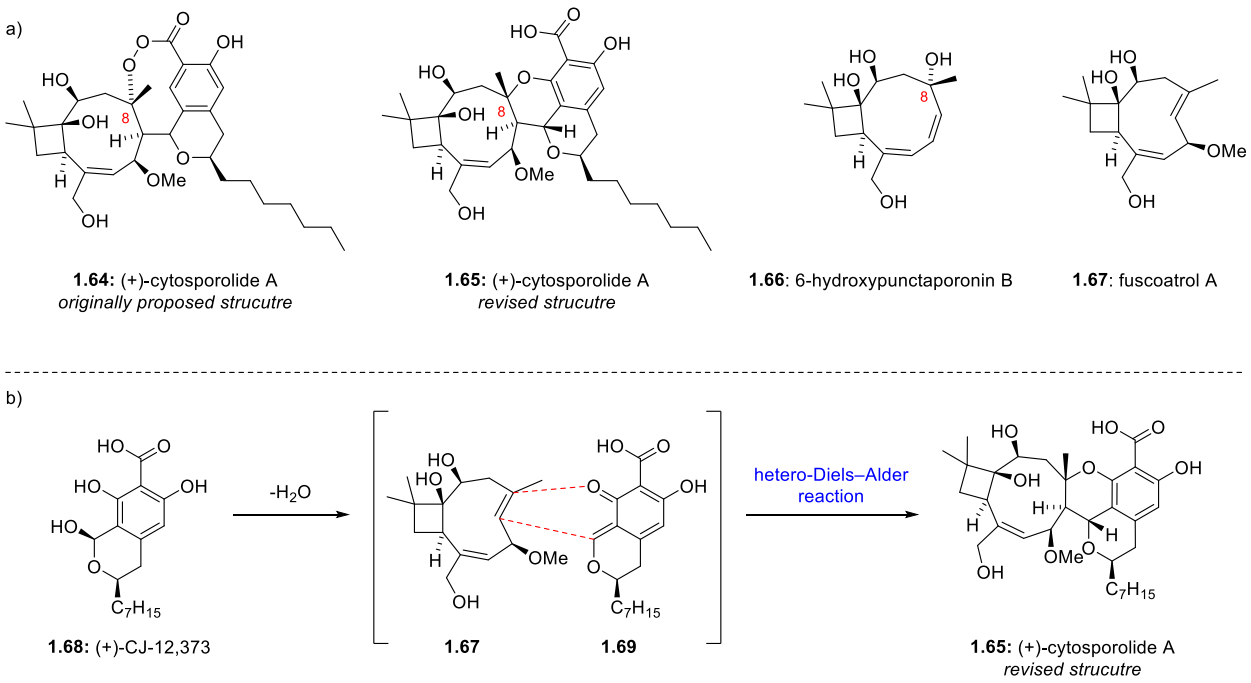

Figure 1.4: a) Original and revised structures of (+)-cytosporolide A as well as related compounds b) Proposed biosynthesis for the formation of (+)-cytosporolide A (**1.65**).

A simplified analogue of the cytosporolide A (**1.73**, Scheme 1.9, a), was synthesized to validate the proposed structural revisions of the cytosporolides. Alcohol **1.70** was treated with TFA and excess $HC(OEt)_3$ (**1.71**). Heating at 100 °C generated *o*-QM **1.72** *in situ*, which was instantly trapped by caryophyllene, affording analogue **1.73** in 53% yield. The data of analogue **1.73**, which contained the proposed 6-membered aryl ether ring, closely matched that of isolated (+)-cytosporolide A, including the key chemical shift at C-8 (δ_c = 88.6 for analogue **1.73**).[40]

The first total synthesis of (+)-cytosporolide A (**1.65**) would be achieved by Takao and co-workers in 2015.[41] As in the model study, the key step in this synthesis is a hetero-Diels–Alder reaction between *o*-QM **1.69** and a protected form of the putative precursor fuscoatrol A (**1.74**). *o*-QM intermediate **1.69** is generated under thermal conditions and readily undergoes the desired cycloaddition with **1.74**. Subsequent deprotection afforded **1.65** in 22% yield over 3 steps. NMR data for synthetic **1.65** unequivocally matched that of isolated (+)-cytosporolide A, verifying its structural revision by George and Spence.

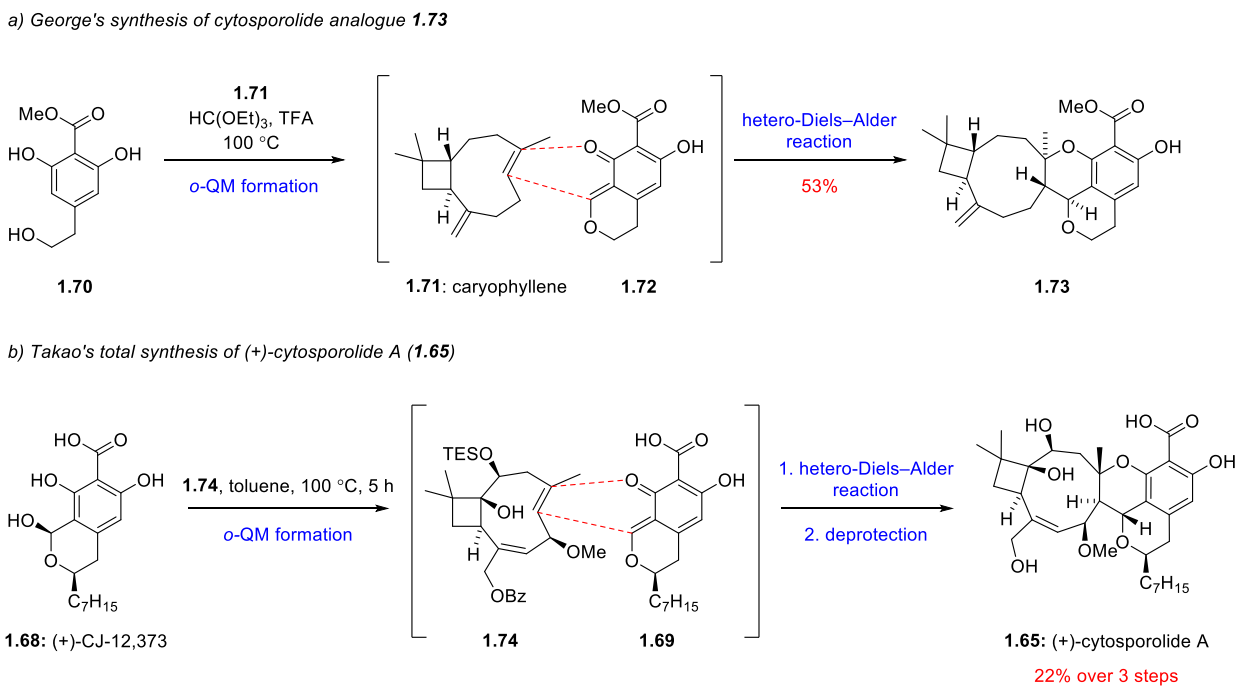

Scheme 1.9: a) The George group's biomimetic synthesis of analogue **1.73**.[40] b) Takao's total synthesis of (+)-cytosporolide A **1.65**.[41]

Once more, biomimetic synthesis proves itself to be a valuable weapon in the in the synthetic chemist's arsenal. Not only does its utility and incorporation in complex syntheses result in elegant pathways to structurally diverse natural products but additionally, as this section has detailed, the biomimetic approach has become an increasingly important and useful tool when isolating new natural products. The consideration of plausible reaction pathways and the formation of likely biosynthetic intermediates, in combination with powerful spectroscopic tools, greatly reduces the assignment of incorrect natural product structures.

1.4 *Ortho*-Quinone Methides in Natural Product Synthesis

The *ortho*-quinone methides (abbreviated as *o*-QMs, **1.75**, Figure 1.5) are ephemeral chemical species that have been exploited by nature, and more recently by organic chemists, in the synthesis of complex natural products. Although *o*-QMs were proposed as early as 1907 by Fries,[42] evidence for their existence would only arrive in 1998 through the pioneering work of Amouri and co-workers who solved their X-ray crystal structure through complexation of *o*-QMs to transition metals.[43] The transient nature of these species can be attributed to their high reactivity, or more specifically, their propensity to rearomatize instantly upon generation. There are several studies which detail the importance of *o*-QMs in important biological processes such as their role in DNA cross-linking and other nucleic acid alkylating reactions.[44-46] Despite their utility, the power of *o*-QMs in total synthesis has only recently been harnessed by synthetic chemists with few examples reported prior to the 1990's. There are already comprehensive reviews detailing the use of *o*-QMs in natural product synthesis up to 2014,[47,48] thus, only some selected syntheses, as well as more recent works, will be covered in this section.

1.4.1 Generation and Reactivity of *ortho*-Quinone Methides

There are many ways to achieve *in situ* generation of *o*-QMs including thermolysis,[49-52] photolysis,[53, 54] treating with acid[55] or base,[56] and oxidation[57] (Figure 1.5), all of which typically involve the elimination of a stable benzylic substituent.

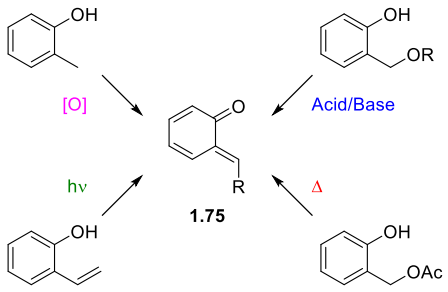

Figure 1.5: General structure of *o*-QMs and common methods of generation.

Reactions of *ortho*-quinone methides can be divided into three major categories: Michael additions, [4+2] cycloadditions and oxa-6π-electrocyclizations (Figure 1.6). The application of these reactions in total synthesis will be discussed in this section.

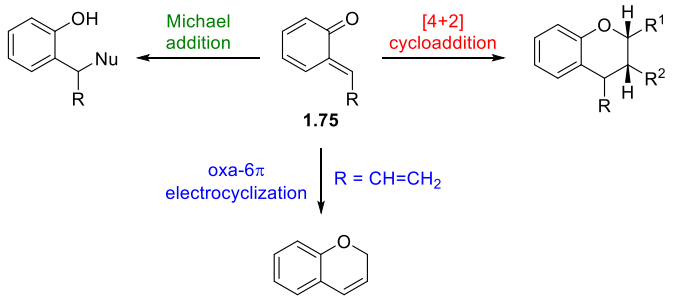

Figure 1.6: Typical reactions of *o*-QMs.

1.4.2 Michael Reactions of *ortho*-Quinone Methides

The use of *o*-QMs as Michael acceptors in organic synthesis has remained underexplored when compared to cycloadditions or electrocyclizations, with fewer examples cited in literature. Generation of *o*-QMs for Michael additions can prove problematic, requiring careful selection of the reaction conditions to minimise unwanted side reactions, a factor which may have discouraged their use as intermediates in total synthesis.

The Pettus group are pioneers in the field of *ortho*-quinone methide chemistry. In addition to the several published total syntheses which utilise *o*-QMs, the group have also distinguished themselves by their use of Grignard reagents to generate *o*-QMs under relatively mild conditions. One such example can be seen in the total synthesis of (+)-rishirilide B (**1.80**), in which an *o*-QM generated by this Grignard reagent strategy undergoes a Michael addition (Scheme 1.10).[58] Excess isobutyl magnesium bromide **1.77** was added dropwise to the Boc-protected phenol **1.76** to form the key *o*-QM **1.78**. This intermediate was trapped by a second equivalent of the Grignard reagent to afford the alkylated phenol **1.79**. The final natural product was achieved from **1.79** in a further 13 steps.

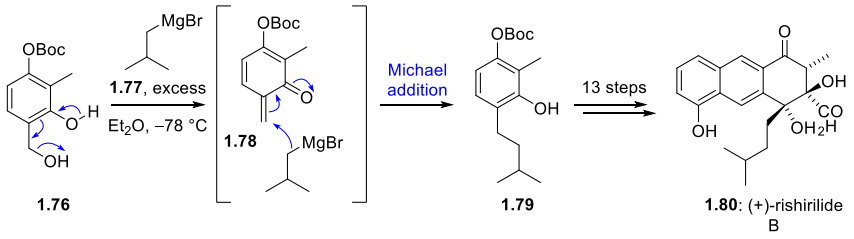

Scheme 1.10: The total synthesis of (+)-rishirilide B (**1.80**) by Pettus.[58]

The George group have firmly established themselves as experts in the realm of biomimetic synthesis and often make use of the *o*-QMs in their natural product syntheses. This is clearly exemplified in their total synthesis of *ent*-penilactone A (**1.86**) and penilactone B (**1.87**) by a common *o*-QM intermediate **1.82** (Scheme 1.11).[59] Heating precursor **1.81** under reflux formed the *ortho*-quinone methide **1.82**. In the presence of a lactone **1.83**, the *o*-QM can react via a Michael addition to give adduct **1.84**. A second equivalent of **1.82** participates in an additional Michael reaction to give compound **1.85**. Finally, a ring closure yielded the desired natural products **1.86** and **1.87** in 46% and 85% yield, respectively.

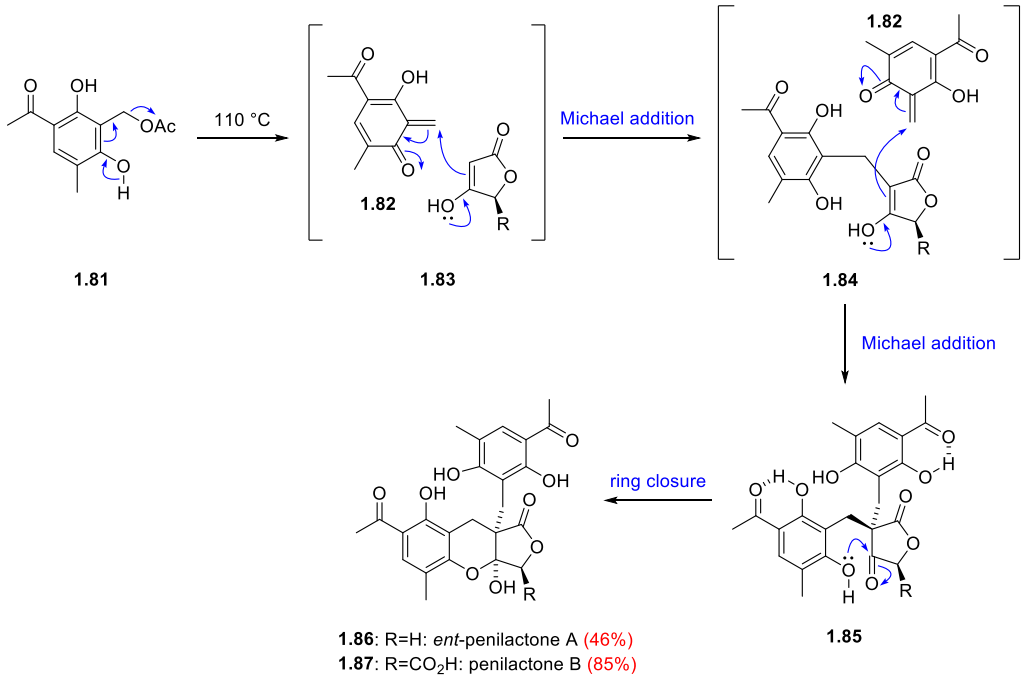

Scheme 1.11: George's biomimetic synthesis of *ent*-penilactone A (**1.86**) and penilactone B (**1.87**).[59]

George et al. would revisit intermediate **1.82** in their biomimetic synthesis of peniphenones A (**1.86**), B (**1.87**) and (*S*)-peniphenone D (**1.88**) (Scheme 1.12).[60] Once more, *o*-QM **1.82** is formed by heating precursor **1.81** under reflux (Scheme 1.11). Doing so in the presence of coupling partners **1.84** and **1.85**, with subsequent manipulations, affords the desired natural products **1.87** and **1.88**, respectively. Peniphenone A (**1.86**) was originally proposed to be the product of a [4+2] cycloaddition with an exocyclic alkene coupling partner, but its synthesis presented some problems and required a revised strategy. An alternative method was worked on which made use of an enolate as a Michael donor. Thus, treatment of the bis-TBS ether **1.83** with LiTMP in THF/HMPA, followed by the addition *o*-QM precursor **1.81**, generated the necessary *o*-QM and enolate

simultaneously. Michael addition followed by bis-TBS deprotection, spiroketalization and a subsequent TPAP oxidation, yielded the desired natural product **1.86**. Peniphenone C (not shown) was achieved by means of an electrophilic aromatic substitution/autoxidation sequence also using intermediate **1.82**.[59]

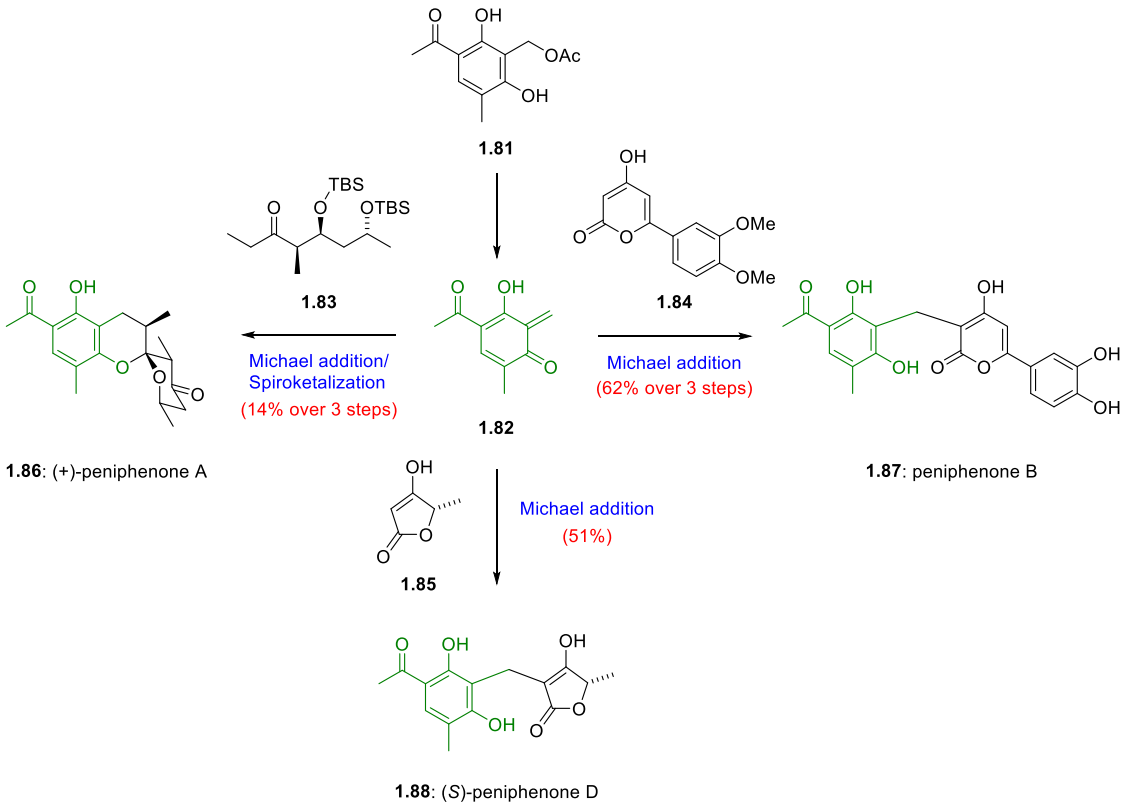

Scheme 1.12: George's synthesis of the peniphenones A (**1.86**), B (**1.87**) and (*S*)-D (**1.88**).[60]

1.4.3 Oxa-6π-electrocyclizations of *ortho*-Quinone Methides

ortho-Quinone methides can readily undergo oxa-6π-electrocyclization reactions to afford chromenes (2*H*-benzopyrans). These chromenes are incredibly versatile building blocks, present in many natural products or acting as key intermediates for their biosynthesis.

Cortistatin A (**1.97**, Scheme 1.13) is a marine natural product with potent anti-angiogenic and anti-proliferative activity and a peculiar, modified steroidal skeleton.[61] Its low abundance, intriguing architecture and potent biological activity quickly made **1.97** an attractive synthetic target. Indeed, several elegant total syntheses of **1.97** have been published by many prestigious research groups.[62-64] From their own investigations into the synthesis of **1.97**, Danishefsky and co-workers published

a concise synthesis of the cortistatin core (**1.96**), which made deft use of *o*-QM chemistry.[65] A 1,2-addition of the bromide **1.89**, via the corresponding aryllithium species, to aldehyde **1.90** generated alkoxide **1.91**. Intramolecular carbamate migration and subsequent elimination formed *o*-QM **1.93** which immediately reacts in an oxa-6π-electrocyclization to give compound **1.94** in 71% yield. Further manipulations of **1.94** produced **1.95.** Treatment with TBAF resulted in simultaneous deprotection and alkylation, yielding the pentacyclic core **1.96** of the cortistatin family in 88% yield.

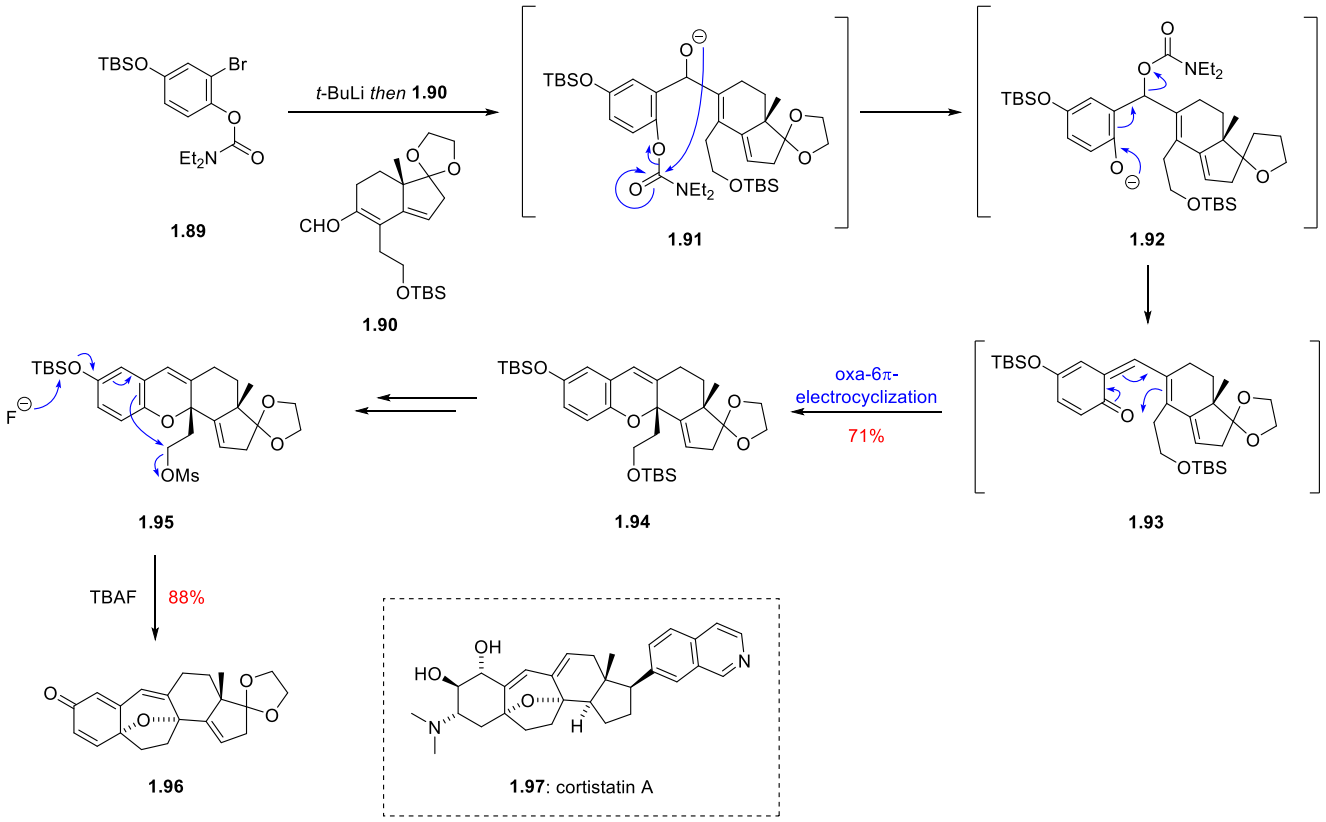

Scheme 1.13: Danishefsky's synthesis of the cortistatin A core (**1.97**).[65]

The Trauner group has also made use of the versatility of *o*-QMs, as seen in their synthesis of the prenylated napthoquinones mollugin (**1.100**) and microphyllaquinone (**1.103**) (Scheme 1.14). By simply treating **1.98** with triethylamine, *o*-QM **1.99** was easily formed, with an oxa-6π-electrocyclization step affording **1.100** in 81% yield. Similarly, **1.102** was generated from napthoquinone dimer **1.101**, also undergoing an oxa-6π-electrocyclization, producing **1.103** in 70% yield.[66]

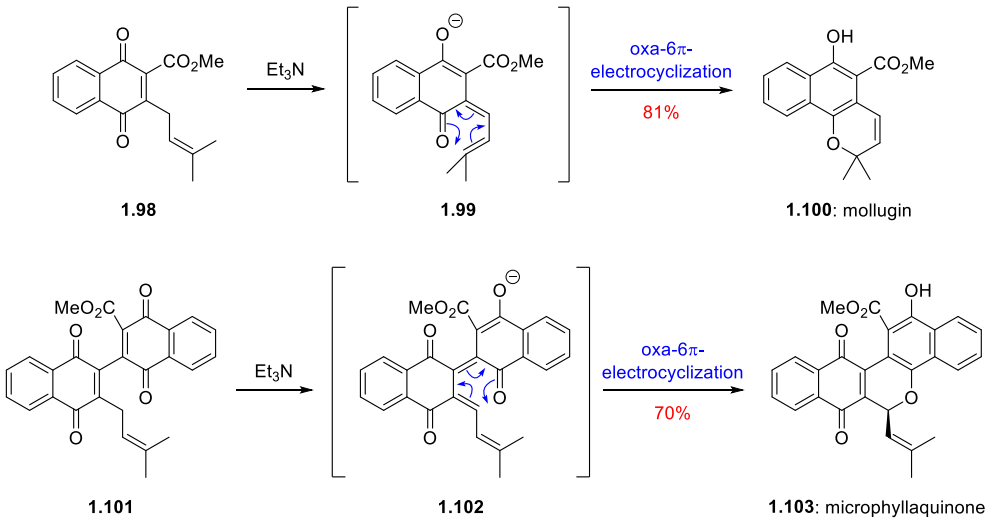

Scheme 1.14: Trauner's biomimetic synthesis of mollugin (**1.100**) and microphyllaquinone (**1.103**).[66]

The George group would once again leverage their expertise of *o*-QM intermediates in their biomimetic synthesis of the rhodonoid natural products. Rhodonoids A (**1.109**), C (**1.113**) and D (**1.114**) are thought to be derived from a common, previously isolated, chromene intermediate **1.107** (Scheme 1.16). This chromene was synthesized in a single step from orcinol (**1.104**) in a tandem Knoevenagel condensation/oxa-6π-electrocyclization cascade via the *o*-QM intermediate **1.106**. A one-pot protocol involving an acetate protection, Schenck ene reaction and Kornblum–DeLaMare rearrangement formed ketone **1.108** from chromene **1.107**. A [2+2] photocycloaddition and same-pot deprotection gave rhodonoid A (**1.109**) in 60% yield.[67] Treatment of **1.107** with *m*-CPBA yielded epoxide **1.110** in 51% yield (1:1 mixture of diastereomers). In the presence of $SnCl_4$, **1.110** may undergo a 6-*endo*-*tet* or a 5-*exo*-*tet* ring opening, affording *o*-QMs **1.111** and **1.112**. Intramolecular nucleophilic attack of intermediates **1.111** and **1.112** by the hydroxyl group generates the natural products rhodonoid C (**1.113**) and rhodonoid D (**1.114**) in 32% and 5% yield respectively.[68]

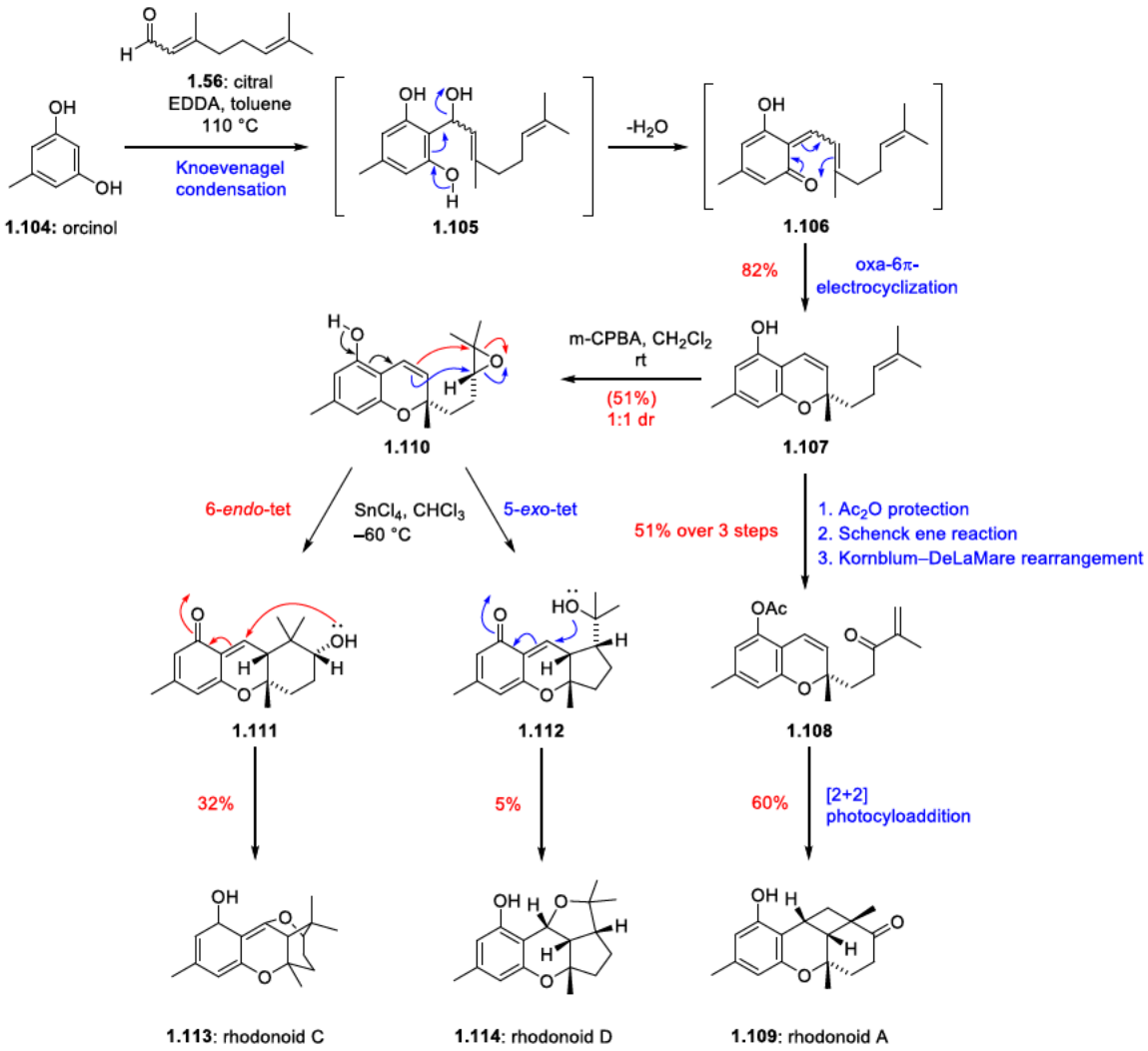

Scheme 1.15: George's biomimetic synthesis of rhodonoids A (**1.109**), C (**1.113**) and D (**1.114**).[67,68]

Other members of this family of natural products – rhodonoids B (**1.119**), E (**1.120**) and F (**1.121**) – were synthesized in similar fashion. Chromene **1.118** (as a mixture of *E* and *Z* isomers) was identified as a precursor to these compounds and could be prepared from orcinol (**1.104**) and farnesal (**1.115**) using the same conditions described in the synthesis of rhodonoids A, C, and D. A Knoevenagel condensation with subsequent oxa-6π-electrocyclization of *o*-QM **1.117** yielded the desired chromene in 84% yield. A [2+2] cycloaddition, followed by a $^1O_2$ reaction produced **1.120** and **1.121**.[67] A [2+2] cycloaddition, protection and Schenck ene reaction allowed for a formal synthesis of **1.119**. The final 2 steps in the sequence to form **1.119** have previously been reported by Hsung and Tang.[69]

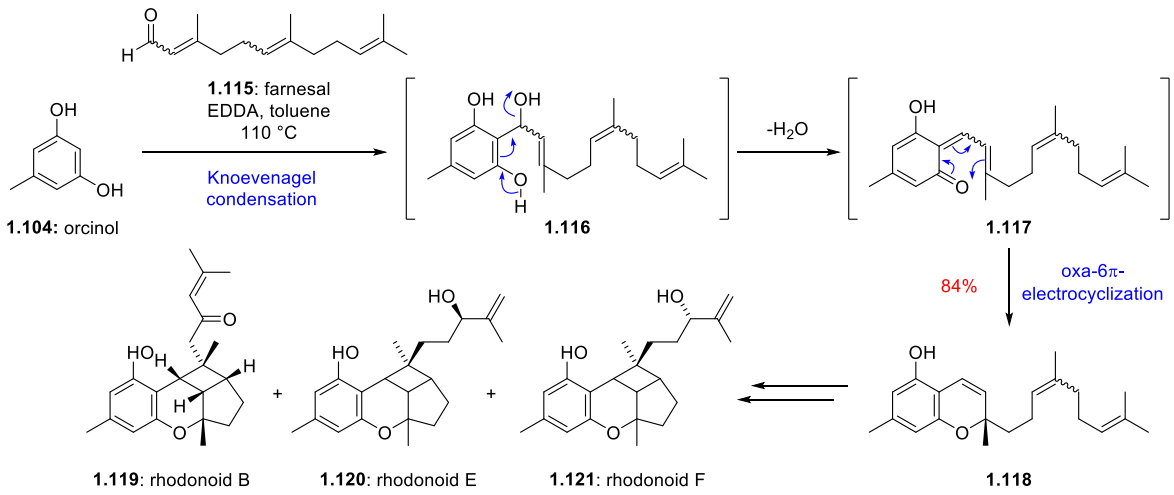

Scheme 1.16: George's biomimetic synthesis of rhodonoids B (**1.119**), E (**1.120**) and F (**1.121**).[67]

1.4.4 [4+2] Cycloadditions of *ortho*-Quinone Methides

The most prominent and well-studied application of *o*-QMs in synthesis is their use in hetero-Diels–Alder reactions. Their capacity to construct six-membered rings under varied conditions and with a wide range of dienophilic partners makes strategies involving [4+2] cycloadditions of *o*-QMs very attractive. The ability to participate in hetero-Diels–Alder reactions has led to numerous successful total syntheses being reported which make use of this reactivity. The first and perhaps the most famous application of *ortho*-quinone methides in total synthesis is in the biomimetic synthesis of carpanone (**1.124**) by Chapman in 1971. A palladium(II) mediated dimerization of phenol **1.122** generated the *o*-QM **1.123**, which immediately reacts in an intramolecular [4+2] cycloaddition yielding **1.124** in 46% yield (Scheme 1.17).[70] In a single step a large degree of molecular complexity was established with the formation 2 new rings as well as 5 stereocentres, making this seminal work a showcase for the potential of *o*-QMs in total synthesis.

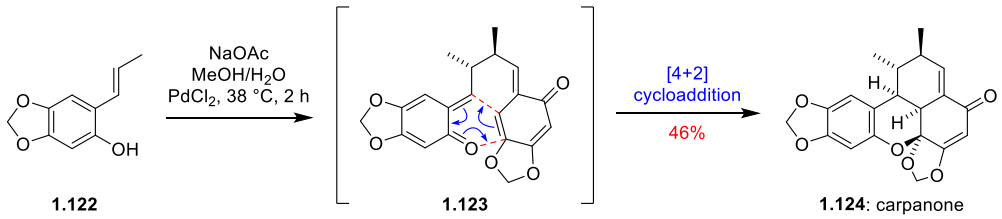

Scheme 1.17: Chapman's biomimetic synthesis of carpanone (**1.124**).[70]

Another excellent example of the use of *o*-QMs in [4+2] cycloadditions is in the biomimetic synthesis of lucidene (**1.128**) by Baldwin (Scheme 1.18).[71] Thermolysis of the hydroxybenzyl alcohol **1.125** at 170 °C generated the necessary *o*-QM **1.127**. Two equivalents of **1.127** react with humulene (**1.126**) to form the desired natural product **1.128** and its diastereoisomer, isolucidene (**1.129**) in 17% overall yield (2.5:1 ratio in favour of **1.128**). The mono-adduct **1.130** was also formed in 28% yield. Re-exposure of **1.130** to the hydroxybenzyl alcohol **1.125** under similar reaction conditions (sealed tube, 160 °C) afforded **1.128** and **1.129** in similar relative amounts as before. This synthesis is also a great display of the regioselectivity of humulene (**1.126**) as the mono-adduct **1.130** is only generated by reaction of **1.127** with the more reactive $\Delta^{1,2}$ alkene of humulene as opposed to the other alkenes present in its structure.

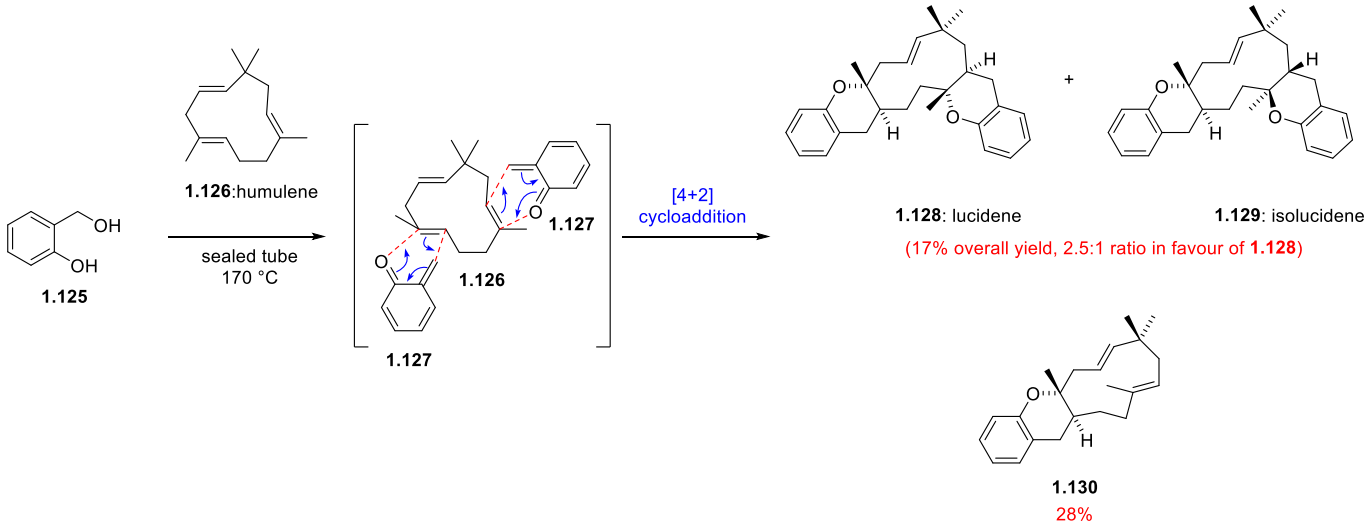

Scheme 1.18: Baldwin's biomimetic synthesis of lucidene (**1.128**).[71]

In 2008, the Trauner group would once again make excellent use of *o*-QM chemistry in their work, this time reporting the total synthesis of the complex natural product rubioncolin B (**1.137**) by utilizing a one-pot oxidation/tautomerisation/Diels–Alder cascade[72] (Scheme 1.19). Starting from the bis-TBS ether **1.131**, a TASF mediated deprotection generated the phenoxide anion **1.132**. Subsequent oxidation with $PhI(OAc)_2$ resulted in the oxonium cation **1.133** which was deprotected by a second equivalent of TASF to form **1.134**. Quinone **1.134** exists in equilibrium with its tautomer, the *o*-QM **1.135**, which undergoes the key [4+2] cycloaddition to give compound **1.136** in 60% yield. Finally, demethylation of **1.136** using BBr_3 afforded the natural product, rubioncolin

B (**1.137**) in 95% yield. Further highlighting the utility of *o*-QMs, this synthesis makes use of another *ortho*-quinone methide reaction that was discussed earlier (See Scheme 1.14). The bis-TBS ether **1.131** is derived from an acid chloride and a tertiary alcohol (alcohol derived portion of the molecule is highlighted in green in Scheme 1.19). This alcohol was made in 4 steps from the natural product mollugin (**1.100**, Scheme 1.14), also synthesized by Trauner via an oxa-6π-electrocyclization of an *o*-QM.[66]

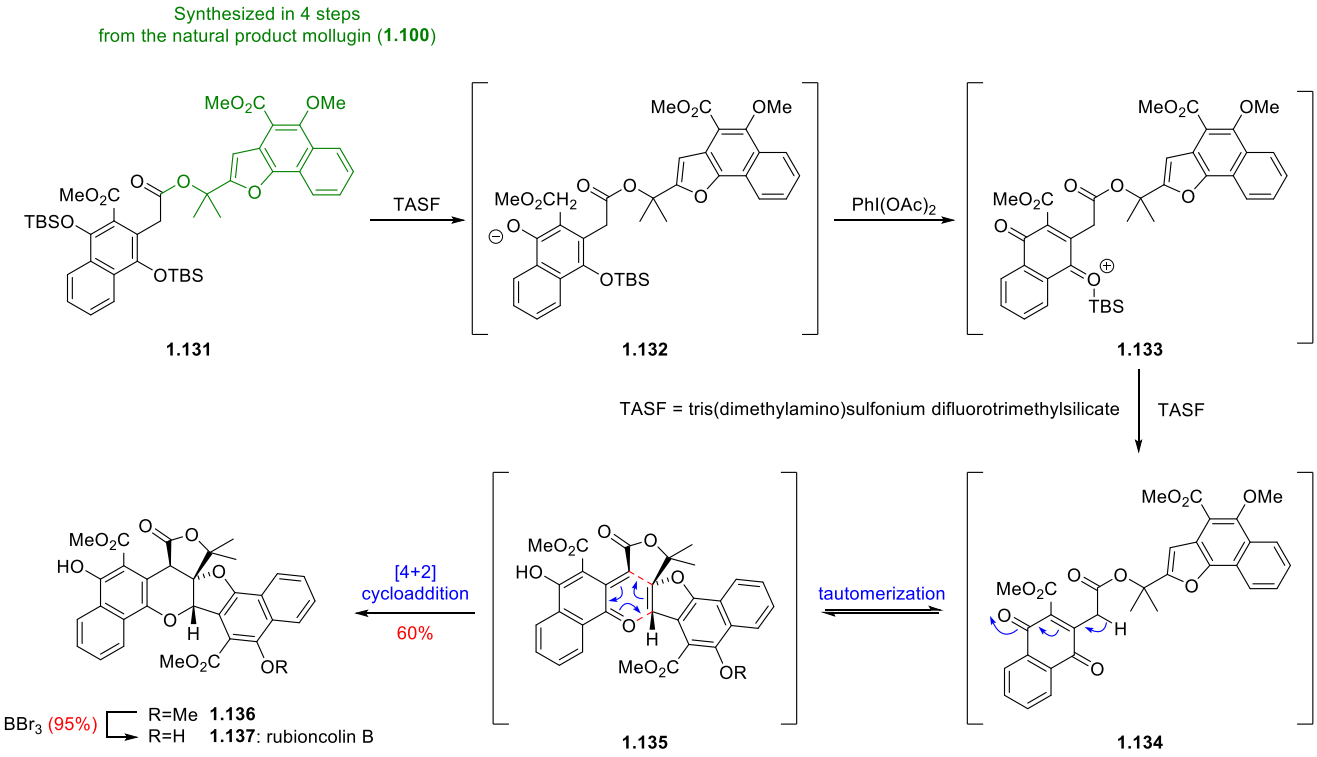

Scheme 1.19: Trauner's total synthesis of rubioncolin B (**1.137**).[72]

Spirooliganones A and B (**1.143** and **1.144**) are a pair of epimer natural products isolated from the roots of *Illicium oligandrum*[73] and contain a complex 5/6/6/5/3 pentacyclic framework, including a rare dioxa-spiro system. At the time of writing, three total syntheses for **1.143** and **1.144** have been reported, all published within a year of each other by the groups of Xie, Tong and Yu.[74-76] Despite varying approaches between syntheses, a common strategy employed by these groups was a [4+2] cycloaddition of an *o*-QM with (−)-sabinene (**1.141**, Scheme 1.20).

In the first synthesis by Xie (Scheme 1.20, a), this cycloaddition strategy is employed early on with the required *o*-QM **1.140** being generated from 1,3-cyclohexadione (**1.138**) and formaldehyde (**1.139**) under Hoffmann conditions. The hetero-Diels–Alder reaction between **1.140** and **1.141** in one-pot afforded the spirocycle **1.142** as a mixture of diastereomers in 79% yield. The resulting diastereomers were separated by flash column chromatography and recrystallisation. Each diastereomer was subjected to identical conditions to yield the two natural products **1.143** and **1.144** in seven steps.[74]

Following a biomimetic approach, the syntheses by Tong and Yu placed a greater emphasis on developing their *o*-QM precursors first and carrying out the key [4+2] cycloaddition later. In both cases, this strategy defers the installation of critical stereocentres which would be introduced by the hetero-Diels–Alder step. This approach minimises the number of late-stage manipulations which can prove problematic due to the presence of an unstable cyclohexadione moiety, as well as avoiding potential obstacles that may arise when separating products. Both syntheses also form their respective *o*-QMs by elimination of a benzylic substituent under thermal conditions. In Tong's synthesis (Scheme 1.20, b), heating of the *o*-QM precursor **1.145** in a sealed tube at 160 °C in the presence of **1.141** resulted in an aromatic Claisen rearrangement and a subsequent [4+2] cycloaddition to generate spirocycle **1.147** in 79% yield. **1.147** was converted to the natural products **1.143** and **1.144** in a further 6 steps.[75] Yu and co-workers employed a similar strategy using compound **1.148** (Scheme 1.20, c). Thermolysis in the presence of **1.141** generates adduct **1.150** in 82% yield which was converted to spirooliganones A and B in 3 more steps.[76]

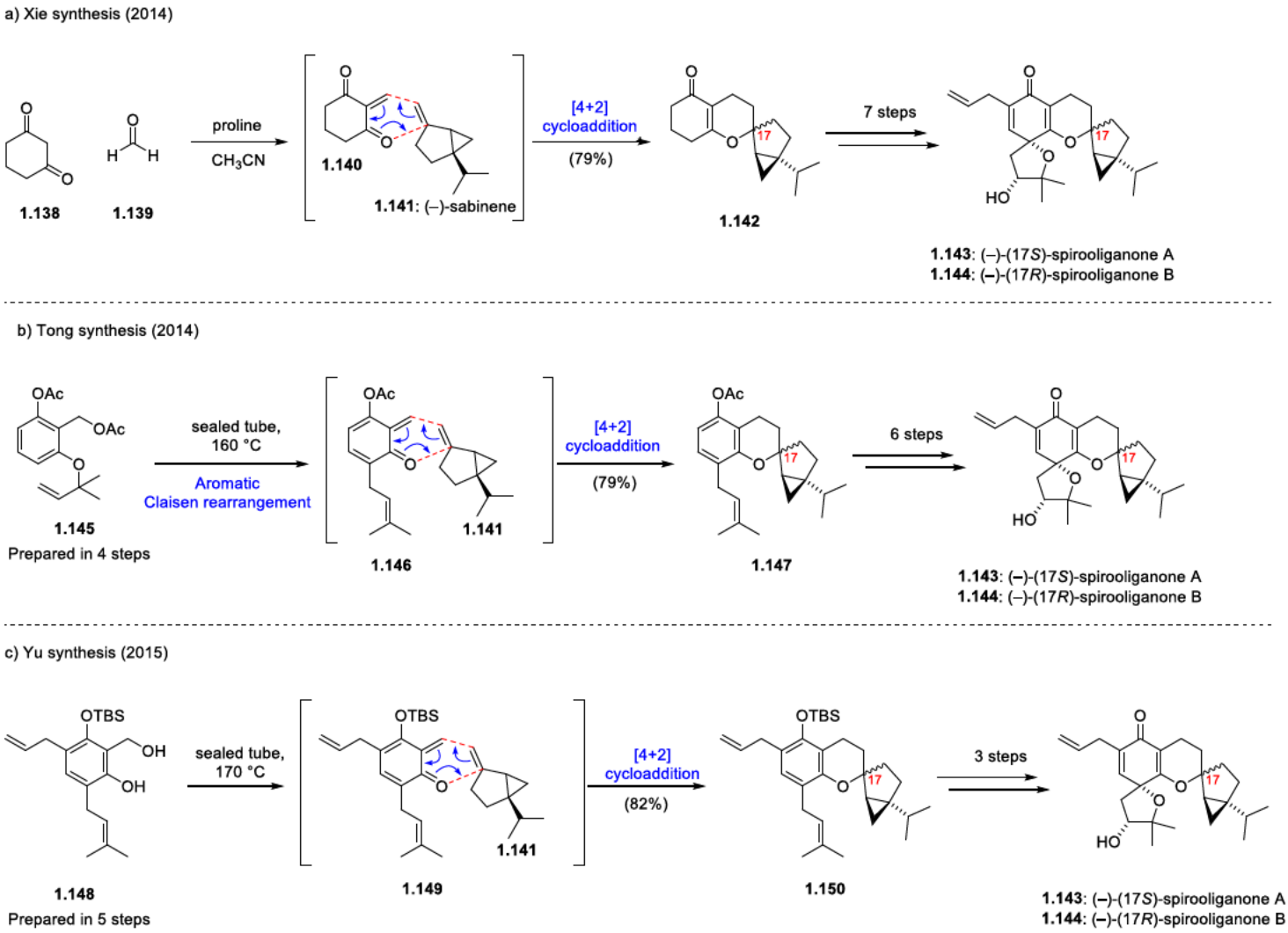

Scheme 1.20: Published total syntheses of spirooliganones A (**1.143**) and B (**1.144**) by the groups of Xie[74], Tong[75] and Yu.[76]

Bruceol (**1.151**, Figure 1.7) is a polycyclic meroterpenoid isolated from the Western Australian shrub, *Philotheca brucei*, in 1963 by Jefferies and co-workers.[77] Bruceol possesses an intriguing pentacyclic framework, with a 5,7-dihydroxycoumarin fused to a "citran" ring system, biosynthetically derived from a geranyl cyclization. The relative configuration of **1.151** was determined by X-ray crystallography of 8-bromobruceol; at the time no detailed NMR studies were conducted. Years later, the absolute configuration of bruceol was confirmed by X-ray analysis of its chloroacetate and iodoacetate derivatives.[78] In 1992, Waterman and co-workers would publish detailed NMR studies of what they believed was **1.151**. As it turns out, Waterman had mistakenly isolated and characterised a related natural product, isobruceol (**1.152,** Figure 1.7).[79]

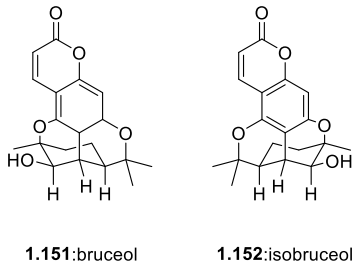

Figure 1.7: The structures of bruceol (**1.151**) and isobruceol (**1.152**).

This misassignment was confirmed in 2019 when George and co-workers achieved the first total synthesis of **1.151** and **1.152** nearly 50 years following the original isolation of bruceol.[80] Both **1.151** and **1.152** were synthesized in a biomimetic fashion by making expert use *o*-QM chemistry, including an intramolecular hetero-Diels–Alder reaction as the final step in both syntheses. Knoevenagel condensation between 5,7-dihydroxycoumarin (**1.153**) and citral (**1.56**) followed by an oxa-6π-electrocyclization of the resulting *o*-QM formed the isomeric chromenes **1.154** and **1.155** in 13% and 15% yield respectively (Scheme 1.21).

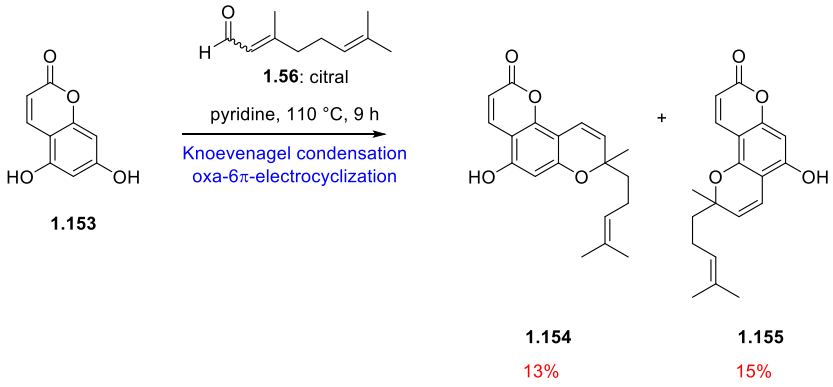

Scheme 1.21: Synthesis of chromenes **1.154** and **1.155**.

A stereoselective Jacobsen–Katsuki epoxidation of chromene **1.155** using 10 mol % of Jacobsen's catalyst (*R,R*)-**1.156**, with *m*-CPBA and NMO as stoichiometric oxidants, gave two epoxides **1.157** and **1.159**. These labile epoxides readily undergo ring openings to give the *o*-QMs **1.158** and **1.160** which are now primed to react in the key [4+2] cycloaddition, finally yielding the natural product (−)-bruceol (**1.151**) in 11% yield and (+)-2′-*epi*-bruceol (**1.161**) in 3% yield (Scheme 1.22). ^{1}H and ^{13}C NMR data between George's synthetic bruceol (**1.151**) and Waterman's isolated sample revealed multiple discrepancies. X-ray crystallography of synthetic **1.151** and a detailed NMR analysis of Jefferies' original, isolated sample of bruceol from 1963 confirmed Waterman's erroneous assignment.

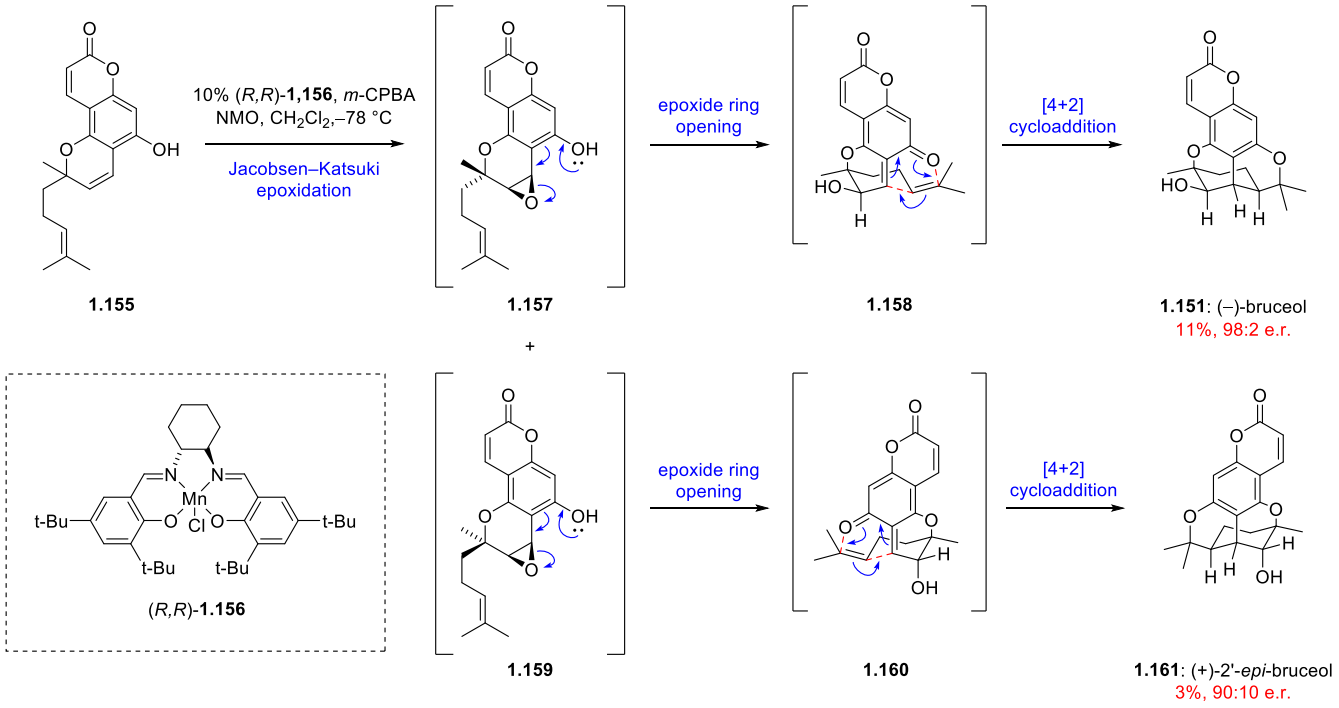

Scheme 1.22: George's biomimetic synthesis of bruceol (**1.151**).[80]

Following a re-isolation of **1.152** and confirmation of its structure by X-ray analysis in the same study,[80] George et al. would also carry out a biomimetic synthesis of isobruceol. Taking the previously synthesized chromene **1.154** and treating with methanolic NaOH gave chromene **1.162**, which exists with **1.154** in a separable equilibrium mixture. This transformation proceeds via a methoxide-induced ring opening of the lactone followed by cyclization of the ester intermediate at the C-9 phenol. Another stereoselective epoxidation, this time using (*S,S*)-**1.156**, triggers the cascade seen in the synthesis of **1.151**, affording (−)-isobruceol (**1.152**) and (+)-2′-epi-isobruceol (**1.163**) in 5% and 2% yield respectively.

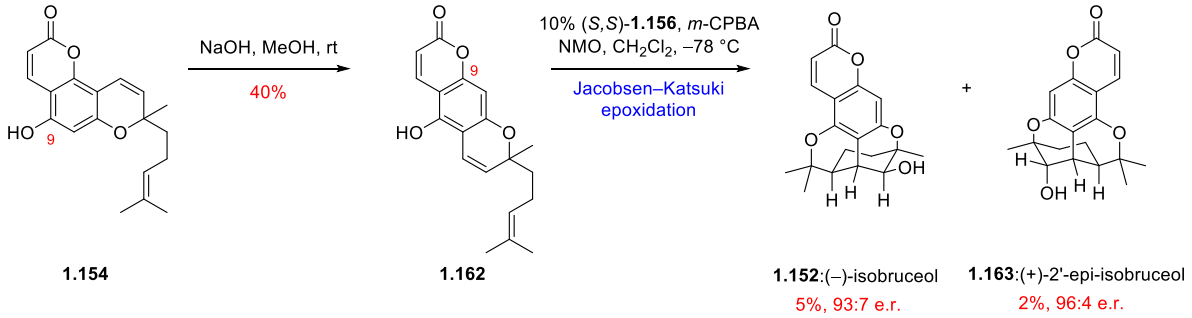

Scheme 1.23: George's biomimetic synthesis of isobruceol (**1.152**).[80]

1.5 Project Aims

The art of organic synthesis has developed exponentially since its inception and the continued development and discovery of novel chemical reagents, methodologies, and reactions has greatly aided chemists on their ambitious quest of resolving and understanding the molecules engineered by nature. The dynamic nature and extensive scope of natural product synthesis lends itself to collaborations across various areas of research including medicinal, biological, and industrial chemistry.[81] This introductory chapter has highlighted a fraction of what is possible in natural product synthesis including: the power of the biomimetic approach as a synthetic strategy, the use of total synthesis in determining the correct structures of newly isolated compounds, and the utility of *ortho*-quinone methides as reactive intermediates.

This thesis will outline the work carried out towards the biomimetic synthesis and the accompanying structural revisions of three meroterpenoid natural products: littordial E, littordial F and drychampone B (Figure 1.7), all while utilizing the concepts covered in this past chapter. Based on our own biosynthetic speculation, we believe the key step in the syntheses of these natural products to involve a hetero-Diels–Alder reaction between an appropriate phloroglucinol-derived *ortho*-quinone methide and caryophyllene or humulene. Our synthetic strategies are based on this biosynthetic proposal. Hopefully, this project will adequately highlight the importance of considering a molecule's plausible biosynthesis when assigning a novel structure and when used in combination with spectroscopic data, significantly reduces the likelihood of error in its initial assignment.

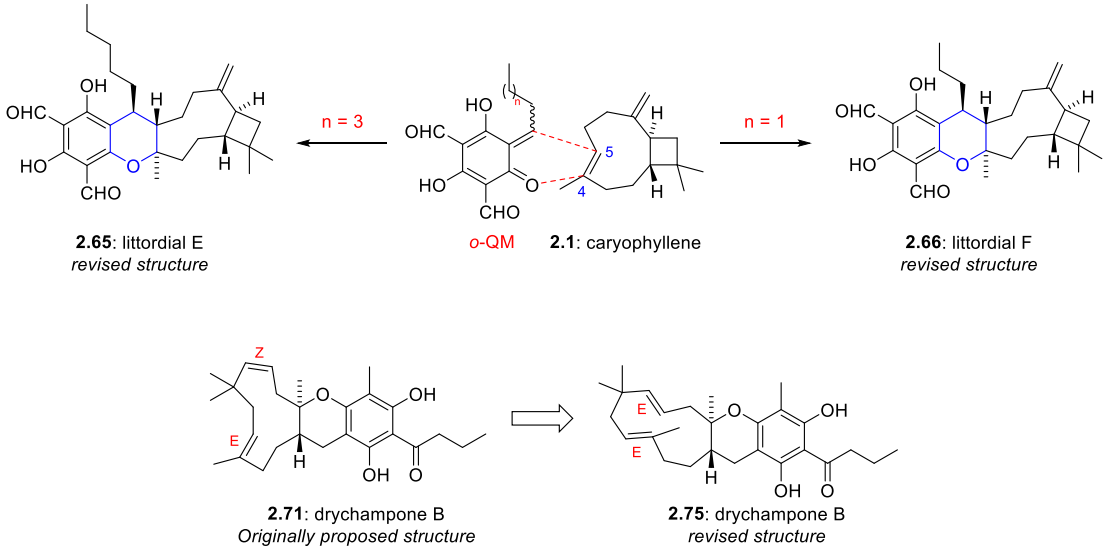

Figure 1.7: Project overview.

1.6 References

1. Dias, D. A.; Urban, S.; Roessner, U. A Historical Overview of Natural Products in Drug Discovery. *Metabolites* **2012**, *2,* 303.

2. Butler, M. S. The Role of Natural Product Chemistry in Drug Discovery. *J. Nat. Prod.* **2004**, *67*, 2141.

3. Harvey, A. L.; Edrada-Ebel, R.; Quinn, R. J. The re-emergence of natural products for drug discovery in the genomics era. *Nat. Rev. Drug Discov.* **2015**, *14*, 111.

4. Newman, D. J.; Cragg, G. M. Natural Products as Sources of New Drugs from 1981 to 2014. *J. Nat. Prod*. **2016**, *79*, 629.

5. Wani, M. C.; Taylor, H. L.; Wall, E. M.; Coggon, P.; McPhail, A. T. Plant Antitumor The Isolation and Structure of Taxol, a Novel Antileukemic and Antitumor Agent from *Taxus brevifolia. J. Am. Chem. Soc.* **1971**, *93*, 2325.

6. Nicolaou, K. C.; Yang, Z.; Liu, J. J.; Ueno, H.; Nantermet, P. G.; Guy, R. K.; Claiborne, C. F.; Renaud, J.; Couladouros, E. A.; Paulvannan, K.; Sorensen, E. J. Total synthesis of taxol. *Nature*, **1994**, *367*, 630.

7. Holton, R. A.; Somoza, C.; Kim, H. B.; Liang, F.; Biediger, R. J.; Boatman, P. D.; Shindo, M.; Smith, C. C.; Kim, S.; Nadizadeh, H.; Suzuki, Y.; Tao, C.; Vu, P.; Tang, S.; Zhang, P.; Murthi, K. K.; Gentile, L. N.; Liu, J. H. First total synthesis of taxol. 1. Functionalization of the B ring. *J. Am. Chem. Soc.* **1994**, *116*, 1597.

8. Holton, R. A.; Somoza, C.; Kim, H. B.; Liang, F.; Biediger, R. J.; Boatman, P. D.; Shindo, M.; Smith, C. C.; Kim, S.; Nadizadeh, H.; Suzuki, Y.; Tao, C.; Vu, P.; Tang, S.; Zhang, P.; Murthi, K. K.; Gentile, L. N.; Liu, J. H. First total synthesis of taxol. 2. Completion of the C and D Rings. *J. Am. Chem. Soc.* **1994**, *116*, 1599.

9. Danishefsky, S. J.; Masters, J. J.; Young, W. B.; Link, J. T.; Snyder, L. B.; Magee, T. V.; Jung, D. K.; Isaacs, R. C. A.; Bornmann, W. G.; Alaimo, C. A.; Coburn, C. A.; Di Grandi, M. J.; Total Synthesis of Baccatin III and Taxol. *J. Am. Chem. Soc.* **1996**, *118*, 2843.

10. Wender, P. A.; Badham, N. F.; Conway, S. P.; Floreancig, P. E.; Glass, T. E.; Gränicher, C.; Houze, J. B; Jänichen, J.; Lee, D.; Marquess, D. G.; McGrane, P. L.; Meng, W.; Mucciaro, T. P.; Mühlebach, M.; Natchus, M. G.; Paulsen, H.; Rawlins, D. B.; Satkofsky, J.; Shuker, A. J.; Sutton, J. C.; Taylor, R. E.; Tomooka, K. The Pinene Path to Taxanes. 5. Stereocontrolled Synthesis of A Versatile Taxane Precursor. *J. Am. Chem. Soc.* **1997**, *119*, 2755.

11. Wender, P.; Badham, N.; Conway, S.; Floreancig, P.; Glass, T.; Houze, J.; Krauss, N.; Lee, D.; Marquess, D.; McGrane, P.; Meng, W.; Natchus, M.; Shuker, A.; Sutton, J.; Taylor, R. The Pinene Path to Taxanes. 6. A Concise Stereocontrolled Synthesis of Taxol. *J. Am. Chem. Soc.* **1997**, *119*, 2757.

12. Morihira, K.; Hara, R.; Kawahara, S.; Nishimori, T.; Nakamura, N.; Kusama, H.; Kuwajima, I. Enantioselective Total Synthesis of Taxol. *J. Am. Chem. Soc.* **1998**, *120*, 12980.

13. Mukaiyama, T.; Shiina, I.; Iwadare, H.; Saitoh, M.; Nishimura, T.; Ohkawa, N.; Sakoh, H.; Nishimura, K.; Tani, Y.; Hasegawa, M.; Yamada, K.; Saitoh, K. Asymmetric Total Synthesis of Taxol. *Chem. Eur. J.* **1999**, *5*, 121.

14. Kanda, Y.; Nakamura, H.; Umemiya, S.; Puthukanoori, R. K.; Appala, V. R. M.; Gaddamanugu, G. K.; Parasellia, B. R.; Baran, P. S. Two-Phase Synthesis of Taxol. *J. Am. Chem. Soc.* **2020**, *142*, 10526.

15. Nelson, T. J.; Sun, M.-K.; Lim, C.; Sen, A.; Khan, T.; Chirila, F. V.; Alkon, D. L. Bryostatin Effects on Cognitive Function and PKCε in Alzheimer's Disease Phase IIa and Expanded Access Trials. *J. Alzheimer's Dis.* **2017**, *58*, 521.

16. Kortmansky, J.; Schwartz, G. K. Bryostatin-1: A Novel PKC Inhibitor in Clinical Development. *Cancer Investig.* **2003**, *21*, 924.

17. Hammond, C.; Shi, Y.; Mena, J.; Tomic, J.; Cervi, D.; He, L.; Millar, A. E.; DeBenedette, M.; Schuh, A. C.; Baryza, J. L.; Wender, P. A.; Radvanyi, L.; Spaner, D. E. Effect of Serum and Antioxidants on the Immunogenicity of Protein Kinase C-Activated Chronic Lymphocytic Leukemia Cells. *J. Immunother.* **2005**, *28*, 28.

18. Bullen, C. K.; Laird, G. M.; Durand, C. M.; Siliciano, J. D.; Siliciano, R. F. New *ex vivo* approaches distinguish effective and ineffective single agents for reversing HIV-1 latency *in vivo. Nat. Med.* **2014**, *20*, 425.

19. Gutiérrez, C.; Serrano-Villar, S.; Madrid-Elena, N.; Pérez-Elías, M.; Martín, M.; Barbas, C.; Ruipérez, J.; Muñoz, E.; Muñoz-Fernández, M.; Castor, T.; Moreno, S. Bryostatin-1 for latent virus reactivation in HIV-infected patients on antiretroviral therapy. *AIDS* **2016**, *30*, 1385.

20. Schaufelberger, D. E.; Koleck, M. P.; Beutler, J. A.; Vatakis, A. M.; Alvarado, A. B.; Andrews, P.; Marzo, L. V.; Muschik, G. M.; Roach, J.; Ross, J. T.; Lebherz, W. B.; Reeves, M. P.; Eberwein, R. M.; Rodgers, L. L.; Testermen, R. P. The Large-Scale Isolation of Bryostatin 1 from *Bugula neritina* Following Current Good Manufacturing Practices. *J. Nat. Prod.* **1991**, *54*, 1265.

21. Keck, G. E.; Poudel, Y. B.; Cummins, T. J.; Rudra, A.; Covel, J. A. Total Synthesis of Bryostatin 1. *J. Am. Chem. Soc.* **2011**, *133,* 744.

22. Wender, P. A.; Hardman, C. T.; Ho, S.; Jeffreys, M. S.; Maclaren, J. K.; Quiroz, R. V.; Ryckbosch, S. M.; Shimizu, A. J.; Sloane, J. L.; Stevens, M. C. Scalable synthesis of bryostatin 1 and analogs, adjuvant leads against latent HIV. *Science* **2017**, *358*, 218.

23. Robinson, R. LXIII. — A synthesis of tropinone. *J. Chem. Soc.* **1917**, *111*, 762.

24. Yagi, S. *Daphniphyllum* Alkaloid. *Kyoto Igaku Zasshi* **1909**, *111*, 208.

25. Chattopadhyay, A. K.; Hanessian, S. Recent progress in the chemistry of daphniphyllum alkaloids. *Chem. Rev.* **2017**, *117*, 4104.

26. Piettre, S.; Heathcock, M. C.; Biomimetic Total Synthesis of *Proto*-Daphniphylline. *Science*. **1990**, *248*, 1532.

27. Pepper, H. P.; Lam, H. C.; Bloch, W. M.; George, J. H. Biomimetic Total Synthesis of (±)-Garcibracteatone. *Org. Lett.* **2012**, *14*, 5162.

28. Chhetri, W. B.; Lavoie, S.; Sweeney-Jones, A. M.; Kabanek, J. Recent trends in the structural revision of natural products. *Nat. Prod. Rep.,* **2018**, *35*, 514.

29. Nicolaou, K. C.; Snyder, S. A. Chasing Molecules That Were Never There: Misassigned Natural Products and the Role of Chemical Synthesis in Modern Structure Elucidation. *Angew. Chem. Int. Ed.* **2005**, *44*, 1012.

30. Sullivan, B.; Djura, P.; McIntyre, D. E.; Faulkner, D. J. Antimicrobial constituents of the sponge *Siphonodictyon coralliphagum. Tetrahedron* **1981**, *37*, 979.

31. Sullivan, B. W.; Faulkner, D. J.; Matsumoto, G. K.; He, C.-H.; Clardy, J. Metabolites of the burrowing sponge *Siphonodictyon coralliphagum. J. Org. Chem*. **1986**, *51*, 4568.

32. Marion, F.; Williams, D. E.; Patrick, B. O.; Hollander, I.; Mallon, R.; Kim, S. C.; Roll, D. M.; Feldberg, L.; Van Soest, R.; Andersen, R. Liphagal, a Selective Inhibitor of PI3 Kinase α Isolated from the Sponge *Aka coralliphaga*: Structure Elucidation and Biomimetic Synthesis. *J. Org. Lett*. **2006**, *8*, 321.

33. Markwell-Heys, A. W.; Kuan, K. K. W.; George, J. H. Total Synthesis and Structure Revision of (−)-Siphonodictyal B and its Biomimetic Conversion into (+)-Liphagal. *Org. Lett*. **2015**, *17*, 4228.

34. da Cunha, E. V. L.; Armstrong, J. A.; Gray, A. I.; Hockless, D. C. R.; Waterman, P. G.; White, A. H. 3-Monoterpenyl 2,4-Dioxygenated Quinoline Alkaloids From the Aerial Parts of *Eriostemon australasius* subsp. *banksii* (Rutaceae). *Aust. J. Chem.* **1993**, *46*, 1507.

35. Coleman, M. A.; Burchill, L.; Sumby, C. J.; George, J. H. Biomimetic Synthesis Enables the Structure Revision of Furoerioaustralasine. *Org. Lett.* **2019**, *21*, 8776.

36. Riveira, M. J.; La-Venia, A.; Mischne, M. P. Pericyclic Cascade toward Isochromenes: Application to the Synthesis of Alkaloid Benzosimuline. *J. Org. Chem.* **2016**, *81*, 7977.

37. Li, Y.; Niu, S.; Sun, B.; Liu, S.; Liu, X.; Che, Y. Cytosporolides A−C, Antimicrobial Meroterpenoids with a Unique Peroxylactone Skeleton from *Cytospora* sp. *Org. Lett.* **2010**, *12*, 3144.

38. Deyrup, S. T.; Swenson, D. C.; Gloer, J. B.; Wicklow, D. T. Caryophyllene Sesquiterpenoids from a Fungicolous Isolate of *Pestalotiopsis disseminata*. *J. Nat. Prod.* **2006**, *69*, 608.

39. Lawrence, A. L.; Adlington, R. M.; Baldwin, J. E.; Lee, V.; Kershaw, J. A.; Thompson, A. L. A Short Biomimetic Synthesis of the Meroterpenoids Guajadial and Psidial A. *Org. Lett*. **2010**, *12*, 1676.

40. Spence, J. T. J.; George, J. H. Structural Reassignment of Cytosporolides A-C via Biomimetic Synthetic Studies and Reinterpretation of NMR. *Org. Lett*. **2011**, *13*, 5318.

41. Takao, K.; Noguchi, S.; Sakamoto, S.; Kimura, M.; Yoshida, K.; Tadano, K. Total Synthesis of (+)-Cytosporolide A via a Biomimetic Hetero-Diels−Alder Reaction. *J. Am. Chem. Soc.* **2015**, *137*, 15971.

42. Fries, K.; Kann, K. I. Ueber die Einwirkung von Brom und von Chlor auf Phenole: Substitutionsproducte, Pseudobromide und Pseudochloride. Ueber *o*-Pseudohalogenide und o-Methylenchinone aus *o*-Oxymesitylalkohol. *Liebigs Ann. Chem*. **1907**, *353*, 335.

43. Amouri, H.; Besace, Y.; Le Bras, J.; Vaissermann, J. General Synthesis, First Crystal Structure, and Reactivity of Stable *o*-Quinone Methide Complexes of Cp*Ir. *J. Am. Chem. Soc*. **1998**, *120*, 6171.

44. Doria, F.; Richter, S. N.; Nadai, M.; Colloredo-Mels, S.; Mella, M.; Palumbo, M.; Freccero, M. BINOL− Amino Acid Conjugates as Triggerable Carriers of DNA-Targeted Potent Photocytotoxic Agents. *J. Med. Chem.* **2007**, *50*, 6570.

45. Di Antonio, M.; Doria, F.; Richter, S. N.; Bertipaglia, C.; Mella, M.; Sissi, C.; Palumbo, M.; Freccero, M. Quinone methides tethered to naphthalene diimides as selective G-quadruplex alkylating agents. *J. Am. Chem. Soc.* **2009**, *131*, 13132.

46. Wang, H.; Rokita, S. E. Dynamic Cross-Linking Is Retained in Duplex DNA after Multiple Exchange of Strands. *Angew. Chem., Int. Ed*. **2010**, 49, 5957.

47. Van De Water, R. W.; Pettus, T. R. R. o-Quinone methides: intermediates underdeveloped and underutilized in organic synthesis. *Tetrahedron* **2002**, *58*, 5367.

48. Willis, N. J.; Bray, C. D. *ortho*-Quinone Methides in Natural Product Synthesis. *Chem. Eur. J.* **2012**, *18*, 9160.

49. Jurd, L. Quinones and quinone-methides—I: Cyclization and dimerisation of crystalline *ortho*-quinone methides from phenol oxidation reactions. *Tetrahedron* **1977**, *33*, 163.

50. Jurd, L.; Roitman, J. N. Quinones and quinone methides—II: cyclization and hydration reactions of 2-cinnamyl-5-methoxy-1,4-benzoquinones. *Tetrahedron* **1978**, *34*, 57.

51. Jurd, L.; Roitman, J. N.; Wong, R. Y. Quinones and quinone methides—IV: Dimerization reactions of 2-phenylmethyl-5-methoxy-1,4-benzoquinones. *Tetrahedron* **1979**, *35*, 1041.

52. Jurd, L.; Roitman, J. N. Quinones and quinone methides—V: Further rearrangements of the dimer from 5-methoxy-2-(4-methoxyphenylmethyl)-1,4-benzoquinone. *Tetrahedron* **1979**, *35*, 1567.

53. Chen, Y.; Steinmetz, M. G. Photoactivation of Amino-Substituted 1,4-Benzoquinones for Release of Carboxylate and Phenolate Leaving Groups Using Visible Light. *J. Org. Chem*. **2006**, *71*, 6053.

54. Nayak, M. K.; Wan, P. Direct and water-mediated excited state intramolecular proton transfer (ESIPT) from phenol OH to carbon atoms of extended *ortho*-substituted biaryl systems. *Photochem. Photobiol. Sci.* **2008**, *7*, 1544.

55. Batsomboon, P.; Phakhodee, W.; Ruchirawat, S.; Ploypradith, P. Generation of *ortho*-Quinone Methides by *p*-TsOH on Silica and Their Hetero-Diels−Alder Reactions with Styrenes. *J. Org. Chem.* **2009**, *74*, 4009.

56. Marsini, M. A.; Huang, Y.; Lindsey, C. C.; Wu, K.-L.; Pettus, T. R. R. Rapid Syntheses of Benzopyrans from o-OBOC Salicylaldehydes and Salicyl Alcohols: A Three-Component Reaction. *Org. Lett.* **2008**, *10*, 1477.

57. Uyanik, M.; Nishioka, K.; Kondo, R.; Ishihara, K. Chemoselective oxidative generation of *o*-quinone methides and tandem transformations. *Nat. Chem.* **2020**, *12*, 353.

58. Mejorado, L. H.; Pettus, T. R. R. Total synthesis of (+)-rishirilide B: development and application of general processes for enantioselective oxidative dearomatization of resorcinol derivatives. *J. Am. Chem. Soc.* **2006**, *128*, 15625.

59. Spence, J. T.; George, J. H. Biomimetic total synthesis of *ent*-penilactone A and penilactone B. *Org. Lett*. **2013**, *15*, 3891.

60. Spence, J. T.; George, J. H. Total synthesis of peniphenones A-D via biomimetic reactions of a common *o*-quinone methide intermediate. *Org. Lett*. **2015**, *17*, 5970.

61. Aoki, S.; Watanabe, Y.; San-Agawa, M.; Setiawan, A.; Kotoku, N.; Kobayashi, M. Cortistatins A, B, C, and D, Antiangiogenic Steroidal Alkaloids, from the Marine Sponge *Corticium simplex*. *J. Am. Chem. Soc.* **2006**, *128*, 3148.

62. Shenvi, R. A.; Guerrero, C. A.; Shi, J.; Li, C.-C.; Baran, P. S. Synthesis of (+)-Cortistatin A. *J. Am. Chem. Soc.* **2008**, *130*, 7241.

63. Nicolaou, K. C.; Sun, Y.-P.; Peng, X.-S.; Polet, D.; Chen, D. Y.-K. Total Synthesis of (+)-Cortistatin A. *Angew. Chem., Int. Ed.* **2008**, *47*, 7310.

64. Flyer, A. N.; Si, C.; Myers, A. G. Synthesis of cortistatins A, J, K and L. *Nat. Chem.* **2010**, *2*, 886.

65. Dai, M.; Danishefsky, S. J. A concise synthesis of the cortistatin core. *Tetrahedron Lett*. **2008**, *49*, 6610.

66. Lumb, J.-P.; Trauner, D. Pericyclic Reactions of Prenylated Naphthoquinones: Biomimetic Syntheses of Mollugin and Microphyllaquinone. *Org. Lett.* **2005**, *7*, 5865.

67. Burchill, L.; George, J. H. Total Synthesis of Rhodonoids A, B, E, and F, Enabled by Singlet Oxygen Ene Reactions. *J. Org. Chem*. **2020**, *85*, 2260.

68. Day, A. J.; Lam, H. C.; Sumby, C. J.; George, J. H. Biomimetic Total Synthesis of Rhodonoids C and D, and Murrayakonine D. *Org. Lett*. **2017**, *19*, 2463.

69. Wu, H.; Hsung, R. P.; Tang, Y. Total Syntheses of (±)-Rhodonoids A and B and C12-*epi*-Rhodonoid B. *J. Org. Chem.* **2017**, *82*, 1545.

70. Chapman, O. L.; Engel, M. R.; Springer, J. P.; Clardy, J. C. Total Synthesis of Carpanone. *J. Am. Chem. Soc.* **1971**, *93*, 6696.

71. Adlington, R. M.; Baldwin, J. E.; Pritchard, G. J.; Williams, A. J.; Watkin, D. J. A Biomimetic Synthesis of Lucidene. *Org. Lett*. **1999**, *1*, 1937.

72. Lumb, J. P.; Choong, K. C.; Trauner, D. *ortho*-Quinone Methides from *para*-Quinones: Total Synthesis of Rubioncolin B. *J. Am. Chem. Soc.* **2008**, *130*, 9230.

73. Ma, S.-G.; Gao, R.-M.; Li, Y.-H.; Jiang, J.-D.; Gong, N.-B.; Li, L.; Lü, Y.; Tang, W.-Z.; Liu, Y.-B.; Qu, J.; Lü, H.-N.; Li, Y.; Yu, S.-S. Antiviral Spirooliganones A and B with Unprecedented Skeletons from the Roots of *Illicium oligandrum*. *Org. Lett.* **2013**, *15*, 4450.

74. Wei, L.; Xiao, M. X.; Xie, Z. X. Total Syntheses of (−)-Spirooliganones A and B. *Org. Lett*. **2014**, *16*, 2784.

75. Song, L.; Yao, H.; Tong, R. Biomimetic Asymmetric Total Syntheses of Spirooliganones A and B. *Org. Lett.* **2014**, *16*, 3740.

76. Zhao, N.; Ren, X.; Ren, J.; Lü, H.; Ma, S.; Gao, R.; Li, Y.; Xu, S.; Li, L.; Yu, S. Total Syntheses of (−)-Spirooliganones A and B and Their Diastereoisomers: Absolute Stereochemistry and Inhibitory Activity against Coxsackie Virus B3. *Org. Lett.* **2015**, *17*, 3118.

77. Duffield, A. M.; Jefferies, P. R.; Maslen, E. N.; Rae, A. I. M. The Structure of Bruceol. *Tetrahedron* **1963**, *19*, 593.

78. Ghisalberti, E. L.; Jefferies, P. R.; Raston, C. L.; Skelton, B. W.; Stuart, A. D.; White, A. H. Structural Studies in the Bruceol System. *J. Chem. Soc., Perkin Trans. 2* **1981**, 583.

79. Gray, A. I.; Rashid, M. A.; Waterman, P. G. NMR Assignments for the Pentacyclic Coumarins Bruceol and Deoxybruceol. *J. Nat. Prod.* **1992**, *55*, 681.

80. Day, A. J.; Lee, J. H. Z.; Phan, Q. D.; Lam, H. C.; Ametovski, A.; Sumby, C. J.; Bell, S. G.; George, J. H. Biomimetic and Biocatalytic Synthesis of Bruceol. *Angew. Chem., Int. Ed.* **2019**, *58*, 1427.

81. Baran, P. S. Natural Product Total Synthesis: As Exciting as Ever and Here To Stay. *J. Am. Chem. Soc.* **2018**, *140*, 4751.

Chapter 2

The Biomimetic Total Synthesis and Structure Revision of Littordials E and F, and Drychampone B

2.1 Introduction

2.1.1 The Chemistry of (−)-Caryophyllene

(−)-Caryophyllene (also called (−)-*trans*-caryophyllene or *β*-caryophyllene, **2.1**, Figure 2.1) is a sesquiterpene natural product found in several different species of plants and fungi and plays a critical role in the chemistry of numerous natural products. Caryophyllene possesses a bicyclic structure with a 9-membered ring *trans*-fused to cyclobutane, as well as two alkene functional groups. These alkenes are responsible for the reactivity of caryophyllene, with the endocyclic $\Delta^{4,5}$ alkene being more reactive than the external alkene as a result of increased substitution and ring strain.[1]

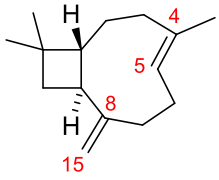

2.1: (–)-caryophyllene

Figure 2.1: The structure of (−)-caryophyllene (**2.1**).

Molecular mechanics calculations and ^{13}C NMR studies have determined that caryophyllene can adopt four possible low energy conformations in solution, denominated *αα*, *αβ*, *βα* and *ββ*. These conformers contrast in the relative disposition of their exocyclic alkene and vinyl methyl moieties (Figure 2.2). From these studies, the ratio between conformations *αα* /*βα* /*ββ* in solution was calculated as 48:28:24 with *αβ* being the only unpopulated conformer of caryophyllene.[2] The conformational flexibility of **2.1** is an important intrinsic feature of the molecule as it governs the stereochemistry of its reaction products.

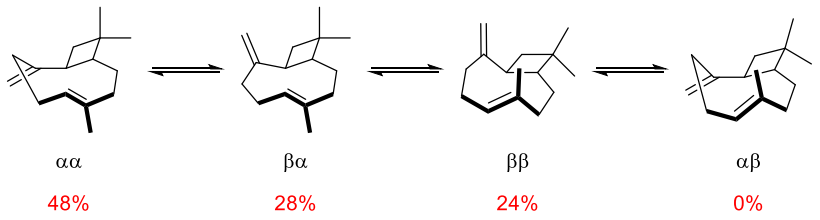

Figure 2.2: Relative populations of (−)-caryophyllene (**2.1**) conformers in solution.[2]

Naturally, caryophyllene's abundance and predisposed reactivity has made it a notable component of many terpenoid natural products. Chemists have made deft use of caryophyllene as a reagent in many total syntheses, a few of which are described further.

2.1.2 Caryophyllene in Natural Product Synthesis

Psiguadial B (**2.9**) is one of many caryophyllene derived meroterpenoid natural products isolated from the leaves of *Psidium guajava* (the common guava) and shows potent inhibitory activity against human HepG2 cells.[3] The bicyclo[4.3.1]decane ring *trans*-fused to cyclobutane (highlighted in red, Scheme 2.1) presents a significant synthetic obstacle. Construction of this complex motif would become the focus of the first total synthesis of **2.9**, achieved in 2016 by the Reisman group in 16 steps using an abiotic approach (not shown).[4] Cramer and co-workers speculated that biosynthetically, **2.9** could be derived from caryophyllene (**2.1**) and an appropriate phloroglucinol derived *ortho*-quinone methide intermediate. Cramer postulated that the bicyclo[4.3.1]decane ring could be formed by an acid-catalysed rearrangement of caryophyllene, resulting in a framework which bears a striking resemblance to caryolanol, a known terpene co-isolated with **2.1** from Brazilian *Cangerana* oil.[5] Using DMEDA as a base catalyst and HFIP as the solvent, psiguadial B was formed in 8% yield in a one-pot reaction between diformylphloroglucinol (**2.2**), benzaldehyde (**2.3**), and caryophyllene (**2.1**). Related products guajadial (**2.10**), psidial A (**2.11**), and a diastereomer **2.12**, were also formed *via* a [4+2] cycloaddition. Experimental observations and DFT calculations support a Michael addition/cyclization cascade as a plausible biosynthetic pathway in the synthesis of psiguadial B (Scheme 2.1).[6]

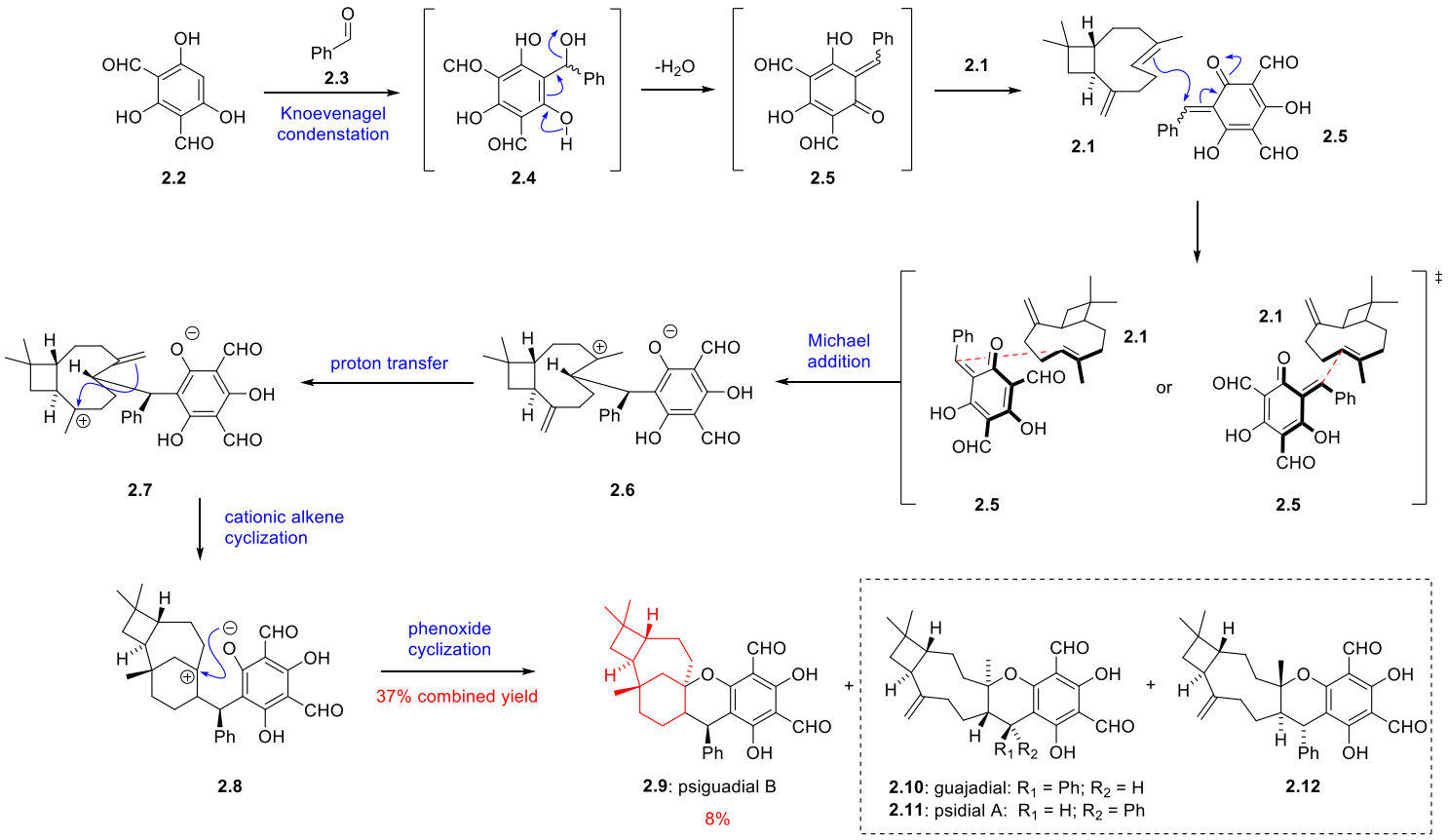

Scheme 2.1: Cramer's biomimetic synthesis of psiguadial B (**2.9**).[6]

Plant species of the Myrtaceae family have provided organic chemists with numerous meroterpenoids of varying biological activities. A common feature of these species is the presence of a *β*-triketone moiety derived from syncarpic acid (**2.14**, highlighted in green Scheme 2.2 but can also be seen as **2.22** in Scheme 2.3). In their studies of this family of compounds, the Porco group reported the isolation and characterization of rhodomyrtusials A and C (**2.15** and **2.16**, the also isolated rhosomyrtusial B is not shown), novel caryophyllene-derived meroterpenoids from *Rhodomyrtus tomentosa* (Scheme 2.2). Additionally, two new biogenetically related isomers, rhotomentodiones A and B (**2.17** and **2.18**), and two known analogues, tomentodiones Q and R (**2.19** and **2.20**), were also obtained from the plant material (Scheme 2.2).[7]

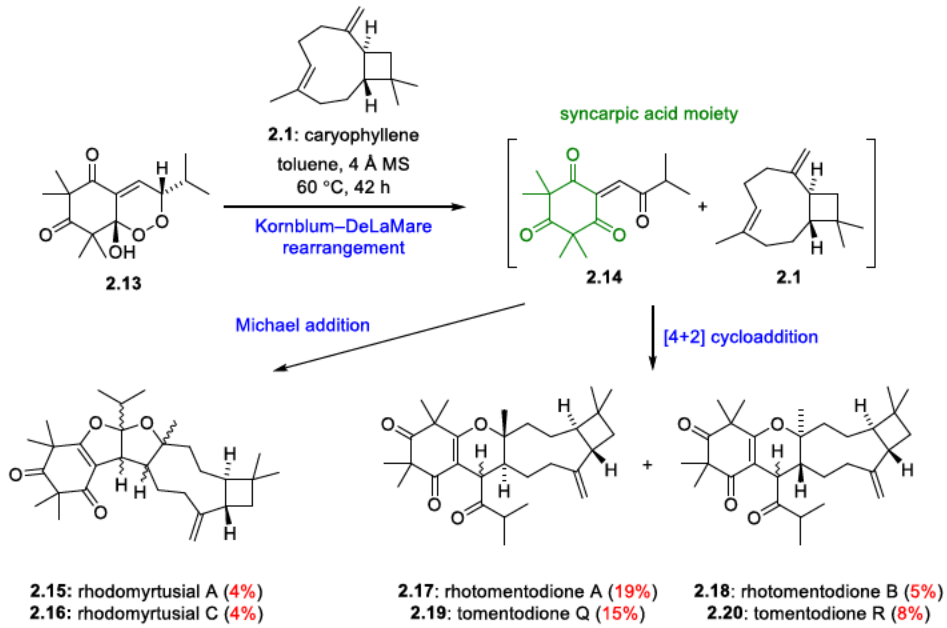

Scheme 2.2: Porco and Liu's biomimetic synthesis of compounds **2.15–2.20**.[7]

Rhodomyrtusials A and C consist of a unique 6/5/5/9/4 fused *bis*-furan ring system, motivating a desire for further synthetic studies. All isolated natural products were proposed to form *via* the reaction of a common enetrione intermediate (**2.14**) with **2.1**. Compounds **2.15** and **2.16** were hypothesized to form *via* a stepwise Michael addition pathway, whereas **2.17**–**2.20** were speculated to be the products of a [4+2] cycloaddition. To validate their biosynthetic speculation, the Porco group carried out biomimetic syntheses of their newly isolated natural products. The desired enetrione intermediate was formed *in situ* by a Kornblum-DeLaMare rearrangement of endoperoxide **2.13**. A hetero-Diels–Alder reaction between **2.14** and **2.1** affords compounds **2.17**–**2.20** as a mixture of diastereomers. The stepwise Michael reaction of the *βα* conformer of caryophyllene in a *re*-face approach affords rhodomyrtusial A (**2.15**) in 4% yield. Rhodomyrtusial C (**2.16**) is generated in 4% yield via the same stepwise Michael reaction pathway but reacts with the *ββ* conformer of caryophyllene in a *si*-face approach.[7] This study is great showcase of caryophyllene's versatility in synthesis; in a single step six natural products are formed from a common intermediate *via* two different pathways, leading to two sets of isomers with distinct structural features.

Continuing with natural products of *Rhodomyrtus tomentosa*, rhodomentones A and B (**2.25** and **2.26**) display an unprecedented oxa-spiro[5.8]tetradecadiene structure (Scheme 2.3). This fascinating architecture was proposed by Qiu to be the result of a caryophyllene cycloaddition via its less reactive exocyclic alkene, rather than the more reactive $\Delta^{4,5}$ alkene that has been discussed up until this point. The structure of **2.25** was determined via X-ray crystallography, confirming the presence of the oxa-spirocycle motif. Furthermore, rhodomentone B (**2.26**) differs from **2.25** only in the presence of a diol located at C-4/C-5. The absolute configurations of these hydroxyl groups were determined by CD spectroscopy, inferring an *anti*-relationship. Biosynthetically, these vicinal diols could be formed by the epoxidation and subsequent H_2O induced ring opening of rhodomentone A (**2.25**). To support their characterization of these natural products, Qiu and co-workers carried out total syntheses of **2.25** and **2.26**. Starting from acetylphloroglucinol (**2.21**), methylation and deacetylation affords syncarpic acid **2.22** in 67% yield. Proline-catalysed Knoevenagel condensation of **2.22** with isovaleraldehyde (**2.23**) generates key intermediate **2.24** in near quantitative yields, which was successfully characterized by NMR. Triketone **2.24** undergoes a biomimetic Diels–Alder reaction with caryophyllene to afford rhodomentone A (**2.25**) in 27% yield.[8] Despite assigning an *anti*-relationship to the hydroxyl groups of **2.26**, the authors inexplicably employ Upjohn dihydroxylation conditions in their conversion of isolated **2.25** to **2.26**; conditions which produce a *syn*-diol rather than the *anti*-diol they have assigned. Their explanation for the use of these conditions is not present in the paper, made more perplexing by the fact that their proposed epoxidation/ring-opening sequence could have been easily investigated. These discrepancies could be indicative of a misassigned structure and may warrant further investigation.

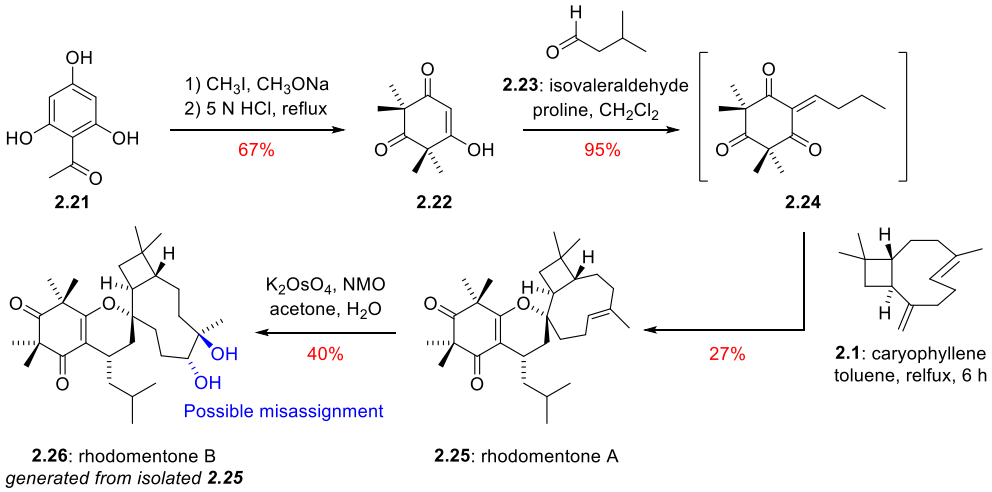

Scheme 2.3: Qiu's synthesis of rhodomentones A (**2.25**) and B (**2.26**).[8]

2.1.3 The Chemistry of Humulene

Humulene (**2.27**) is a naturally occurring cyclic sesquiterpene found in *Humulus lupus*, the common hop, and can constitute up to 40% of the plant's essential oil make up.[9] Aside from giving beer its characteristic flavour, humulene and its oxidation products are found as fundamental components of many natural products, a few of which will be discussed further in this chapter. The reactivity of humulene originates from its three alkenes, which can undergo regioselective functionalization. Fujita et al. set out to determine the structures of humulene's oxidation products using a crystalline sponge method.[10] Treatment of humulene with one equivalent of *m*-CPBA yielded epoxides **2.28**–**2.30** in 75, 14 and 5% yield respectively. Using two equivalents of oxidant formed the diepoxide **2.31** exclusively and confirmed the order of alkene reactivity as $\Delta^{1,2} > \Delta^{8,9} > \Delta^{4,5}$ (Scheme 2.4).

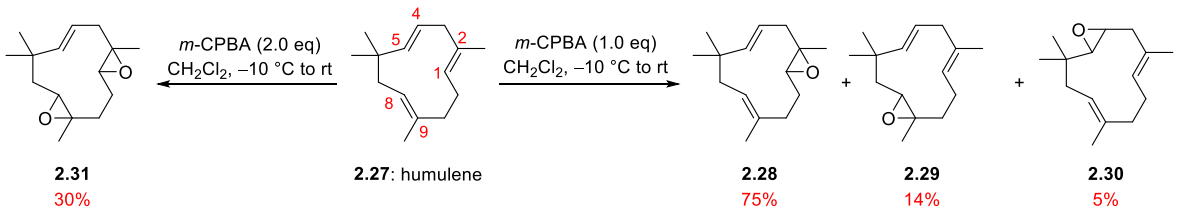

Scheme 2.4: Fujita's epoxidation of humulene (**2.27**).[10]

To further elucidate its unique regioselectivity, Hermans and co-workers performed DFT calculations and temperature dependent NMR experiments in a full structural analysis study of humulene.[11] Four conformations of humulene were reported, each of which was chiral, leading to a total of eight possible humulene conformers, in line with previous work done by Shirahama.[12] Hermans et al. note that the electron density of the humulene alkenes, thus their reactivity toward electrophiles, is substantially affected by hyperconjugation of the allylic $\sigma_{C\text{-}C}$ orbital. This hyperconjugation is only possible when these allylic orbitals are perpendicular to the alkene. The calculated relative reactivity shows the $\Delta^{1,2}$ alkene is more reactive than the $\Delta^{8,9}$ alkene by factor of 6.2, which is in good agreement with experimental data.[10] Humulene has seen extensive use in the field of total synthesis predominantly as a coupling partner in [4+2] cycloaddition reactions.

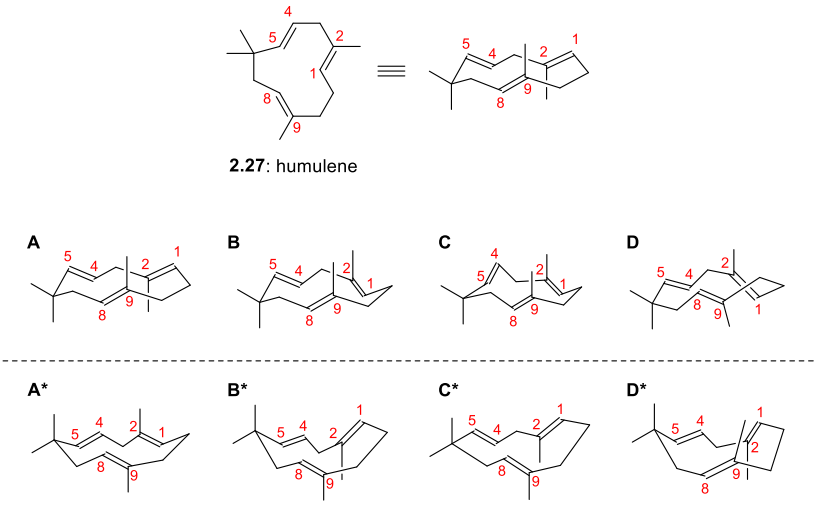

Figure 2.3: The structure of humulene (**2.27**) and its conformers.[11,12]

2.1.4 Humulene in Natural Product Synthesis

As discussed in Chapter 1 (Scheme 1.18), Baldwin's seminal synthesis of lucidene is an excellent showcase of humulene's regioselectivity.[13] In another work, Baldwin and co-workers carried out an investigation into the tropolone family of natural products which include pycnidione (**2.32**), eupenifeldin (**2.33**) and epolone B (**2.34**) (Figure 2.4).[14] These three natural products feature identical tropolone rings (highlighted in red) all connected to sesquiterpene backbone. The addition of two equivalents of a tropolone derived *o*-QM to humulene would hopefully afford the desired natural product analogues with the correct regio- and stereoselectivity.

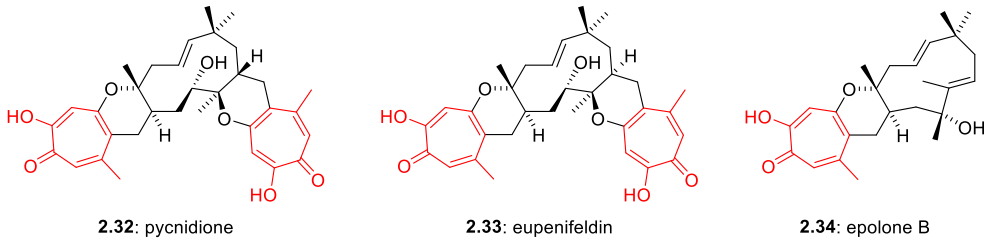

Figure 2.4: Structures of pycnidione (**2.32**), eupenifeldin (**2.33**), epolone B (**2.33**).

Protected tropolone **2.35** was synthesized in 5 steps from commercially available phthalic acid (Scheme 2.5). Heating **2.35** in a sealed tubed at 150 °C for 24 hours generated heterodiene **2.36**. Initially, **2.36** was trapped by methylcylcohexene (**2.37**) to test the feasibility of the cycloaddition. Gratifyingly, a hetero-Diels–Alder reaction between **2.36** and the **2.37** generates adduct **2.38** in good yield. In the presence of humulene, **2.36** undergoes an initial cycloaddition to produce monosubstituted compound **2.39**. A second cycloaddition proved less facile most likely due to steric factors. Nonetheless, in the presence of excess **2.27** a second hetero-Diels–Alder reaction is achieved, giving analogue **2.40** in 20% yield.

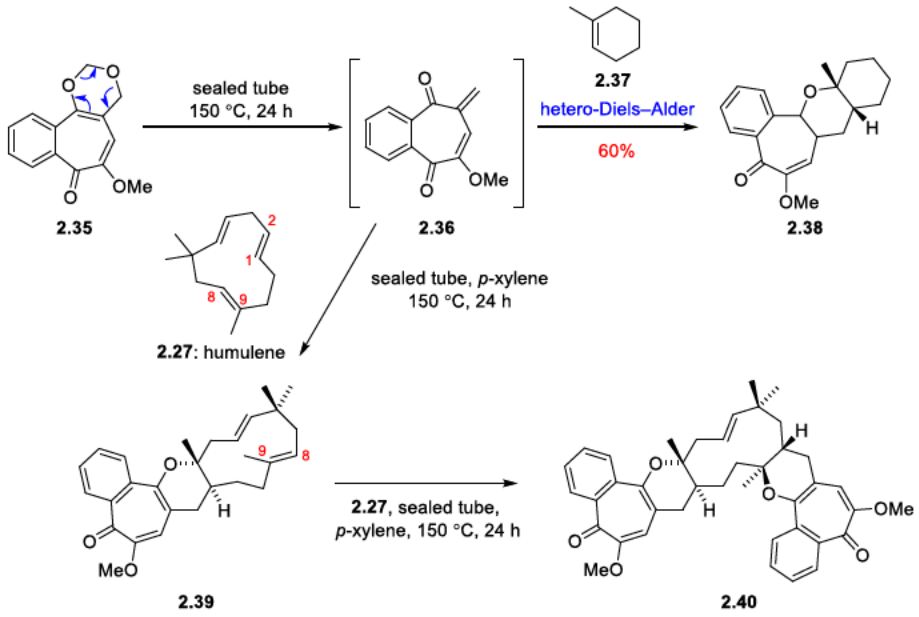

Scheme 2.5: Baldwin's biomimetic synthesis of tropolone analogue **2.40**.[14]

The George group has made use of humulene in their biomimetic syntheses of the hyperjapone and hyperjaponol family of meroterpenoid natural products (Scheme 2.6).[15] The simplest of these compounds, hyperjapone A (**2.43**), is unmistakably formed *via* a hetero-Diels–Alder reaction between humulene (**2.27**) and an *α,β*-unsaturated ketone species (**2.42**) derived from the natural product norflavesone (**2.41**). This reaction occurs regioselectively with respect to humulene, in line with Baldwin's previous studies.[13,14] The proposed biosynthesis of the hyperjaponols (Scheme 2.6 a. Hyperjaponols A and B not shown) is based upon hyperjapone A (**2.43**) acting as a common biosynthetic precursor. Hyperjaponol C (**2.48**), the most structurally complex of these molecules, elicited the greatest interest from the George group thanks to its intricate *trans*-isodaucane framework. This ornate architecture could theoretically be synthesized by a cyclization/alkyl shift sequence starting with epoxidation of **2.43** at the exposed face of the $\Delta^{8,9}$ alkene to form **2.44**. Subsequent acid-catalysed ring opening of this epoxide generates the key tertiary carbocation **2.45**, which is primed for the crucial biomimetic cascade. A stereoselective cation-alkene cyclization of **2.45** affords the secondary carbocation **2.46**. Finally, a stereospecific 1,2-alkyl shift generates tertiary carbocation **2.47** which, after deprotonation, produces hyperjaponol C (**2.48**). According to computational work done by Tantillo and co-workers,[16] these types of carbocation rearrangements in terpene biosynthesis tend to form *via* concerted processes, so it is likely that the rearrangement of **2.45** to **2.47** occurs in a single step.

The biomimetic synthesis of hyperjapone A (**2.43**) and hyperjaponol C (**2.48**) begins with the trimethylation of phloroglucinol (**2.49**) to give norflavesone (**2.41**) in 69% yield over two steps. The hetero-Diels–Alder reaction is achieved by oxidation of **2.41** using Ag_2O/TEMPO in the presence of humulene (**2.27**), furnishing hyperjapone A in 32% yield. The rearrangement cascade to give **2.48** starts with the epoxidation of **2.43** to give **2.50** in 76% yield. In the presence of *para*-toluenesulfonic acid, **2.50** is converted to the natural product hyperjaponol C (**2.48**) in 43% yield. The length of the synthesis can be reduced by telescoping these final two steps, epoxidation followed immediately by acid-catalysed ring opening in one-pot produces **2.48** in 34% yield (Scheme 2.6 b).

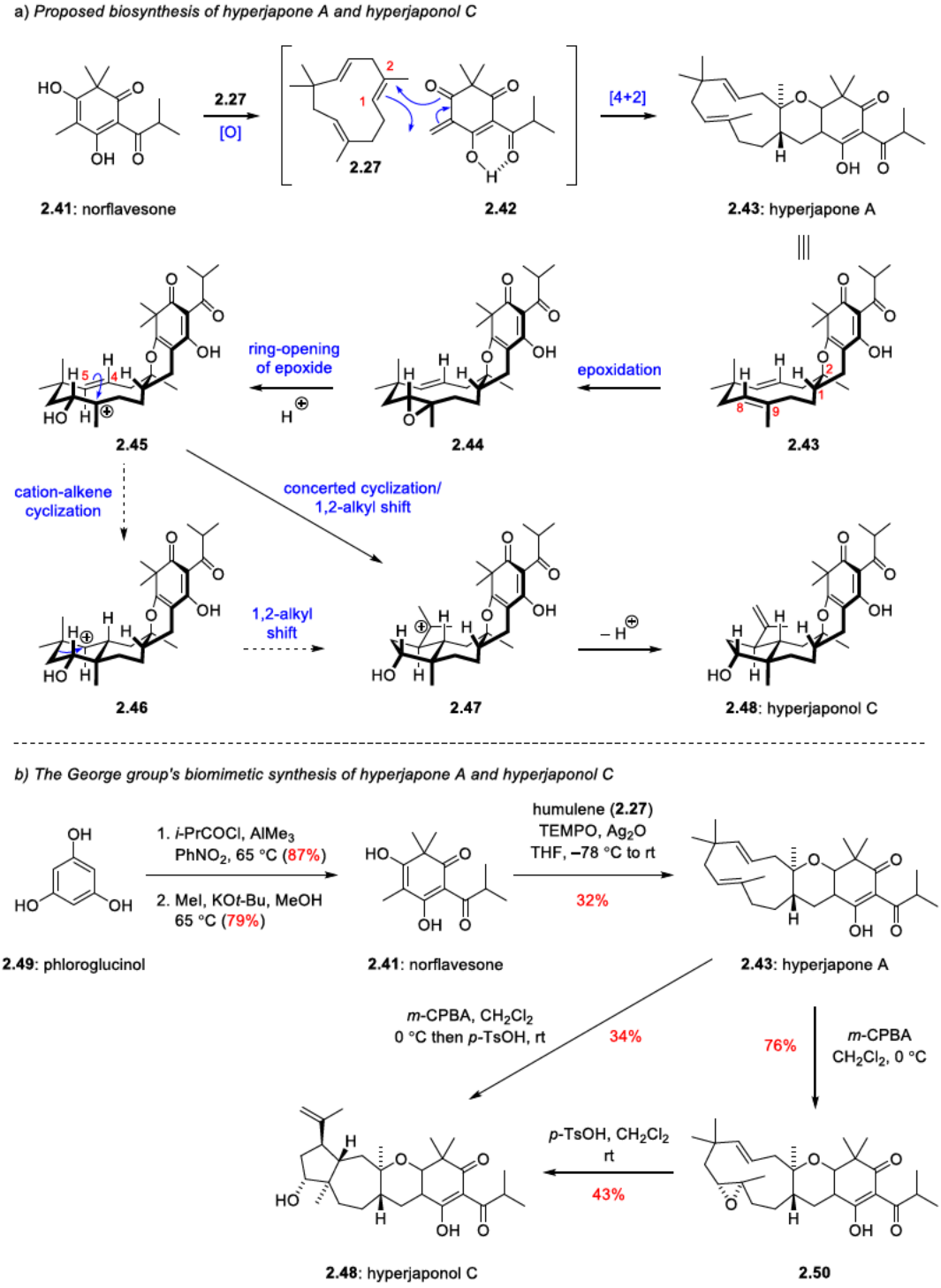

Scheme 2.6: a) The proposed biosynthesis of hyperjapone A (**2.43**) and hyperjaponol C (**2.48**) b) The biomimetic synthesis of **2.43** and **2.48** by the George group.[15]

Xenovulene A (**2.51**) is a sesquiterpenoid natural product isolated from *Acremonium strictum* and acts as a benzodiazepine inhibitor, binding to human GABA receptors.[17] Structurally analogous to **2.51** are sterhirsutins A and B (**2.52** and **2.53**) which were isolated from *Stereum hirsutum* a fungus located in the Tibetan Plateau. Sterhirsutins A and B show moderate antiproliferative activities against human myelogenous leukemia (K562) cells.[18] Despite originating from different fungal species, these compounds share 5/6/11 tricyclic cores with a sesquiterpene motif (highlighted in red) likely derived from humulene (Figure 2.5).

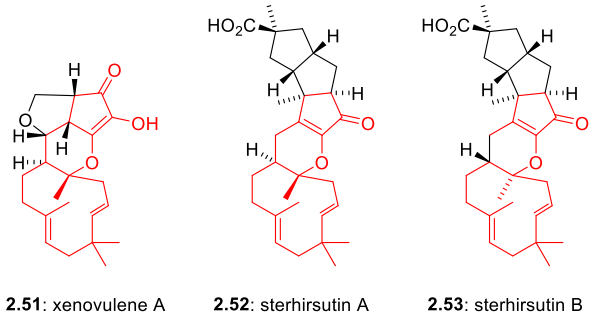

2.51: xenovulene A **2.52**: sterhirsutin A **2.53**: sterhirsutin B

Figure 2.5: The strucutures of xenovulene A (**2.51**) and sterhirsutins A and B (**2.52** and **2.53**).[17,18]

Kirschning et al. rationalized that the core of xenovulene and the sterhirsutins may be formed in nature by a cycloaddition between humulene and a ribose-derived vinyl ketone.[19] The requisite vinyl ketone **2.54** was arduously prepared in 10 steps from D-ribose for the key cycloaddition reaction (Scheme 2.7). Heating a solvent-free mixture of **2.54** and excess **2.27** at 150 °C for 5 days with subsequent TBAF-mediated deprotection afforded two diastereomers **2.55** and **2.56** in 51% combined yield, with **2.55** assigned as the xenovulene A core. A derivative of compound **2.55** (not shown) yielded crystals for X-ray diffraction analysis, confirming its structure. Investigations into the diastereoselectivity of the reaction by the authors suggest the *re*-face approach by **2.54** in the transition state is favoured due to minimised steric clash between the methyl group of humulene and the acetonide group of **2.54**. Finally, an acid-catalysed acetonide rearrangement of **2.55** and **2.56** yielded **2.57** and **2.58** respectively, in 65% combined yield.

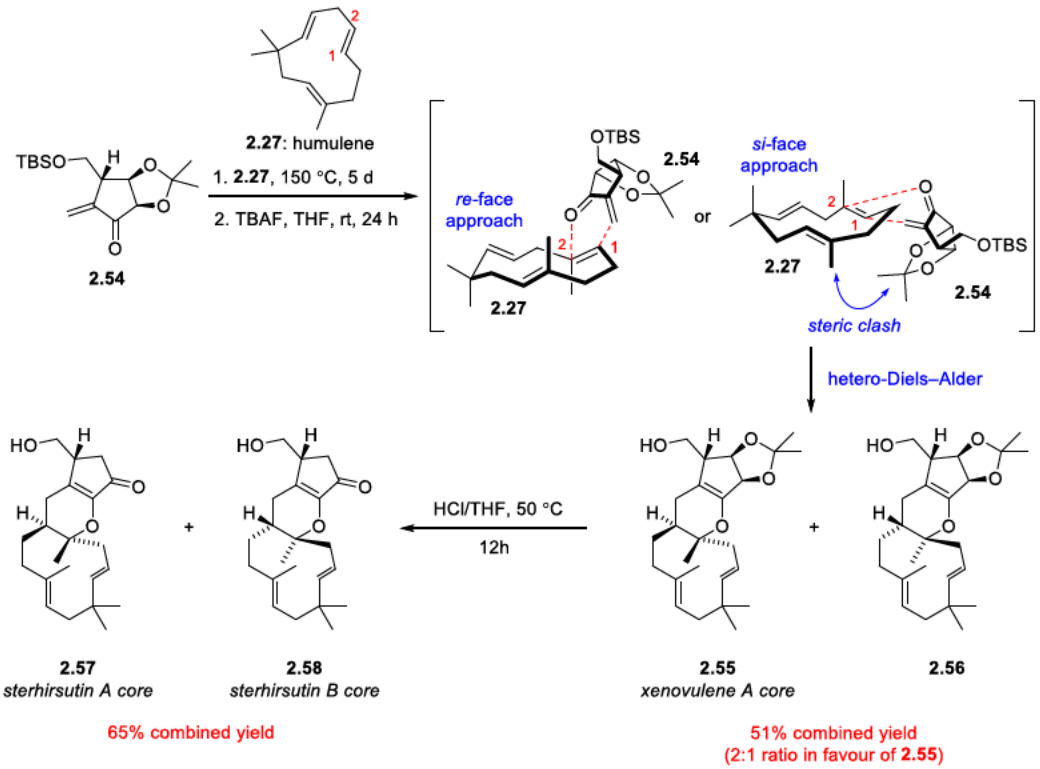

Scheme 2.7: Kirschning's biomimetic synthesis of the tricyclic cores of xenovulene A (**2.55**) and sterhirsutins A and B (**2.75** and **2.58**).[19]

2.2 Isolation of Littordials A–F

Littordials A–E (**2.59**–**2.64**, Figure 2.6) are phloroglucinol-derived meroterpenoid natural products isolated in 2019 from the leaves of *Psidium littorale*. Better known as the strawberry guava, this plant's edible fruits are widely popular due to their sweetness and high nutritious value.[20] A sixth natural product, Littordial F (**2.64**) was isolated from the same plant later that year.[21] Compounds **2.60**, **2.61**, **2.64** showed moderate cytotoxic activity against the MDA-MB-231 and B16 human cancer cell lines; **2.64** showed activity against the A549, B16, and HepG-2 cell lines.

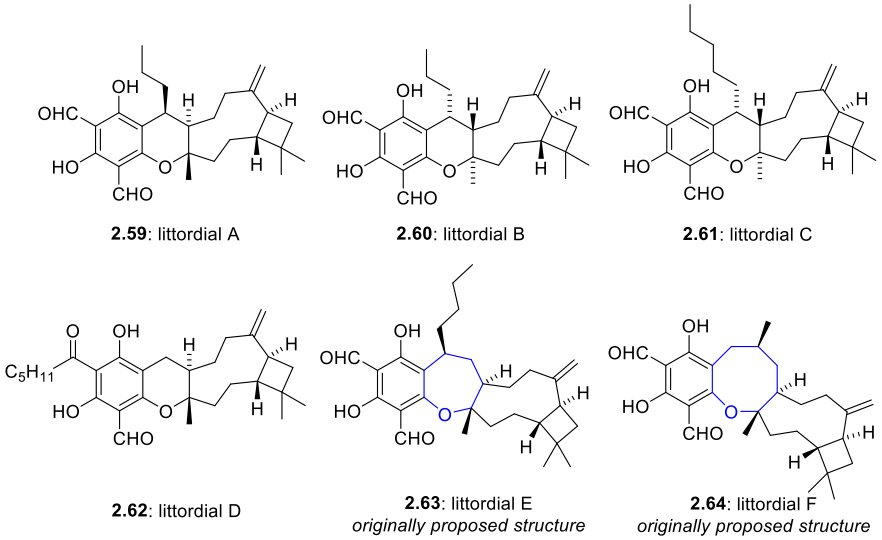

Figure 2.6: Littordials A–F (**2.59**–**2.64**), as assigned by Qu and Xu.[20,21]

Littordials A–D (**2.59**–**2.60**) all possess a 6/6/9/4 tetracyclic framework, which is presumably synthesized in nature via a reaction of (–)-caryophyllene (**2.1**) with a diformylphloroglucinol-derived coupling partner. This union could be achieved by a hetero-Diels–Alder reaction between an appropriate *o*-QM and the reactive $\Delta^{4,5}$ alkene of caryophyllene. There is strong literature precedent for this proposed biosynthesis, with compounds such as psiguajdianone,[22] myrtucommulones K and N[23] and guajadial and psidial A,[24] among others, having been synthesized through similar [4+2] cycloadditions. Of these natural products, we found littordials E (**2.63**) and F (**2.64**) to be of particular interest due to their uncommon structures, which feature seven- and eight membered rings respectively (highlighted in blue, Figure 2.6).

2.3 Proposed Biosynthesis of Littordials E and Littordial F

Though they still contained the same phloroglucinol and caryophyllene derived moieties as the other littordials, **2.63** and **2.64** were assigned unique 6/7/9/4 and 6/8/9/4 ring systems respectively. Qu and Xu rationalize that the proposed seven- and eight-membered rings of littordials E and F could be formed via an uncommon Michael addition between (–)-caryophyllene and a suitable phloroglucinol-derived *o*-QM.[19,20] Despite evidence suggesting caryophyllene's potential to undergo Michael additions,[6] we find the formation of the seven- and eight-membered rings of **2.63** and **2.64** in this manner to be biosynthetically implausible, leading us to believe that the structures of these compounds have been misassigned. Furthermore, the formation of diastereomeric natural products also suggests a non-enzymatically mediated biosynthesis with stereochemical configurations most likely derived from the isomeric complexity of the caryophyllene and *o*-QM reactants (these factors are discussed in the Computational Methods section, 2.4.5). The complexity of isolated compound spectra also makes assigning these compounds with full confidence a challenge, as extensive signal overlap may obscure key signals or in some cases suggest implausible correlations leading to erroneous structures.

Instead, we propose that littordials E and F are likely diastereomers of other littordial natural products (Figure 2.7). Specifically, we believe littordial E (**2.65**) is a diastereomer of littordial C (**2.61**) and that littordial F (**2.66**) is a diastereomer of littordials A and B (**2.59** and **2.60**). We propose that all these compounds may be readily synthesized via a hetero-Diels–Alder reaction between (–)-caryophyllene and *o*-QMs of varying alkyl side chain lengths. In the following sections, we will detail the biomimetic synthesis of these natural products as well as revising their originally proposed structures, all based on our biosynthetic speculation.

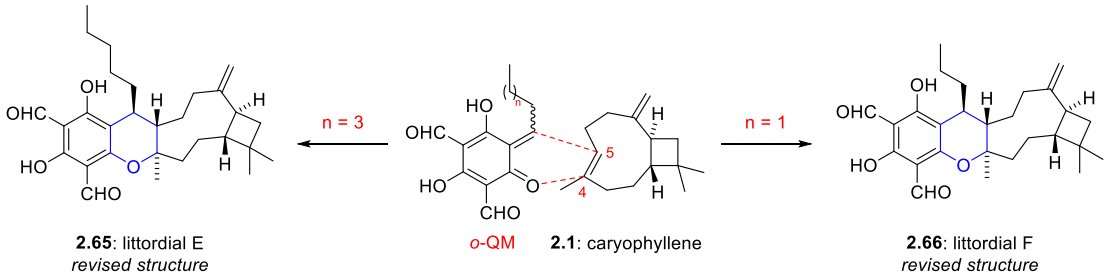

Figure 2.7: Proposed biomimetic synthesis and structural revisions of littordials E and F (**2.65** and **2.66**).

2.4 Biomimetic Synthesis and Structure Revision of Littordials E and F

Our biomimetic synthesis of littordials E and F was initially guided by the synthesis of closely related natural products guajadial (**2.10**) and psidial A (**2.11**) by Lee and co-workers.[24] These compounds, as well as diastereomer **2.12**, were isolated as by-products in Cramer's synthesis of psiguadial B (**2.9**, Scheme 2.1). As is expected for the littordials, both guajadial and psidial A were synthesized via a hetero-Diels–Alder reaction between (–)-caryophyllene and a diformylphloroglucniol-derived *o*-QM (**2.5**) (Scheme 2.8). Under the authors' optimized conditions, a Knoevenagel condensation of diformylphloroglucinol (**2.2**) with benzaldehyde (**2.3**) generated the key *o*-QM **2.5** which is sequestered by caryophyllene, giving compounds **2.10**, **2.11** and **2.12** in 25% combined yield (60:20:20 ratio of **2.10**:**2.11**:**2.12**). We hypothesized that replacing benzaldehyde with hexanal in this multicomponent cascade could successfully generate littordials C and E (**2.61** and **2.65**). Alternatively, using butanal as the aldehyde component of the Knoevenagel condensation should produce littordials A, B and F (**2.59**, **2.60**, **2.66**).

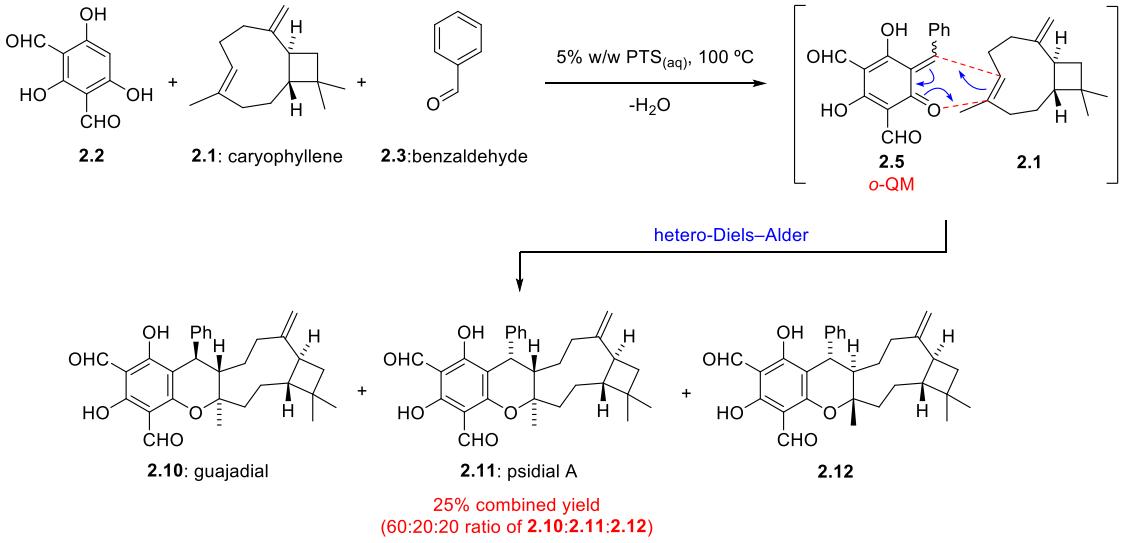

Scheme 2.8: The biomimetic synthesis of guajadial (**2.10**) and psidial A (**2.11**) by Lee et al.[24]

2.4.1 Synthesis of diformylphloroglucinol (2.2)

Our synthesis of littordials E and F began with the preparation of diformylphloroglucinol (**2.2**) using previously reported conditions by Hintermann et al.[25] Diformylation of anhydrous phloroglucinol (**2.49**) using Vilsmeier–Haack conditions was achieved on a multigram scale in 83% yield, affording **2.2** (Scheme 2.9).

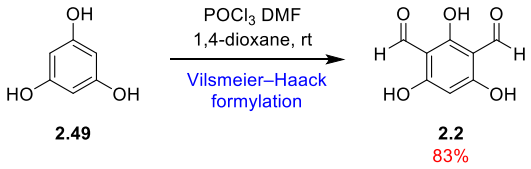

Scheme 2.9: Synthesis of diformylphloroglucinol (**2.2**).

^{1}H NMR spectra of the final product in d_6-DMSO revealed a significant amount of water still present following its synthesis. The presence of 3 hydroxyl groups and 2 carbonyls in **2.2** make it a formidable H-bond donor and acceptor, facilitating bonding with water molecules. As such, **2.2** required significant drying prior to use, which was done in a 110 °C oven and on a high vacuum line. Diformylphloroglucinol was typically prepared a few days prior to use in order to remove as much water from the product as possible. Fortunately, we discovered during this project that **2.2** is available for purchase, avoiding the need for laborious syntheses. We were kindly gifted some commercial diformylphloroglucinol by Dr. Chris Newton, who was working at the University of Adelaide at the time, which proved more than sufficient for the completion of this project.

2.4.2 Total Synthesis of Littordials A, B, C, E and F

With a healthy stock of **2.2** now available, we turned our attention to the key hetero-Diels–Alder step. Once again, we looked to the work done by Lee et al. as a starting point. For their optimized conditions, the multicomponent reaction was carried out in 5% w/w PEG-600/α-Tocopherol-based diester of Sebacic acid (PTS) solution while heating under reflux.[24] As these reagents were unavailable to us at the time, we began searching for alternative conditions. During our exploration of the literature, the results reported by the Cramer group in their synthesis of psiguadial B (**2.9**)

caught our attention. In generating this meroterpenoid, Cramer et al. reported the formation of appreciable amounts of both guajadial (**2.10**) and psidial A (**2.11**) as side products in their reactions (see Scheme 2.1).[6] Thus, we selected the conditions which maximized the yield of the side products, **2.10** and **2.11**, and applied these to our synthesis of littordials E and F in the hope that these compounds would form in good yields. To our delight, reacting **2.2** and hexanal in the presence of (–)-caryophyllene with catalytic EDDA in HFIP afforded littordial C (**2.61**) and littordial E (**2.65**) in 40% and 17% yield, respectively. Under the same reaction conditions, replacing hexanal with butanal gave littordials A and B as an inseparable mixture in 42% yield (5:1 ratio in favour **2.60** by NMR) and littordial F (**2.66**) in 3% yield (Scheme 2.10).

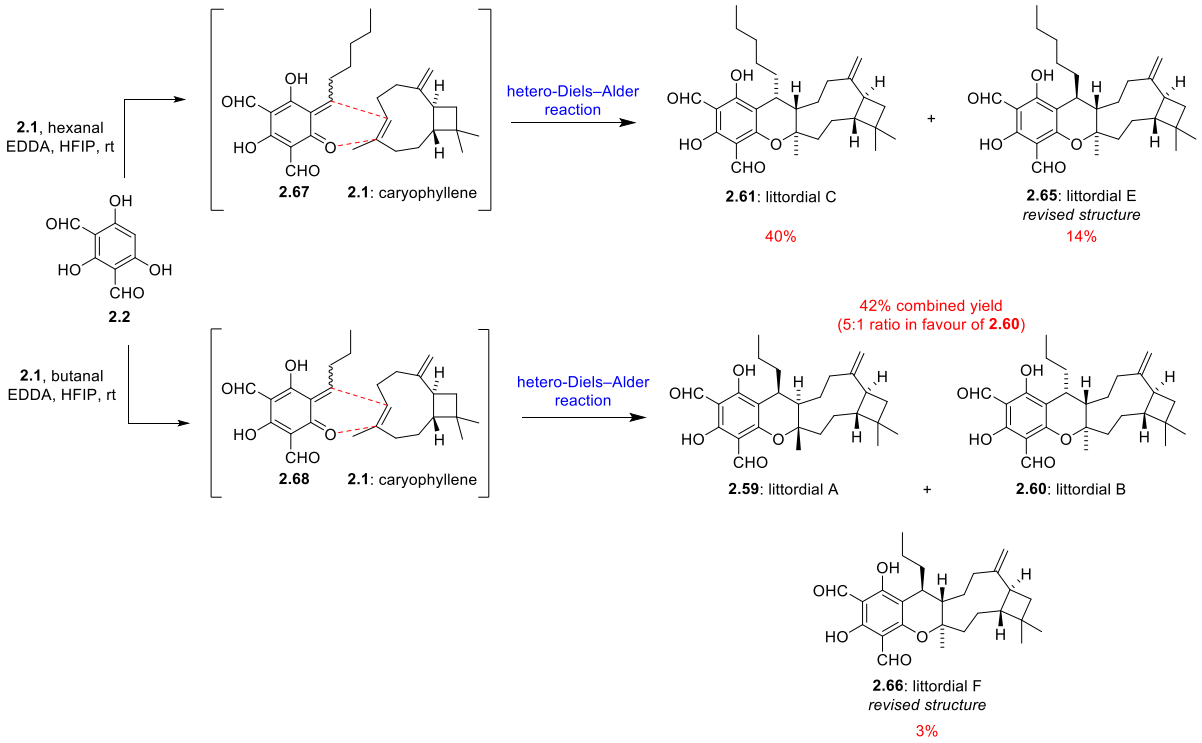

Scheme 2.10: Biomimetic synthesis of littordials A, B, C, E and F.

Considering the dubious nature of the proposed structures **2.63** and **2.64**, the assignment of littordial C (**2.61**) was also called into question at an early stage of the project. Single crystals of synthetic littordial C for X-ray analysis were obtained by recrystallisation from ethanol. The crystal structure of littordial C (**2.61**) is given in Figure 2.8, showing the H-atoms at key stereocentres (remaining H-atoms were omitted for clarity). The diffraction data matches the

originally proposed structure of **2.61**[20] and confirms what we observed in our 2D NMR studies. Unfortunately, we were unable to grow crystals for both **2.65** and **2.66**. The structures of these two compounds were reassigned by 2D NMR spectroscopy, supported by computational studies.

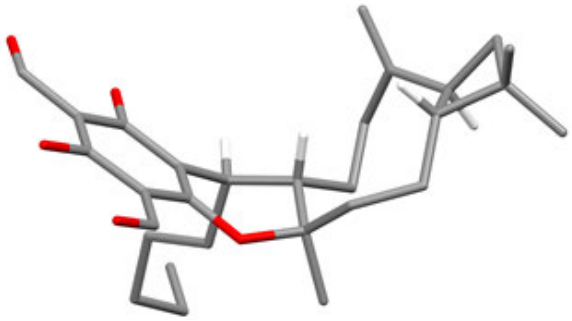

Figure 2.8: X-ray crystal structure of littordial C (**2.61**).

A thorough structural analysis of **2.65** and **2.66** was initially impeded by the constant presence of diastereomeric impurities in our "clean" samples. One such example can be seen in a ^{1}H NMR spectrum of littordial C (Figure 2.9, a). Our 1D NMR spectra remained relatively unaffected by the presence of these contaminants but 2D NMR analysis proved challenging due to extensive signal overlap. Although the structure of **2.61** was unambiguously assigned by X-ray crystallography, early characterization attempts by 2D NMR required us to develop more a meticulous purification procedure to achieve clean samples for analysis. After much trial and error, it was found that trituration of the crude mixture using diethyl ether, following the straightforward removal of excess aldehyde and caryophyllene, yielded a mixture of natural products as an orange gum. This gum, which was composed only of our natural product diastereomers, was separated by flash chromatography using a Biotage Isolera^{TM} One Flash Chromatography System (see Experimental Procedures for more detail) giving a clean natural product sample (Figure 2.9, b)). This protocol would be adopted for the purification of all our synthesized littordials. The difficulty in separating these compounds may have also hindered spectroscopic analysis in the isolation work, contributing to the misassignment of the natural product structures.

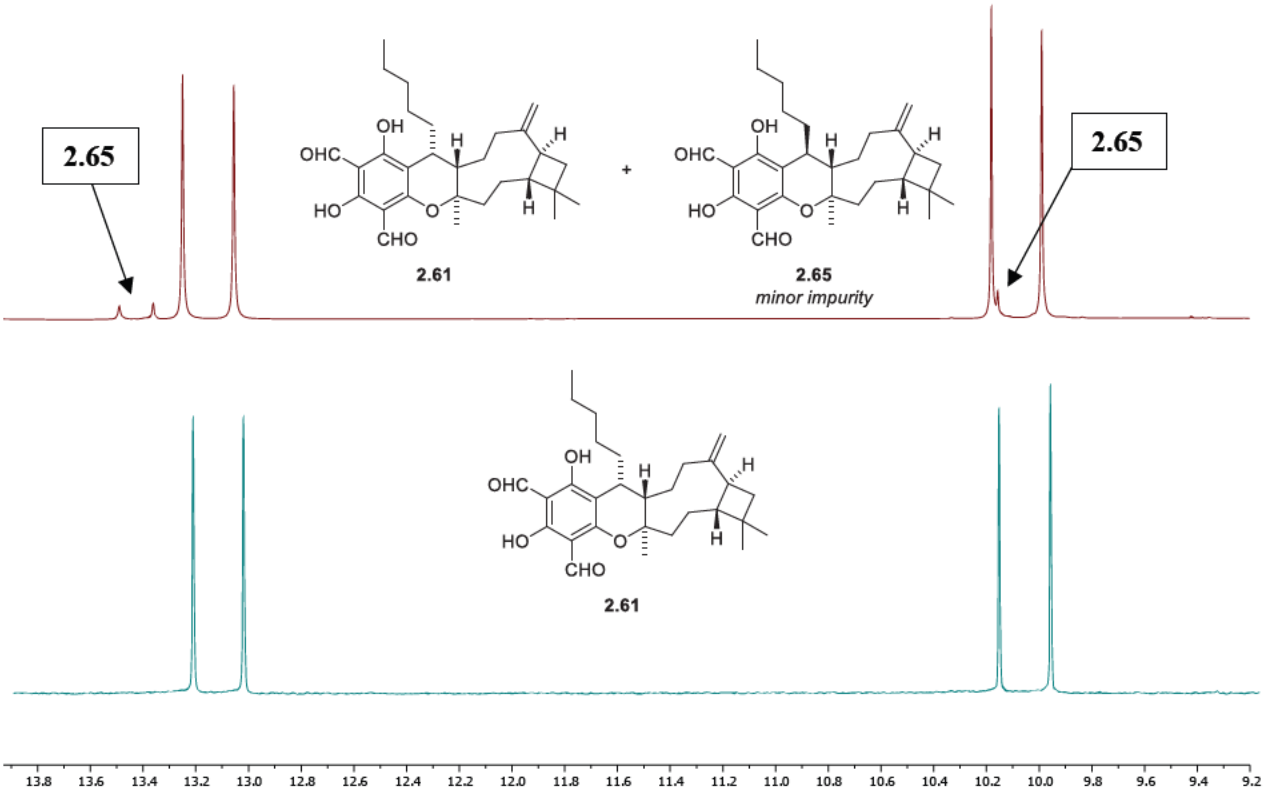

Figure 2.9: Section of the ^{1}H NMR spectra of an impure sample of littordial C (red) and clean sample of **2.61** (blue). The impurity was identified as the diastereomeric natural product, littordial E (**2.65**).

Whilst comparing the data for our synthetic littordial samples with that of the isolated compounds we observed an intriguing discrepancy. The optical rotations for the isolated littordials C, E and F are given as $[\alpha]_D^{25}$ = +36.9, –16.7 and –42.0, respectively.[20,21] In comparison, our synthetic samples of **2.61**, **2.65**, and **2.66** gave optical rotations of $[\alpha]_D^{25}$ = –50.4, +45.1, and +44.4. While we considered this inconsistency the result of an initial error during the data recording process, subsequent measurements proved that this was not the case. The absolute configuration of littordial A (**2.59**) was determined by single-crystal X-ray diffraction analysis with Ga Kα radiation and was supported by comparisons between calculated and experimental CD spectra.[20] The configuration of **2.59** arises from the natural, (–) enantiomer of caryophyllene, available for purchase from commercial sources. This (–) enantiomer was purchased from the Sigma-Aldrich as used as received for all our reactions. As we expected, the CD spectra of our synthetic littordials C, E and F matched the spectra of the isolated compounds (see Section 2.11.3 for our CD spectra). Despite the considerable variation in optical rotation values, we believe that CD spectroscopy and single

crystal X-ray diffraction analysis removes any doubt as to the absolute configuration of the natural products. These differences in optical rotation values could be explained by the presence of minor diastereomeric impurities, which may exist in either the synthetic or the isolated samples and contribute greatly to optical activity. Joyce and co-workers discuss these issues, focusing on CD spectroscopy and optical rotation, in the case of the famously misassigned absolute configuration of frondosin B.[26]

2.4.3 Structural Revision of Littordial E by 2D NMR Spectroscopy

With an adequate sample of littordial E (**2.65**) in hand, a comprehensive structural revision could now be carried out. Our 1D NMR spectra closely matched data reported for the isolated natural product. However, key differences in the 2D spectra required closer inspection. Full NMR spectra for our synthesized natural products as well the isolated natural product spectra[20] can be found in Section 2.11.1.

The structural reassignment of littordial E begins with the examination of C-14′ which the isolation team had assigned as a methylene sub-unit belonging to their proposed seven-membered ring.[20] The isolation team's claimed COSY correlation between one of the H-14′ signals (δ_H = 0.77) and H-5 (δ_H = 2.17) is difficult to assess due to overlapped peaks around the region of H-5. Although we observe a correlation from this region to H-14′, the proximity of one of the H-10′ signals (δ_H = 2.18) makes this H-14′/H-5 coupling highly ambiguous. Additionally, in our spectra we observe a clear COSY correlation in the region of δ_H = 1.41-1.45 to H-14′ (δ_H = 0.77). Signals from this region are assigned to the second proton of H-10′ (δ_H = 1.43) and H-2 (δ_H = 1.44). Considering that a COSY correlation from H-2 to H-14′ would be impossible, this correlation of δ_H = 1.41-1.45 to H-14′ can only arise from the coupling of the H-10′ proton to H-14′. These two couplings, δ_H = 2.18 to δ_H = 0.77 and δ_H = 1.43 to δ_H = 0.77, therefore imply a correlation of H-10′ to H-14′ rather than H-14′ to H-5, which is only possible with our proposed structure **2.65** (Figure 2.10).

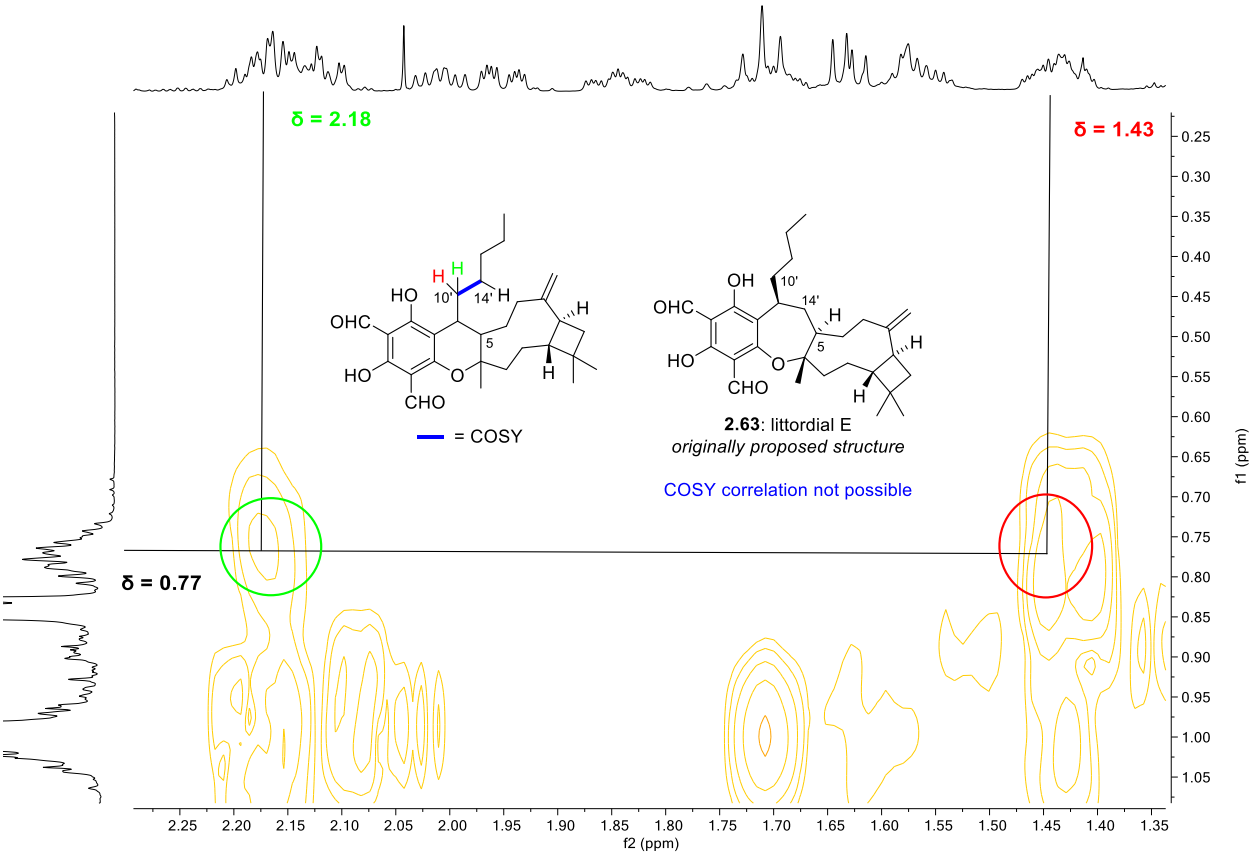

Figure 2.10: Section of the COSY spectrum (in $CDCl_3$) of synthetic littordial E (**2.65**). The key coupling of H-14′ to H-10′ suggests C-14′ is located within the branching alkyl chain of **2.65** and not within a seven-membered ring as originally proposed.

HMBC correlations from H-14′ to C-9′ /C-10′/C-11′/C-12′ also suggest that C-14′ is likely located within the alkyl chain connected at C-9′ rather forming part of a seven-membered ring. Furthermore, HMBC correlations from H-9′ to C-1′/C-6′/C-5/C-6 along with H-5 to C-4 and H-14 to C-4/C-5 implies the presence of a six-membered ring as seen in the other littordial natural products. The NOESY spectrum of **2.65** is challenging to interpret due to a large degree of peak overlap in key regions. From the NOESY spectrum in $CDCl_3$ there is an unambiguous coupling of H-14 (δ = 1.12) to H-9′ (δ = 2.47) showing that these centres possess the same relative configuration. The stereochemistry of H-5 is far more difficult to characterize due to significant peak overlap. Though one could infer the presence of some couplings to H-5, many of these do not aid the assignment of its stereochemistry and are far too ambiguous to assign with any degree of certainty. To resolve these issues, NOESY and ROESY experiments were carried out using d_d-

benzene as the solvent. Using d_6-benzene resolved some of the overlapping peaks seen in $CDCl_3$. As before, we see a clear coupling from H-14 ($\delta = 0.76$) to H-9′ ($\delta = 2.45$) confirming their relative configuration. In d_6-benzene there is also a clear coupling of H-5 ($\delta = 2.13$) to H-1 ($\delta = 2.04$). Couplings to H-1/H-9 are crucial for stereochemistry determination as their absolute configurations (which arise from (–)-caryophyllene) are known. Knowing the stereochemistry of H-5 one can deduce that H-14 will have an opposite configuration resulting from the *trans* $\Delta^{4,5}$ alkene of (–)-caryophyllene (**2.1**). The NOESY correlation of H-9′ to H-14 means that H-9′ will also be opposite to H-1/H-5. Our structural revision of littordial E is summarised in Figure 2.11, showing key couplings from our 2D NMR experiments.

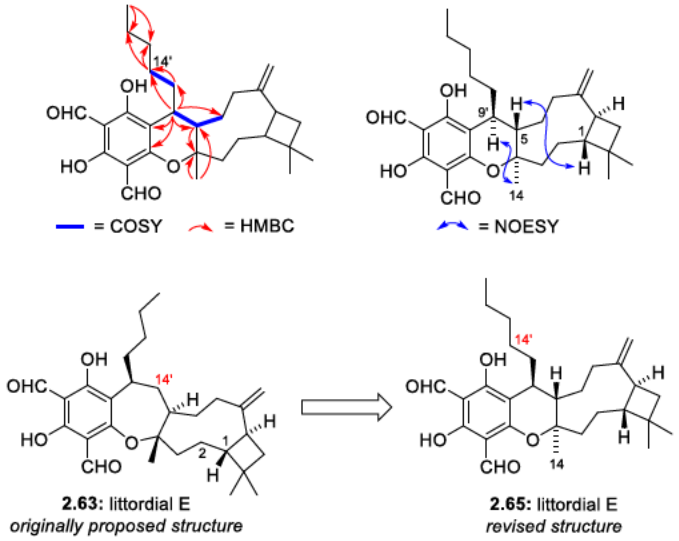

Figure 2.11. Key 2D NMR correlations supporting the structural revision of littordial E (**2.65**).

2.4.4 Structural Revision of Littordial F by 2D NMR Spectroscopy

The structural revision of littordial F (**2.66**) is described here and proceeds in a similar manner to what is written for littordial E (**2.65**). Once more, our 1D NMR spectra match the data for the isolated natural product fully. Differences between isolated and synthetic 2D NMR data support our structural revision, the key correlations supporting this are displayed in Figure 2.12. Full NMR spectra for our synthesized natural products as well as spectra of isolated **2.66**[21] can be found in Section 2.11.1.

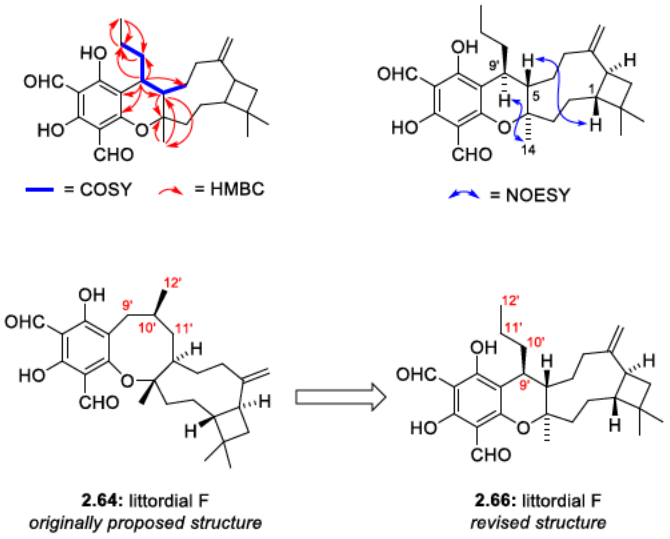

Figure 2.12. Key 2D NMR correlations supporting the structural revision of littordial F (**2.66**).

From the HSQC spectrum of our synthetic **2.66**, the coupling of C-9′ to a single proton at $\delta_H = 2.47$ is in contradiction to what is reported from the isolation, which assigns C-9′ as a -CH_2 unit within the originally proposed 8-membered ring. Furthermore, the authors also state C-10′ is a tertiary carbon but we see coupling to protons at $\delta = 1.43$ and $\delta = 2.16$.[21] The COSY spectrum establishes correlations from H-9′/H-5/-H-6 as previously seen in **2.65**, connections which would be impossible in the isolation team's proposed structure. The isolation chemists' observed correlation between H-12′ to H-10′ is also questionable. Although correlations to H-10′ are observed, the significant overlap around $\delta = 0.85–0.80$ makes distinguishing between signals from H-12′ and H-11′ difficult. However, we do see a coupling from a multiplet around $\delta = 1.03$ to H-10′, corresponding to the second proton of C-11′. Other signals around the region of $\delta = 1.03$ are designated as the *gem*-dimethyl protons located on the cyclobutane ring of caryophyllene, making this assignment much less ambiguous.

From the HMBC spectrum, we observe many of the same correlations present in the spectrum for **2.65** including H-9′ to C-1′/C-6′/C-5/C-6, H-5 to C-4/C-14 and H-14 to C-4/C-5. These couplings were used to establish the six-membered ring. The proximity of the proton signal of H-9′ (δ = 2.47) to that of H-7 (δ = 2.51) obscures the coupling of H-9′ to C-5/C-6, a factor which may have contributed to Xu's misassigned structure (Figure 2.13). The correlation from H-9′ to C-6 is particularly important, as in the proposed structure this would represent an uncommon five-bond correlation, the fact that it is seen in our data is further evidence of the presence of a six-membered ring in **2.66**. Finally, the *n*-propyl side chain of **2.66** is established by the correlations H-9′ to C-10′/C-11′, H-10′ to C-11′, H-11′ to C-10′/C-12′ and H-12′ to C-10′/C-11′. We observe the same NOESY correlations for **2.66** that are also seen in **2.65**. Spectra of **2.66** obtained in d_6-benzene is consistent with spectra collected in $CDCl_3$. Therefore, **2.65** and **2.66** are assigned the same relative configurations.

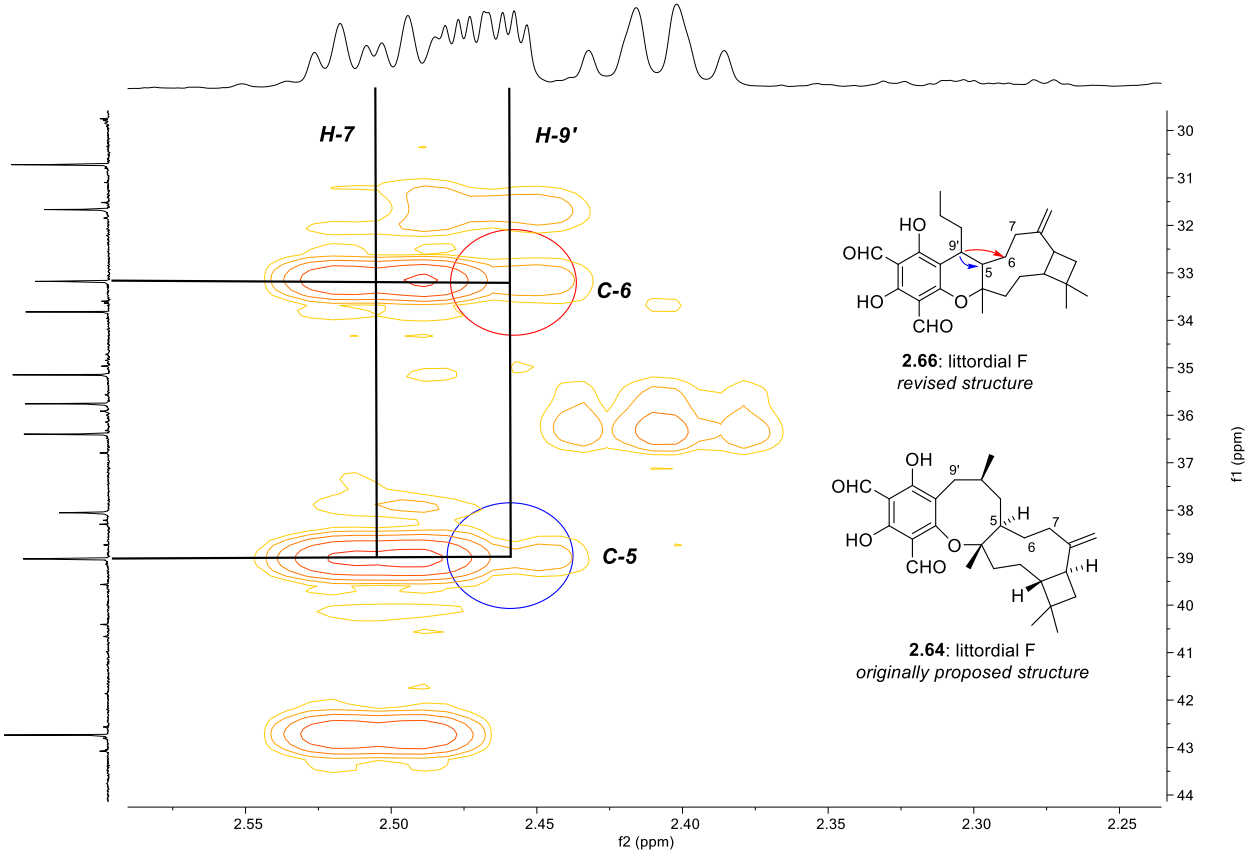

Figure 2.13: Section of the HMBC spectrum of littordial F (**2.66**). The strong coupling of H-7 to C-5 and C-6 obscures couplings from H-9′ (red and blue arrows) to these carbon atoms which may have contributed to Xu's misassigned structure.

2.4.5 Computational Methods

As mentioned previously in this chapter, caryophyllene (**2.1**) can adopt four possible low energy conformations in solution termed *αα*, *αβ*, *βα* and *ββ* (See Figure 2.2). Based on the relative population of these low energy conformers in solution and on the work of Lee et al.,[24] we have proposed that littordials B and C (**2.60** and **2.61**) and littordials E and F (**2.65** and **2.66**) are formed from the [4+2] cycloaddition between an *o*-QM and the *βα* conformer of **2.1**. Littordial A (**2.59**) is likely derived from the less populated *ββ* conformer of caryophyllene (Figure 2.14). The single crystal X-ray diffraction analysis of isolated **2.59**, our X-ray crystal structure of synthetic **2.61** and our extensive 2D NMR studies support this hypothesis. To verify our structural revisions further, computational modelling was performed to investigate the proposed cycloaddition pathways that produce littordials A (**2.59**), B (**2.60**), F (**2.66**) and an unknown diastereomer **2.69**. These computational studies were performed by one of our collaborators at the University of Adelaide, Dr. Thomas Fallon. Calculations were performed using DFT with the M06-2X functional and the 6-31+G(d) basis set for geometry optimizations and frequency analysis, with single-point energies calculated at the 6-311+(d,p) level.

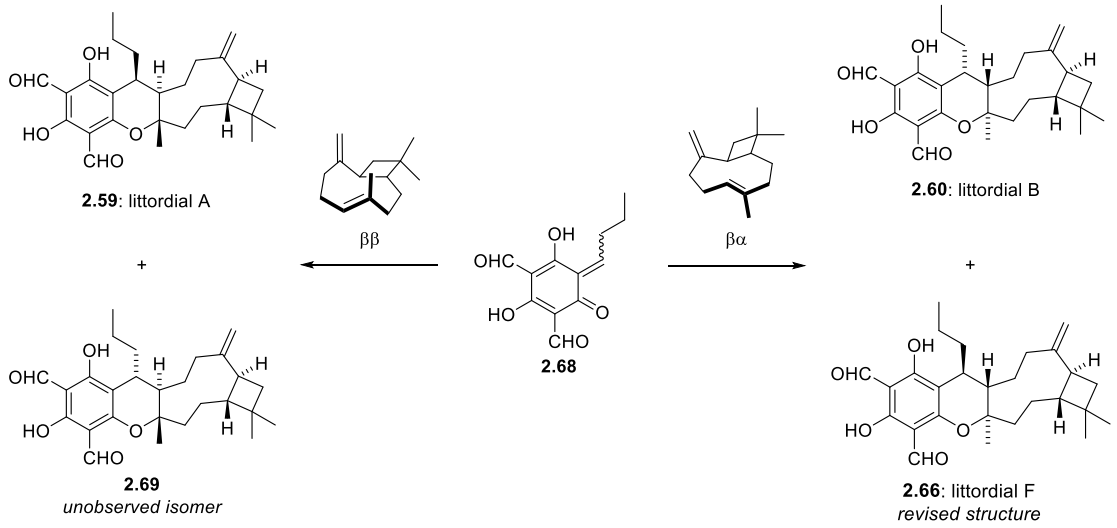

Figure 2.14: Proposed stereochemical outcomes for reactions with different caryophyllene (**2.1**) conformations.

When considering possible reaction pathways, we must take into account the various conformations of caryophyllene (**2.1**), the formation of either the *E* or *Z* isomer of *o*-QM **2.68**, and the *endo*/*exo* stereoselectivity of the hetero-Diels–Alder reaction. Firstly, calculated energies for

the *E*- and *Z*-isomers of **2.68** are nearly identical (*Z*-**2.68** relative $\Delta G = -1.2$ kJ mol^{-1}) and given that the selectivity in the formation of **2.68** is unknown, we must assume that both *E*- and *Z*-configurations are plausible reactants. Secondly, given the *αβ* conformer of **2.1** is non-populated, any pathways involving this conformation were not considered. Thus, there are a total of 12 possible reaction pathways which could form littordials A, B, F and diastereomer **2.69** (see Section 2.11.5 for full computational data). The lowest energy transition states leading to **2.59**, **2.61** and **2.66** are given in Figure 2.15. Our computational study revealed an energetically feasible, concerted cycloaddition between **2.1** and **2.68**, under our reaction conditions. Our calculations give transition states with C-O forming bond lengths between 2.64 and 2.96 Å, consistent with previous computational studies of Diels–Alder reactions of *o*-QMs.[27]

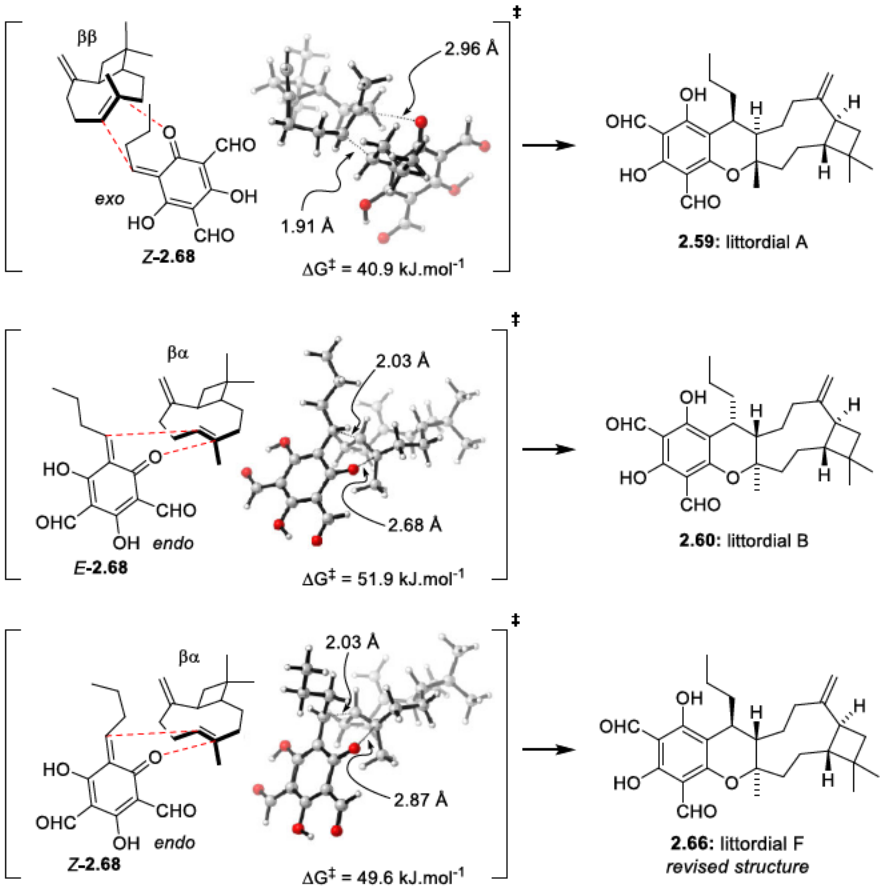

Calculated at M06-2X/6-311+G(d,p)//M06-2X/6-31+G(d), smd = hexafluoroisopropanol, 298 K

Figure 2.15: Calculated lowest energy transition states leading to littordials A, B and F.

Of all pathways, the formation of **2.59** (caryophyllene-*ββ*−*Z*-*o*-QM−*exo*-TS) possesses the lowest calculated energy barrier at $\Delta G^{\ddagger} = 40.9$ kJ mol^{-1}. Littordial A (**2.59**) was isolated as a minor isomer and synthesized in a 1:5 ratio with **2.60** (42% combined yield, mixture of diastereomers), observations which are consistent with the fact that is derived from the minor, *ββ*, conformer of **2.1**. Littordials B (**2.60**) and F (**2.66**) are both derived from more populated *βα* conformer of **2.1** via *endo* transition states. Littordial B (**2.60**) is formed from the *E*-**2.68** species with a predicted lowest-energy barrier of $\Delta G^{\ddagger} = 51.9$ kJ mol^{-1}. On the other hand, **2.66** is furnished by the *Z*-*o*-QM **2.68** with a predicted lowest-energy barrier of $\Delta G^{\ddagger} = 49.6$ kJ mol^{-1}. From our synthesis, littordial B is formed is greater yield than littordial F despite being predicted to have a higher energy barrier for its transition state. Although our calculations have shown feasible reaction pathways under our conditions, obtaining complete predictive power over the product distributions given by our study is unrealistic. This is due to both the conformational flexibility of caryophyllene (**2.1**) and the configurational uncertainty of **2.68**. Additionally, challenges with purification, degradation and other experimental uncertainties contribute to the unpredictability of these outcomes.

One final observation to make regarding this computational study is the possible formation of a fourth unknown diastereoisomer **2.69**. Our calculations show that the lowest-energy pathway (caryophyllene-*ββ*−*Z*-*o*-QM−*endo*-TS, see Figure 2.81 in Section 2.11.5) to generate **2.69** has a predicted barrier of $\Delta G^{\ddagger} = 55.6$ kJ mol^{-1}. This higher energy barrier might explain the absence of this diastereomer both in our synthesis and the original isolation studies.

2.5 Isolation of Drychampones A–C

Drychampones A–C (**2.70**–**2.72**) were isolated in 2016 from the ethanol extract of the aerial part of *Dryopteris championii*; a fern species used in traditional Chinese medicine to treat a variety of ailments.[28] These meroterpenoid natural products all possess an 11/6/6 ring-system featuring a humulene moiety coupled to an acylphloroglucinol derivative through a six-membered heterocyclic ring. Additionally, drychampones A and C contain a pyrone tethered to the phloroglucinol derived functionality (Figure 2.16). All compounds were isolated as racemates, implying a non-enzymatic biosynthesis.

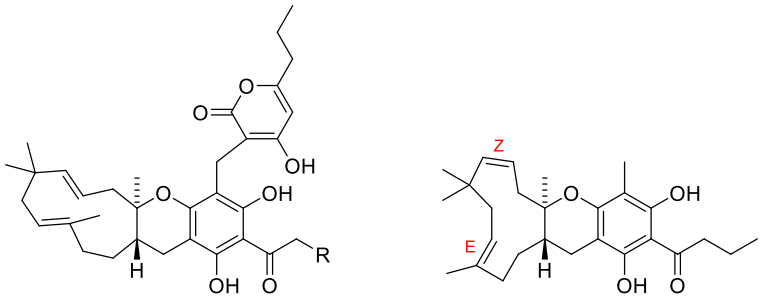

2.70: (±)-drychampone A R = CH_2CH_3
2.72: (±)-drychampone C R = H

2.71: (±)-drychampone B
Originally proposed structure

Figure 2.16: Structures of drychampones A–C (**2.70**–**2.72**) as assigned by Li and Wang.[28]

2.6 Proposed Biosynthesis of Drychampones A–C

Wang and co-workers proposed that drychampones A–C are formed biosynthetically via a hetero-Diels–Alder reaction between humulene (**2.27**) and *ortho*-quinone methides **2.74** and **2.78**, which can be traced back to two co-isolated phloroglucinol derived precursors **2.73** and **2.77** (Figure 2.17). Drychampones A and C (**2.70** and **2.72**) are furnished through an additional pyrone coupling of intermediates **2.75** and **2.79**. Interestingly, Wang et al. propose that in the biosynthesis of **2.71**, humulene undergoes an isomerisation event to a *cis*-humulene species.[28] This isomerization was proposed on the basis of an alkene signal seen in the ^{1}H NMR spectrum, which the authors assigned as being *cis*-configured on the basis of its coupling constant. This is despite extensive signal overlap in this region which would impede any accurate characterization of these signals.

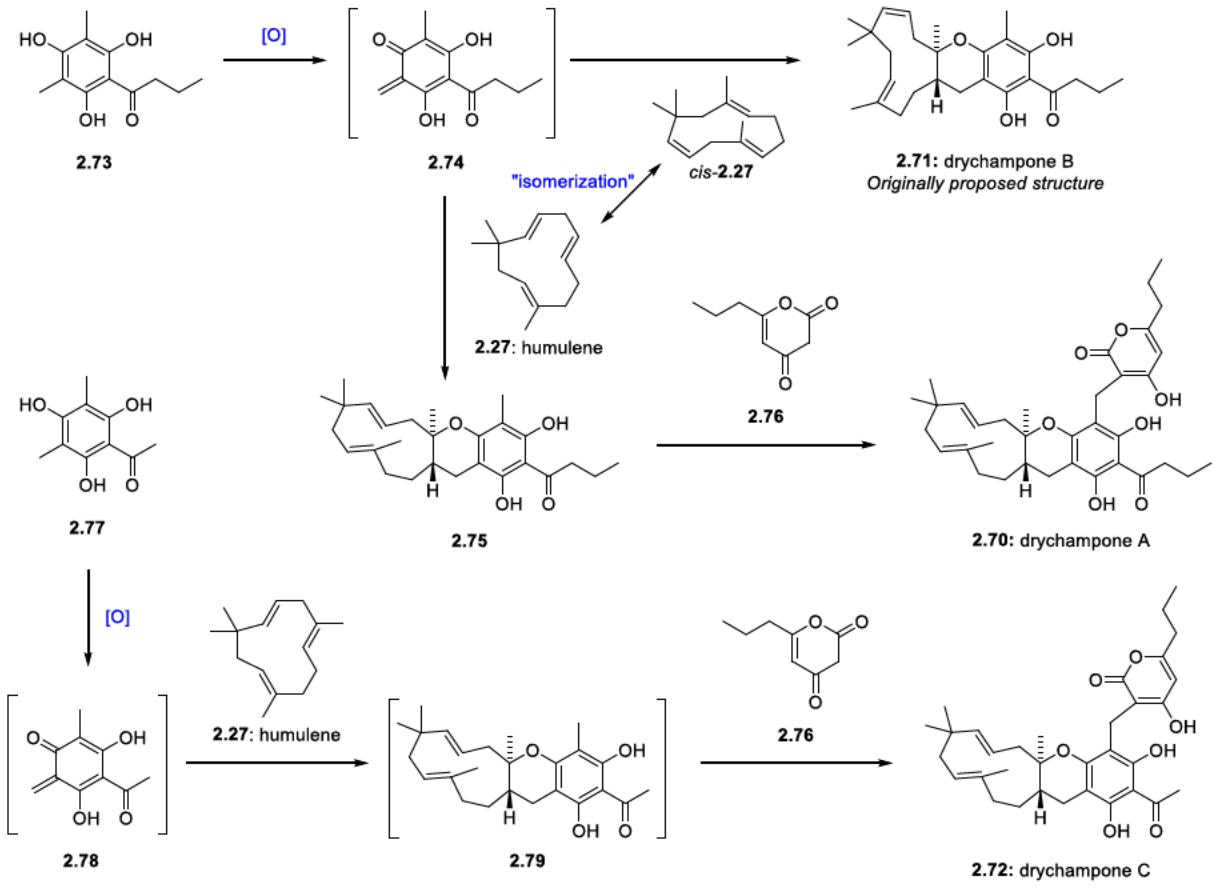

Figure 2.17: Wang's originally proposed biosynthesis of drychampones A–C (**2.70**–**2.72**), featuring an unusual humulene isomerization step.[28]

While there is substantial literature precedent for cycloaddition reactions between humulene and *o*-QMs in the context of meroterpenoid natural products (some examples discussed in detail in Section 2.1.4), the originally proposed humulene isomerization step is highly questionable. We envisage a hetero-Diels–Alder reaction to still be the crucial step of this synthesis, but without the formation of this dubious *cis*-humulene species (Scheme 2.11). Under oxidative conditions, *o*-QM **2.74** may be generated from precursor **2.73**. This *o*-QM can then be trapped *in situ* with humulene to yield drychampone B (**2.75**), which should now contain two *E*-configured alkenes. Additionally, our revised structure of drychampone B matches a compound Wang et al. believe is a precursor to drychampone A (**2.70**). Re-subjecting **2.75** to the same oxidative conditions could generate a second *o*-QM (**2.80**) which may undergo a Michael reaction with pyrone **2.76** to afford **2.70** (Scheme 2.11). If proved correct, this proposed biosynthesis may allow for this synthesis of drychampone A from precursor **2.73** in a one-pot procedure.

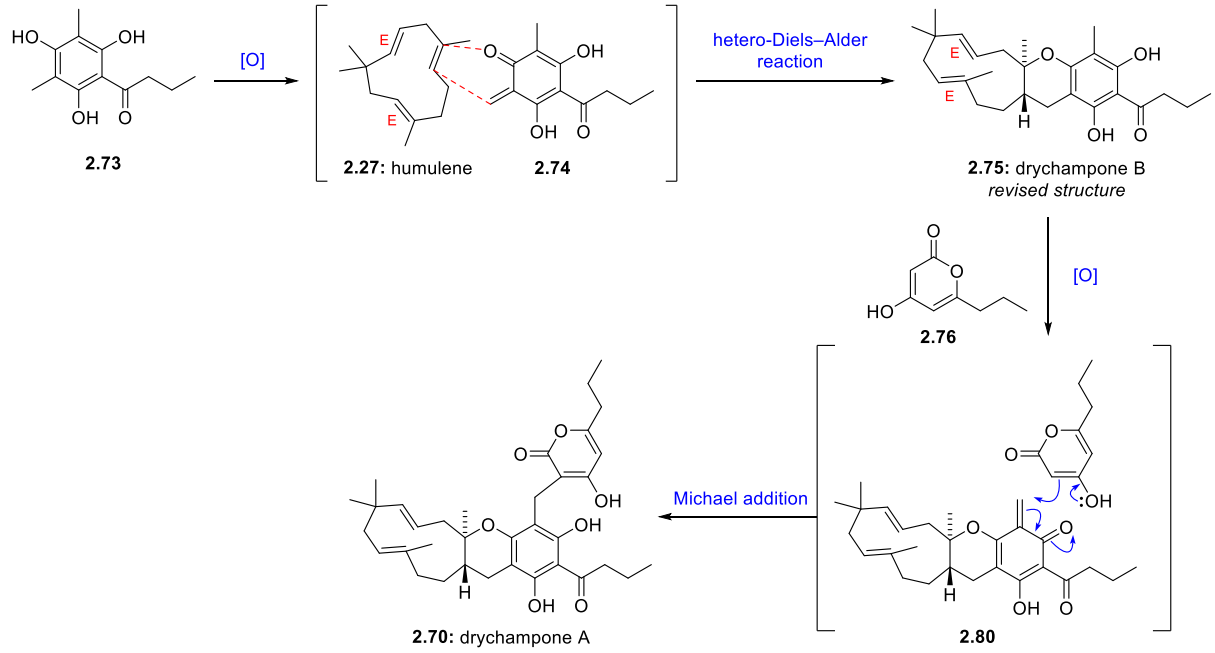

Scheme 2.11: Our proposed biosynthesis of drychampones A and B (**2.70** and **2.75**).

2.7 Biomimetic Synthesis and Structure Revision of Drychampone B

2.7.1 Synthesis of the *o*-QM precursor

The synthesis of the necessary *o*-QM precursor (**2.73**) begins with a reduction of commercially available diformylphloroglucinol (**2.2**). Initial attempts at a stepwise reduction of the aldehyde functional groups using $LiAlH_4$ proved unsuccessful, often leading to unclean material and poor yields. Fortunately, a simple protocol for the simultaneous reduction to the desired methyl substituents has been reported by Jung and co-workers.[29] Treating diformylphloroglucinol with $NaBH_3CN$ in the presence of hydrochloric acid gave dimethylphloroglucinol (**2.81**) in 46% yield after purification (Scheme 2.12). Despite the consistently modest yields (approximately 40% for every reaction), this double reduction protocol was easily scalable and afforded clean product. Additionally, the efficiency of a simultaneous reduction avoided the need for a more laborious, and potentially more inefficient, stepwise procedure. With **2.81** in hand, the requisite *o*-QM precursor was synthesized in just one more step using Friedel–Crafts chemistry. Acylation of **2.81**

with butyryl chloride using a modified literature procedure,[30] furnished our desired *ortho*-quinone methide precursor **2.73** in 59% yield (Scheme 2.12)

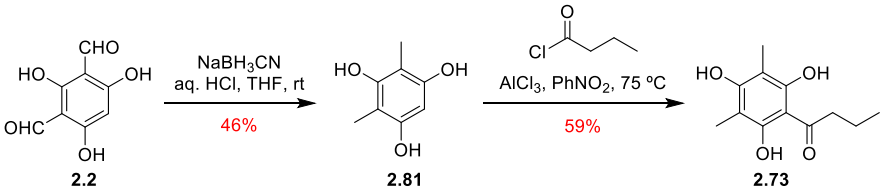

Scheme 2.12: Synthesis of *o*-QM precursor **2.73**.

2.7.2 Biomimetic Synthesis of Drychampone B

With a route to precursor **2.73** secured all that remained to synthesize drychampone B (**2.75**) was carrying out the hetero-Diels–Alder reaction. We initially tested oxidation conditions previously reported by the George group in the synthesis of the hyperjapone and hyperjaponol natural products.[15] To our delight, oxidation using Ag_2O and TEMPO generated *o*-QM **2.74** which was trapped *in situ* by humulene (**2.27**) to give drychampone B (**2.75**) in 17% yield after purification (Scheme 2.13).

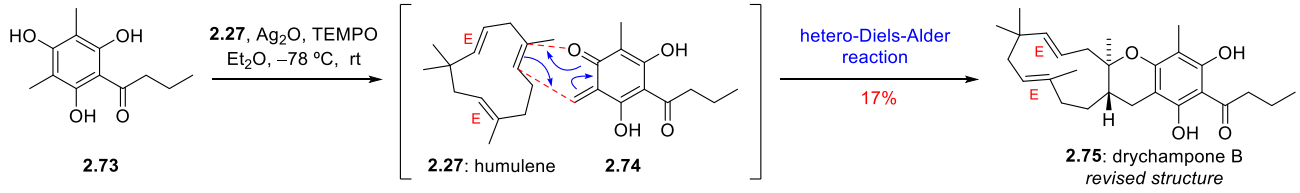

Scheme 2.13: Biomimetic synthesis of drychampone B (**2.75**)

Following the successful synthesis of drychampone B, we continued to investigate alternative conditions to improve the yield of the hetero-Diels–Alder reaction (Table 2.1). The low yields were initially attributed to the low reactivity of humulene but increasing the equivalents of **2.27** had no pronounced effect on yield (Table 2.1, entry 2). Both catalytic and equivalent amounts of TEMPO resulted in no reaction (Table 2.1, entries 3 and 4). The required use of excess TEMPO in our reaction could be indicative of the quality of the reagent present in our lab, which had seen extensive use over several years. Replicating the original Ag_2O conditions described by Lei[31] for oxidative *o*-QM generation saw no reaction (Table 2.1, entry 5). Likewise, using MnO_2 as the

singular oxidant gave no results (Table 2.1, entry 6). Going back to TEMPO but replacing Ag_2O with other co-oxidants such as PIDA, PIFA and CAN (Table 2.1, entries 7-10) showed only decomposition. Finally, using only TEMPO while open to air gave no indication of reaction despite running for 5 days (Table 2.1, entry 11).

Table 2.1. Optimization of the biomimetic synthesis of drychampone B (2.75):

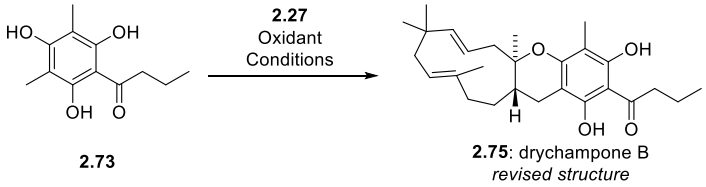

2.73 **2.75**: drychampone B *revised structure*

Entry	Humulene equivalents	Oxidants (eq)	Solvent	Conditions	Result
1	1.2	Ag_2O (1.2) TEMPO (2.0)	Et_2O	–78 °C → rt, 18 h	17%
2	2.0	Ag_2O (1.2) TEMPO (2.0)	Et_2O	–78 °C → rt, 17 h	15%
3	2.0	Ag_2O (1.2) TEMPO (0.4)	Et_2O	–78 °C → rt, 17 h	No reaction
4	2.0	Ag_2O (1.2) TEMPO (1.1)	Et_2O	–78 °C → rt, 17 h	No reaction
5	2.0	Ag_2O (1.2)	Benzene	rt, 17 h	No reaction
6	2.0	MnO_2 (2.2)	Benzene	rt, 24 h	No reaction
7	2.0	PIDA (1.2) TEMPO (2.0)	Et_2O	–78 °C → rt, 4 h	Decomposition
8	2.0	PIFA (1.2) TEMPO (2.0)	THF	–78 °C → rt, 2 h	Decomposition
9	2.0	CAN (1.2) TEMPO (2.0)	MeOH	–78 °C → rt, 3 h	Decomposition
10	2.0	CAN (1.2) TEMPO (1.2)	MeOH	–78 °C →rt, 3 h	Decomposition
11	2.0	TEMPO (2.0)	Et_2O	Air, rt, 5 d	No reaction

2.7.3 Structural Revision of Drychampone B by NMR Spectroscopy

With enough material available to us, we began our structural revision of drychampone B (**2.75**) by means of NMR spectroscopy. Attempts were made at growing crystals of **2.75** for X-ray crystallography, but these were unsuccessful. However, considering the originally proposed structure of drychampone B is the result of a single, dubious coupling constant, NMR data should prove more than sufficient for the reassignment.

Our 1D NMR data for synthetic **2.75** perfectly matched that of the isolated natural product with both ^{1}H NMR and ^{13}C NMR spectra in $CDCl_3$ matching the peaks for the isolated sample exactly.[28] Our synthetic compound data as well as isolated material NMR spectra[28] can be found in section 2.11.1. There was a minor impurity that could be seen in the ^{1}H NMR spectrum, identified as H-grease, but this was negligible and would have no impact on the structural reassignment. Likewise, our 2D NMR spectra in $CDCl_3$ matched isolated product data. COSY correlations between H-4/H-5/H-6/H-7′ as well as HMBC correlations from H-13 to C-9/C-8/C-7/C-6 and H-7′ to C-6/C-7 establish the connectivity between the acylphloroglucinol and humulene moieties. Additionally, HMBC correlations from H-7′ to C-1′/C-2′/C-6′ confirm the central six-membered ring of **2.75** (Figure 2.18). Reassignment of the structure of **2.75** proved trivial, as observation of the coupling constants of H-9 and H-10 would be indicative of the alkene bond geometry in humulene. In the $CDCl_3$ spectrum of **2.75**, these proton signals appear as an overlapped multiplet. After much trial and error, running a ^{1}H NMR spectrum in d_6-benzene resolved these overlapped peaks well, indicating a *trans* coupling constant ($^{3}J_{9\text{-}10}$ = 15.8 Hz) thus proving our structural reassignment of drychampone B (**2.75**).

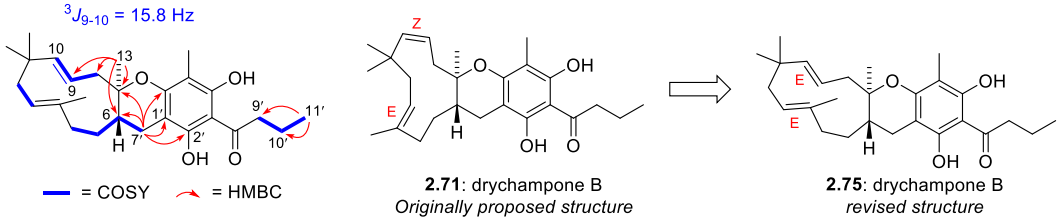

Figure 2.18. Structural revision of drychampone B (**2.75**).

2.8 Conclusions and Future Directions

We have achieved concise biomimetic total syntheses of littordials C, E and F (**2.61**, **2.65**, and **2.66**) by means of an intermolecular hetero-Diels–Alder reaction between and *o*-QM intermediate and (–)-caryophyllene (**2.1**). Additionally, littordials A and B (**2.59** and **2.60**) were produced as an inseparable mixture of diastereomers in 42% combined yield (a 5:1 ratio in favour of **2.60** based on NMR spectra). The originally proposed structure for littordial C was confirmed by our 2D NMR studies and single crystal X-ray diffraction analysis. Revised structures of littordials E and F (**2.65** and **2.66**) were proposed on the basis of our biosynthetic speculation and were confirmed by their biomimetic synthesis and subsequent 2D NMR experiments. Computational studies supported the feasibility of our proposed cycloadditions in the formation of littordials A, B and F (**2.59**, **2.60**, **2.66**).

Drychampone B (**2.75**) was synthesized in 3 steps from diformylphloroglucinol (**2.2**). The key step in this synthesis involved an intermolecular hetero-Diels–Alder reaction between an *o*-QM and humulene (**2.27**). A structural revision of **2.75** was performed on the basis of dubious $\Delta^{9,10}$ alkene coupling constant, suggested by the isolation chemists to belong to a *cis*-humulene species. The proposed structural reassignment was confirmed by our ^{1}H NMR spectrum of **2.75** in d_6-benzene, which showed $^{3}J_{9\text{-}10}$ coupling constant of 15.8 Hz, consistent with the presence of an *E*-configured alkene. The revised drychampone B (**2.75**) was also proposed to be a biosynthetic precursor to drychampone A (**2.70**) and could theoretically be formed by the Michael addition of a pyrone (**2.76**) to *o*-QM **2.74**. The success of this Michael addition could also open the door for a one-pot synthesis of **2.70** from precursor **2.73** and should be investigated further.

This project highlights the important role biomimetic synthesis plays in structural characterization of newly isolated small molecules. Despite the ever expanding, powerful arsenal of analytical techniques available for structure elucidation, isolation chemists are still prone to error when it comes time to assign novel structures. In many cases this is simply due to the proposal of structures that may satisfy analytical data but whose formation in nature is poorly rationalized, or entirely non-existent in the worst of cases. In combination, modern spectroscopic techniques and biomimetic synthesis significantly reduce the number of these misassigned structures by combining the spectroscopic data with logical structures that are the result of feasible biosynthetic pathways.

2.9 Experimental

2.9.1 General Methods

All chemicals were purchased from commercial suppliers and used as received. All reactions, unless otherwise stated, were performed under an inert atmosphere of N_2. All organic extracts were dried over anhydrous magnesium sulfate. Thin layer chromatography was performed using aluminium sheets coated with silica gel F_{254}. Visualization was aided by viewing under a UV lamp and staining with ceric ammonium molybdate or $KMnO_4$ stain followed by heating. All R_f values were measured to the nearest 0.05. Flash column chromatography was performed using 40-63-micron grade silica gel. Melting points were recorded on a digital melting point apparatus and are uncorrected. Infrared spectra were recorded using an FT-IR spectrometer as the neat compounds. High field NMR spectra were recorded using either a 500 MHz spectrometer (^{1}H at 500 MHz, ^{13}C at 125 MHz) or 600 MHz spectrometer (^{1}H at 600 MHz, ^{13}C at 150 MHz). The solvent used for NMR spectra was $CDCl_3$ unless otherwise specified. ^{1}H chemical shifts are reported in ppm on the δ-scale relative to TMS (δ 0.0) or $CDCl_3$ (δ 7.26) and ^{13}C NMR chemical shifts are reported in ppm relative to CDCl3 (δ 77.16). Multiplicities are reported as (br) broad, (s) singlet, (d) doublet, (t) triplet, (q) quartet, (quin) quintet, (sext) sextet, (hept) heptet and (m) multiplet. All *J*-values were rounded to the nearest 0.1 Hz. ESI high resolution mass spectra were recorded on an ESI-TOF mass spectrometer. Circular dichroism (CD) spectra were measured using a JASCO J-715 spectropolarimeter.

2.9.2 Experimental Procedures

Synthesis of diformylphloroglucinol (2.2)

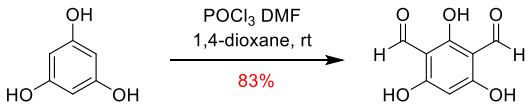

2.49 **2.2**

$POCl_3$ (15.6 mL, 167 mmol) was added dropwise to DMF (12.8 mL, 166 mmol) with vigorous stirring. The solution was stirred under a N_2 atmosphere at room temperature for 30 min. This Vilsmeier reagent was transferred dropwise, *via* cannula, to a stirred solution of anhydrous phloroglucinol (10.1 g, 79.9 mmol) in 1,4-dioxane (50 mL) under a N_2 atmosphere. This mixture was vigorously stirred at room temperature for 16 h. The resulting yellow solid was cooled to 0 °C and subsequently added to an ice-water slurry (approx. 400 mL). The mixture was slowly warmed to room temperature and stirred for a further 4 h. The resulting orange precipitate was filtered and washed with cold H_2O. This solid was dissolved in H_2O (50 mL), heated under reflux for 5 min and then cooled to 0 °C. The resulting solid was filtered, washed with cold H_2O and dried in an oven at 110 °C to constant weight to yield diformylphloroglucinol (**2.2**) as a red-orange powder (12.1 g, 66.4 mmol, 83%). Data for **2.2** matched that of published literature.[24, 25]

R_f: 0.15 (petrol/EtOAc, 1:1)
IR (neat): 2887, 1598, 1502, 1438, 1393, 1253, 1187, 1096, 947, 846 cm^{-1}
^{1}H NMR (500 MHz, d_6-DMSO): δ 12.56 (br s, 2H), 10.01 (s, 2H), 5.89 (s, 1H)
^{13}C NMR (125 MHz, d_6-DMSO): δ 191.4, 169.5, 169.2, 103.8, 93.9

Synthesis of littordial C (2.61) and littordial E (2.65)

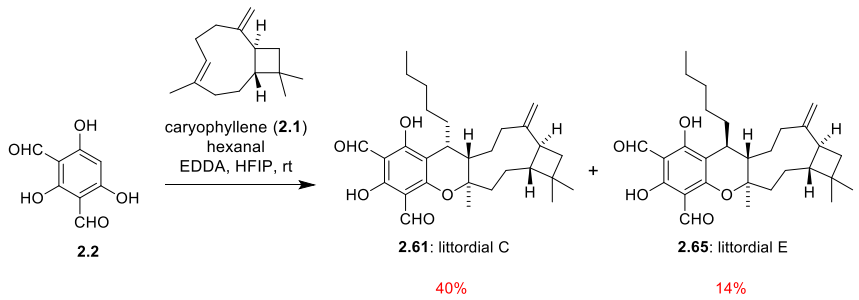

To a round-bottom flask open to air was added (–)-caryophyllene (**2.1**) (1.52 mL, 7.25 mmol), HFIP (20 mL), and hexanal (0.85 mL, 6.81 mmol). To this biphasic mixture was added **2.2** (400 mg, 2.20 mmol). The reaction mixture was stirred vigorously for 5 min after which, EDDA (60 mg, 0.33 mmol) was added in a single portion. The mixture was stirred at room temperature for 4 h. The solvent was removed under reduced pressure. Excess hexanal was removed on the rotary evaporator and on a high vacuum pump. Unreacted caryophyllene (**2.1**) was removed by eluting the reaction mixture through a pad of SiO_2 using neat petrol as the eluent. Trituration of the resulting mixture with diethyl ether yielded a mixture of diastereomers as an orange gum. These diastereomers were separated by flash chromatography using a Biotage Isolera™ One Flash Chromatography System with iLOK™ Empty Solid Load Cartridges, and Carl Roth silica gel 60 (230 - 400 mesh grade), and 1% Et_2O/petrol as eluent, to give **2.61** (400 mg, 0.85 mmol, 40%) as a yellow powder and **2.65** (139 mg, 0.30 mmol, 14%) as a yellow oil. To obtain single crystals suitable for X-ray analysis, littordial C (20 mg, 43 μmol) was dissolved in ethanol (0.5 mL) in a 5 mL vial and left at room temperature overnight to afford colourless prisms (10 mg, 50 %).

Data for 2.61:

Mp: 105 – 108 °C

R_f: 0.65 (5% EtOAc/petrol)

$[\alpha]_D^{25} = -50.4$ (c 1.0, CH_2Cl_2), c.f. $[\alpha]_D^{25} = +36.9$ (c 0.1, CH_2Cl_2) from Xu et al.

IR (neat): 2951, 1633, 1441, 1382, 1304, 1178, 890 cm^{-1}

^{1}H NMR (600 MHz, $CDCl_3$): δ 13.25 (s, 1H), 13.06 (s, 1H), 4.92 (s, 1H), 4.90 (s, 1H), 2.93 (m, 1H), 2.41 (q, J = 8.7 Hz, 1H), 2.32 (td, J = 13.1, 11.9, 3.2 Hz, 1H), 2.19 (dd, J = 16.8, 3.9 Hz, 1H), 2.02 (dd, J = 12.6, 9.2 Hz, 1H), 1.77 – 1.65 (overlapped, m, 5H), 1.61 – 1.53 (overlapped, m, 2H), 1.46 (s, 3H), 1.39 – 1.35 (overlapped, m, 3H), 1.31 – 1.22 (overlapped, m, 8H), 1.17 (overlapped, m, 1H), 0.97 (s, 3H), 0.92 (s, 3H), 0.85 (t, J = 7.1 Hz, 3H)

^{13}C NMR (150 MHz, $CDCl_3$): δ 192.2, 192.0, 168.0, 167.5, 164.0, 150.9, 111.3, 111.2, 105.8, 104.3, 88.2, 59.5, 47.8, 42.5, 40.7, 36.1, 35.6, 34.8, 32.3, 29.7, 29.6, 29.5, 28.6, 24.8, 23.6, 23.3, 22.8, 21.8, 14.2

HRMS (ESI) m/z: $[M + H]^+$ Calculated for $C_{29}H_{42}O_5$ 469.2949; found 469.2955

Data for 2.65:

R_f: 0.60 (5% EtOAc/petrol)

$[\alpha]_D^{25}$ = +45.1 (c .7, CH_2Cl_2), c.f. $[\alpha]_D^{25}$ = –16.7 (c 0.1, CH_2Cl_2) from Xu et al.

IR (neat): 2953, 2926, 1631, 1440, 1382, 1306, 1177, 855 cm^{-1}

^{1}H NMR (600 MHz, $CDCl_3$): δ 13.42 (s, 1H), 13.33 (s, 1H), 4.94 (s, 1H), 4.90 (s, 1H), 2.51 (dt, *J* = 13.9, 5.2 Hz, 1H), 2.46 (ddd, *J* = 9.2, 5.0, 2.6 Hz, 1H), 2.43 – 2.38 (m, 1H), 2.24 – 2.06 (overlapped, m, 4H), 2.01 (ddd, *J* = 11.8, 10.1, 5.5 Hz, 1H), 1.95 (ddd, *J* = 15.4, 5.6, 3.1 Hz, 1H), 1.84 (dddd, *J* = 15.1, 12.6, 5.5, 3.1 Hz, 1H), 1.71 (overlapped, m, 2H), 1.63 (dd, *J* = 10.7, 7.7 Hz, 1H), 1.59 – 1.53 (m, 1H), 1.48 – 1.37 (overlapped, m, 2H), 1.14 (m, 1H), 1.12 (s, 3H), 1.02 (overlapped, m, 1H), 1.01 (s, 3H), 1.00 (s, 3H), 0.84 (t, *J* = 7.1 Hz, 4H), 0.77 (m, 1H).

^{13}C NMR (150 MHz, $CDCl_3$): δ 192.4, 192.1, 169.1, 168.0, 164.6, 152.3, 110.5, 106.0, 105.0, 104.2, 84.0, 53.4, 42.8, 38.8, 37.9, 36.4, 35.7, 35.1, 33.8, 33.4, 32.3, 30.7, 29.0, 24.6, 22.8, 22.7, 22.3, 21.6, 14.3

HRMS (ESI) m/z: $[M+H]^+$ Calculated for $C_{29}H_{42}O_5$ 469.2949; found 469.2936

Synthesis of littordial A (2.59), littordial B (2.60) and littordial F (2.66)

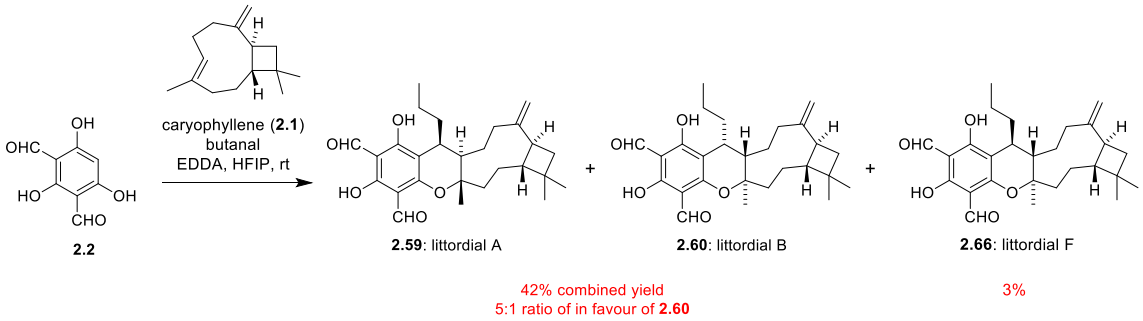

To a round-bottom flask open to air, was added (–)-caryophyllene (**2.1**) (1.73 mL, 8.23 mmol), HFIP (25 mL), and butanal (0.75 mL, 8.23 mmol). To this biphasic mixture was added **2.2** (500 mg, 2.75 mmol). The reaction mixture was stirred vigorously for 5 min after which EDDA (99.0 mg, 0.55 mmol) was added in a single portion. The mixture was stirred at room temperature for 4 h. The solvent was removed under reduced pressure. Excess butanal was removed on the rotary evaporator and on a high vacuum pump. Unreacted caryophyllene (**2.1**) was removed by eluting the reaction mixture through a pad of SiO_2 using petrol. Trituration of the resulting mixture with diethyl ether yielded a mixture of diastereomers as an orange gum. These compounds were separated by flash chromatography using a Biotage Isolera™ One Flash Chromatography System with iLOK™ Empty Solid Load Cartridges, and Carl Roth silica gel 60 (230 - 400 mesh grade), and with 1% Et_2O/petrol as eluent, to give **2.66** (40.8 mg, 0.09 mmol, 3%) as a pale yellow oil and an inseparable mixture of **2.59** and **2.60** (5:1 ratio in favour of littordial B, 492 mg, 1.15 mmol, 42%) as a yellow powder.

Data for 2.66:

R_f: 0.60 (5% EtOAc/petrol)

$[\alpha]_D^{25}$ = +44.4 (c 0.62, CH_2Cl_2), c.f. $[\alpha]_D^{25}$ = –42.0 (c 0.2, CH_2Cl_2) from Zhu et al.

IR (neat): 2954, 2929, 1631, 1441, 1383, 1306, 1178, 846 cm^{-1}

^{1}H NMR (600 MHz, $CDCl_3$): δ 13.42 (s, 1H), 13.32 (s, 1H), 10.16 (s, 1H), 10.01 (s, 1H), 4.95 (s, 1H), 4.90 (s, 1H), 2.51 (dt, *J* = 13.9, 5.4, 1H), 2.47 (m, 1H), 2.41 (m, 1H), 2.22 – 2.10 (overlapped, 4H), 1.99 (m, 1H), 1.95 (ddd, *J* = 15.4, 5.7, 3.0 Hz, 2H), 1.84 (dddd, *J* = 15.1, 12.2, 5.3, 3.0 Hz, 1H), 1.72 – 1.69 (overlapped, m, 2H), 1.63 (dd, *J* = 10.7, 7.7 Hz, 1H), 1.57 (m, 1H), 1.43 (m, overlapped, 1H), 1.12 (s, 3H), 1.04 (m, 1H), 1.01 (s, 3H), 1.00 (s, 3H), 0.83 (overlapped, m, 1H), 0.81 (overlapped, m, 3H)

^{13}C NMR (150 MHz, $CDCl_3$): δ 192.3, 192.1, 169.1, 168.0, 164.6, 152.4, 110.5, 106.1, 105.0, 104.2, 84.1, 53.6, 42.7, 39.0, 38.1, 36.4, 35.8, 35.2, 33.8, 33.2, 31.7, 30.7, 22.7, 22.3, 21.5, 18.4, 14.6

HRMS (ESI) m/z: $[M + H]^+$ Calculated for $C_{27}H_{38}O_5$ 441.2636; found 441.2640

Synthesis of dimethylphloroglucinol (2.81)

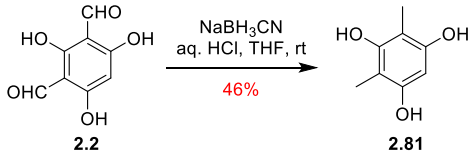

To a stirred solution of **2.2** (5.47 g, 30.0 mmol) and $NaBH_3CN$ (9.42 g, 150 mmol) in THF (85 mL) was added 3M HCl (50 mL, 150 mmol) dropwise. The reaction mixture was stirred at room temperature for 3 h. Upon completion, the mixture was diluted with H_2O and extracted with EtOAc (3 x 150 mL). The combined organic extracts were washed with H_2O (150 mL), brine (2 x 150 mL), dried over anhydrous $MgSO_4$, filtered and concentrated *in vacuo*. The crude residue was purified by flash column chromatography on SiO_2 (petrol/EtOAc, 5:1) to afford **2.81** (2.12 g, 13.8 mmol, 46%) as a pale orange solid. Data for **2.81** matched that of published literature.[29]

Mp: 158.6 – 161.0 °C

R_f: 0.50 (petrol/EtOAc, 1:1)

IR (neat): 3525, 3423, 2942, 1611, 1511, 1460, 1280, 1249, 1150 cm^{-1}

^{1}H NMR (500 MHz, CD_3OD): δ 5.97 (s, 1H), 2.00 (s, 6H)

^{13}C NMR (125 MHz, CD_3OD): δ 154.3, 104.2, 96.1, 8.5

Synthesis of *ortho*-quinone methide precursor (2.73)

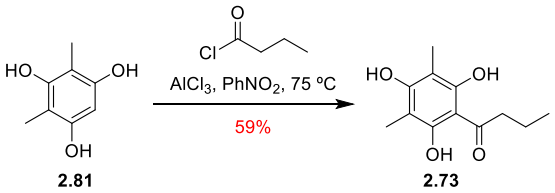

To a stirred of solution of **2.81** (258 mg, 1.67 mmol) in $PhNO_2$ (6 mL) at 0 °C, was added $AlCl_3$ (885 mg, 6.64 mmol). This mixture was stirred at 0 °C for 10 min. Butyryl chloride (0.19 mL, 1.83 mmol) was added dropwise to the reaction which was then warmed to 75 °C using an aluminium heating block and stirred for 3.5 h. The resulting dark red solution was cooled to room temperature and diluted with cold water. This mixture was extracted with EtOAc (3 x 20 mL). The combined organic phases were extracted with 1M NaOH (2 x 15 mL). The aqueous extracts were acidified by conc. HCl. The aqueous layer was extracted with EtOAc (3 x 20 mL). The combined organic extracts were dried over $MgSO_4$, filtered, and concentrated *in vacuo*. The crude residue was purified by flash column chromatography on SiO_2 (pet/EtOAc, 10:1 → 4:1 gradient elution) to afford **2.73** (223 mg, 0.99 mmol, 59%) as a pale orange solid. Data for **2.73** matched that of published literature.[30]

Mp: 136.4 – 138.6 °C

R_f: 0.30 (petrol/EtOAc, 4:1)

IR (neat): 3468, 2964, 2875, 1612, 1432, 1379, 1320, 1284, 1238, 1199, 1159 cm^{-1}

^{1}H NMR (500 MHz, d_6-DMSO): δ 11.49 (s, 2H), 9.20 (s, 1H), 3.04 (t, J = 7.3 Hz, 2H), 1.96 (s, 6H), 1.62 (h, J = 7.3 Hz, 1H), 0.91 (t, J = 7.3 Hz, 3H)

^{13}C NMR (125 MHz, d_6-DMSO): δ 206.0, 160.3, 158.4, 105.3, 102.6, 45.5, 18.0, 14.0, 8.6

HRMS (ESI) m/z: $[M+H]^+$ Calculated for $C_{12}H_{17}O_4$ 225.1121; found 225.1116

Synthesis of drychampone B (2.75)

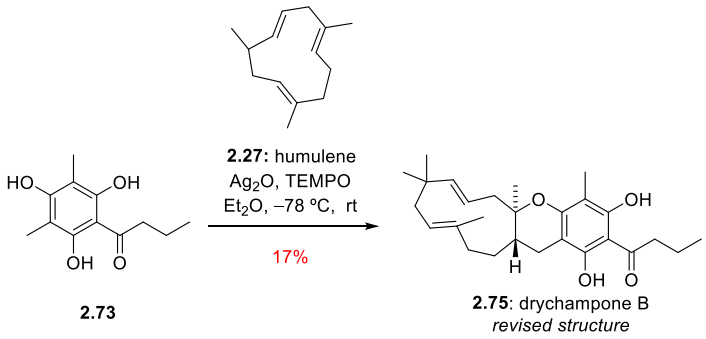

To a solution of **2.73** (53.8 mg, 0.24 mmol) and humulene (**2.27**) (0.07 mL, 0.30 mmol) in Et_2O (5 mL) at −78 °C in a cooling bath of dry ice and acetone was added Ag_2O (69 mg, 0.30 mmol) and TEMPO (78.3 mg, 0.50 mmol). The reaction was stirred at −78 °C for 1 h, then slowly warmed to room temperature where it was stirred for a further 16 h. The mixture was filtered and concentrated *in vacuo*. The crude residue was purified by flash column chromatography on SiO_2 (1:0 → 30:1 petrol/EtOAc gradient elution) to yield **2.75** as a yellow gum (18.8 mg, 0.04 mmol, 17%).

R_f: 0.65 (petrol/EtOAc, 5:1)

IR (neat): 3520, 3422, 2932, 1610, 1421, 1379, 1202, 1159, 1106 cm^{-1}

^{1}H NMR (600 MHz, $CDCl_3$): δ 5.18 – 5.14 (m, 2H), 5.03 (m, 1H), 3.00 (td, *J* = 7.4, 3.8 Hz, 2H), 2.92 (dd, *J* = 16.1, 5.7 Hz, 1H), 2.60 (d, *J* = 14.5 Hz, 1H), 2.37 (ddd, *J* = 14.5, 7.1, 3.0 Hz, 1H), 2.19 (t, *J* = 12.4 Hz, 1H), 2.16 – 2.09 (m, 1H), 2.07 (overlapped, 4H), 1.89 – 1.82 (m, 2H), 1.77 (dd, *J* = 12.9, 4.4 Hz, 1H), 1.70 (q, *J* = 7.4 Hz, 2H), 1.63 (s, 3H), 1.34 (m, 1H), 1.21 – 1.15 (m, 1H), 1.14 (s, 3H), 1.06 (s, 3H), 1.02 (s, 3H), 0.97 (t, *J* = 7.4 Hz, 3H)

^{13}C NMR (150 MHz, $CDCl_3$): δ 206.4, 162.8, 157.5, 154.7, 143.1, 136.7, 123.2, 120.2, 105.8, 101.5, 99.5, 82.2, 46.7, 42.9, 41.5, 38.4, 37.9, 34.8, 30.5, 30.4, 24.4, 23.9, 20.1, 19.0, 17.3, 14.2, 7.2

HRMS (ESI) m/z: $[M+H]^+$ Calculated for $C_{27}H_{40}O_4$ 427.2843; found 427.2837

2.10 References

1. Collado, I. G.; Hanson, J. R.; Macías-Sanchez, A. J. Recent advances in the chemistry of caryophyllene. *Nat. Prod. Rep*. **1998**, *15*, 187.
2. Hübner, M.; Rissom, B.; Fitjer, L. Conformation and Dynamics of (−)-*β*-Caryophyllene. *Helv. Chim. Acta* **1997**, *80*, 1972.
3. Shao, M.; Wang, Y.; Liu, Z.; Zhang, D.; Cao, H.; Jiang, R.; Fan, C.; Zhang, X.; Chen, H.; Yao, X.; Ye, W. Psiguadials A and B, Two Novel Meroterpenoids with Unusual Skeletons from the Leaves of *Psidium Guajava*. *Org. Lett.* **2010**, *12*, 5040.
4. Chapman, L.; Beck, J.; Wu, L.; Reisman, S. Enantioselective Total Synthesis of (+)-Psiguadial B. *J. Am. Chem. Soc*. **2016**, *138*, 9803.
5. Weyerstahl, P.; Schneider, S.; Marschall, H. Constituents of the Brazilian *Cangerana* Oil. *Flavour Fragr. J.* **1996**, *11*, 81.
6. Newton, C. G.; Tran, D. N.; Wodrich, M. D.; Cramer, N. One-Step Multigram-Scale Biomimetic Synthesis of Psiguadial B. *Angew. Chem. Int. Ed*. **2017**, *56*, 13776.
7. Qin, X.- J.; Rauwolf, T. J.; Li, P.-P.; Liu, H.; McNeely, J.; Hua, Y.; Liu, H.-Y.; Porco, J. A., Jr. Isolation and Synthesis of Novel Meroterpenoids from *Rhodomyrtus tomentosa*: Investigation of a reactive Enetrione Intermediate. *Angew. Chem. Int. Ed*. **2019**, *58*, 4291.
8. Liu, H.-X.; Chen, K.; Yuan, Y.; Xu, Z.-F.; Tan, H.-B.; Qiu, S.-X. Rhodomentones A and B, novel meroterpenoids with unique NMR characteristics from *Rhodomyrtus tomentosa*. *Org. Biomol. Chem.* **2016**, *14*, 7354
9. Katsiotis, S.; Langezaal, C.; Scheffer, J. Analysis of the Volatile Compounds from Cones of Ten *Humulus Lupulus* Cultivars. *Planta Medica* **1989**, *55,* 634.
10. Zigon, N.; Hoshino, M.; Yoshioka, S.; Inokuma, Y.; Fujita, M. Where is the Oxygen? Structural Analysis of *α*-Humulene Oxidation Products by the Crystalline Sponge Method. *Angew. Chem. Int. Ed.* **2015**, *54,* 9033.
11. Neuenschwander, U.; Czarniecki, B.; Hermans, I. Origin of Regioselectivity in *α*-Humulene Functionalization. *J. Org. Chem.* **2012**, *77*, 2865.
12. Shirahama, H.; Osawa, E.; Matsumoto, T. Conformational studies on humulene by means of empirical force field calculations. Role of stable conformers of humulene in biosynthetic and chemical reactions. *J. Am. Chem. Soc*. **1980**, *102*, 3208.
13. Adlington, R. M.; Baldwin, J. E.; Pritchard, G. J.; Williams, A. J.; Watkin, D. J. A Biomimetic Synthesis of Lucidene. *Org. Lett.* **1999**, *1*, 1937.
14. Baldwin, J. E.; Mayweg, A. V. W.; Neumann, K.; Pritchard, G. J. Studies toward the Biomimetic Synthesis of Tropolone Natural Products via a Hetero Diels−Alder Reaction. *Org. Lett*. **1999**, *1*, 1933.
15. Lam, H. C.; Spence, J. T. J.; George, J. H. Biomimetic Total Synthesis of Hyperjapones A-E and Hyperjaponols A and C. *Angew. Chem. Int. Ed.* **2016**, *55*, 10368.
16. Tantillo, D. The Carbocation Continuum In Terpene Biosynthesis—Where Are The Secondary Cations? *Chem. Soc. Rev.* **2010**, *39*, 2847.

17. Ainsworth, A.; Chicarelli-Robinson, M.; Copp, B.; Fauth, U.; Hylands, P.; Holloway, J.; Latif, M.; O'beirne, G.; Porter, N.; Renno, D.; Richards, M.; Robinson, N. Xenovulene A, A Novel GABA-Benzodiazepine Receptor Binding Compound Produced by *Acremonium Strictum*. *J. Antibiot.* **1995**, *48*, 568.

18. Qi, Q.-Y.; Bao, L.; Ren, J.-W.; Han, J.-J.; Zhang, Z.-Y.; Li, Y.; Yao, Y.-J.; Cao, R.; Liu, H.-W. Sterhirsutins A and B, Two New Heterodimeric Sesquiterpenes with a New Skeleton from the Culture of *Stereum hirsutum* Collected in Tibet Plateau. *Org. Lett*. **2014**, *16*, 5092.

19. Li, P.-J.; Dräger, D.; Kirschning, A. A General Biomimetic Hetero-Diels−Alder Approach to the Core Skeletons of Xenovulene A and the Sterhirsutins A and B. *Org. Lett*. **2019**, *21*, 998.

20. Xu, J.; Zhu, H.-L.; Zhang, J.; Liu, W.-Y.; Luo, J.-G.; Pan, K.; Cao, W.-Y.; Bi, Q.-R.; Feng, F.; Qu, W. Littordials A−E, novel formyl- phloroglucinol-β-caryophyllene meroterpenoids from the leaves of *Psidium littorale*. *Org. Chem. Front.* **2019**, *6*, 1667.

21. Zhu, H.-L.; Hu, Y.-W.; Qu, W.; Zhang, J.; Guo, E.-Y.; Jiang, X.-Y.; Liu, W.-Y.; Feng, F.; Xu, J. Littordial F, a novel phloroglucinol meroterpenoid from the leaves of *Psidium littorale*. *Tetrahedron Lett.* **2019**, *60*, 1868.

22. Ning, S.; Liu, Z.; Wang, Z.; Liao, M.; Xie, Z. Biomimetic Synthesis of Psiguajdianone Guided Discovery of the Meroterpenoids from *Psidium guajava*. *Org. Lett.* **2019**, *21*, 8700.

23. Lv, L.; Li, Y.; Zhang, Y.; Xie, Z. Biomimetic synthesis of myrtucommulone K, N and O. *Tetrahedron* **2017**, *73*, 3691.

24. Lawrence, A. L.; Adlington, R. M.; Baldwin, J. E.; Lee, V.; Kershaw, J. A.; Thompson, A. L. A Short Biomimetic Synthesis of the Meroterpenoids Guajadial and Psidial A. *Org. Lett*. **2010**, *12*, 1676.

25. Dittmer, C.; Raabe, G.; Hintermann, L. Asymmetric Cyclization of 2′-Hydroxychalcones to Flavanones: Catalysis by Chiral Brønsted Acids and Bases. *Eur. J. Org. Chem*. **2007**, 5886

26. Joyce, L. A.; Nawrat, C. C.; Sherer, E. C.; Biba, M.; Brunskill, A.; Martin, G. E.; Cohen, R. D.; Davies, I. W. Beyond optical rotation: what's left is not always right in total synthesis. *Chem. Sci.* **2018**, *9*, 415.

27. Wang, H.; Wang, Y.; Han, K.-L.; Peng, X.-J. A DFT Study of Diels−Alder Reactions of o-Quinone Methides and Various Substituted Ethenes: Selectivity and Reaction Mechanism. *J. Org. Chem.* **2005**, *70*, 4910.

28. Chen, N.-H.; Zhang, Y.-B.; Huang, X.-J.; Jiang, L.; Jiang, S.-Q.; Li, G.-Q.; Li, Y.-L.; Wang, G.-C. Drychampones A−C: Three Meroterpenoids from *Dryopteris championii*. *J. Org. Chem.* **2016**, *81*, 9443.

29. Jung, J.-W.; Damodar, K.; Kim, J.-K.; Jun, J.-G. First synthesis and in vitro biological assessment of isosideroxylin, 6,8-dimethylgenistein and their analogues as nitric oxide production inhibition agents. *Chin. Chem. Lett.* **2017**, *28*, 1114.

30. Wu, J.; Mu, R.; Sun, M.; Zhao, N.; Pan, M.; Li, H.; Dong, Y.; Sun, Z.; Bai, J.; Hu, M.; Nathan, C. F.; Javid, B.; Liu, G. Derivatives of Natural Product Agrimophol as Disruptors of Intrabacterial pH Homeostasis in Mycobacterium tuberculosis. *ACS Infect. Dis*. **2019**, *5*, 1087.

31. Liao, D.; Li, H.; Lei, X. Efficient Generation of *ortho*-Quinone Methide: Application to the Biomimetic Syntheses of (±)-Schefflone and Tocopherol Trimers. *Org. Lett.* **2012**, *14*, 18

32. Sheldrick, G. M. Phase annealing in SHELX-90: direct methods for larger structures. *Acta Crystallogr. Sect. A* **1990**, *46*, 467.

33. Sheldrick, G. M. A short history of SHELX. *Acta Crystallogr. Sect. A* **2008**, *64*, 112.

34. Barbour, L. J. X-seed - A software tool for supramolecular crystallography. *J. Supramol. Chem.* **2001**, *1*, 189.

35. Bourhis, L. J.; Dolomanov, O. V.; Gildea, R. J.; Howard, J. A. K; Puschmann, H. The anatomy of a comprehensive constrained, restrained refinement program for the modern computing environment - Olex2 dissected. *Acta Crystallogr. Sect. A* **2015**, *71*, 59.

36. Zhao, Y.; Truhlar, D. The M06 suite of density functionals for main group thermochemistry, thermochemical kinetics, noncovalent interactions, excited states, and transition elements: two new functionals and systematic testing of four M06-class functionals and 12 other functionals. *Theor. Chem. Acc.* **2008**, *120*, 215.

37. Hratchian, H. P.; Schlegel, H. B. Accurate reaction paths using a Hessian based predictor–corrector integrator. *J. Chem. Phys.* **2004**, *120*, 9918

38. Marenich, A. V.; Cramer, C. J.; Truhlar, D. G. Universal Solvation Model Based on Solute Electron Density and on a Continuum Model of the Solvent Defined by the Bulk Dielectric Constant and Atomic Surface Tensions. *J. Phys. Chem. B* **2009**, *113*, 6378.

39. Richmond, E.; Yi, J.; Vuković, V. D.; Sajadi, F.; Rowley, C. N.; Moran, J. Ring-opening hydroarylation of monosubstituted cyclopropanes enabled by hexafluoroisopropanol. *Chem. Sci.* **2018**, *9*, 6411.

2.11 Supporting Information

2.11.1 NMR Spectra

Figure 2.19: ^{1}H NMR spectrum of diformylphloroglucinol (**2.2**) in d_6-DMSO

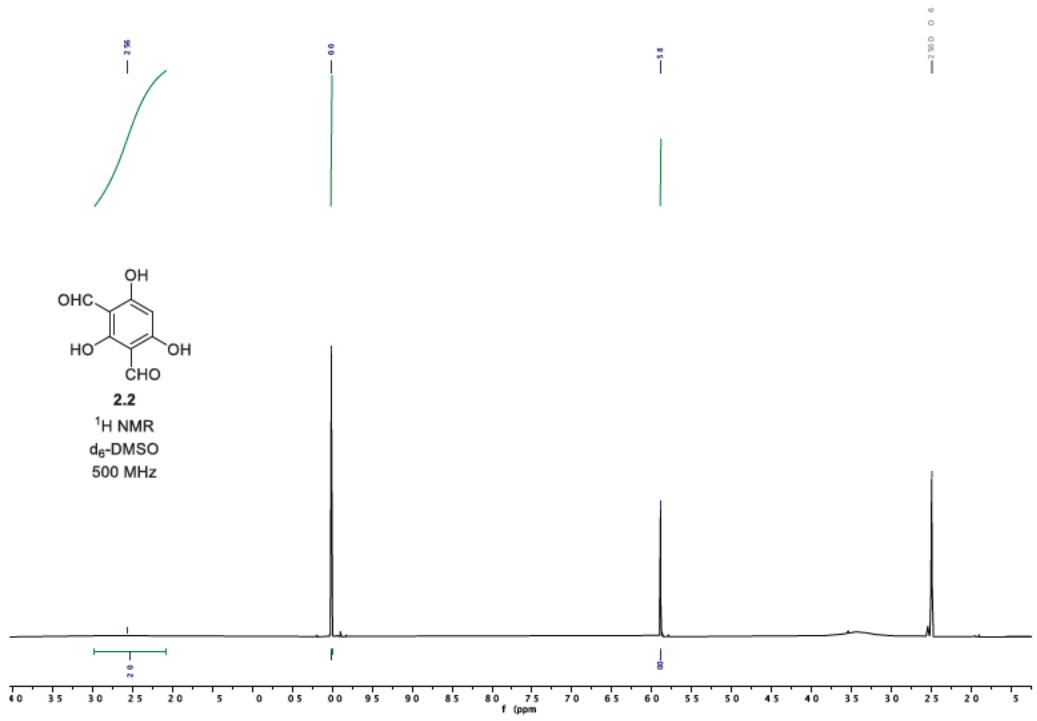

Figure 2.20: ^{13}C NMR spectrum of diformylphloroglucinol (**2.2**) in d_6-DMSO

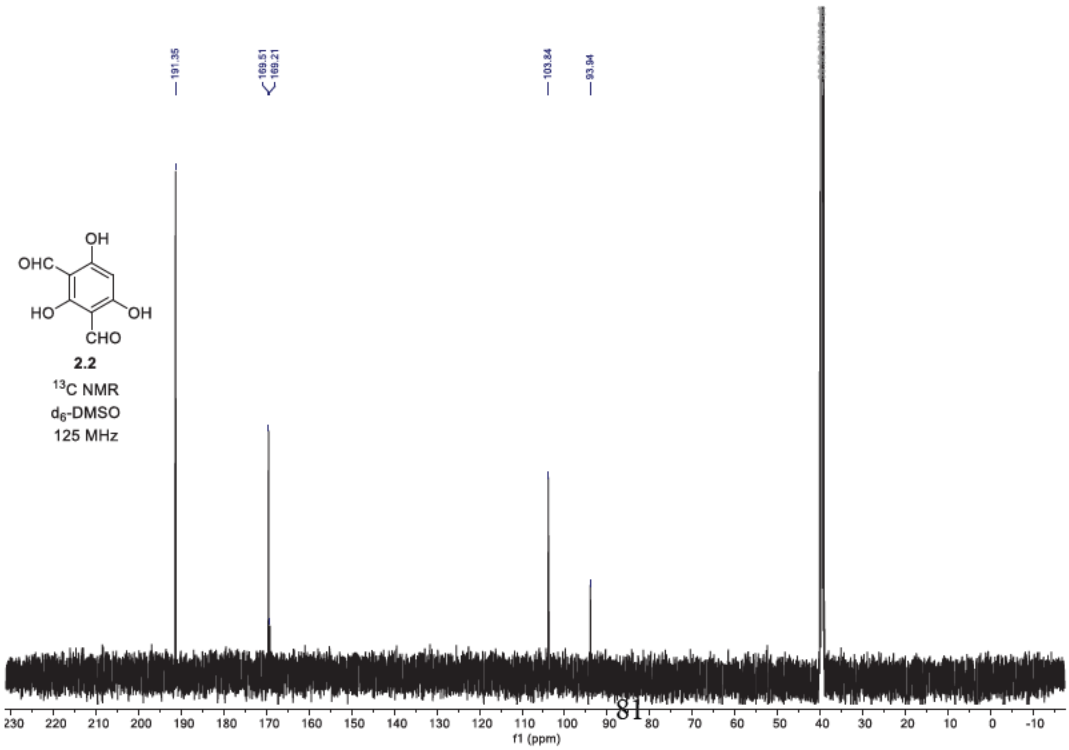

Figure 2.21: ^{1}H NMR spectrum of the mixture of littordials A (**2.59**) and B (**2.60**) in $CDCl_3$

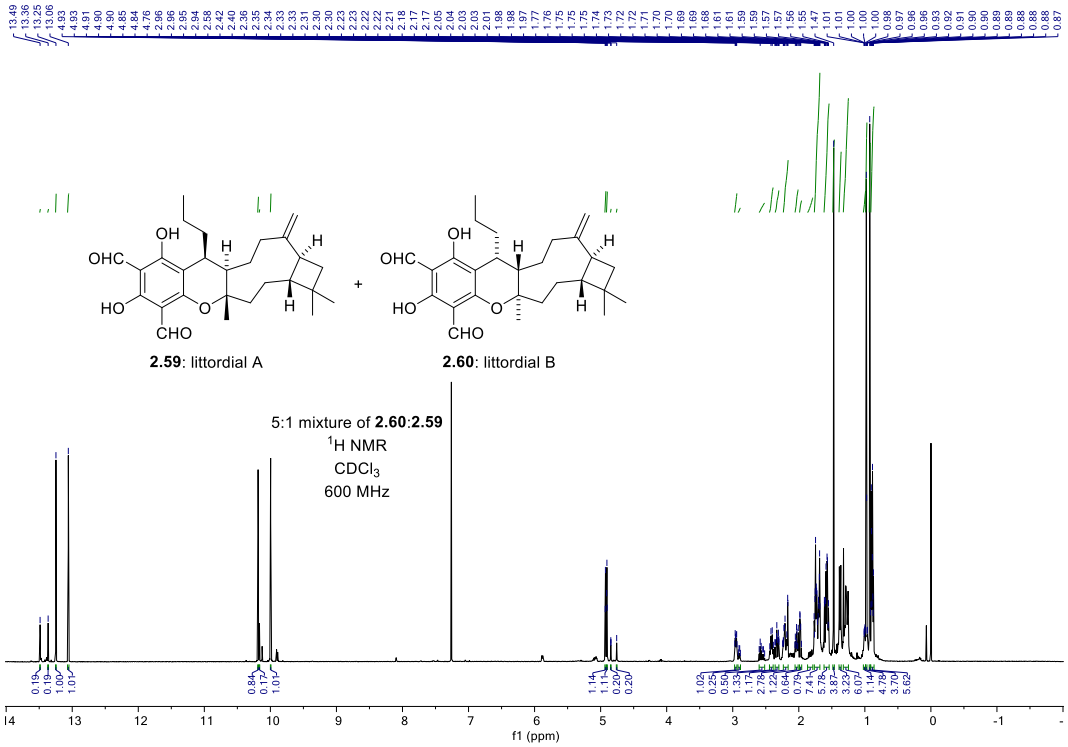

Figure 2.22: ^{13}C NMR spectrum of the mixture of littordials A (**2.59**) and B (**2.60**) in $CDCl_3$

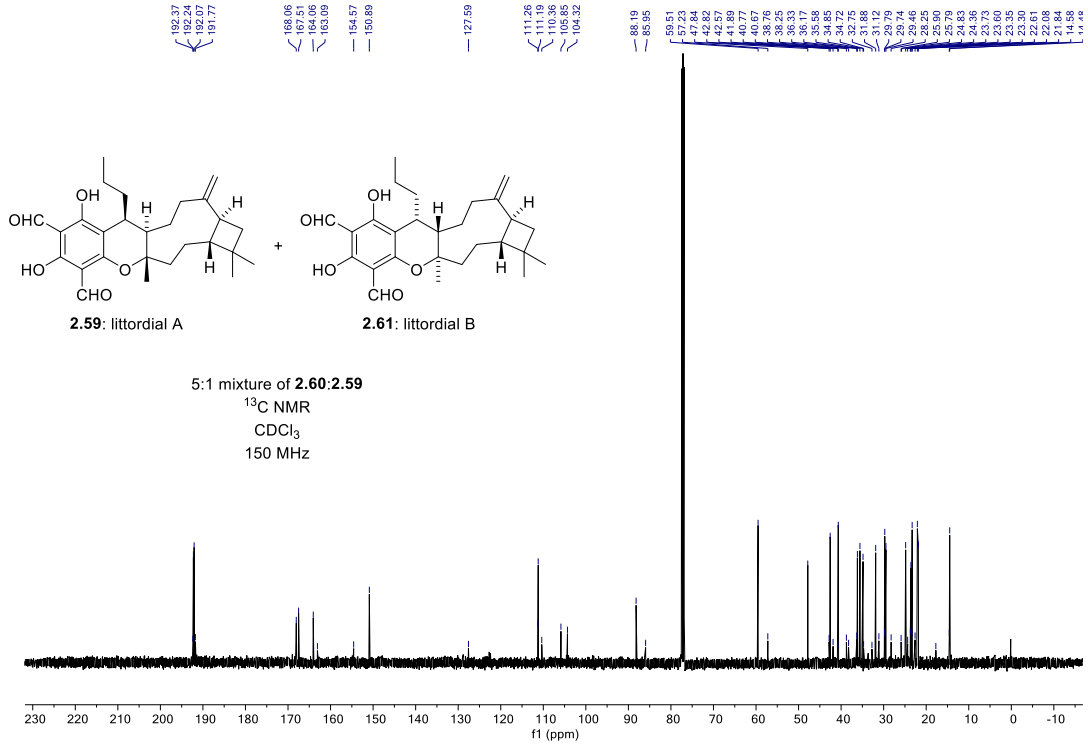

Figure 2.23: ^{1}H NMR spectrum of littordial C (**2.61**) in $CDCl_3$

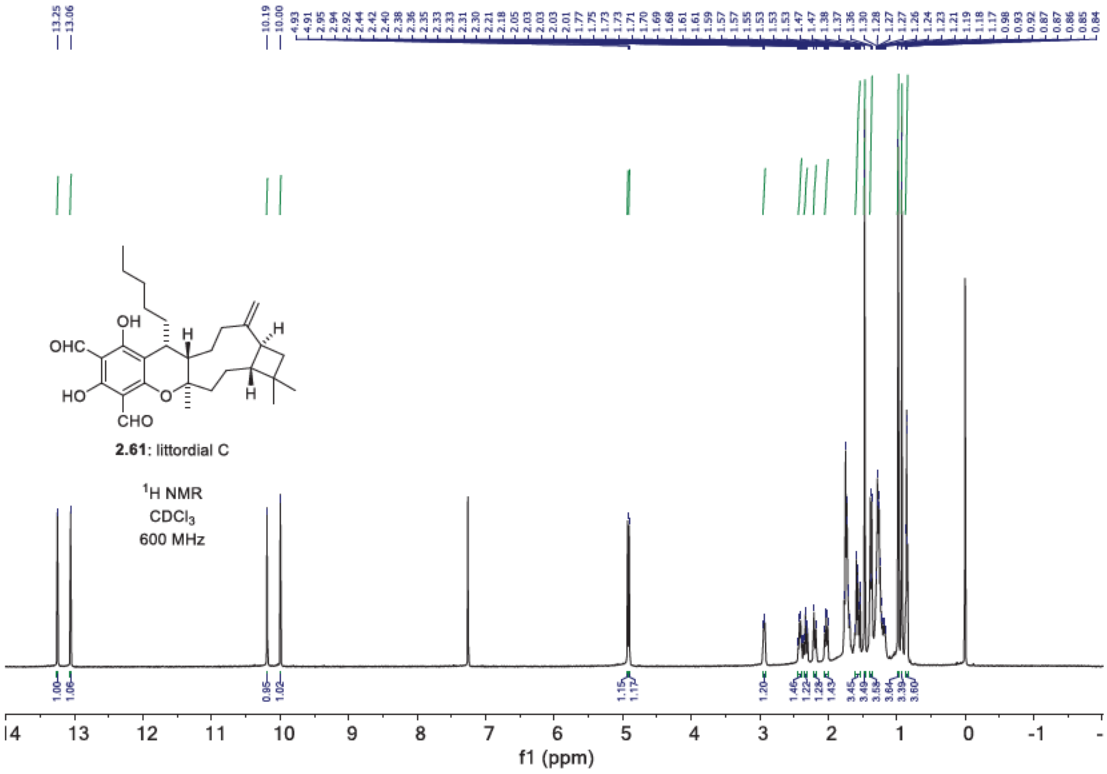

Figure 2.24: ^{13}C NMR spectrum of littordial C (**2.61**) in $CDCl_3$

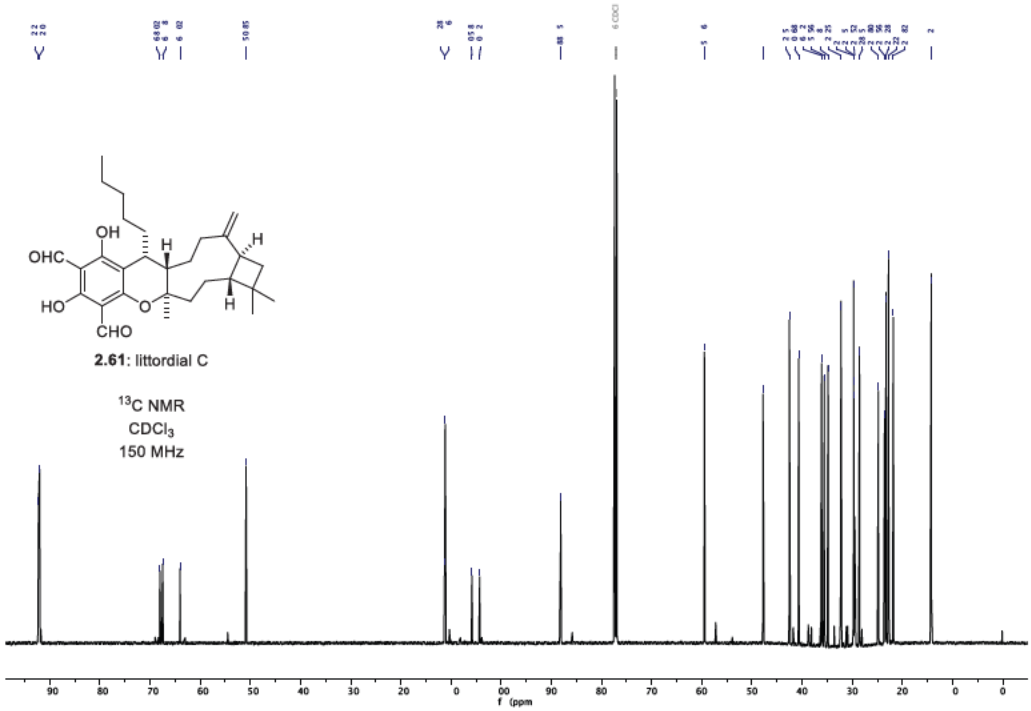

Figure 2.25: COSY spectrum of littordial C (**2.61**) in $CDCl_3$

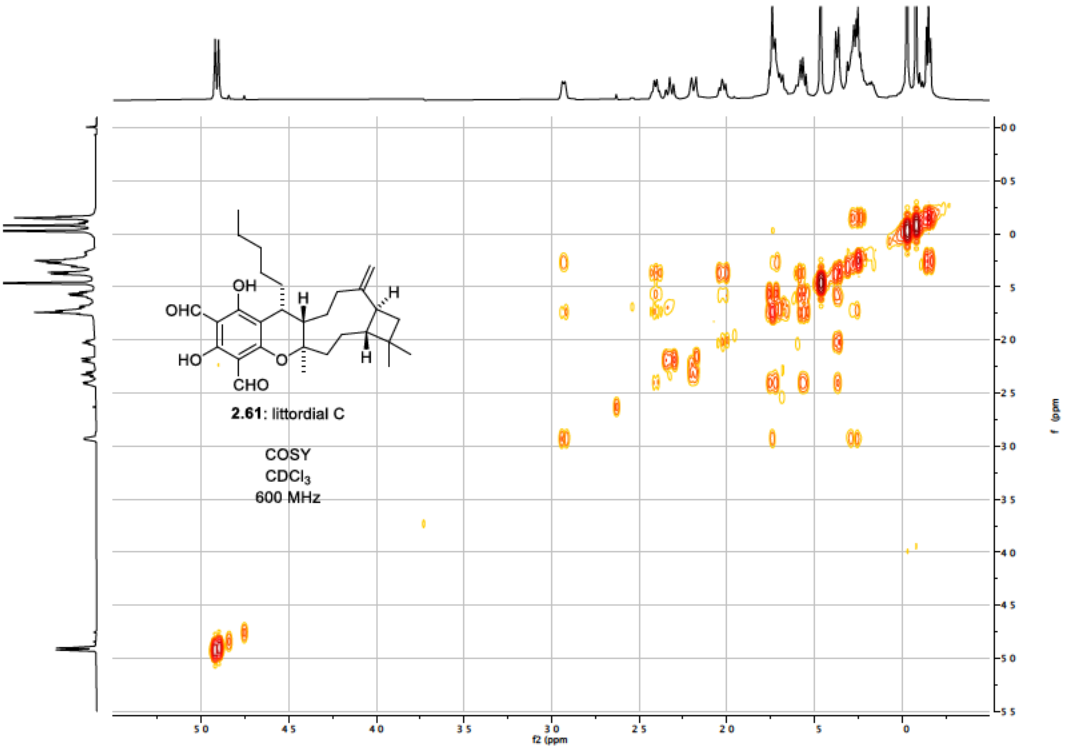

Figure 2.26: NOESY spectrum of littordial C (**2.61**) in $CDCl_3$

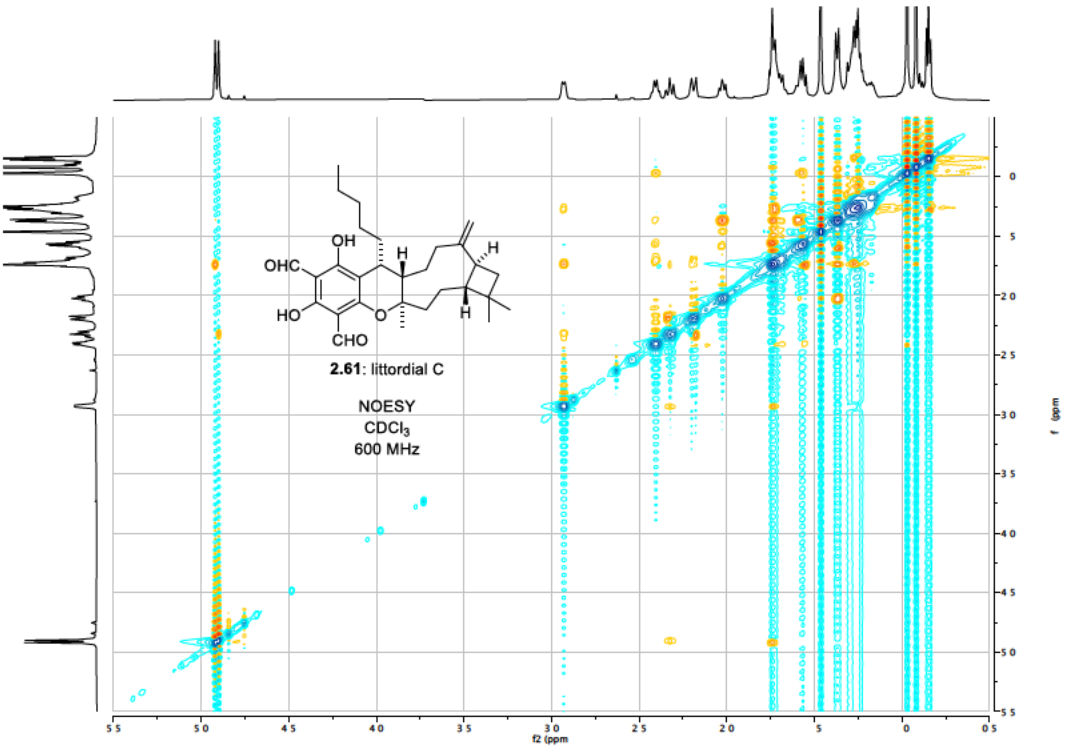

Figure 2.27: HSQC spectrum of littordial C (**2.61**) in $CDCl_3$

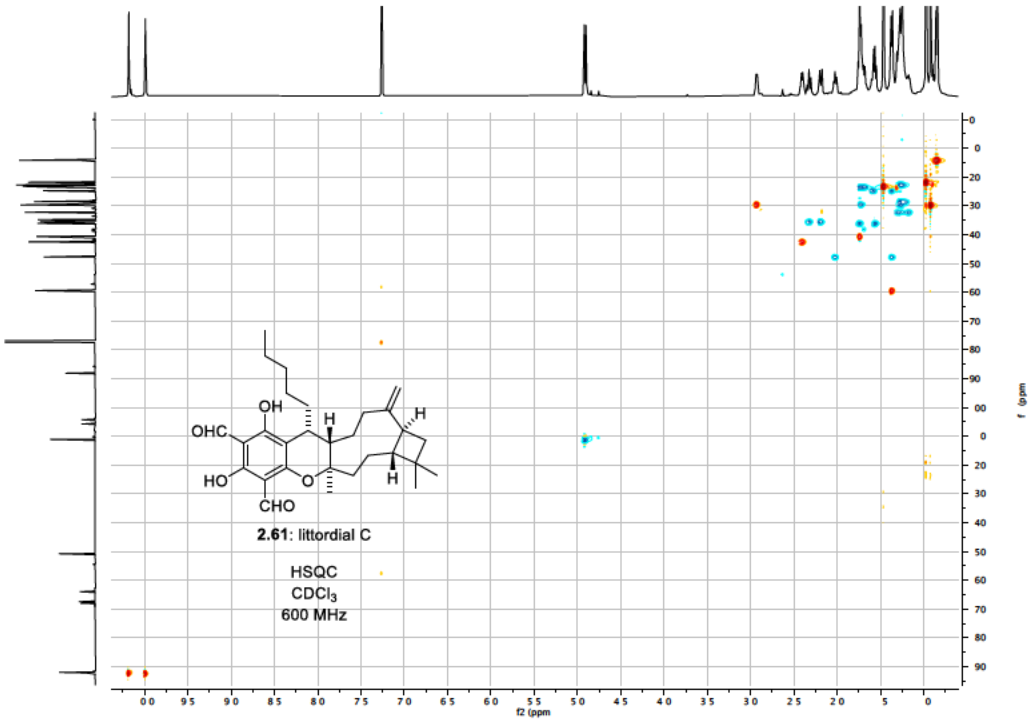

Figure 2.28: Enlarged section of the HSQC spectrum of littordial C (**2.61**) in $CDCl_3$

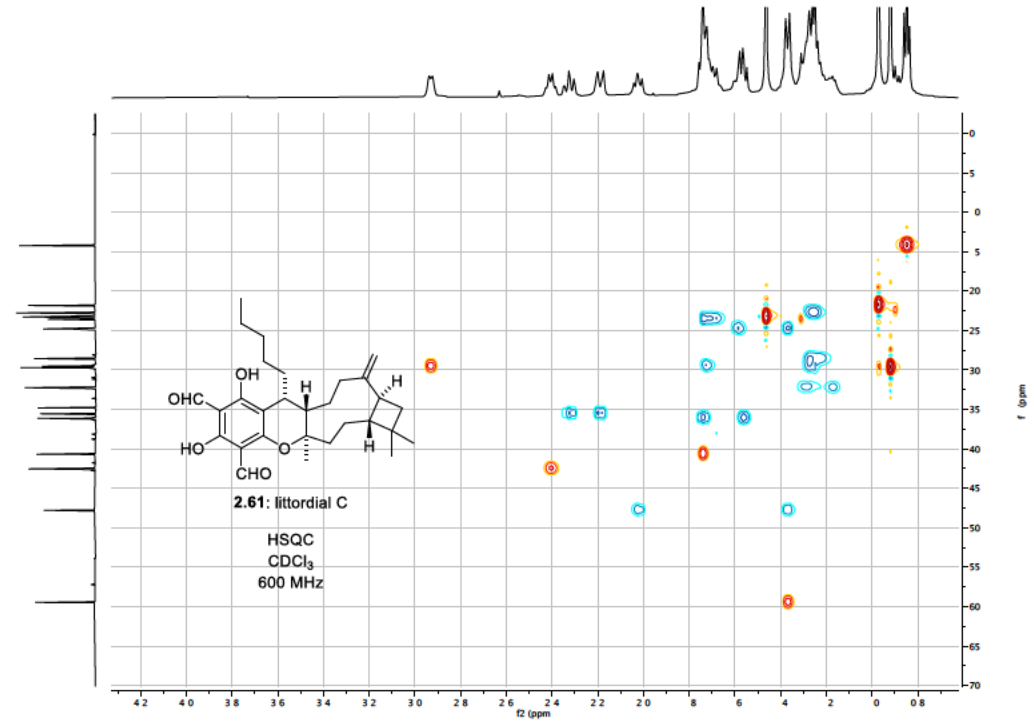

Figure 2.29: HMBC spectrum of littordial C (**2.61**) in $CDCl_3$

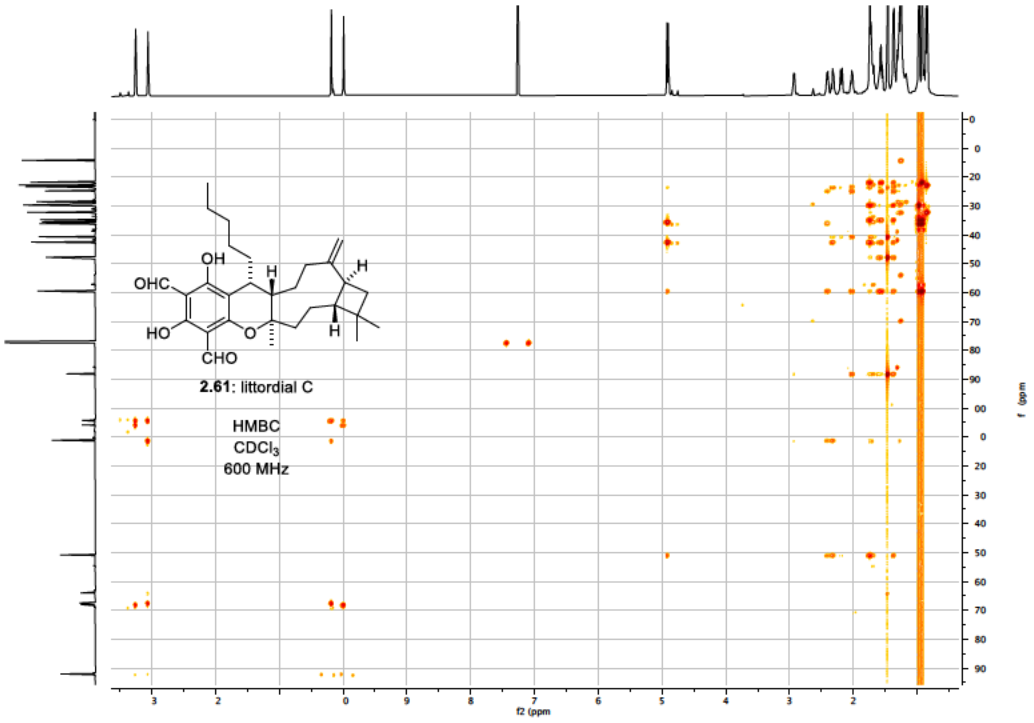

Figure 2.30: Enlarged section of the HMBC spectrum of littordial C (**2.61**) in $CDCl_3$

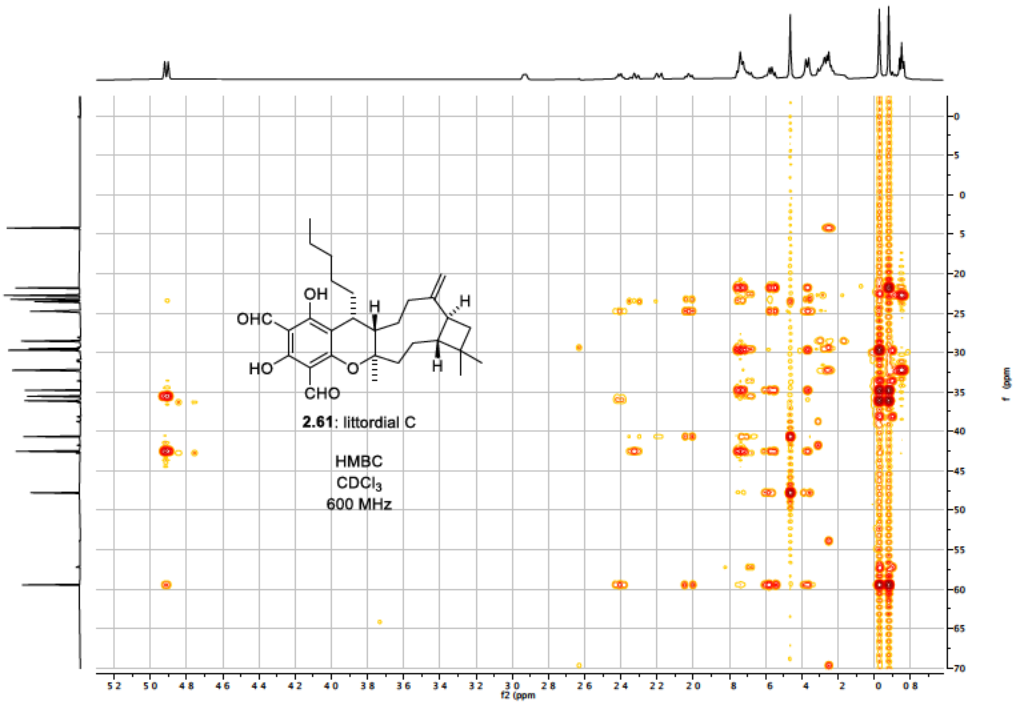

Figure 2.31: ^{1}H NMR spectrum of littordial E (**2.65**) in $CDCl_3$

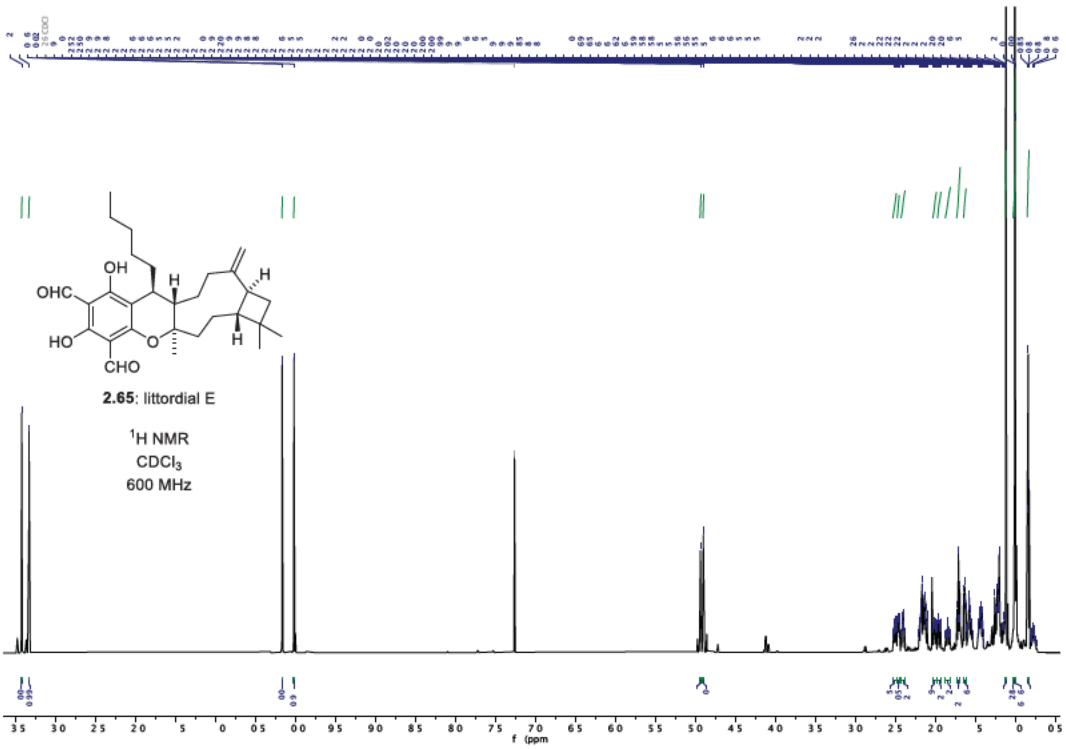

Figure 2.32: ^{13}C NMR spectrum of littordial E (**2.65**) in $CDCl_3$

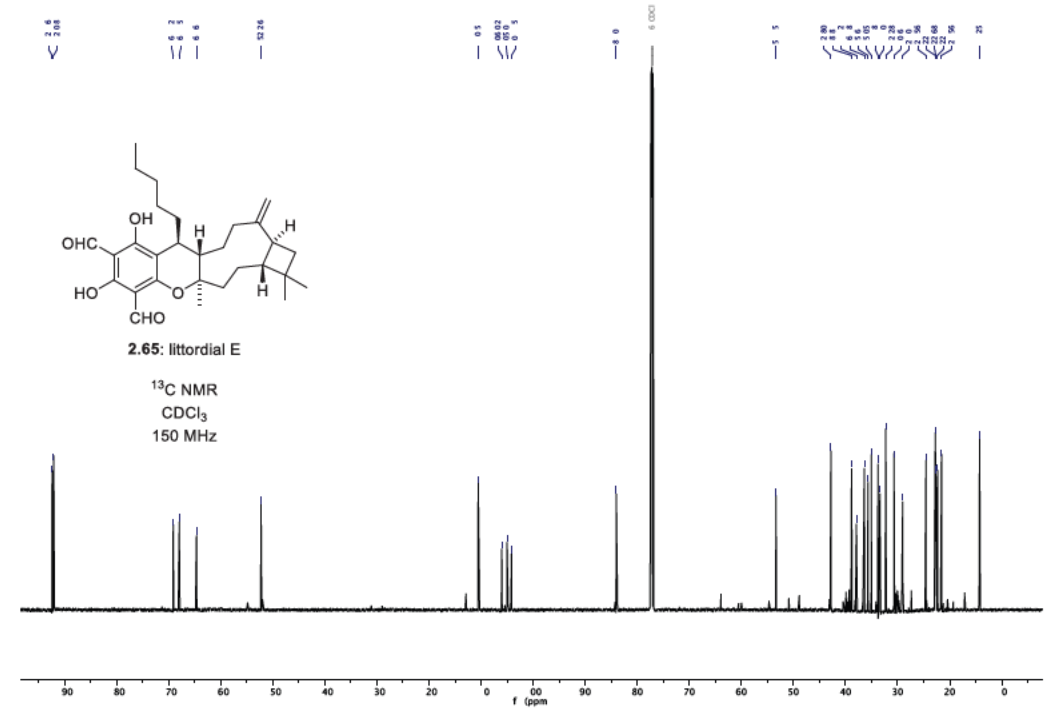

Figure 2.33: COSY spectrum of littordial E (**2.65**) in $CDCl_3$

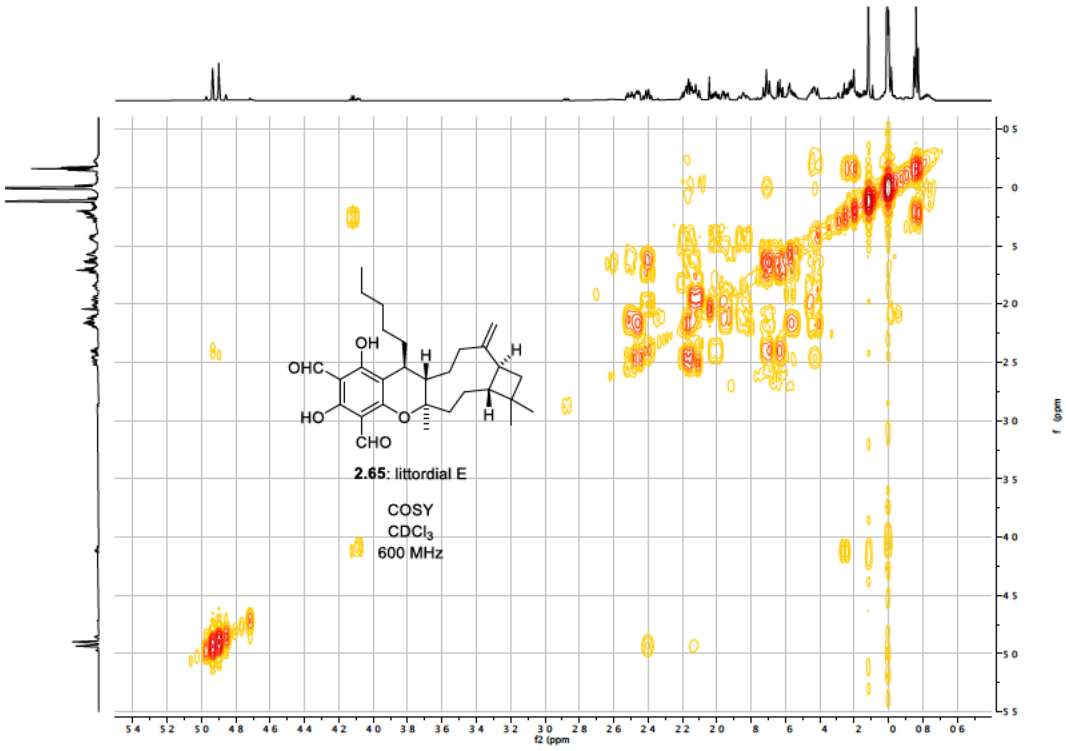

Figure 2.34: NOESY spectrum of littordial E (**2.65**) in $CDCl_3$

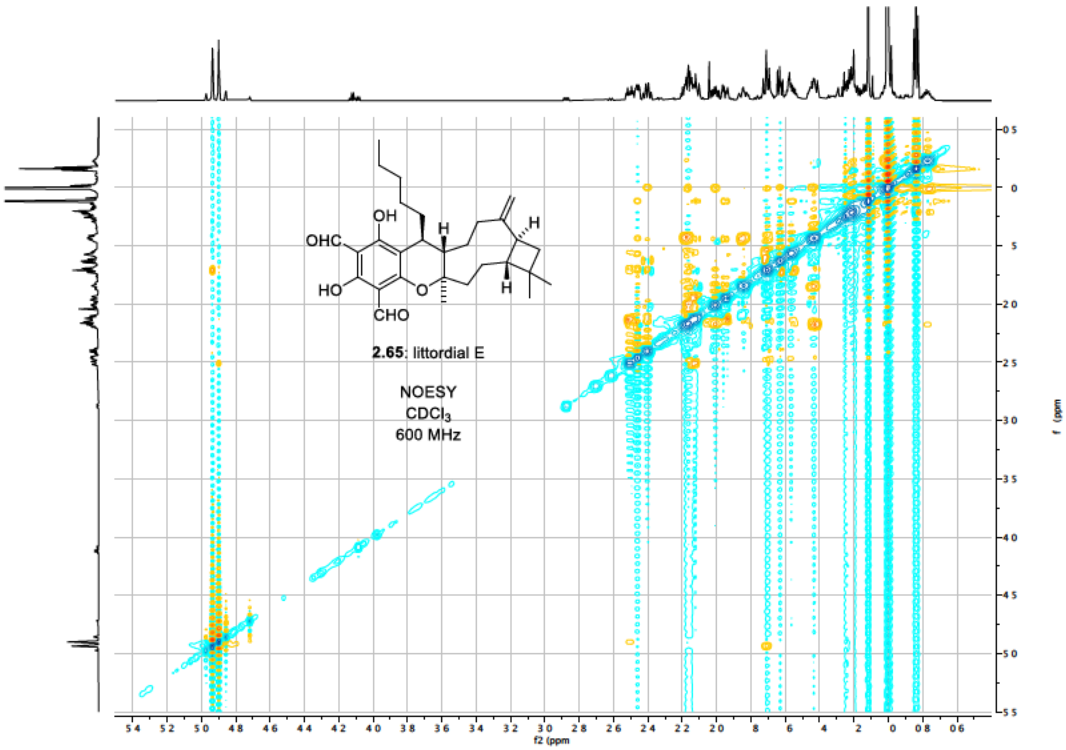

Figure 2.35: HSQC spectrum of littordial E (**2.65**) in $CDCl_3$

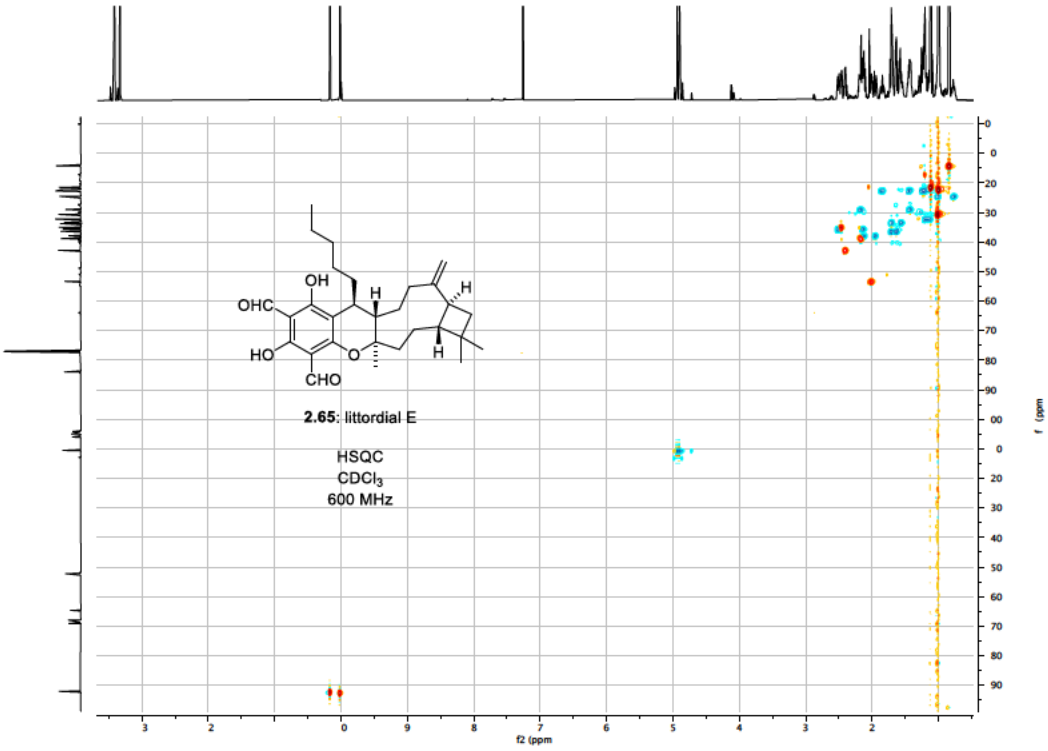

Figure 2.36: Enlarged section of the HSQC spectrum of littordial E (**2.65**) in $CDCl_3$

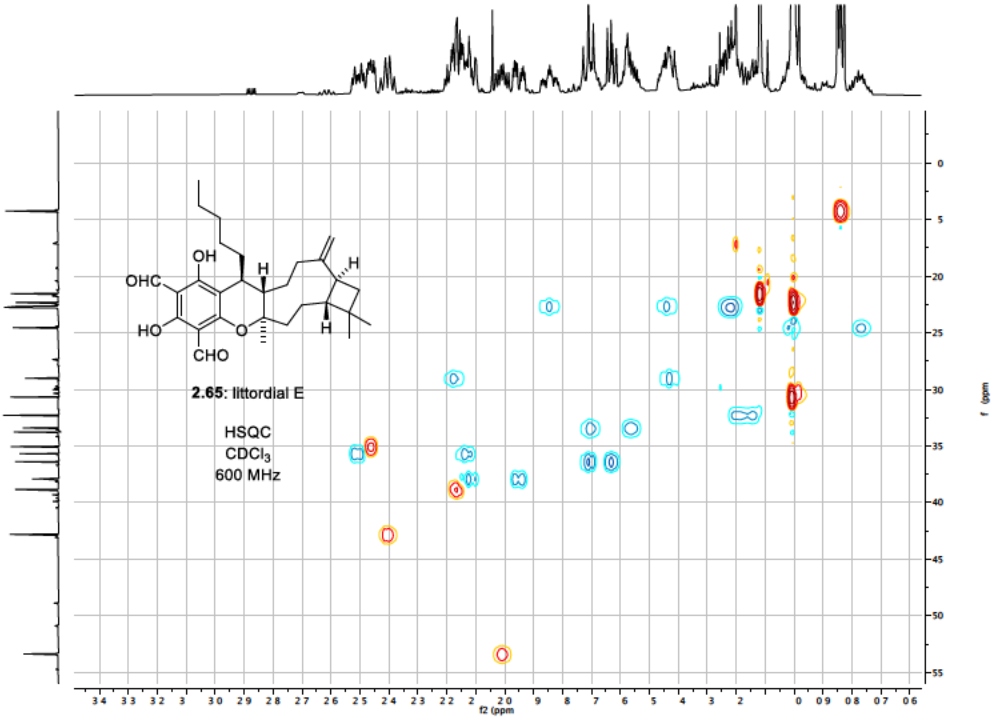

Figure 2.37: HMBC spectrum of littordial E (**2.65**) in $CDCl_3$

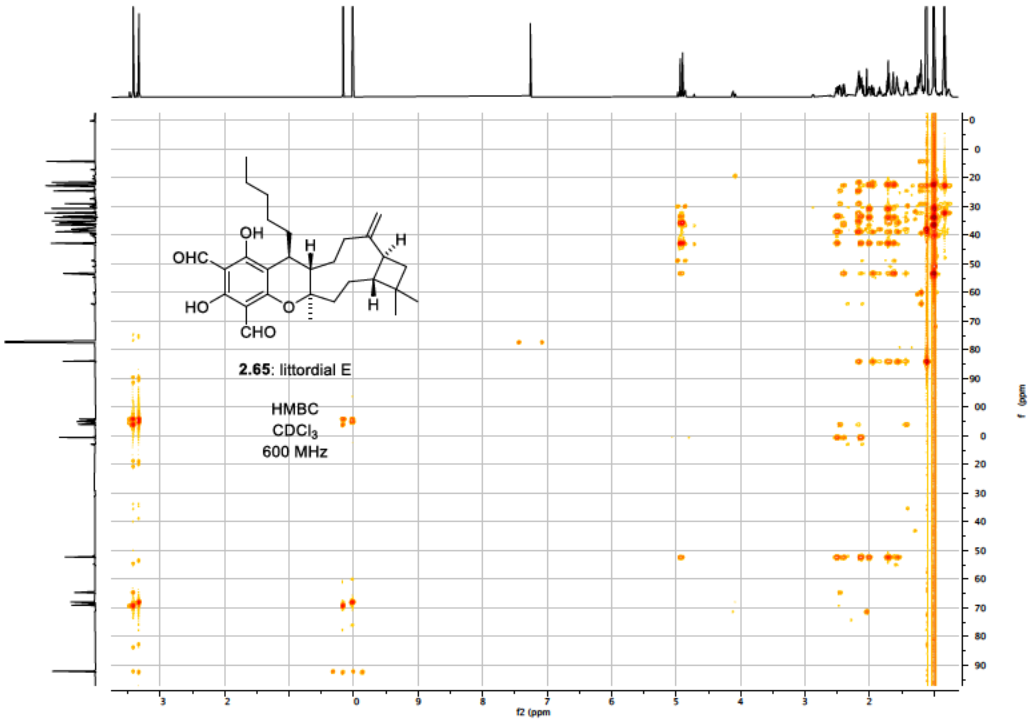

Figure 2.38: Enlarged section of the HMBC spectrum of littordial E (**2.65**) in $CDCl_3$

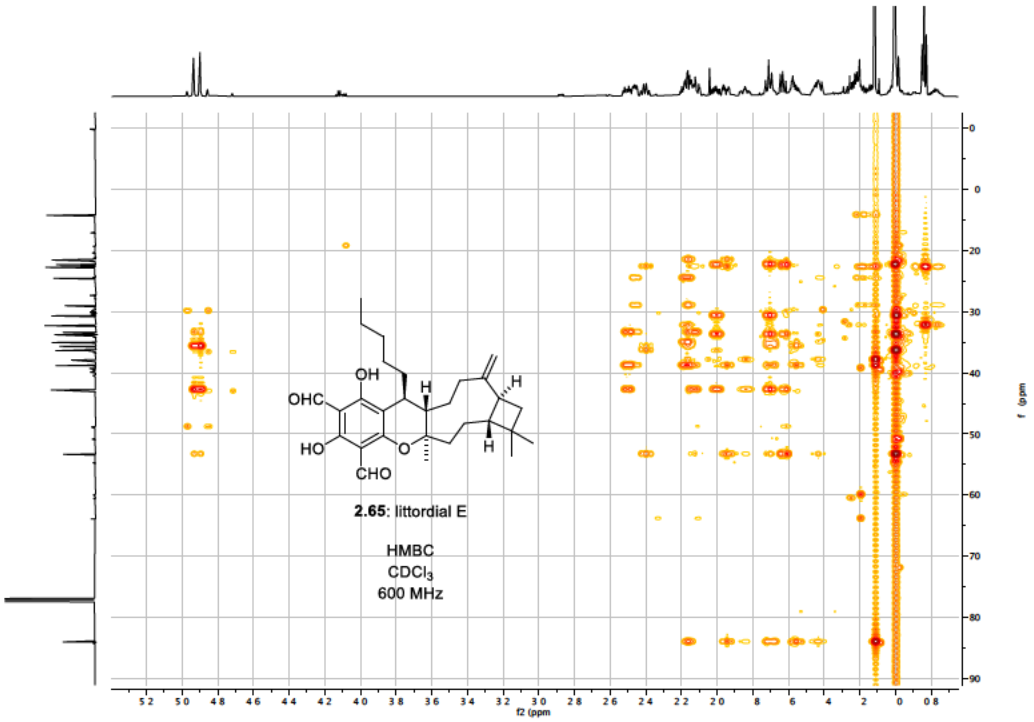

Figure 2.39: ^{1}H NMR spectrum of littordial E (**2.65**) in d_6-benzene

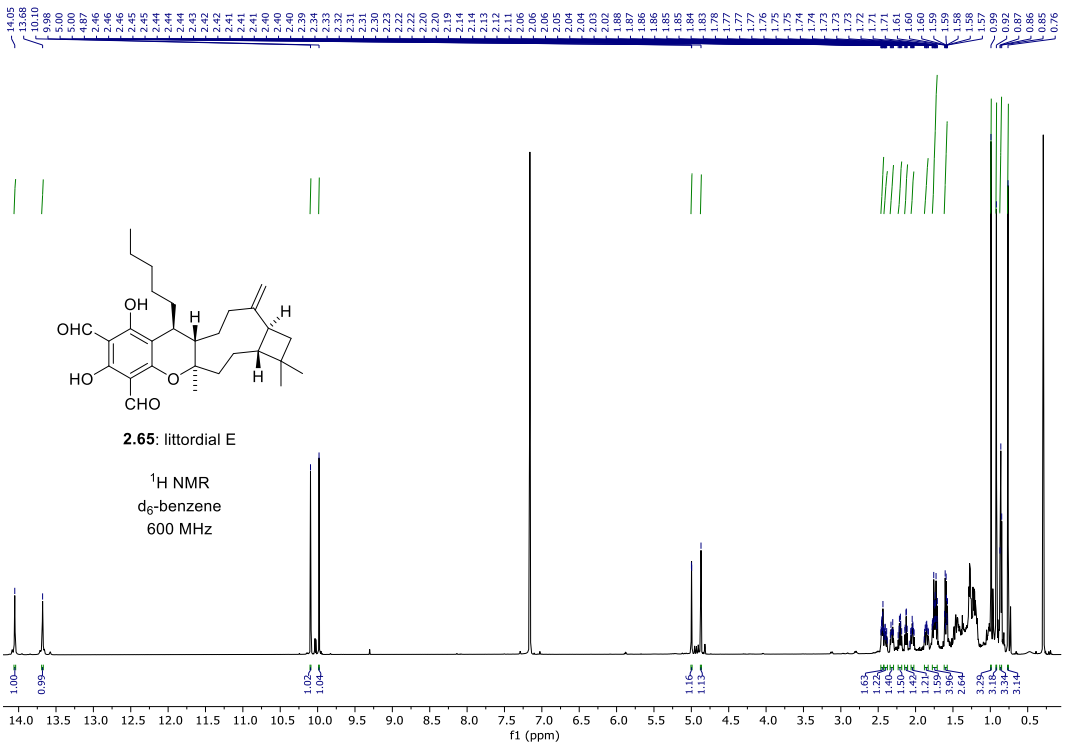

Figure 2.40: ^{13}C NMR spectrum of littordial E (**2.65**) in d_6-benzene

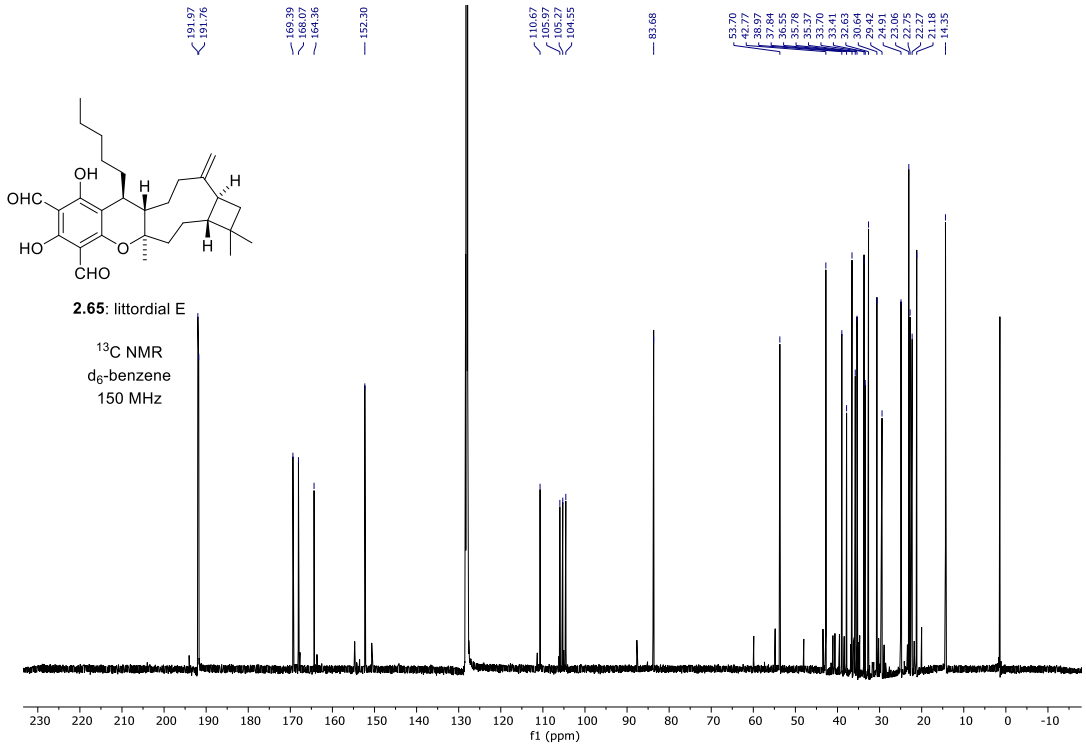

Figure 2.41: COSY spectrum of littordial E (**2.65**) in d_6-benzene

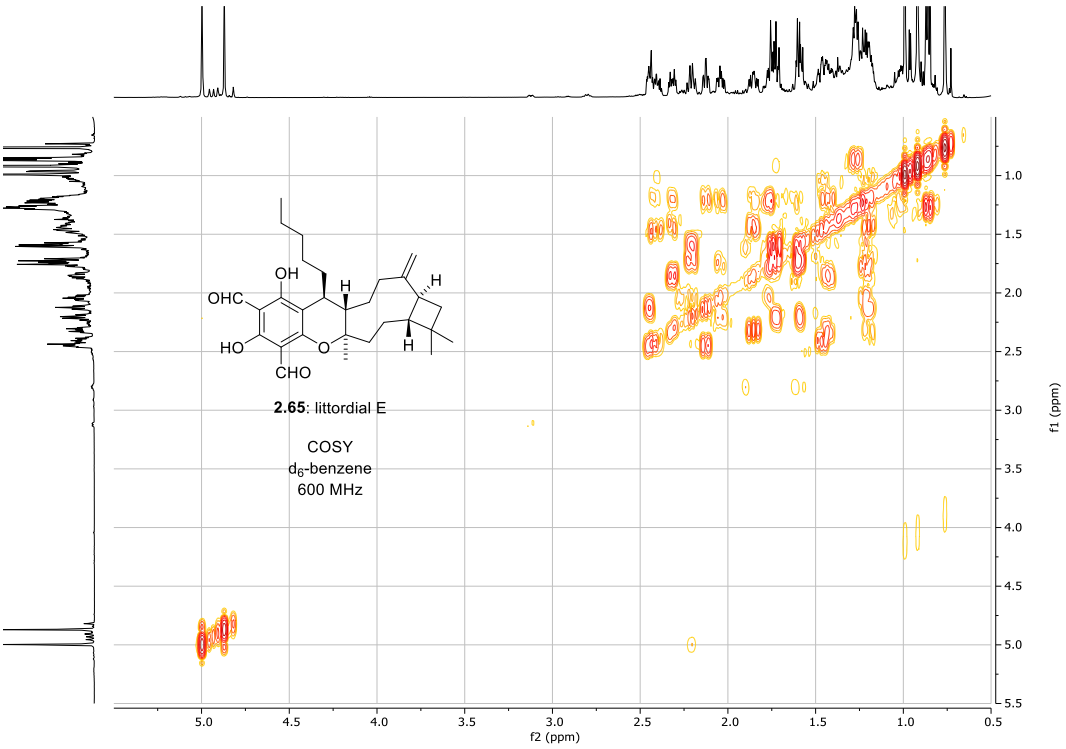

Figure 2.42: TOCSY spectrum of littordial E (**2.65**) in d_6-benzene

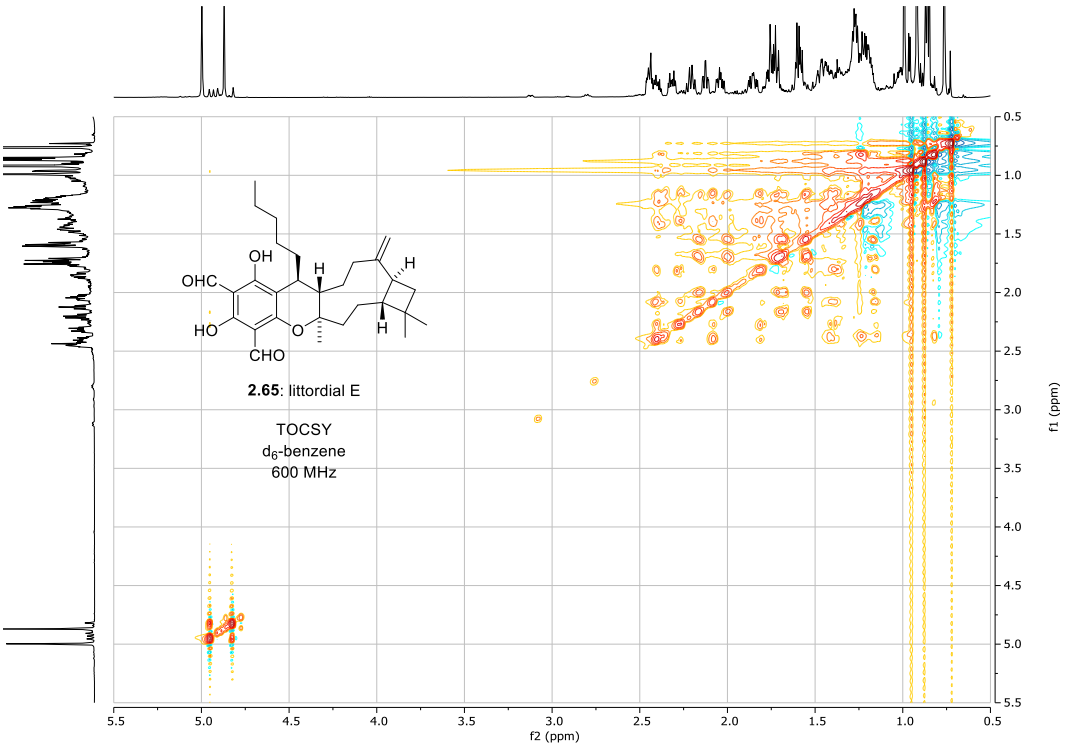

Figure 2.43: ROESY spectrum of littordial E (**2.65**) in d_6-benzene

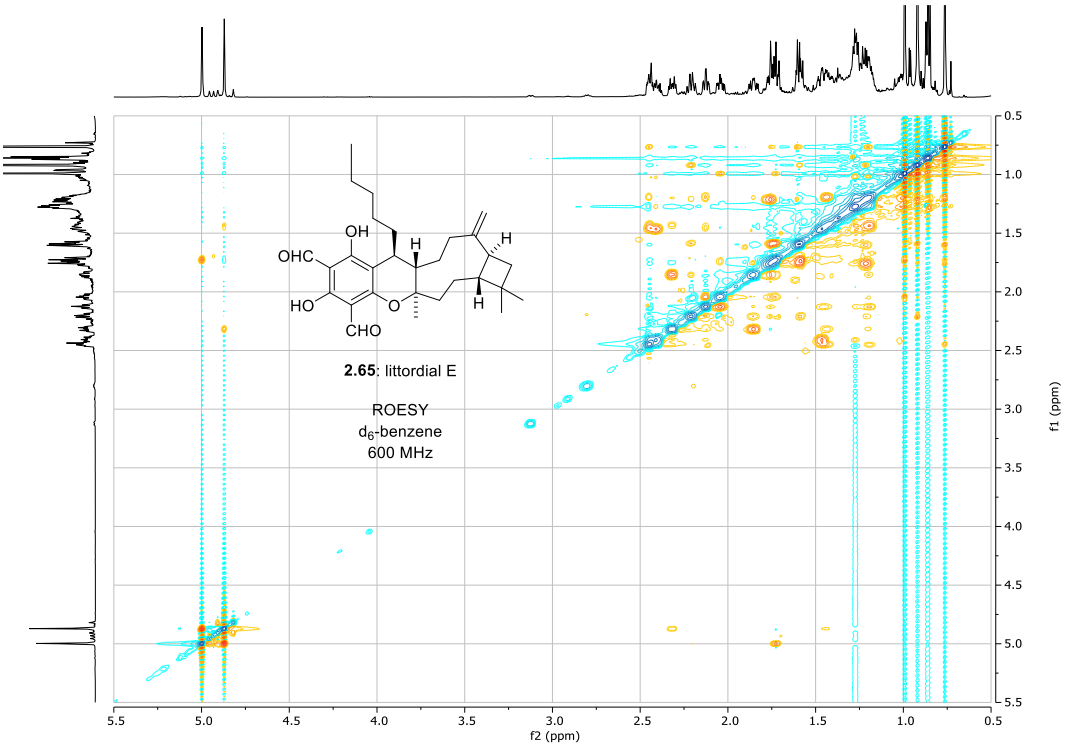

Figure 2.44: NOESY spectrum of littordial E (**2.65**) in d_6-benzene

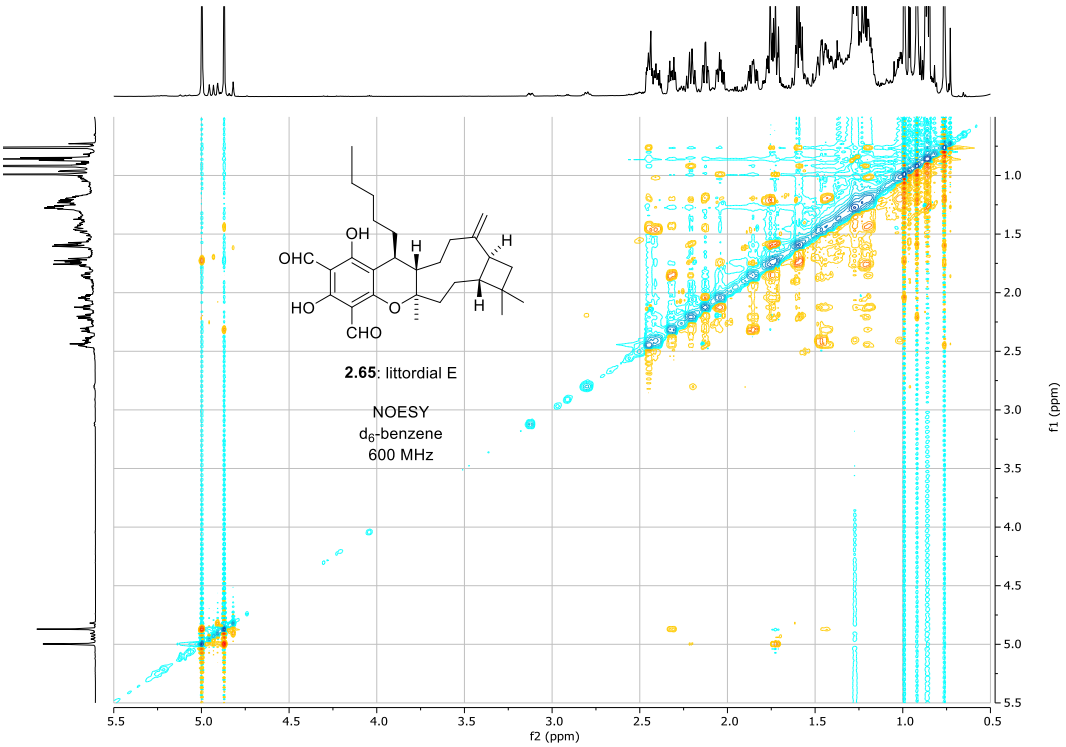

Figure 2.45: HSQC spectrum of littordial E (**2.65**) in d_6-benzene

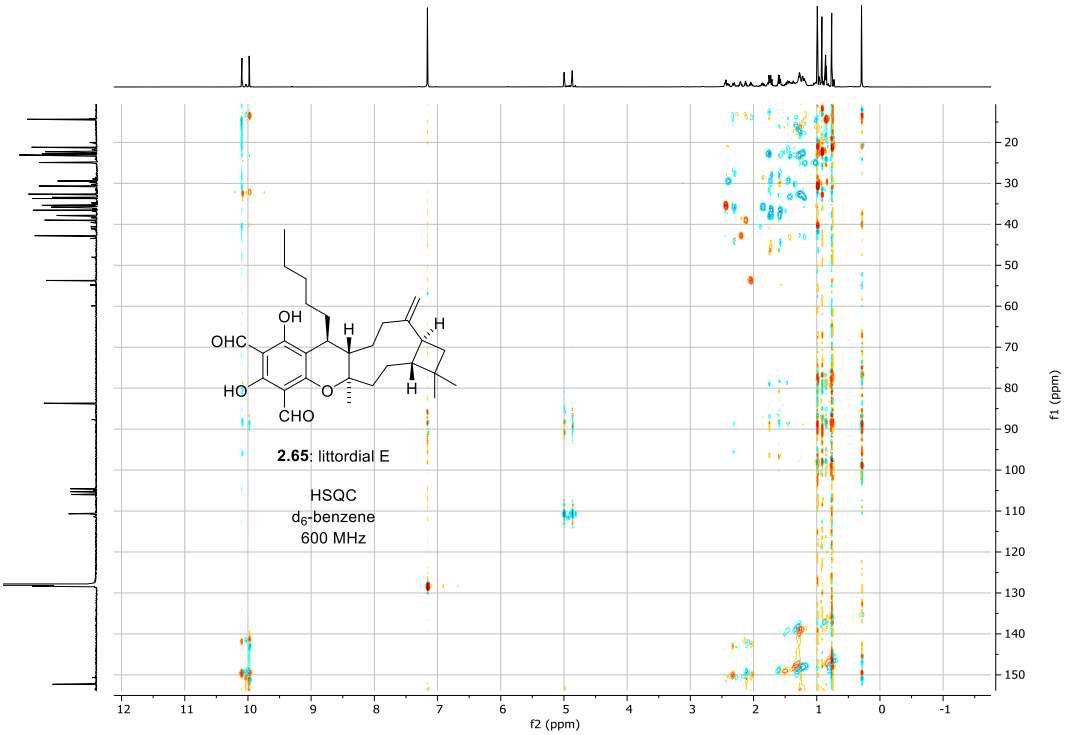

Figure 2.46: Enlarged section of the HSQC spectrum of littordial E (**2.65**) in d_6-benzene

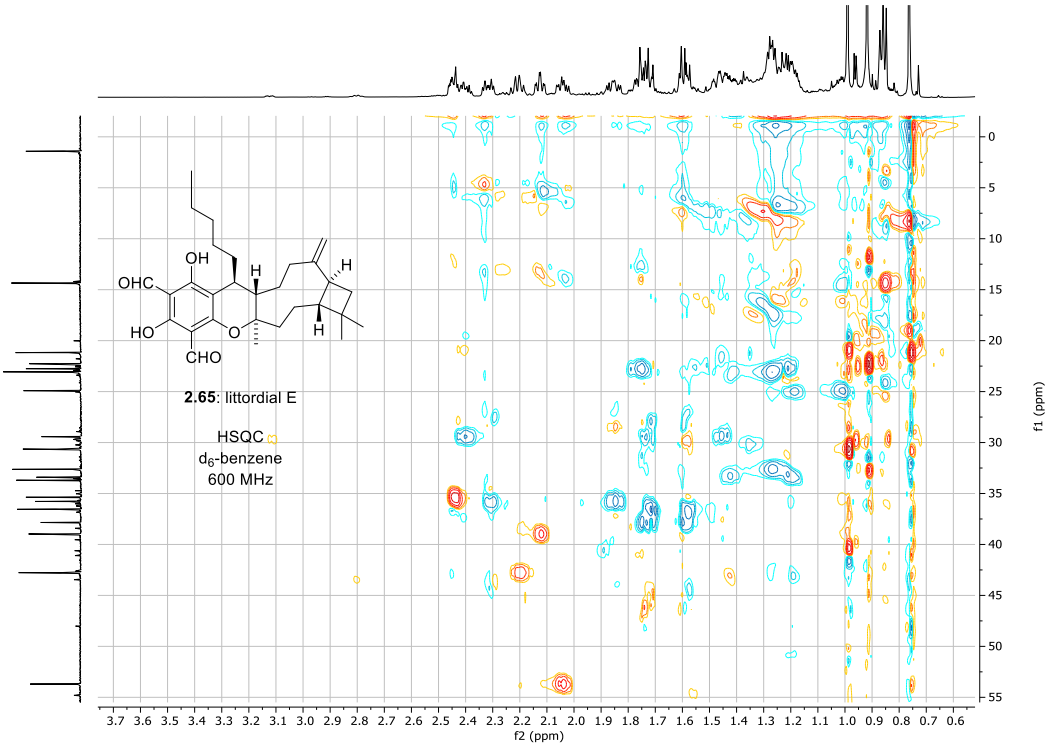

Figure 2.47: HMBC spectrum of littordial E (**2.65**) in d_6-benzene

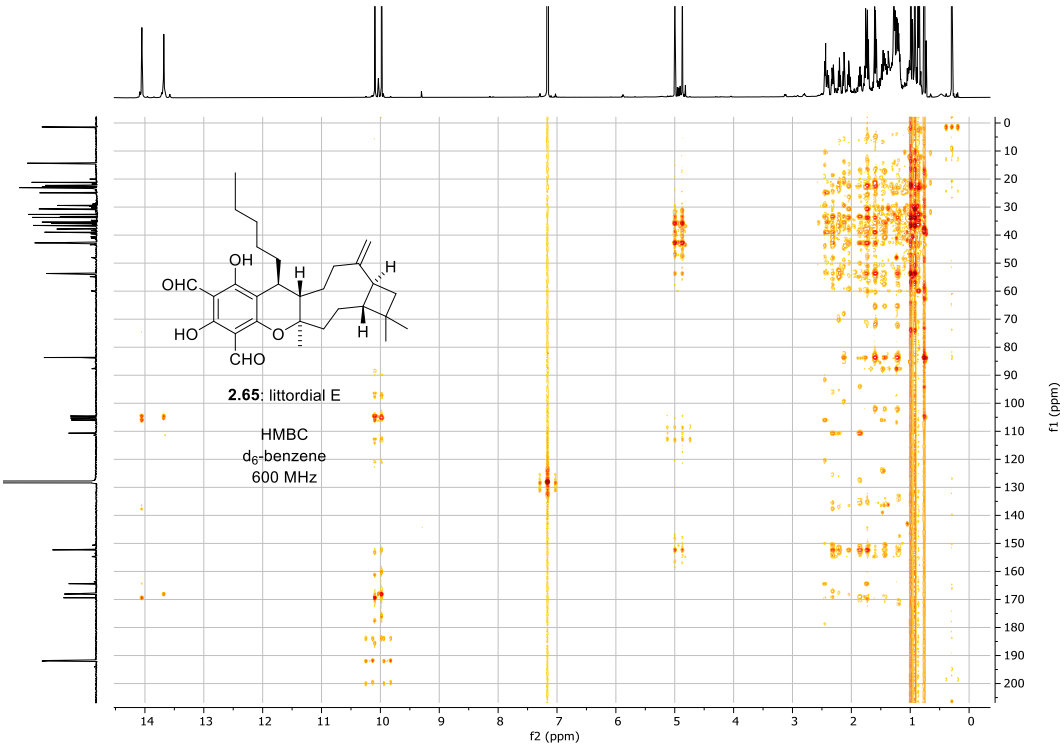

Figure 2.48: Enlarged section of the HMBC spectrum of littordial E (**2.65**) in d_6-benzene

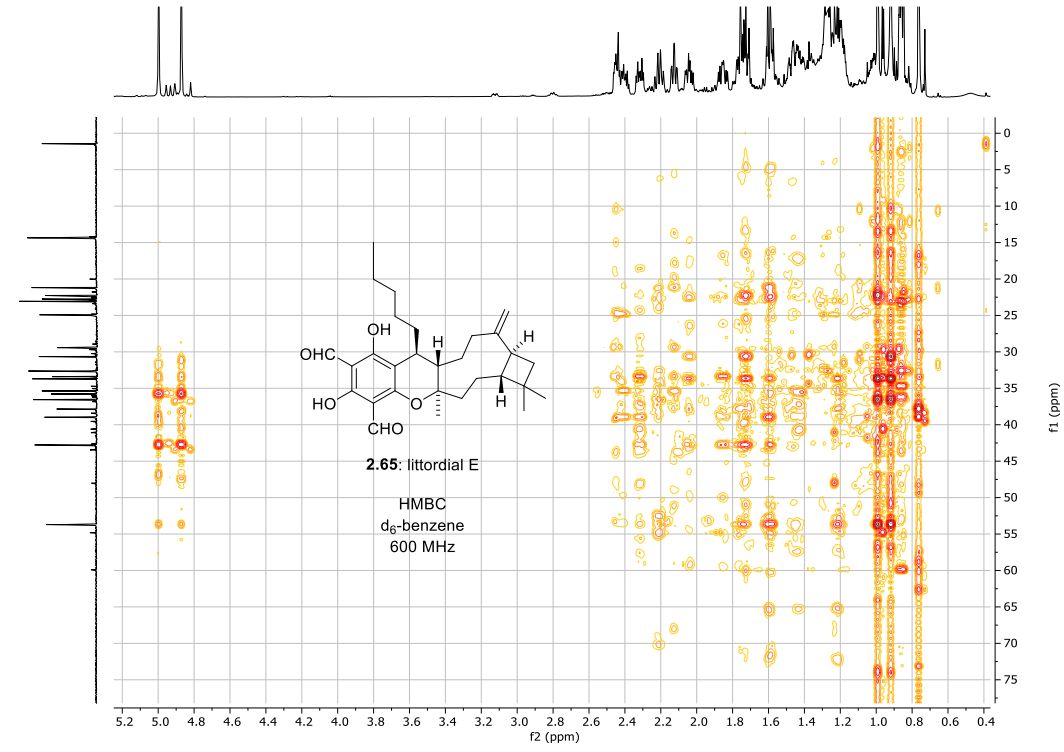

Figure 2.49: ^{1}H NMR spectrum of littordial F (**2.66**) in $CDCl_3$

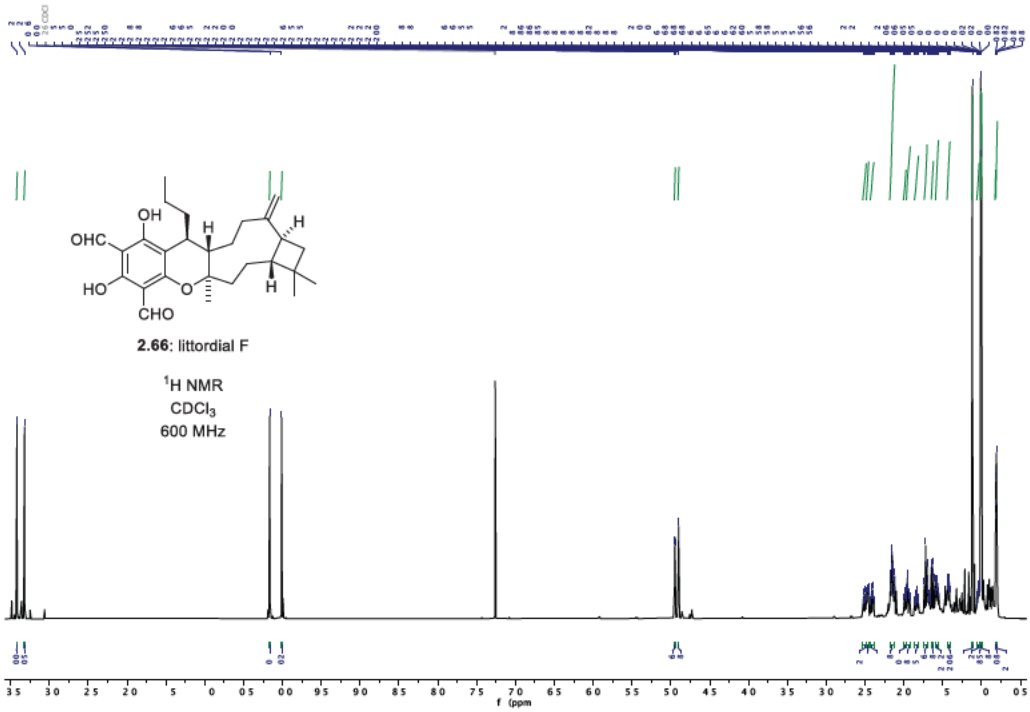

Figure 2.50: ^{13}C NMR spectrum of littordial F (**2.66**) in $CDCl_3$

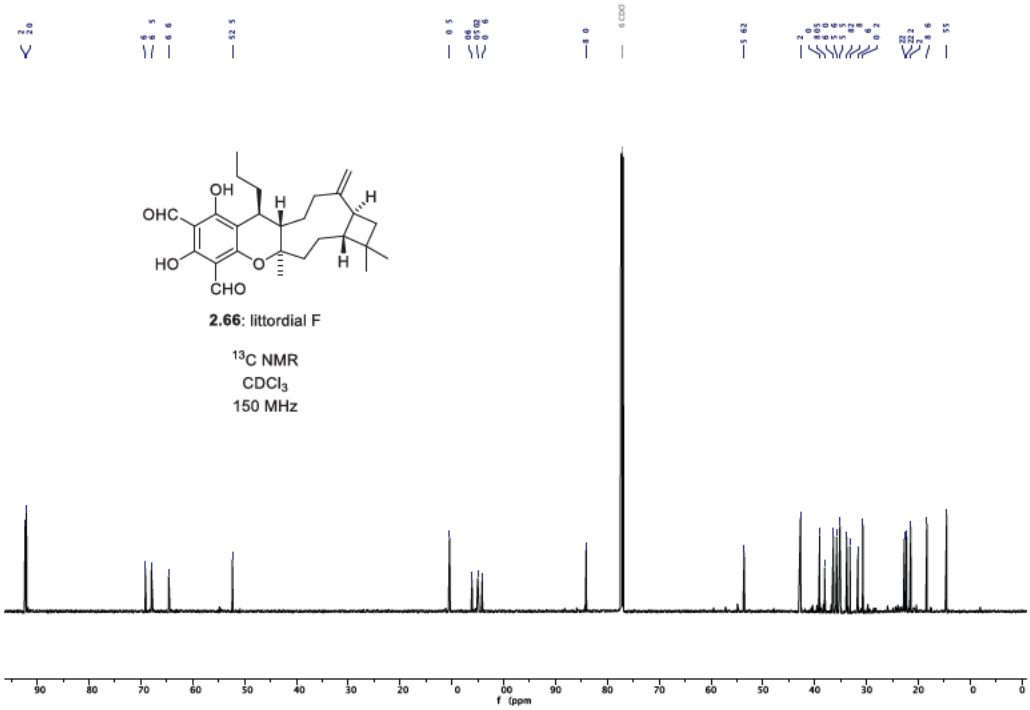

Figure 2.51: COSY spectrum of littordial F (**2.66**) in $CDCl_3$

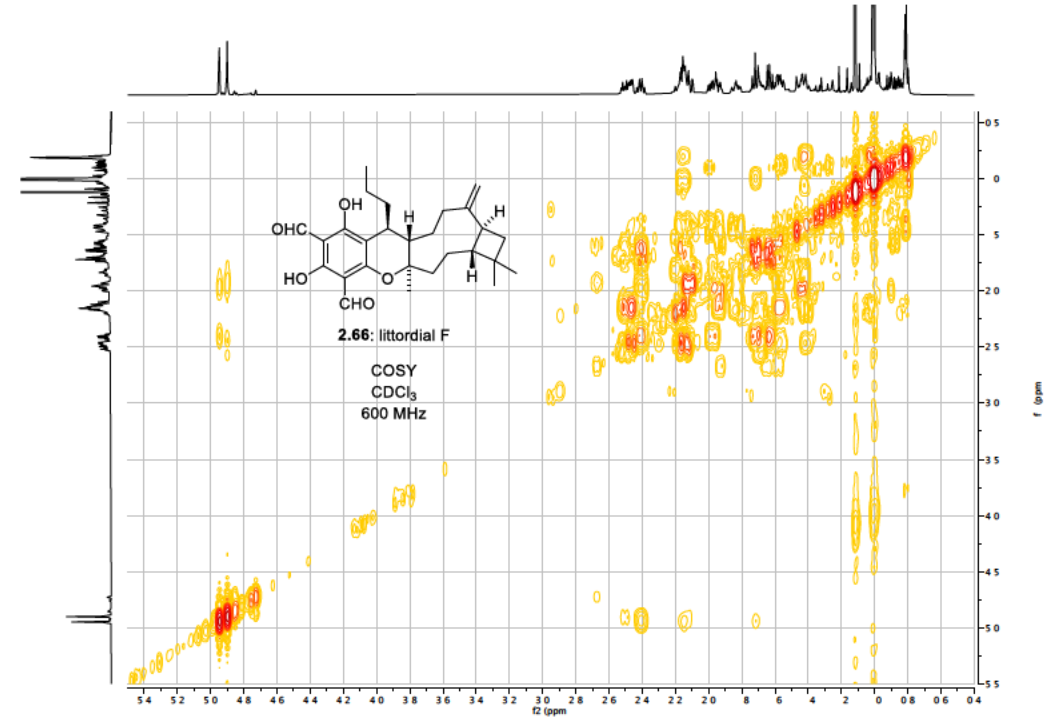

Figure 2.52: NOESY spectrum of littordial F (**2.66**) in $CDCl_3$

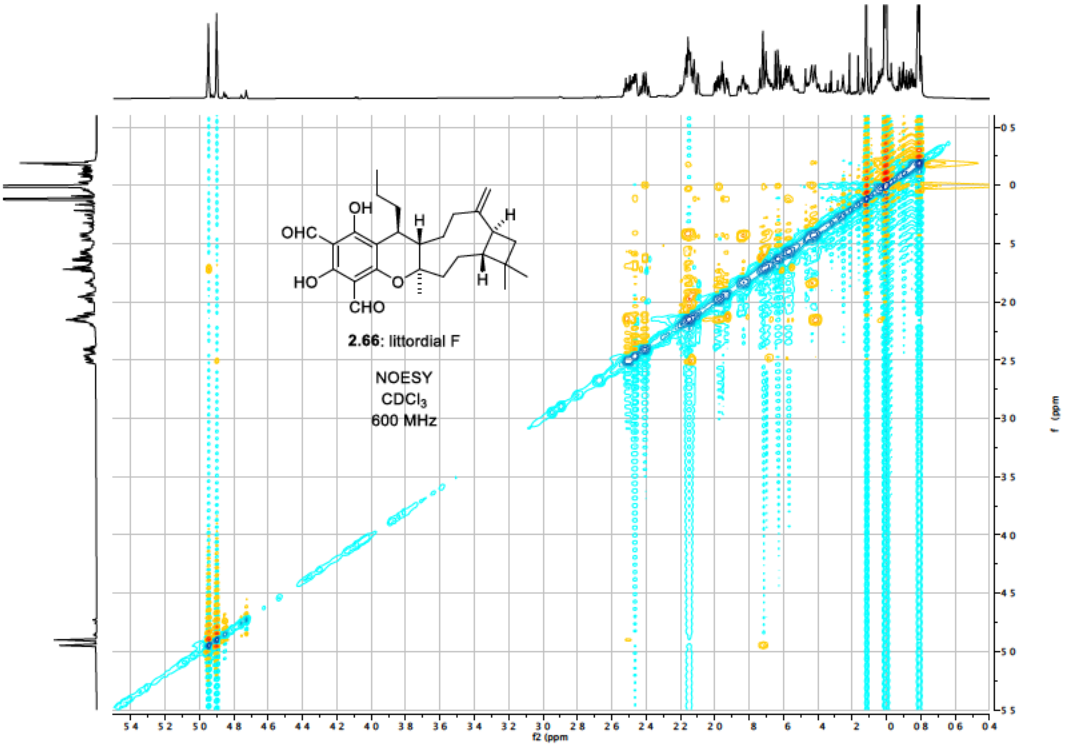

Figure 2.53: HSQC spectrum of littordial F (**2.66**) in $CDCl_3$

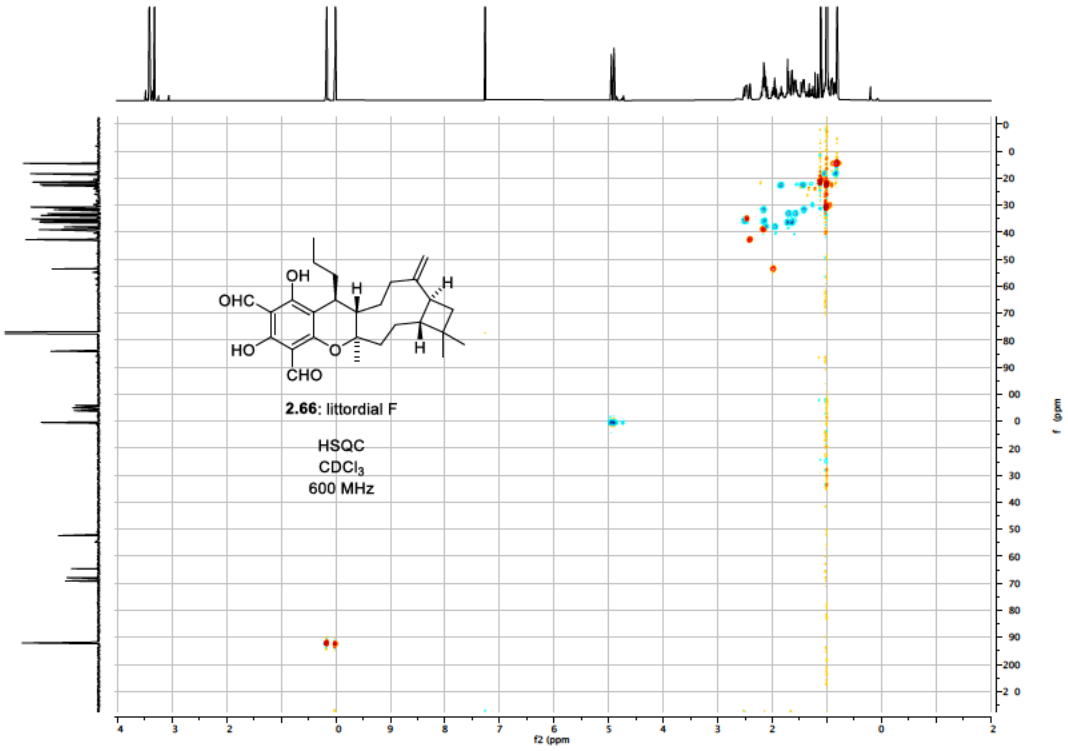

Figure 2.54: Enlarged section of the HSQC spectrum of littordial F (**2.66**) in $CDCl_3$

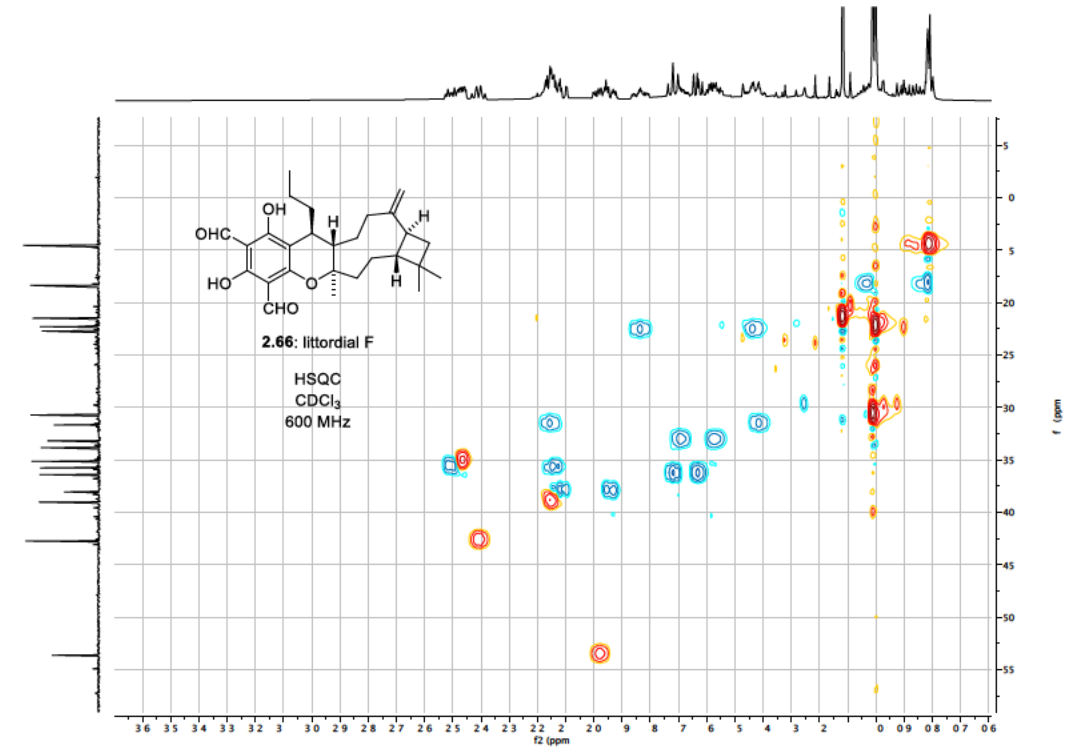

Figure 2.55: HMBC spectrum of littordial F (**2.66**) in $CDCl_3$

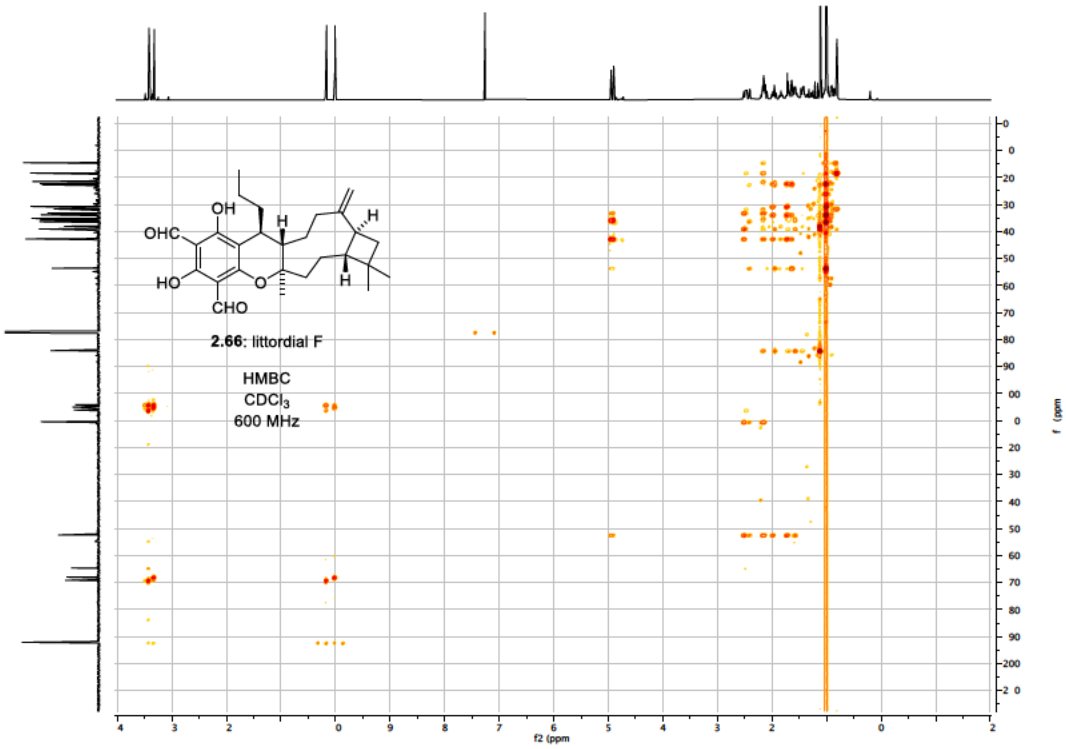

Figure 2.56: Enlarged section of the HMBC spectrum of littordial F (**2.66**) in $CDCl_3$

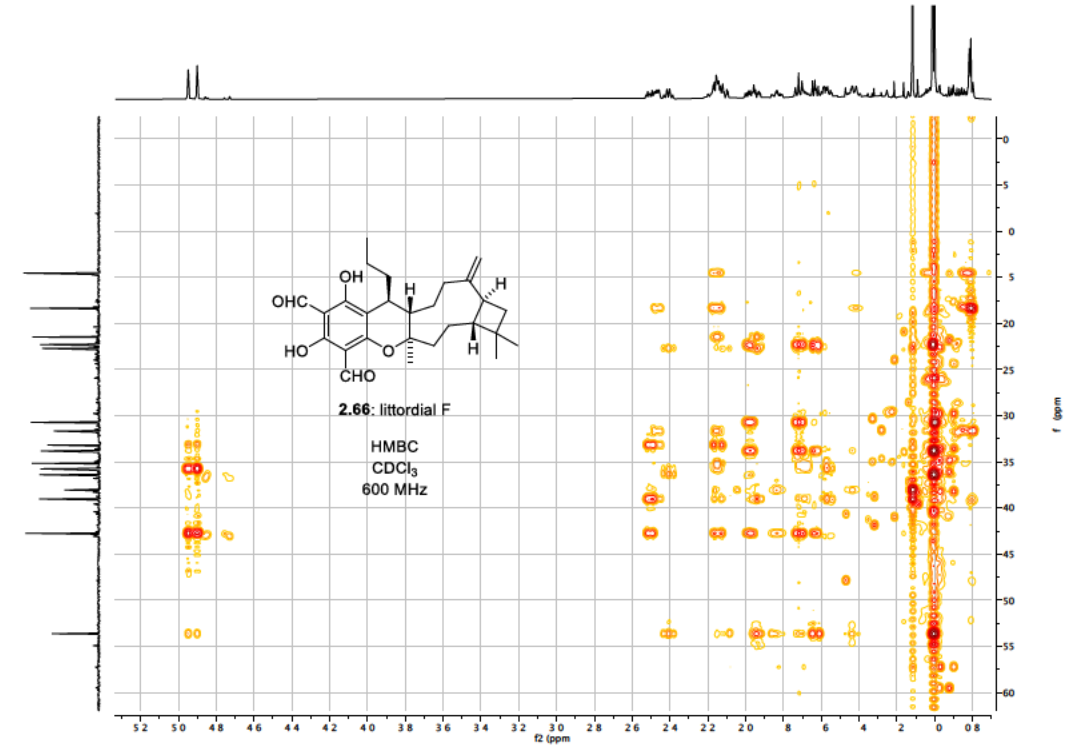

Figure 2.57: ^{1}H NMR spectrum of littordial F (**2.66**) in d_6-benzene

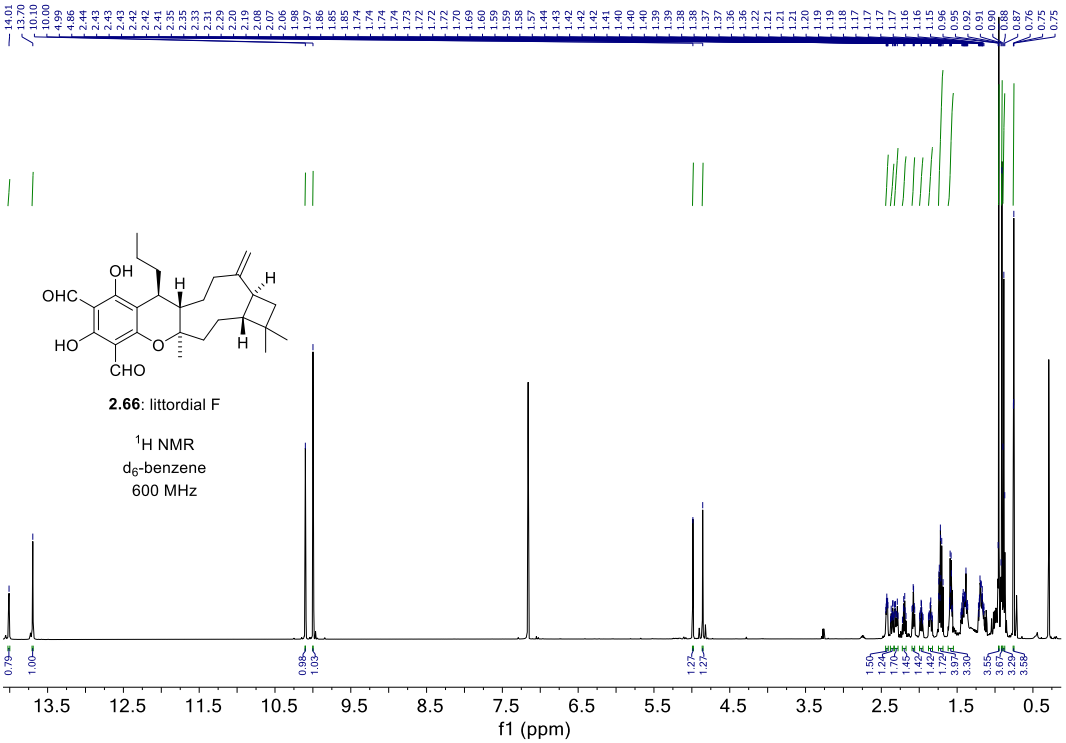

Figure 2.58: ^{13}C NMR spectrum of littordial F (**2.66**) in d_6-benzene

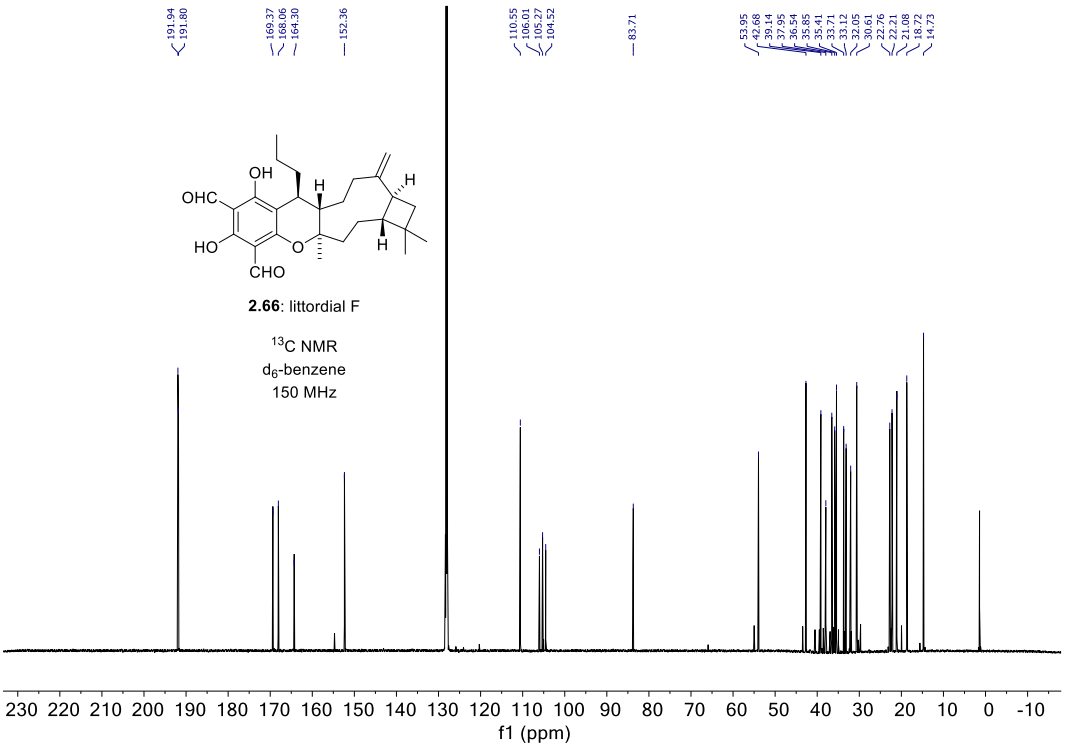

Figure 2.59: COSY spectrum of littordial F (**2.66**) in d_6-benzene

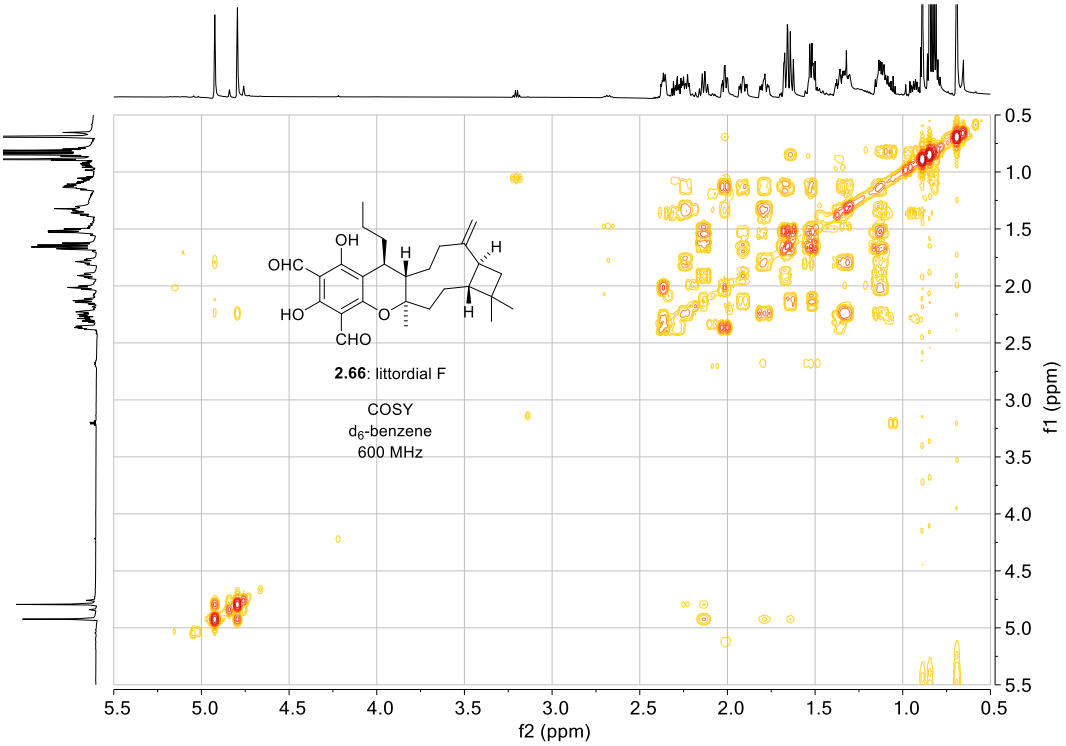

Figure 2.60: NOESY spectrum of littordial F (**2.66**) in d_6-benzene

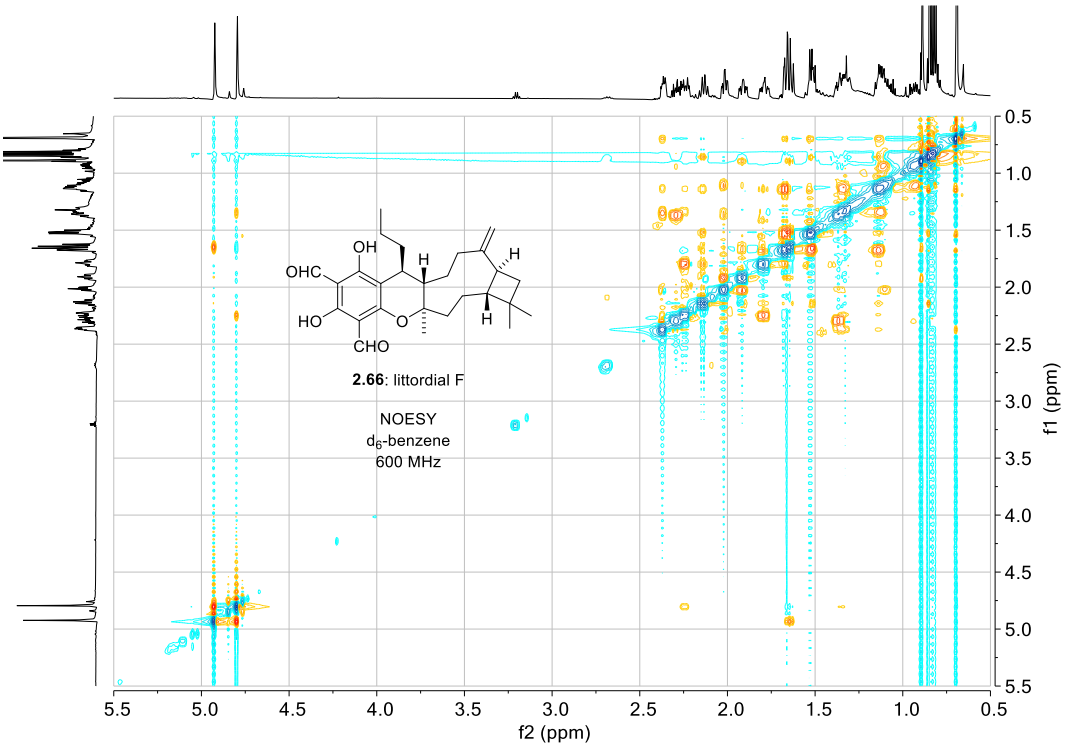

Figure 2.61: HSQC spectrum of littordial F (**2.66**) in d_6-benzene

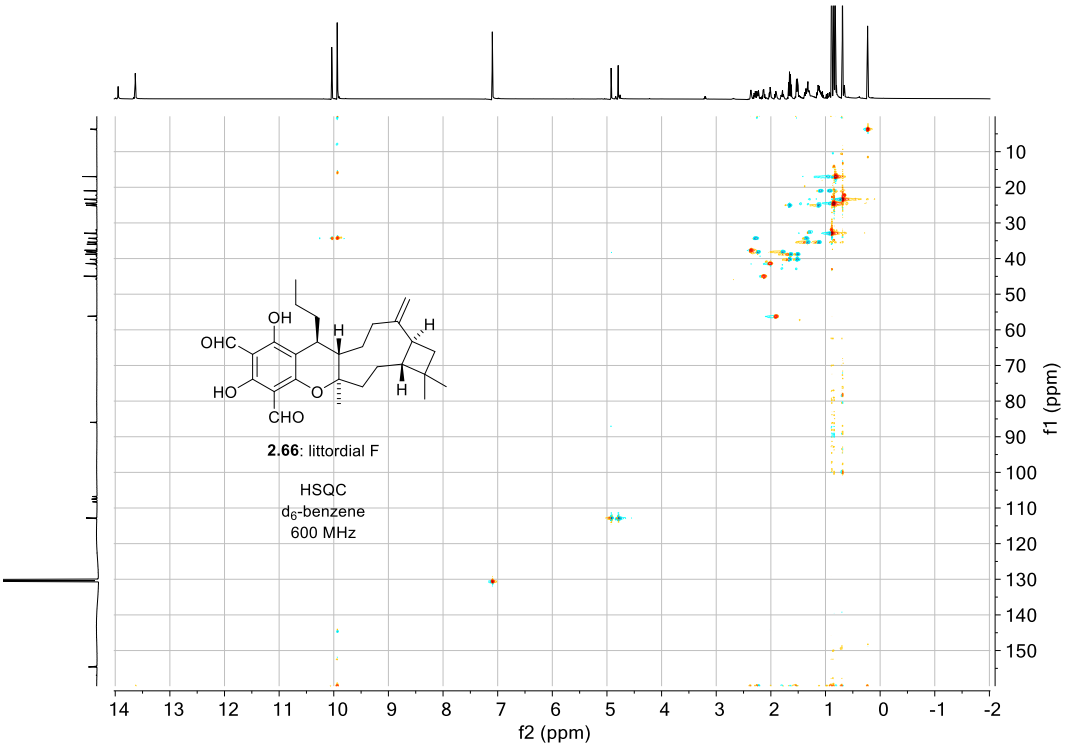

Figure 2.62: Enlarged section of the HSQC spectrum of littordial F (**2.66**) in d_6-benzene

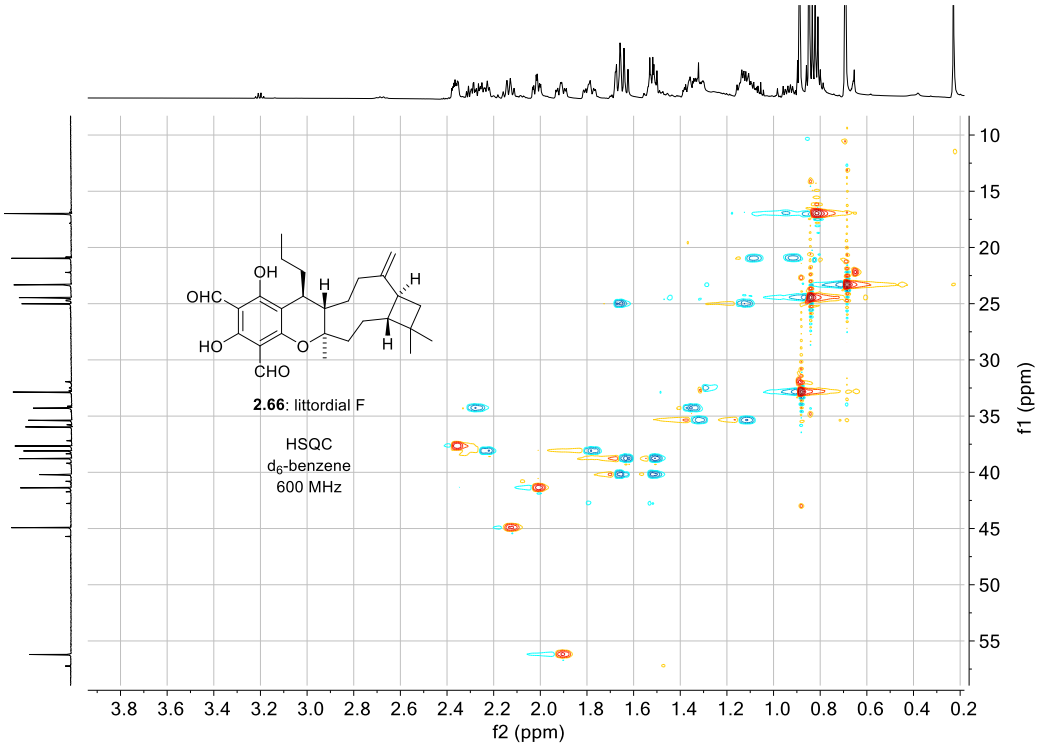

Figure 2.63: HMBC spectrum of littordial F (**2.66**) in d_6-benzene

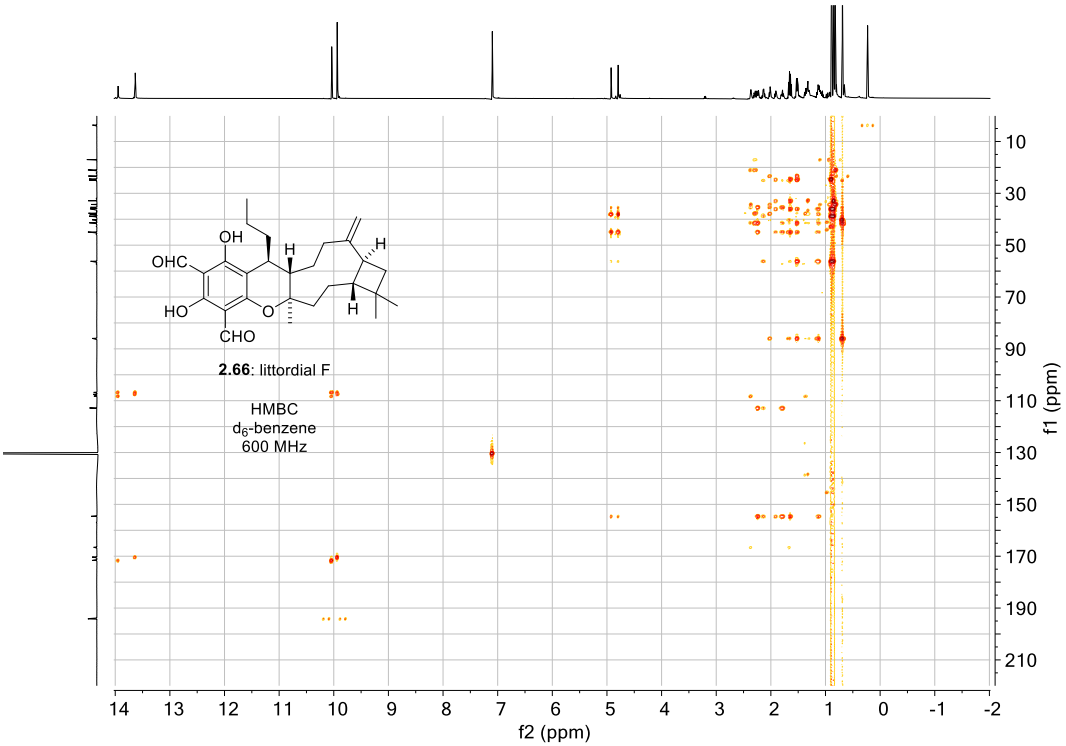

Figure 2.64: Enlarged section of the HMBC spectrum of littordial F (**2.66**) in d_6-benzene

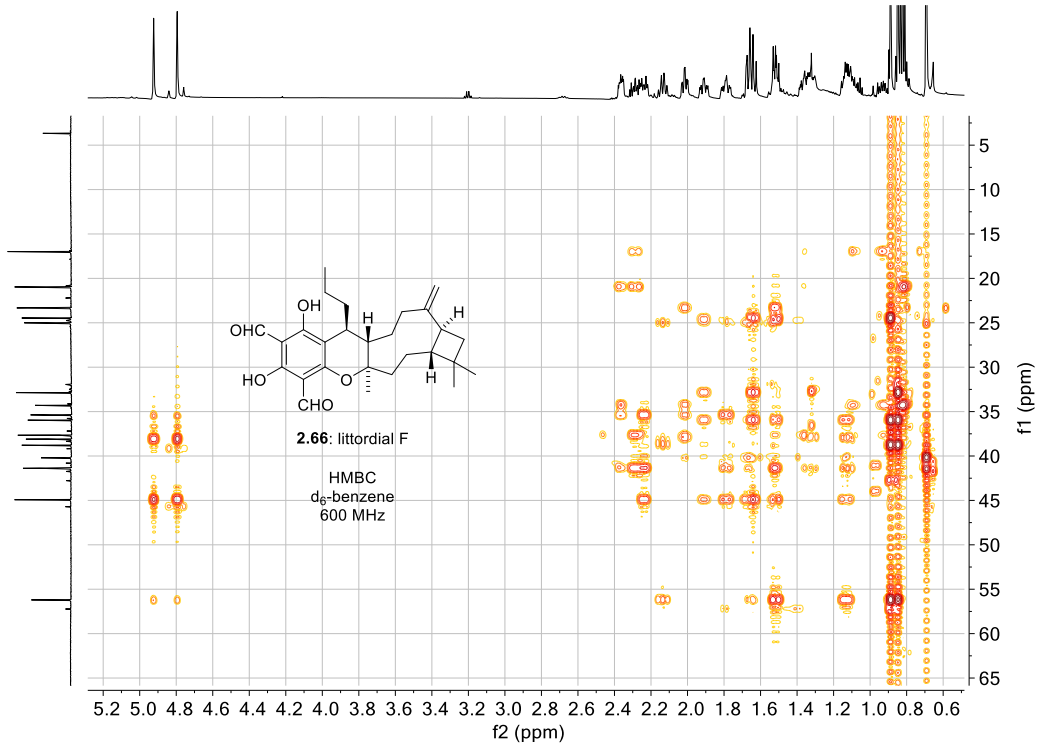

Figure 2.65: ^{1}H NMR spectrum of dimethylphloroglucinol (**2.81**) in CD_3OD

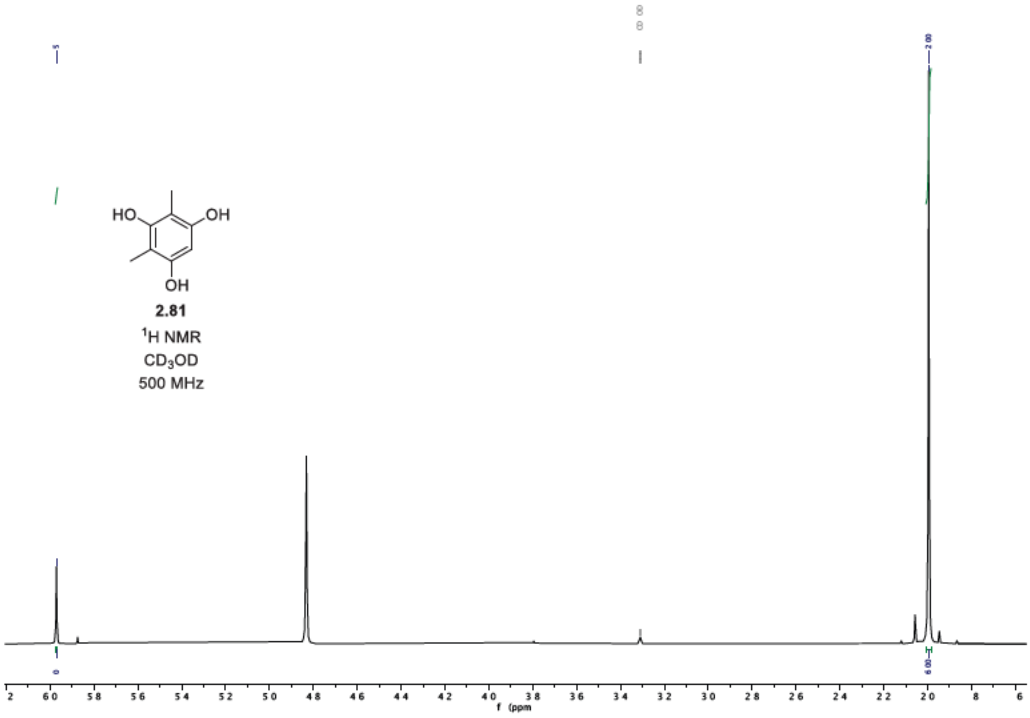

Figure 2.66: ^{13}C NMR spectrum of dimethylphloroglucinol (**2.81**) in CD_3OD

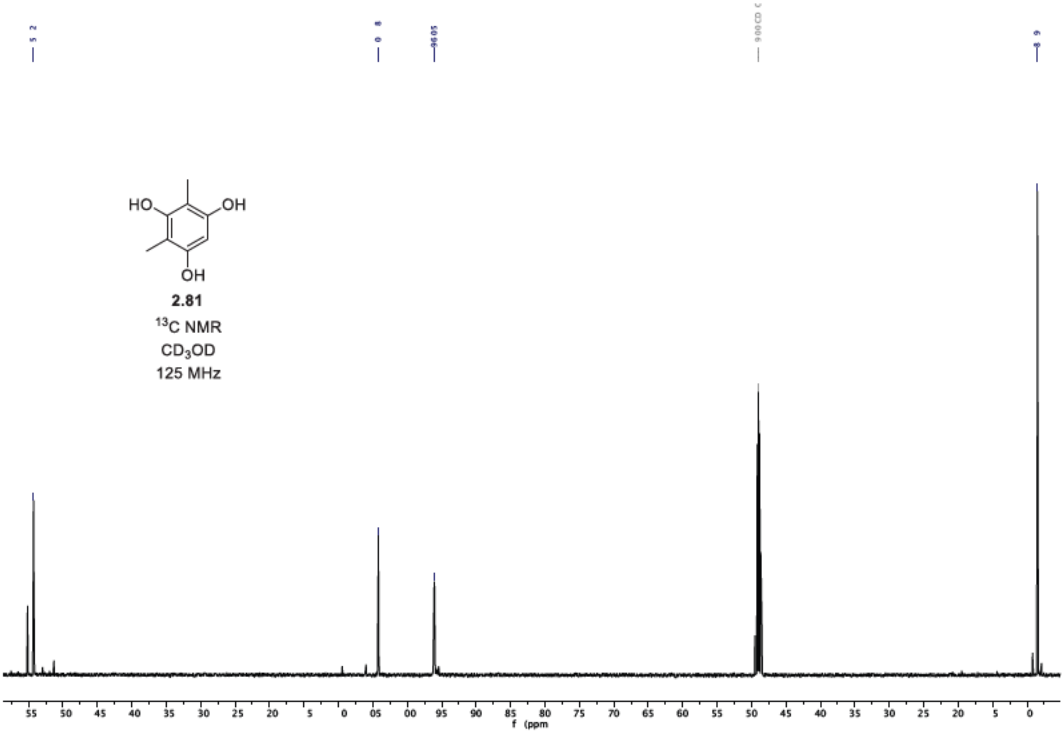

Figure 2.67: ^{1}H NMR spectrum of *o*-QM precursor (**2.73**) in CD_3OD

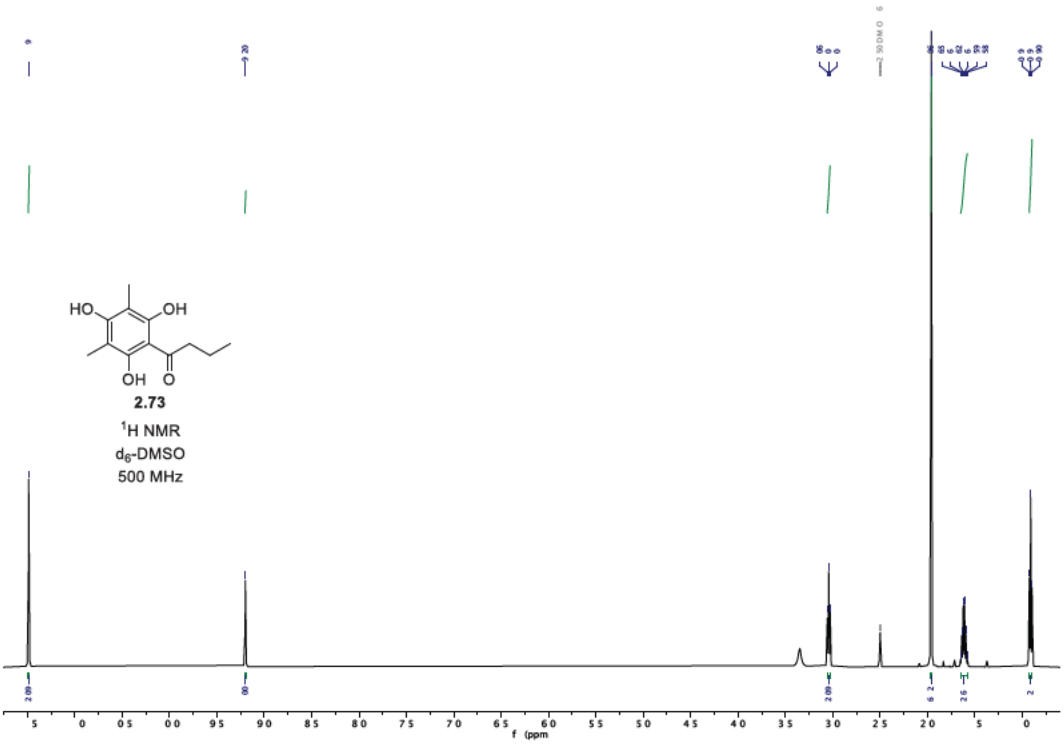

Figure 2.68: ^{13}C NMR spectrum of *o*-QM precursor (**2.73**) in CD_3OD

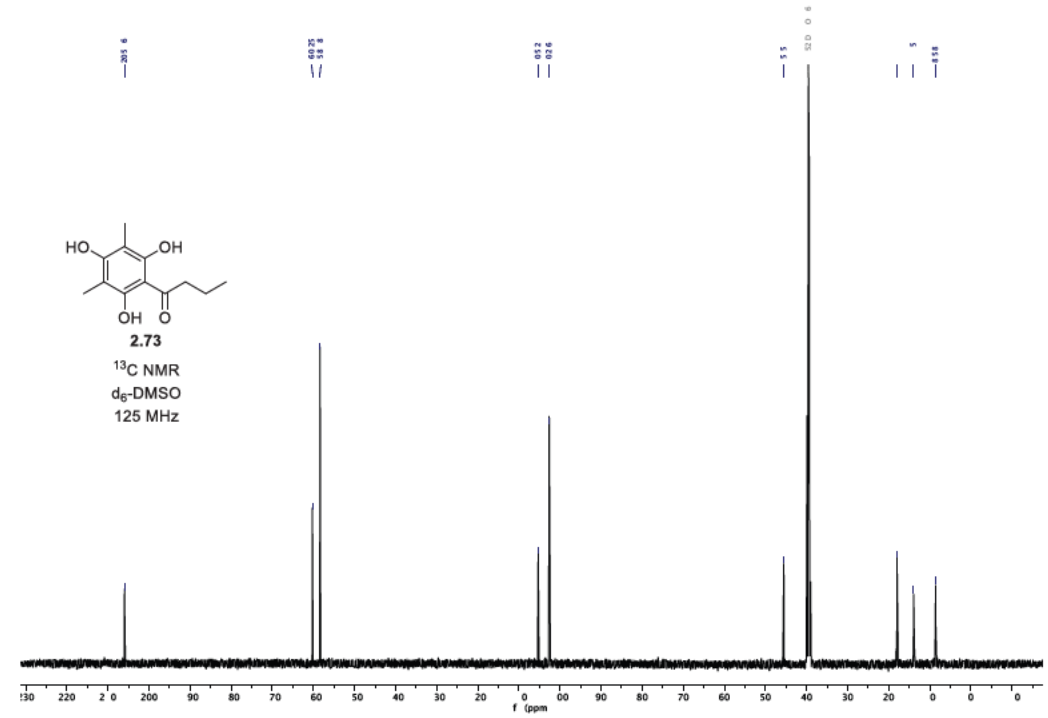

Figure 2.69: ^{1}H NMR spectrum of drychampone B (**2.75**) in $CDCl_3$

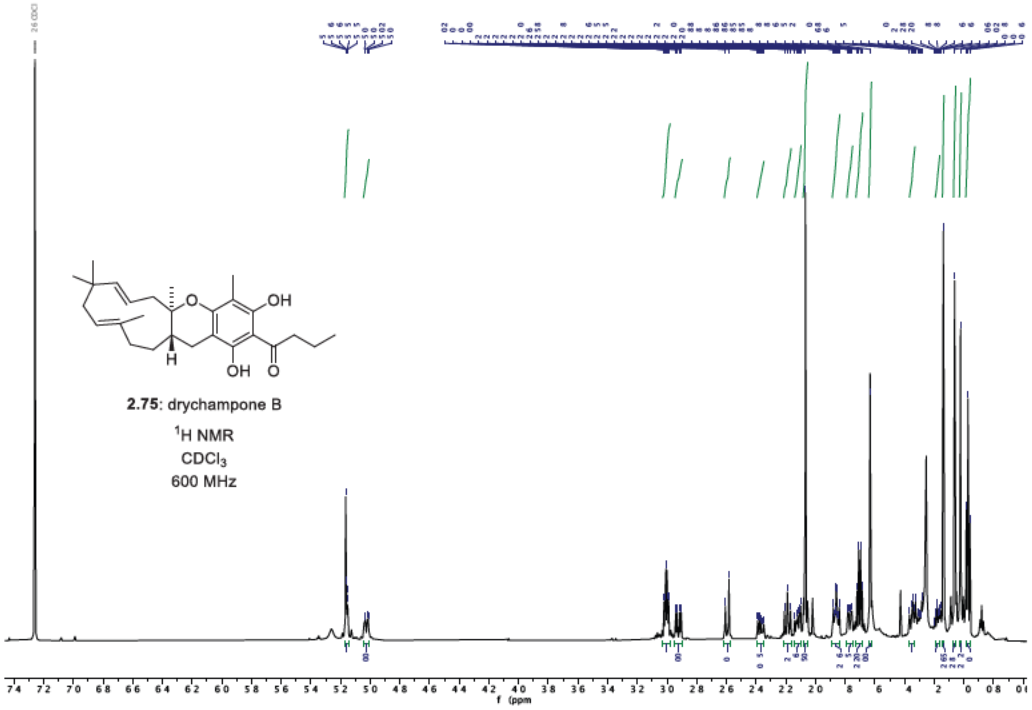

Figure 2.70: ^{1}H NMR spectrum of drychampone B (**2.75**) in d_6-benzene highlighting the key coupling

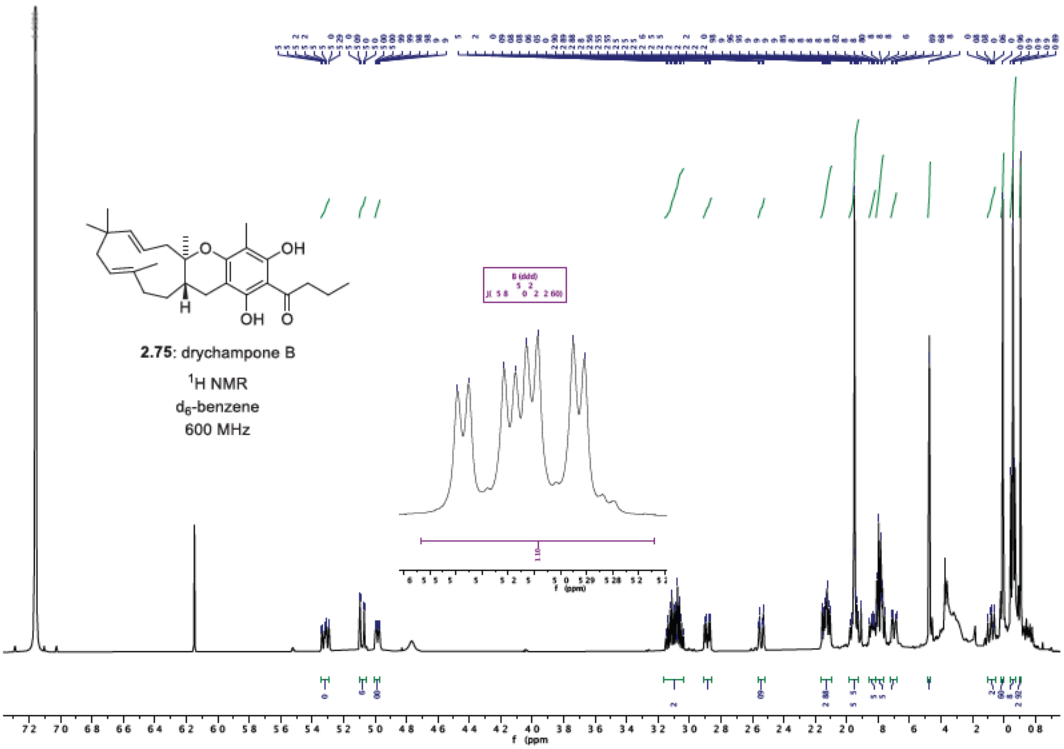

Figure 2.71: ^{13}C NMR spectrum of drychampone B (**2.75**) in $CDCl_3$

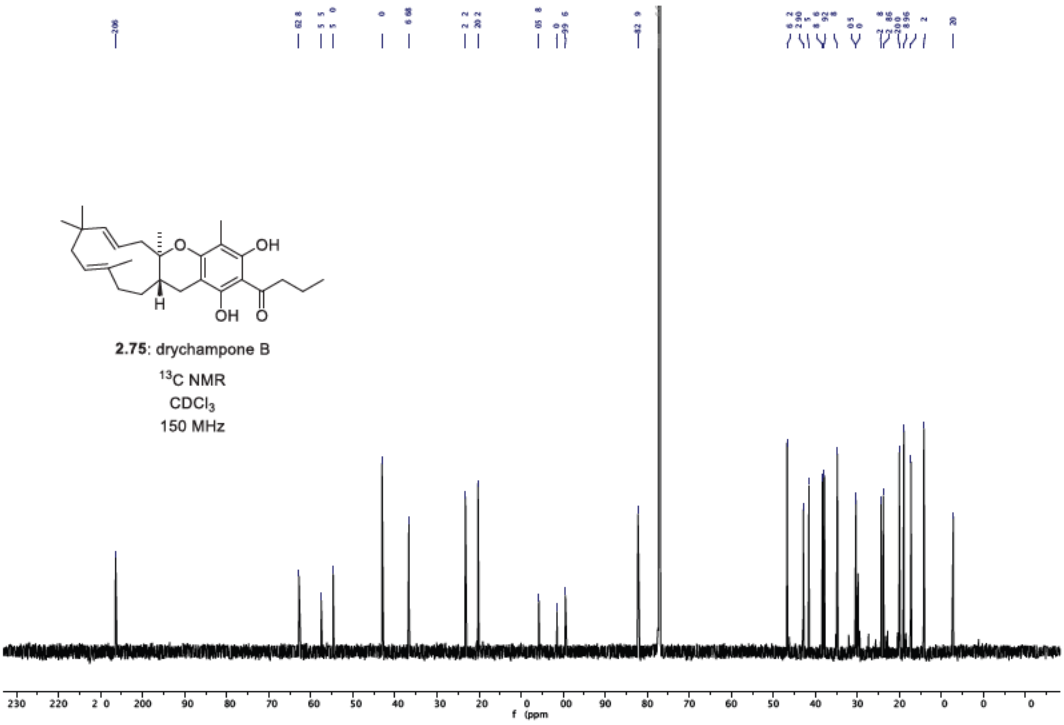

Figure 2.72: COSY spectrum of drychampone B (**2.75**) in $CDCl_3$

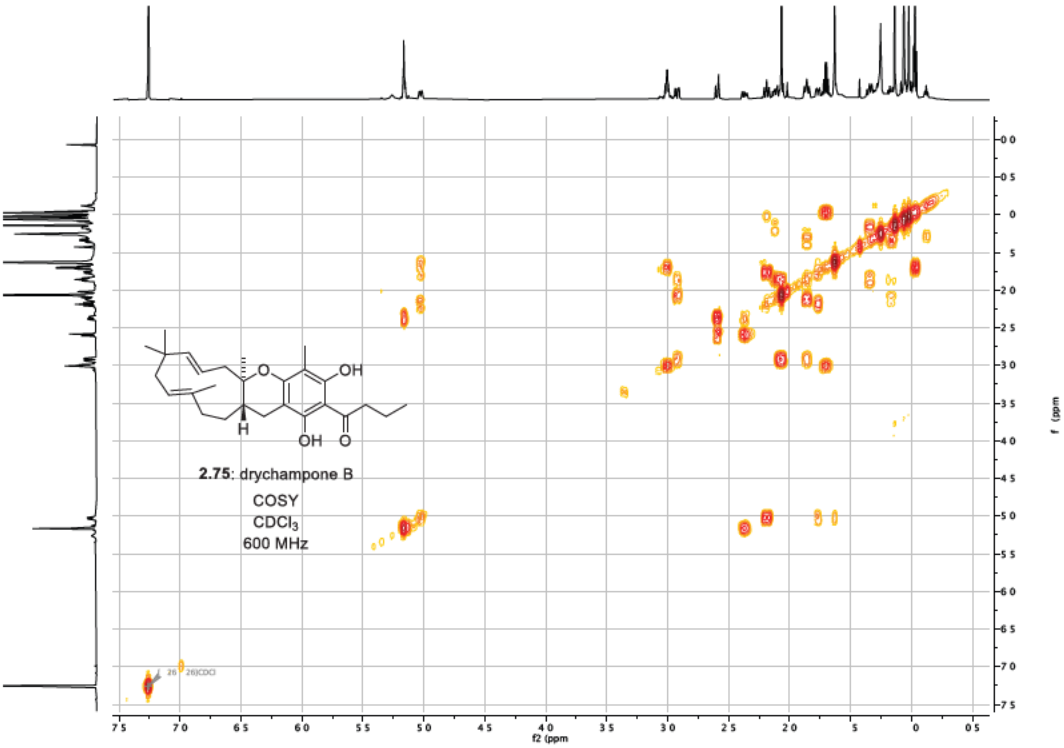

Figure 2.73: HSQC spectrum of drychampone B (**2.75**) in $CDCl_3$

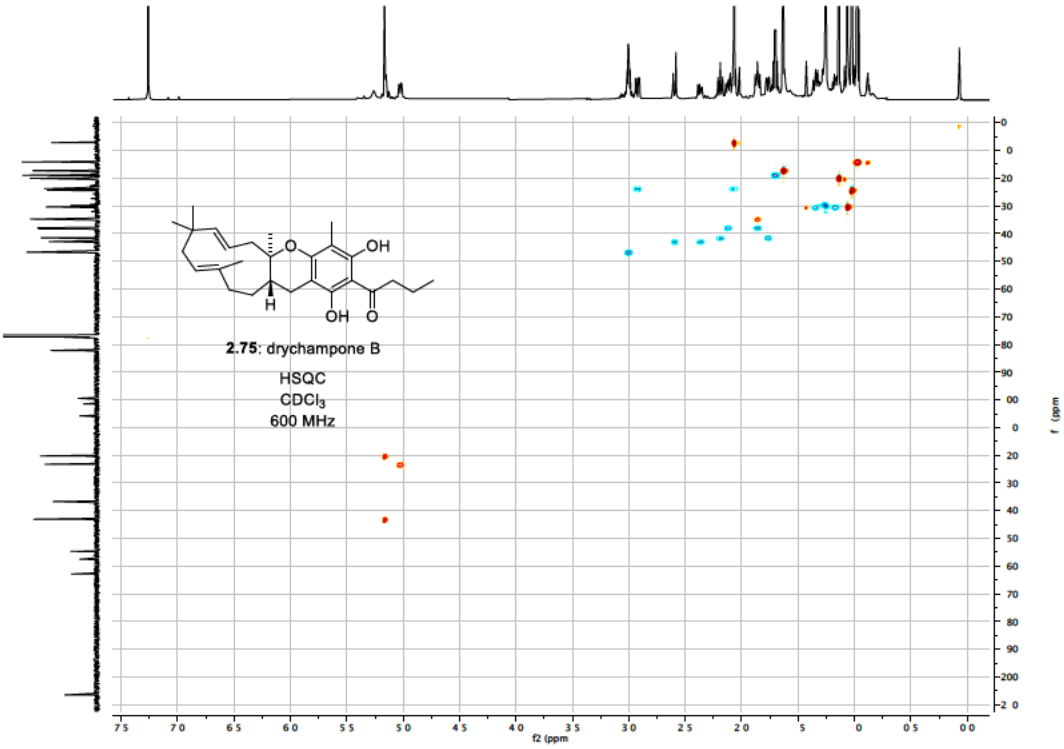

Figure 2.74: Enlarged section of the HSQC spectrum of drychampone B (**2.75**) in $CDCl_3$

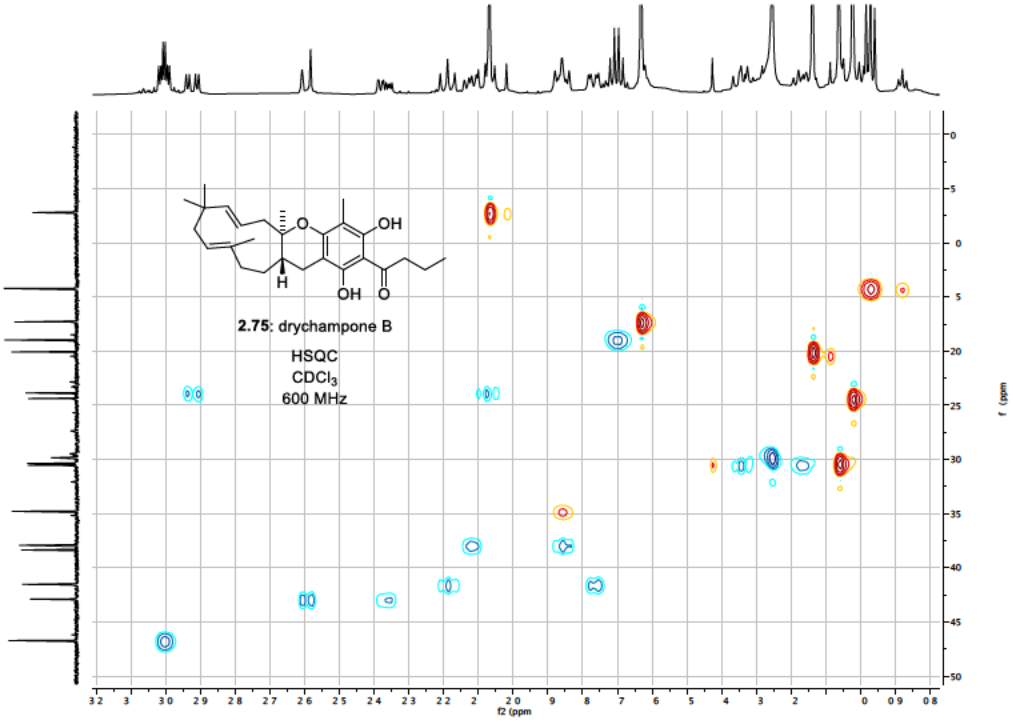

Figure 2.75: HMBC spectrum of drychampone B (**2.75**) in $CDCl_3$

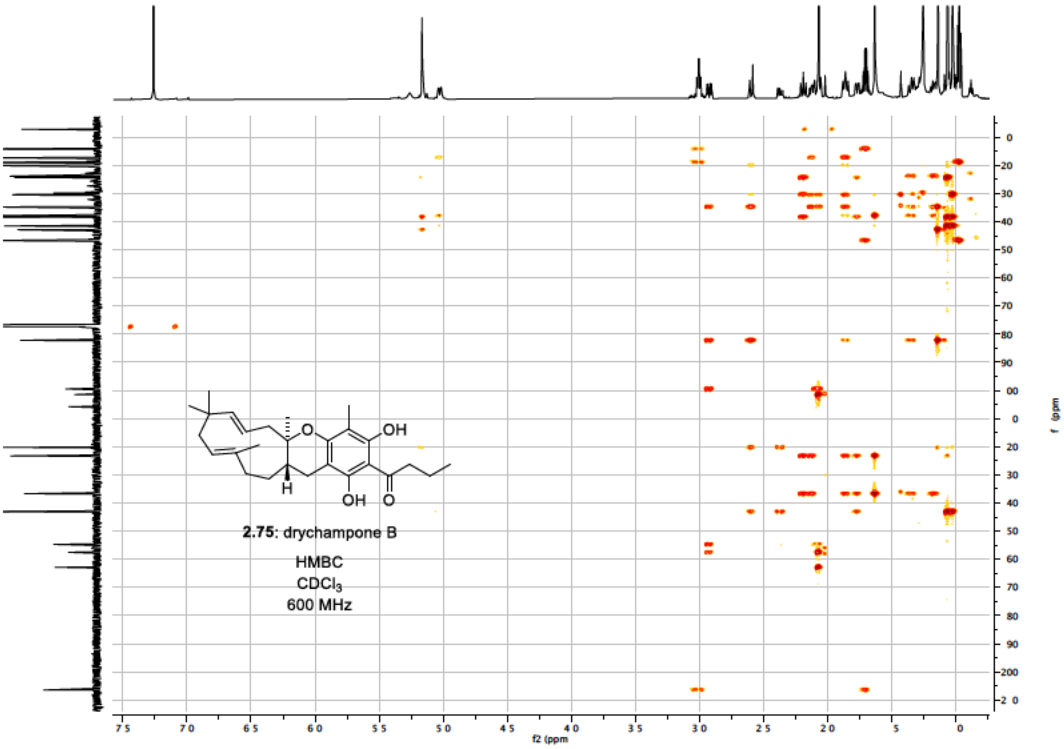

Figure 2.76: Enlarged section of the HMBC spectrum of drychampone B (**2.75**) in $CDCl_3$

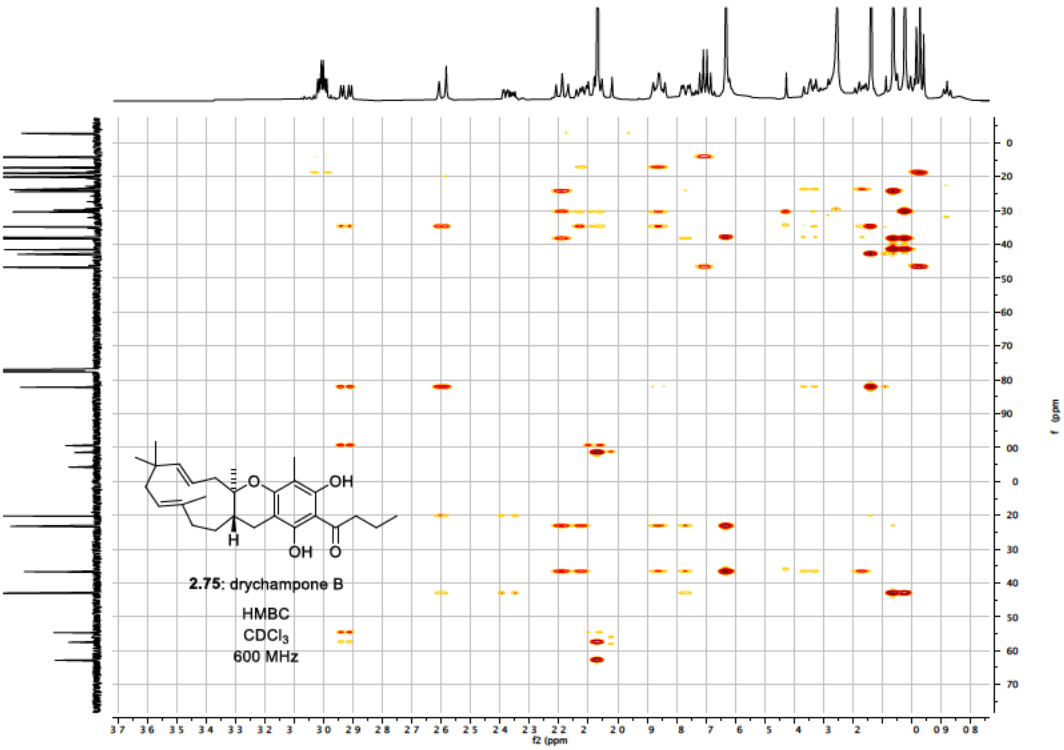

Figure 2.77: ^{1}H NMR spectrum of isolated littordial C (**2.61**) in $CDCl_3$[20]

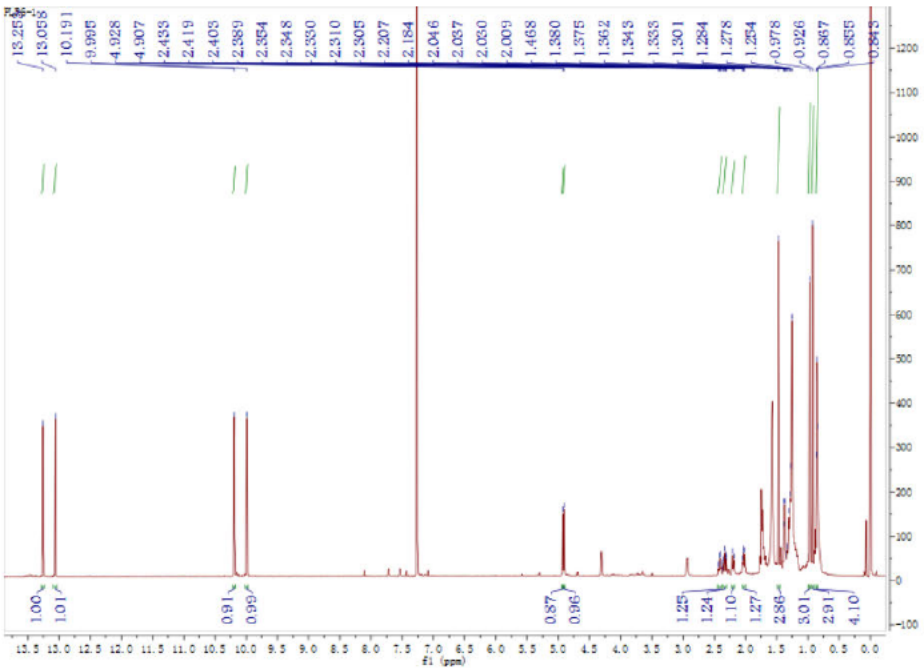

Figure 2.78: ^{13}C NMR spectrum of isolated littordial C (**2.61**) in $CDCl_3$[20]

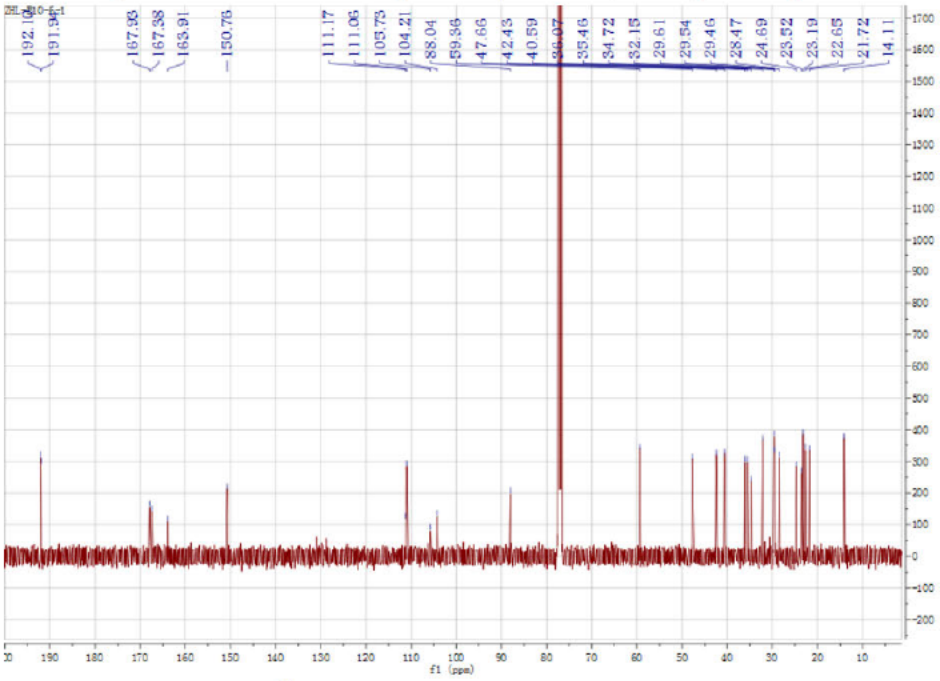

Figure 2.79: HSQC spectrum of isolated littordial C (**2.61**) in $CDCl_3$[20]

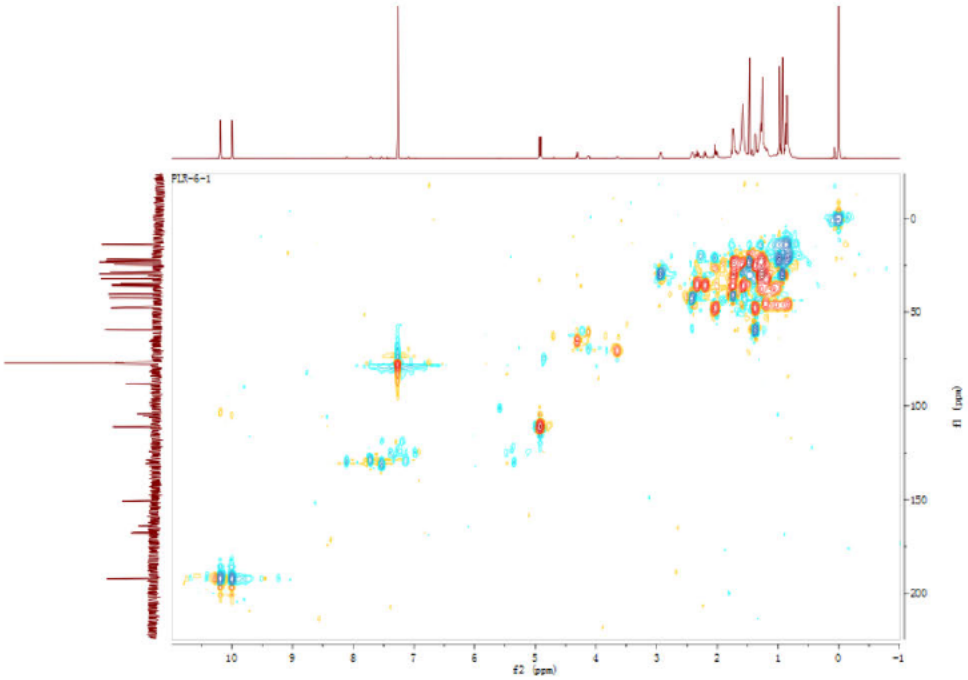

Figure 2.80: HMBC spectrum of isolated littordial C (**2.61**) in $CDCl_3$[20]

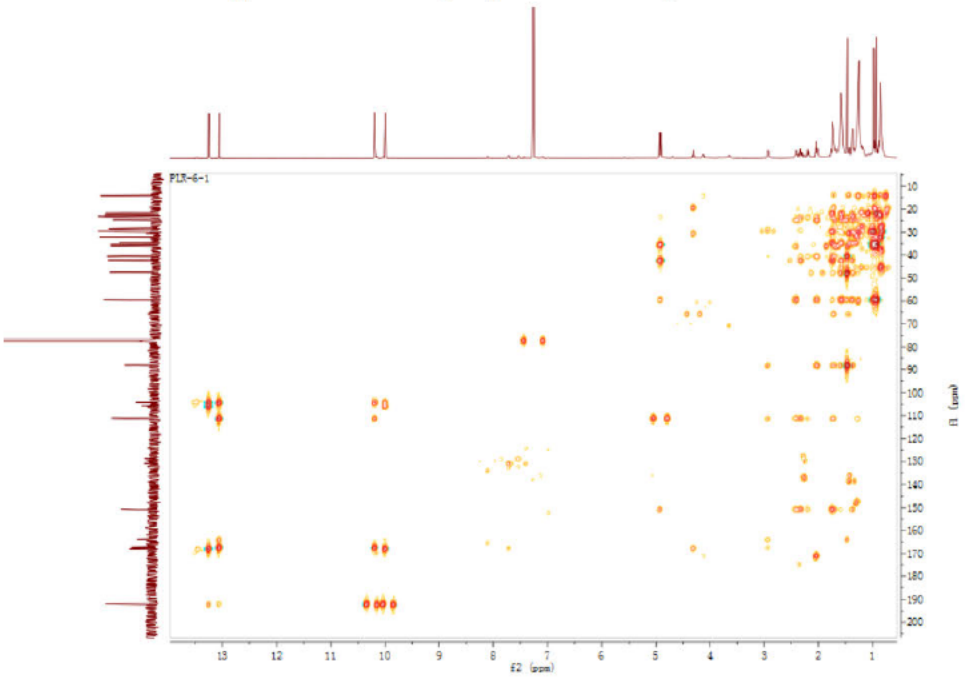

Figure 2.81: COSY spectrum of isolated littordial C (**2.61**) in $CDCl_3$[20]

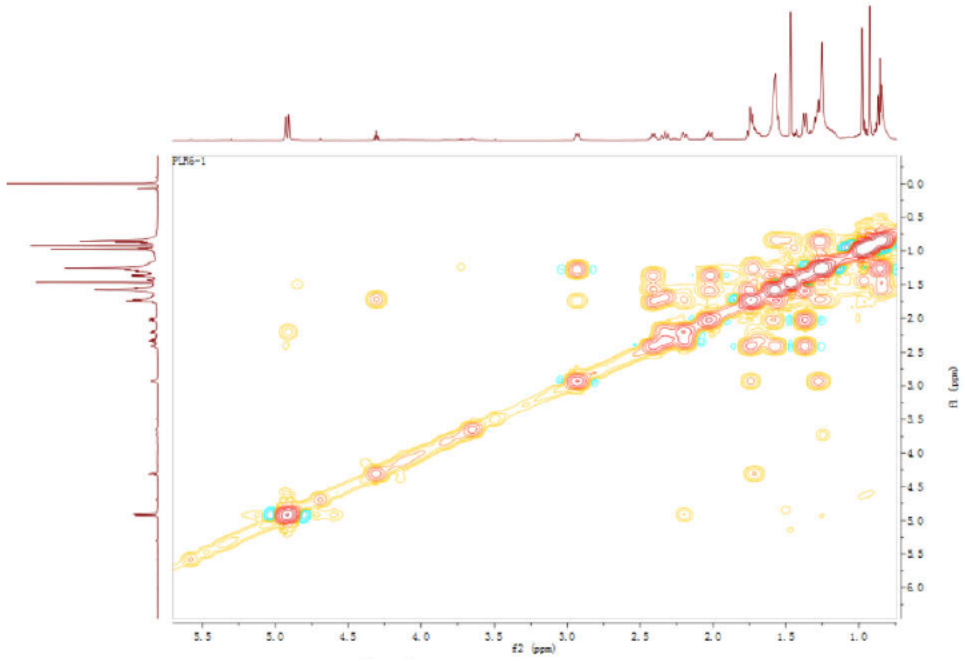

Figure 2.82: NOESY spectrum of isolated littordial C (**2.61**) in $CDCl_3$[20]

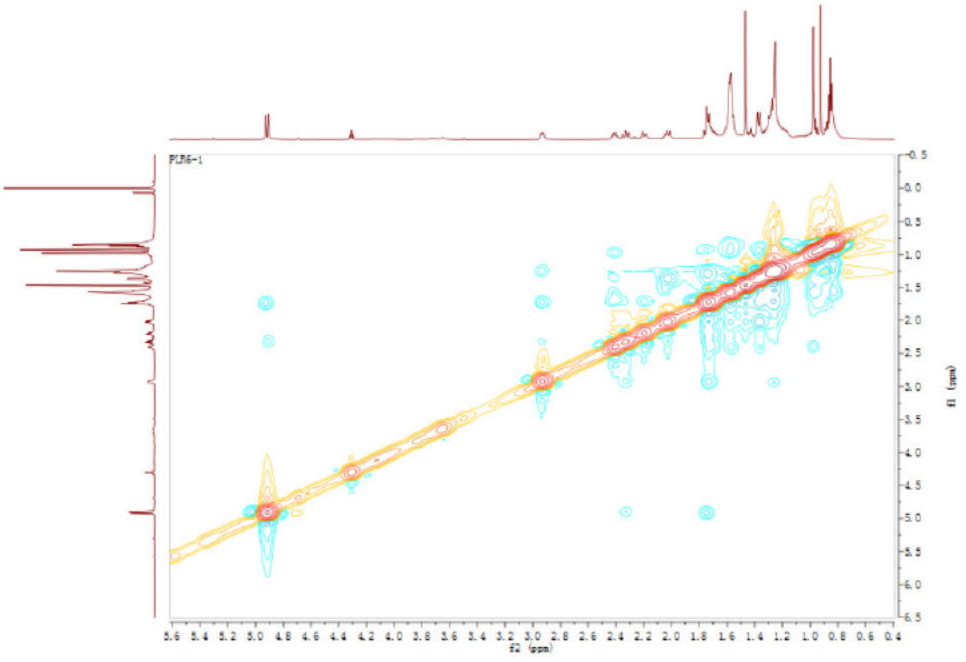

Figure 2.83: ^{1}H NMR spectrum of isolated littordial E (**2.65**) in $CDCl_3$[20]

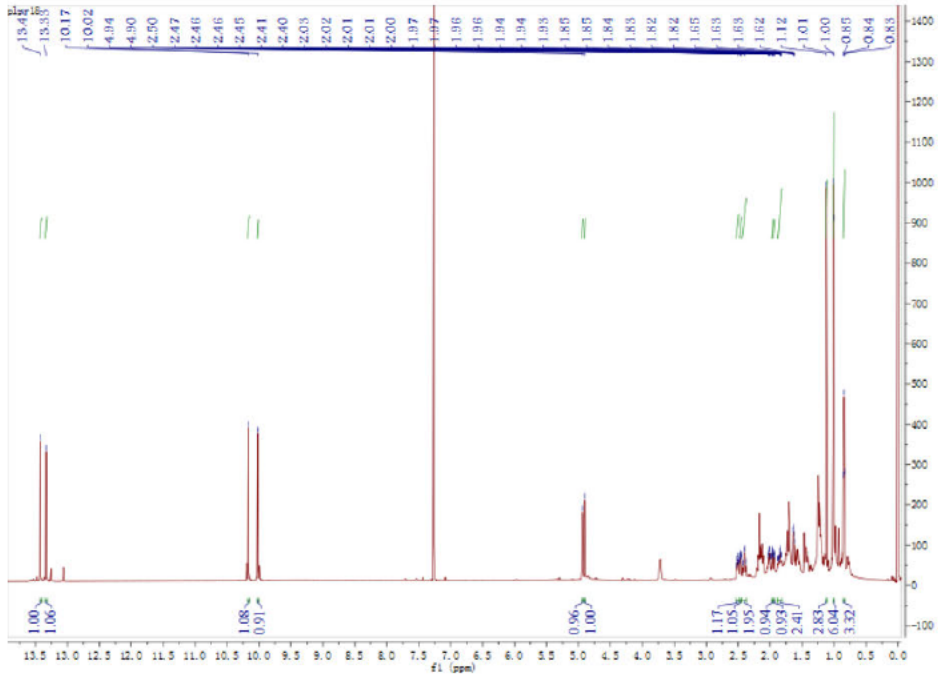

Figure 2.84: ^{13}C NMR spectrum of isolated littordial E (**2.65**) in $CDCl_3$[20]

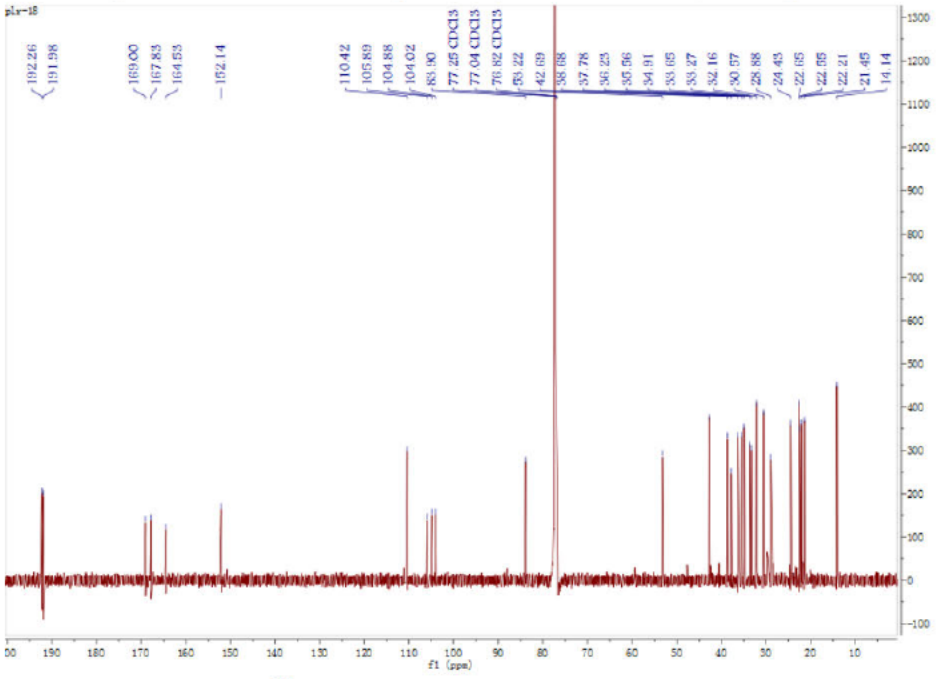

Figure 2.85: HSQC spectrum of isolated littordial E (**2.65**) in $CDCl_3$[20]

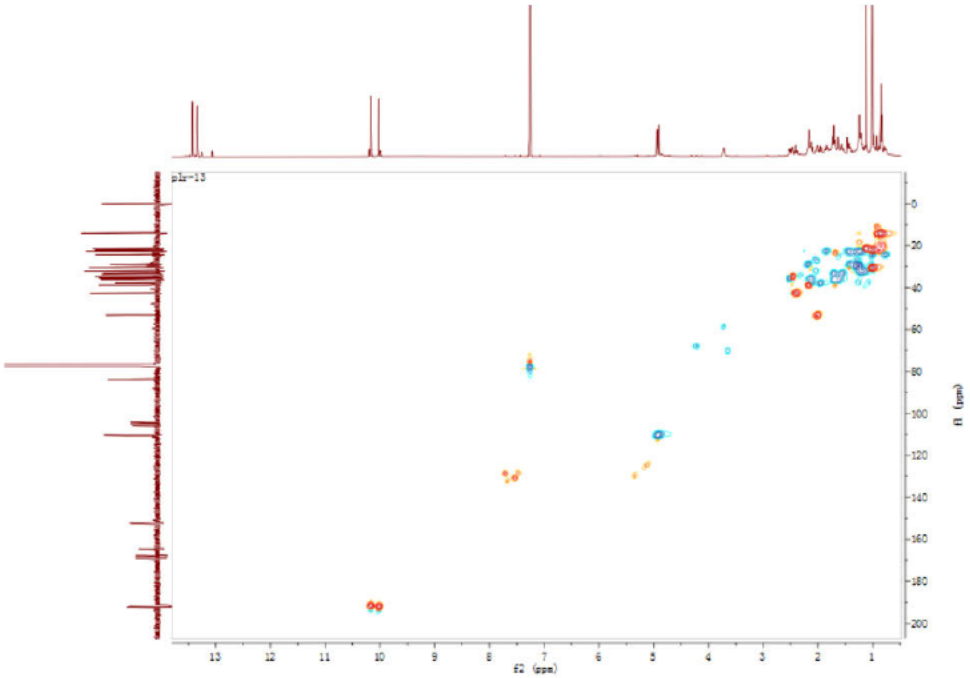

Figure 2.86: HMBC spectrum of isolated littordial E (**2.65**) in $CDCl_3$[20]

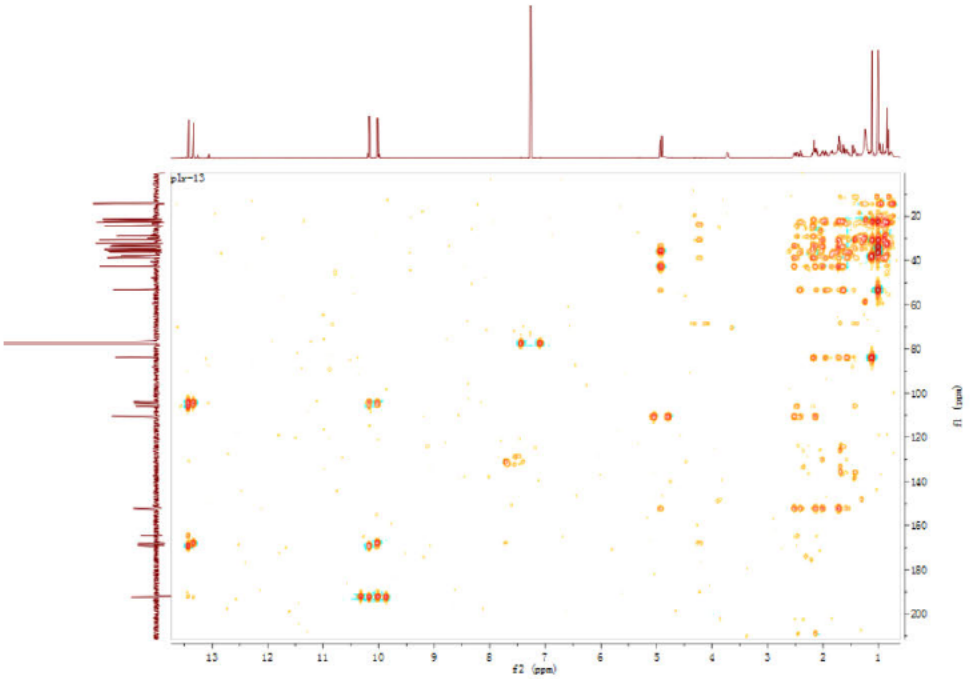

Figure 2.87: COSY spectrum of isolated littordial E (**2.65**) in $CDCl_3$[20]

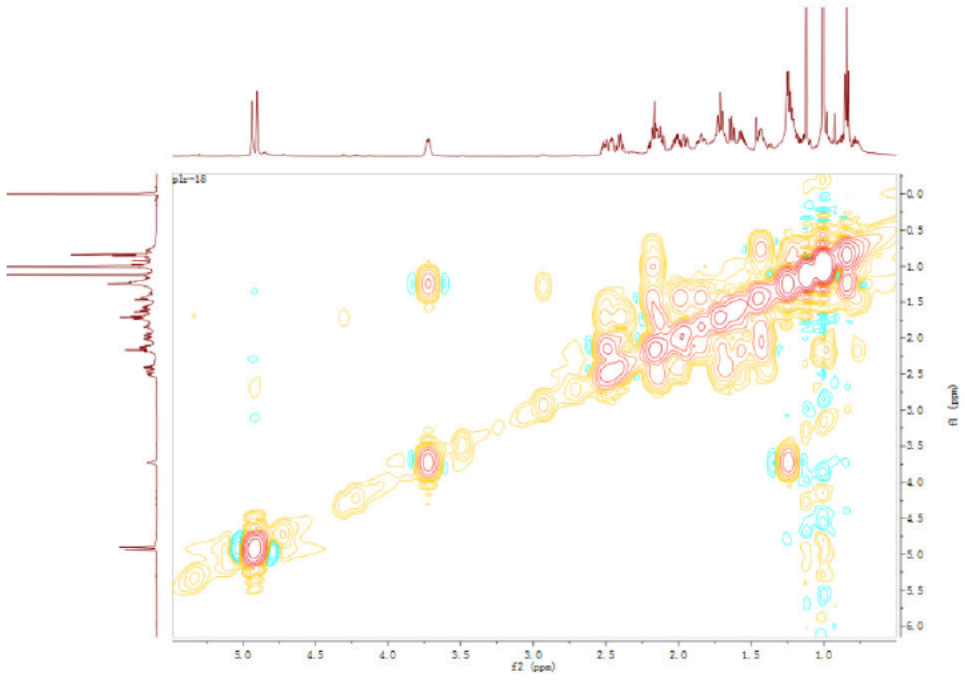

Figure 2.88: NOESY spectrum of isolated littordial E (**2.65**) in $CDCl_3$[20]

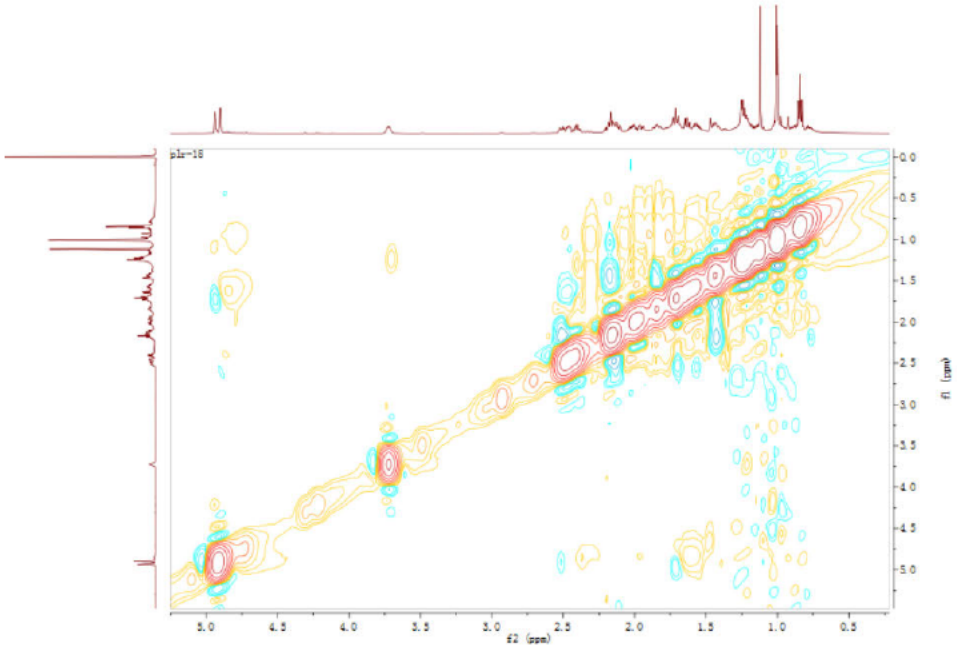

Figure 2.89: ^{1}H NMR spectrum of isolated littordial F (**2.66**) in $CDCl_3$[21]

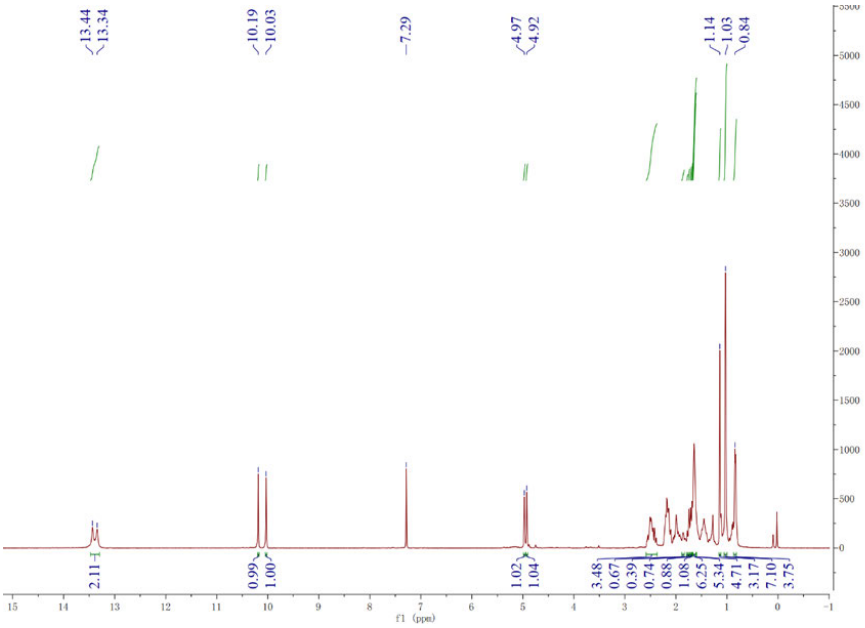

Figure 2.90: ^{13}C NMR spectrum of isolated littordial F (**2.66**) in $CDCl_3$[21]

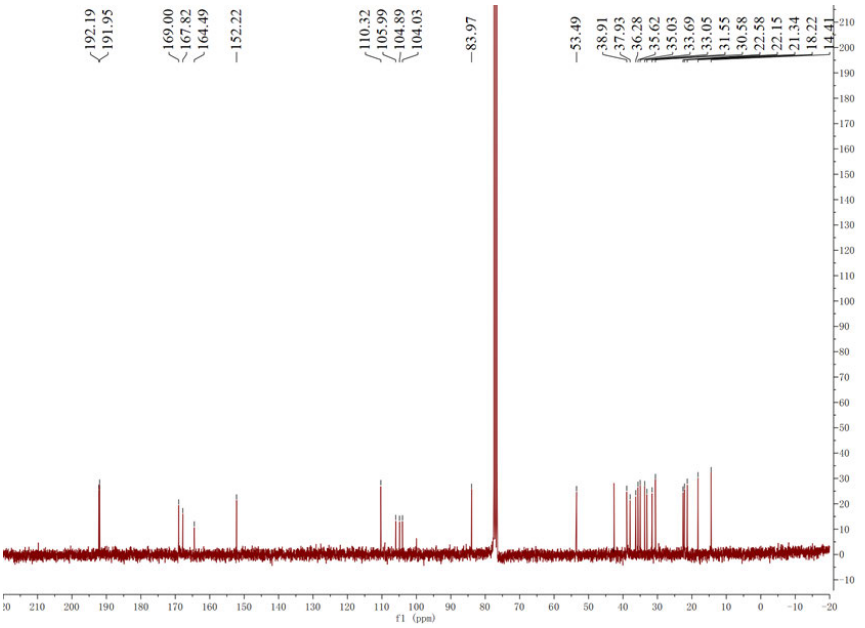

Figure 2.91: HSQC spectrum of isolated littordial F (**2.66**) in $CDCl_3$[21]

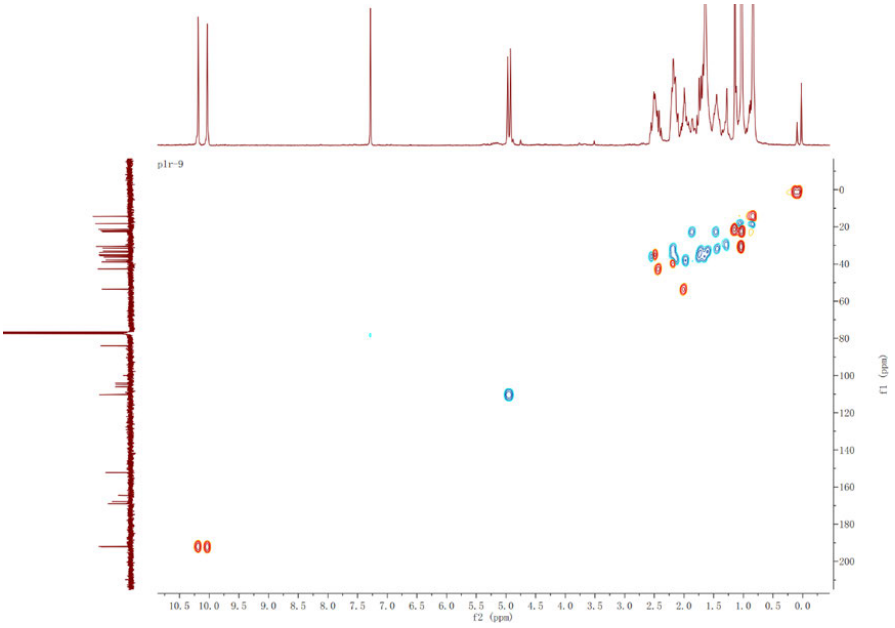

Figure 2.92: HMBC spectrum of isolated littordial F (**2.66**) in $CDCl_3$[21]

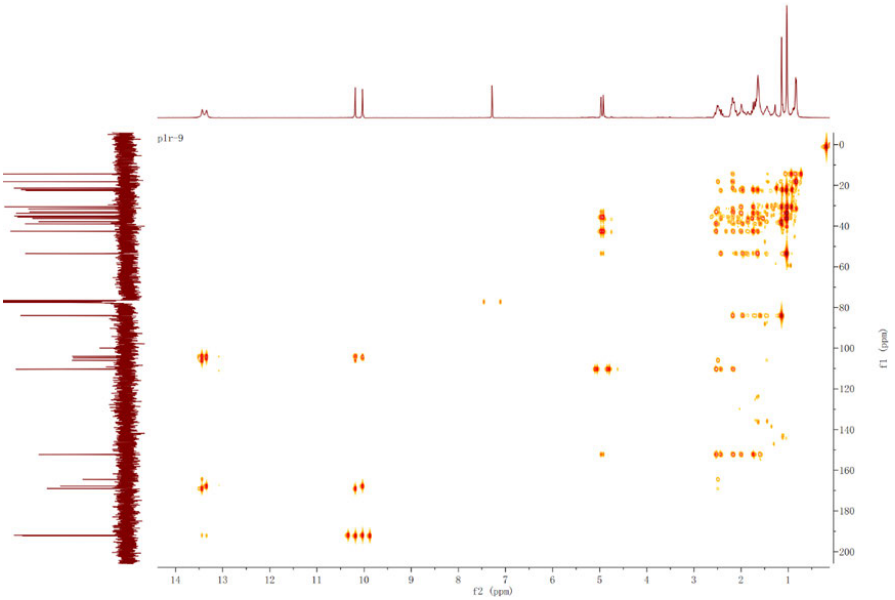

Figure 2.93: COSY spectrum of isolated littordial F (**2.66**) in $CDCl_3$[21]

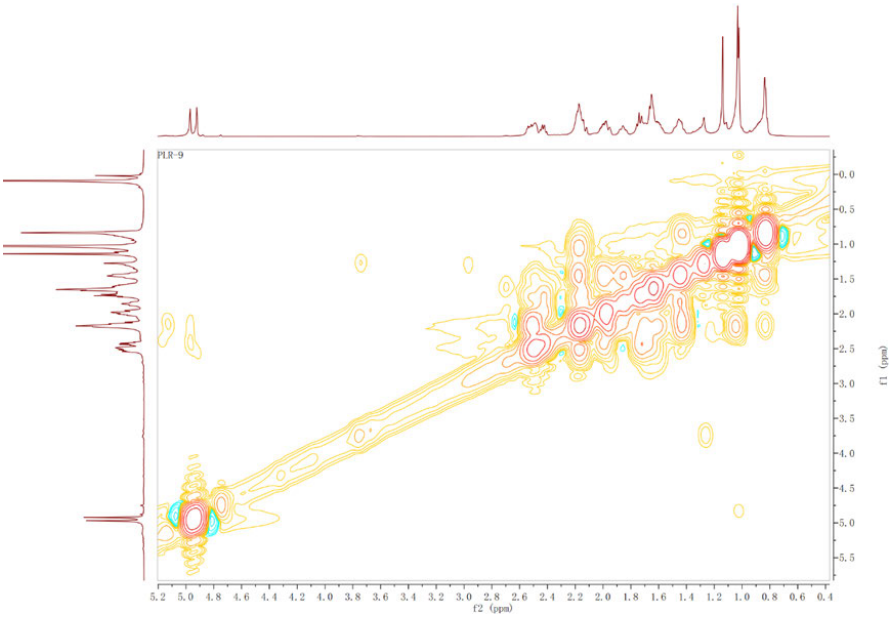

Figure 2.94: NOESY spectrum of isolated littordial F (**2.66**) in $CDCl_3$[21]

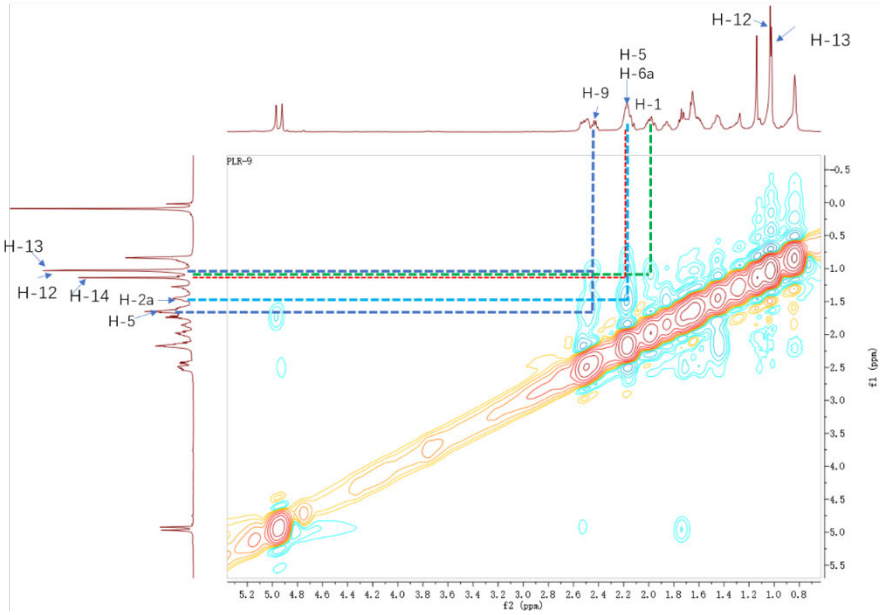

Figure 2.95: ^{1}H NMR spectrum of isolated drychampone B (**2.75**) in $CDCl_3$[28]

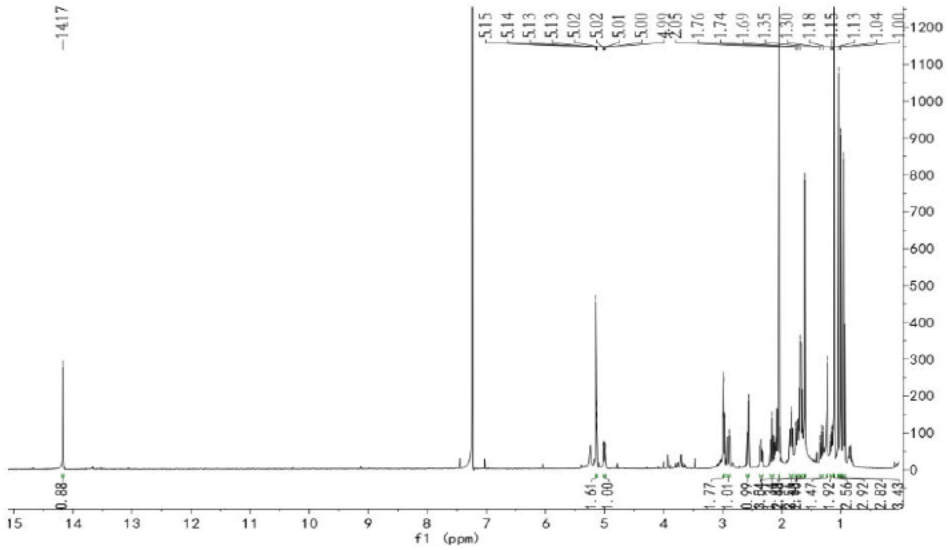

Figure 2.96: ^{13}C NMR spectrum of isolated drychampone B (**2.75**) in $CDCl_3$[28]

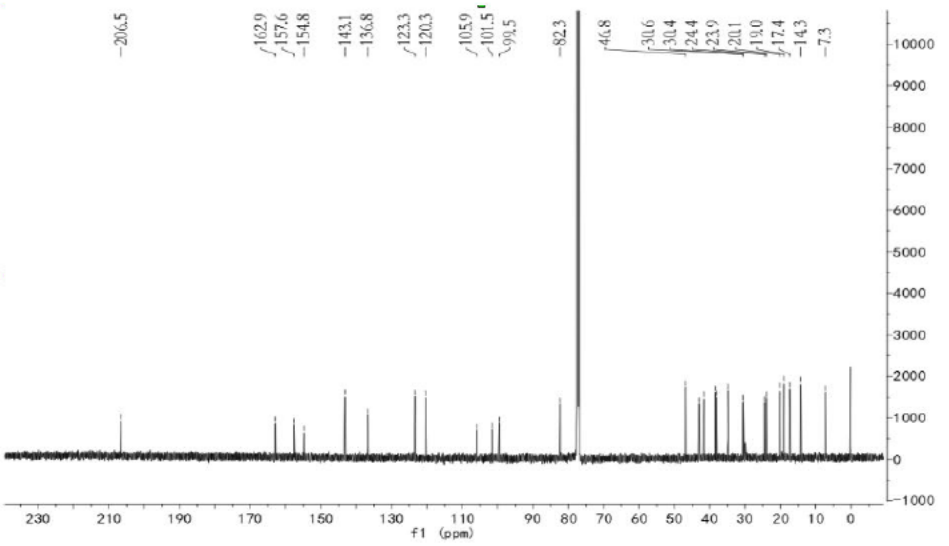

Figure 2.97: COSY spectrum of isolated drychampone B (**2.75**) in $CDCl_3$[28]

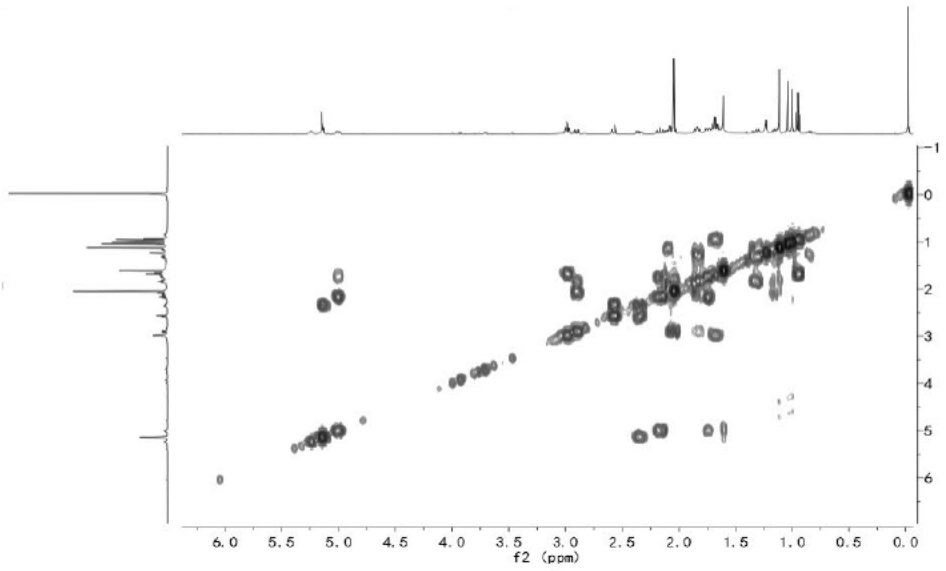

Figure 2.98: HSQC spectrum of isolated drychampone B (**2.75**) in $CDCl_3$[28]

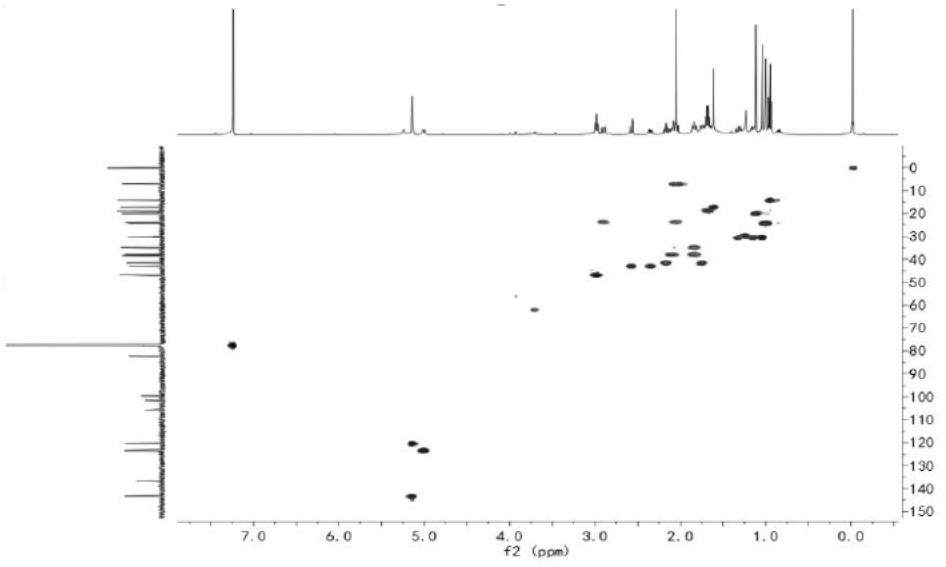

Figure 2.99: HMBC spectrum of isolated drychampone B (**2.75**) in $CDCl_3$[28]

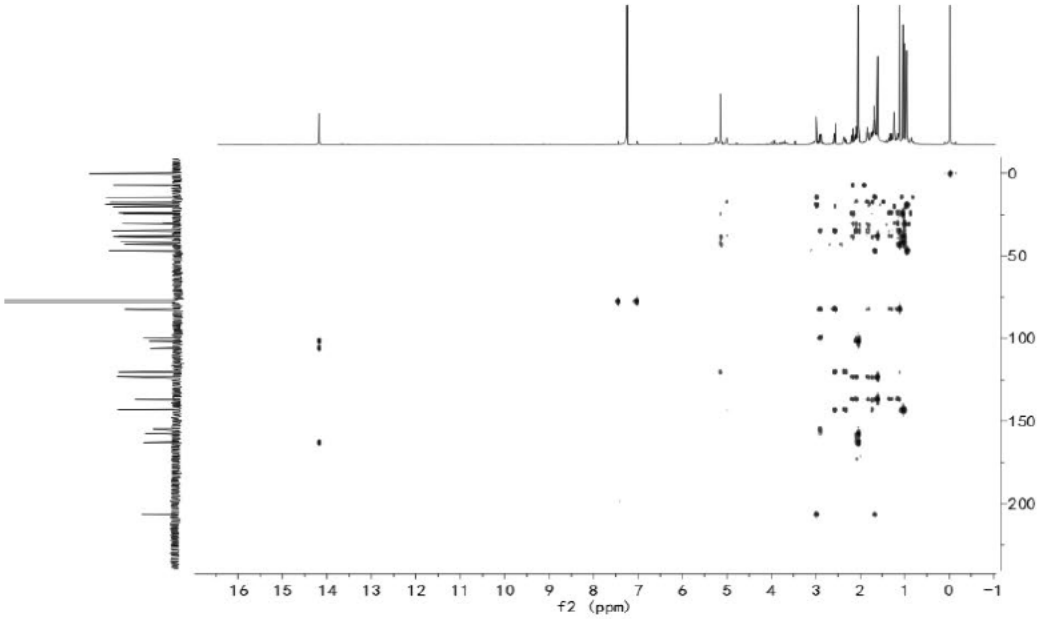

Figure 2.100: NOESY spectrum of isolated drychampone B (**2.75**) in $CDCl_3$[28]

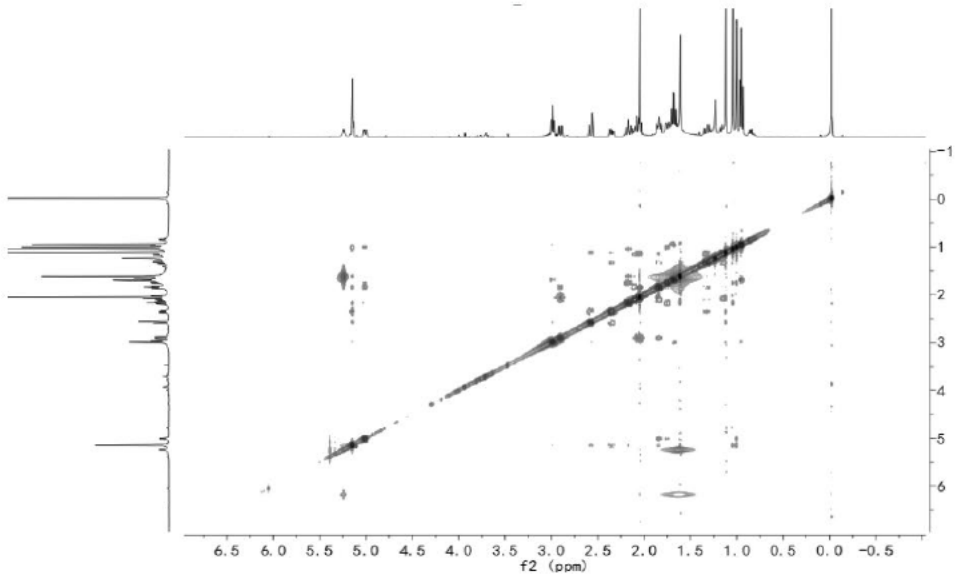

2.11.2 Comparison of natural and synthetic NMR data

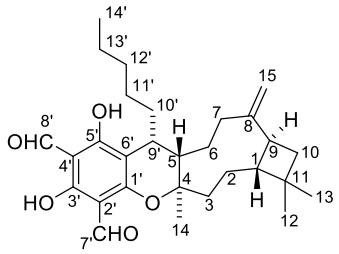

2.61: littordial C

Assignment	Isolated sample, ^{1}H NMR, 600 MHz, $CDCl_3$, (J, Hz)[20]	Synthetic sample, ^{1}H NMR, 600 MHz, $CDCl_3$, (J, Hz)	Isolated sample, ^{13}C NMR, 150 MHz, $CDCl_3$, (J, Hz)[20]	Synthetic sample ^{13}C NMR, 150 MHz, $CDCl_3$, (J, Hz)
1	1.36, overlapped	1.37, overlapped	59.4	59.5
2	1.37, overlapped	1.37, overlapped	24.7	24.8
	1.60, overlapped	1.59, overlapped		
3	1.37, overlapped	1.36, overlapped	47.7	47.8
	2.03 dd (12.6, 10.8)	2.03, dd (12.6, 9.2)		
4			88.1	88.2
5	1.70, overlapped	1.74, overlapped	40.6	40.7
6	1.56, overlapped	1.56, overlapped	36.1	36.1
	1.75, overlapped	1.74, overlapped		
7	2.20, d (13.8)	2.19, dd (16.8, 3.9)	35.5	35.6
	2.33, ddd (14.8, 12.0, 3.0)	2.32, td (13.1, 11.9, 3.3)		
8			150.8	150.9
9	2.41, dd (18.0, 8.4)	2.41, q (8.7)	42.4	42.5
10	1.73, overlapped	1.73, overlapped	23.5	23.6
11			34.7	34.8
12	0.98, s	0.97, s	21.7	21.8
13	0.93, s	0.92, s	29.5	29.7
14	1.47, s	1.46, s	23.2	23.3
15	4.93, s	4.92, s	111.0	111.2
	4.91, s	4.90, s		
1′			163.9	164.0
2′			105.7	105.8
3′			167.9	168.0
4′			104.2	104.3
5′			167.4	167.5
6′			111.1	111.3
7′	10.00, s	9.99, s	192.1	192.2
8′	10.18, s	10.18, s	191.9	192.0
9′	2.93, d (10.2)	2.93, m	29.6	29.6
10′	1.27, overlapped	1.27, overlapped	29.5	29.5
	1.73, overlapped	1.73, overlapped		
11′	1.58, overlapped	1.23, overlapped	28.4	28.6
		1.27, overlapped		
12′	1.18, overlapped	1.17, overlapped	32.2	32.3
		1.28, overlapped		
13′	1.27, overlapped	1.26, overlapped	22.7	22.8
14′	0.86, t (7.2)	0.85, t (7.1)	14.1	14.2
3′-OH	13.25, s	13.25, s		
5′-OH	13.06, s	13.06, s		

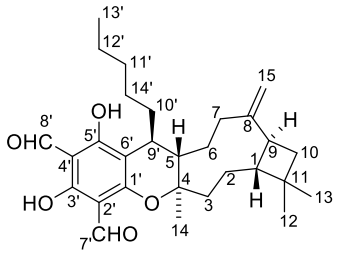

2.65: littordial E
revised structure

Assignment	Isolated sample, ^{1}H NMR, 600 MHz, $CDCl_3$, (J, Hz)[20]	Synthetic sample, ^{1}H NMR, 600 MHz, $CDCl_3$, (J, Hz)	Isolated sample, ^{13}C NMR, 150 MHz, $CDCl_3$, (J, Hz)[20]	Synthetic sample ^{13}C NMR, 150 MHz, $CDCl_3$, (J, Hz)
1	2.00, overlapped	2.01, ddd (11.8, 10.1 5.5)	53.2	53.4
2	1.84, tdd (13.8, 5.4, 3.0)	1.44, overlapped 1.84, dddd (15.1, 12.6, 5.3, 3.1)	22.6	22.8
3	1.95, ddd (15.0, 5.4, 3.0) 2.10, d (2.4)	1.95, ddd (15.4, 5.6, 3.1) 2.13, overlapped	37.8	37.9
4			84.0	84.0
5	2.17, overlapped	2.17, overlapped	38.7	38.8
6	1.56, m 1.70, overlapped	1.56, overlapped 1.70, overlapped	33.3	33.4
7	2.13, m 2.52, dt (13.8, 5.4)	2.14, overlapped 2.51, dt (13.9, 5.2)	35.6	35.7
8			152.1	152.3
9	2.40, dd (18.0, 9.6)	2.40, m	42.7	42.8
10	1.63, dd (10.8, 7.8) 1.69, overlapped	1.63, dd (10.7, 7.7) 1.71, overlapped	36.2	36.4
11			33.6	33.8
12	1.01, s	1.01, s	22.2	22.3
13	1.00, s	1.00, s	30.6	30.7
14	1.11, s	1.12, s	21.5	21.6
15	4.94, s 4.90, s	4.94, s 4.90, s	110.5	110.5
1′			164.6	164.6
2′			104.1	104.2
3′			167.7	168.0
4′			104.9	105.0
5′			168.8	169.1
6′			105.9	106.0
7′	10.02, s	10.02, s	192.0	192.1
8′	10.17, s	10.16, s	192.3	192.4
9′	2.45, m	2.46, ddd (9.2, 5.0, 2.6)	34.9	35.1
10′	1.42, overlapped 2.18, overlapped	1.43, overlapped 2.18, overlapped	28.8	29.0
11′	1.19, m 2.03, overlapped	1.14, overlapped 1.20, overlapped	32.2	32.3
12′	1.24, overlapped	1.22, overlapped	22.5	22.7
13′	0.84, t (7.2)	0.84, t (7.1)	14.1	14.3
14′	0.77, m 1.00, overlapped	0.77, m 1.02, overlapped	24.3	24.6
3′-OH	13.3, s	13.33, s		
5′-OH	13.4, s	13.42, s		

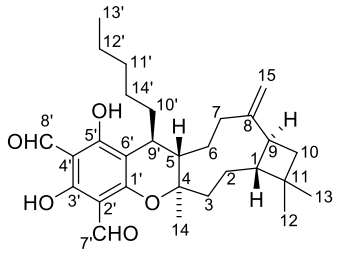

2.65: littordial E
revised structure

Assignment	Isolated sample, ^{1}H NMR, 600 MHz, $CDCl_3$, (J, Hz)[20]	Synthetic sample, ^{1}H NMR, 600 MHz, d_6-benzene, (J, Hz)	Isolated sample, ^{13}C NMR, 150 MHz, $CDCl_3$, (J, Hz)[20]	Synthetic sample ^{13}C NMR, 150 MHz, d_6-benzene
1	2.00, overlapped	2.04, ddd (15.4, 7.5, 3.7)	53.2	53.7
2	1.84, tdd (13.8, 5.4, 3.0)	1.21, overlapped	22.6	22.8
		1.76, overlapped		
3	1.95, ddd (15.0, 5.4, 3.0)	1.60, overlapped	37.8	37.8
	2.10, d (2.4)	1.75, overlapped		
4			84.0	83.7
5	2.17, overlapped	2.13, td (9.1, 2.8)	38.7	39.0
6	1.56, m	1.21, overlapped	33.3	33.4
	1.70, overlapped	1.44, overlapped		
7	2.13, m	1.85, ddd (13.5, 11.3, 4.8)	35.6	35.8
	2.52, dt (13.8, 5.4)	2.32, dt (13.9, 5.3)		
8			152.1	152.3
9	2.40, dd (18.0, 9.6)	2.21, td (10.2, 7.8)	42.7	42.8
10	1.63, dd (10.8, 7.8)	1.59, overlapped	36.2	36.6
	1.69, overlapped	1.73, overlapped		
11			33.6	33.7
12	1.01, s	0.92 (s)	22.2	22.3
13	1.00, s	0.99 (s)	30.6	30.6
14	1.11, s	0.76 (s)	21.5	21.2
15	4.94, s	4.87 (s)	110.5	110.7
	4.90, s	5.00 (s)		
1′			164.6	164.4
2′			104.1	104.6
3′			167.7	168.1
4′			104.9	105.3
5′			168.8	169.4
6′			105.9	106.0
7′	10.02, s	9.98, s	192.0	191.8
8′	10.17, s	10.10, s	192.3	192.0
9′	2.45, m	2.45, m	34.9	35.4
10′	1.42, overlapped	1.46, overlapped	28.8	29.4
	2.18, overlapped	2.40, m		
11′	1.19, m	1.28, overlapped	32.2	32.6
	2.03, overlapped	1.60, overlapped		
12′	1.24, overlapped	1.27, overlapped	22.5	23.1
		1.42, overlapped		
13′	0.84, t (7.2)	0.86, t (7.0)	14.1	14.4
14′	0.77, m	1.02, overlapped	24.3	24.9
	1.00, overlapped	1.20, overlapped		
3′-OH	13.3, s			
5′-OH	13.4, s			

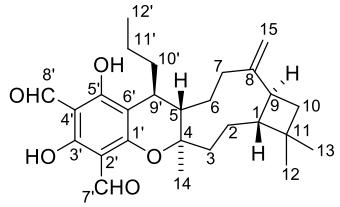

2.66: littordial F
revised structure

Assignment	Isolated Sample, ^{1}H NMR, 600 MHz, $CDCl_3$, (J, Hz)[21]	Synthetic Sample, ^{1}H NMR, 600 MHz, $CDCl_3$, (J, Hz)	Isolated Sample, ^{13}C NMR, 150 MHz, $CDCl_3$, (J, Hz)[21]	Synthetic Sample, ^{13}C NMR, 150 MHz, $CDCl_3$, (J, Hz)
1	2.00, m	1.98, overlapped	53.5	53.6
2	1.46, m 1.86, m	1.43, overlapped 1.84, dddd (15.1, 12.2, 5.3, 3.0)	22.6	22.7
3	1.97, m	1.95, ddd (15.4, 5.7, 3.0) 2.12, overlapped	37.9	38.1
4			84.0	84.1
5	2.18, overlapped	2.16, overlapped	38.9	39.1
6	1.60, overlapped 2.18, overlapped	1.57, overlapped 1.69, overlapped	33.7	33.2
7	1.74, overlapped 2.54, overlapped	2.14, overlapped 2.51, overlapped	35.6	35.8
8			154.0	152.4
9	2.43, overlapped	2.41, m	42.5	42.7
10	1.65, overlapped	1.63, dd (10.7, 7.7) 1.72, overlapped	36.3	36.4
11			33.1	33.8
12	1.04, s	1.00, s	22.2	22.3
13	1.02, s	1.01, s	30.6	30.7
14	1.14, s	1.12, s	21.3	21.5
15	4.92, s 4.97, s	4.90, s 4.95, s	110.3	110.5
1′			164.5	164.6
2′			104.9	105.1
3′			167.8	168.0
4′			104.0	104.2
5′			169.0	169.2
6′			106.0	106.1
7′		10.01	192.2	192.3
8′		10.16	192.0	192.1
9′	2.14, m 2.48, m	2.47, m	35.0	35.2
10′	1.44, m	1.43, overlapped 2.16, overlapped	31.6	31.7
11′	0.88, m 1.05, m	0.83, overlapped 1.04, overlapped	18.3	18.4
12′	0.83, d (3.6)	0.81, m	14.5	14.6
3′-OH	13.3, s	13.32, s		
5′-OH	13.4, s	13.42, s		

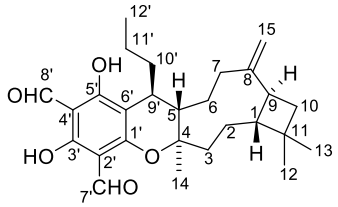

2.66: littordial F
revised structure

Assignment	Isolated Sample, ^{1}H NMR, 600 MHz, $CDCl_3$, (J, Hz)[21]	Synthetic Sample, ^{1}H NMR, 600 MHz, d_6-benzene, (J, Hz)	Isolated Sample, ^{13}C NMR, 150 MHz, $CDCl_3$, (J, Hz)[21]	Synthetic Sample, ^{13}C NMR, 150 MHz, d_6-benzene, (J, Hz)
1	2.00, m	1.97, m	53.5	54.0
2	1.46, m 1.86, m	1.20, overlapped 1.73, overlapped	22.6	22.8
3	1.97, m	1.59, overlapped 1.73, overlapped	37.9	38.0
4			84.0	83.7
5	2.18, overlapped	2.08, td (8.9, 3.0)	38.9	39.1
6	1.60, overlapped 2.18, overlapped	1.19, overlapped 1.39, overlapped	33.7	33.7
7	1.74, overlapped 2.54, overlapped	1.85, overlapped 2.30, overlapped	35.6	35.9
8			154.0	152.4
9	2.43, overlapped	2.20, td (9.9, 7.6)	42.5	42.3
10	1.65, overlapped	1.58, overlapped 1.71, overlapped	36.3	36.5
11			33.1	33.1
12	1.04, s	0.91, s	22.2	22.2
13	1.02, s	0.95, s	30.6	30.6
14	1.14, s	0.75, s	21.3	21.1
15	4.92, s 4.97, s	4.86, s 4.99, s	110.3	110.6
1′			164.5	164.3
2′			104.9	105.3
3′			167.8	168.1
4′			104.0	104.5
5′			169.0	169.4
6′			106.0	106.1
7′			192.2	191.8
8′			192.0	191.9
9′	2.14, m 2.48, m	2.43, m	35.0	35.4
10′	1.44, m	1.43, overlapped 2.35, overlapped	31.6	32.1
11′	0.88, m 1.05, m	0.99, overlapped 1.16, overlapped	18.3	18.7
12′	0.83, d (3.6)	0.88, t (7.2)	14.5	14.7
3′-OH	13.3, s			
5′-OH	13.4, s			

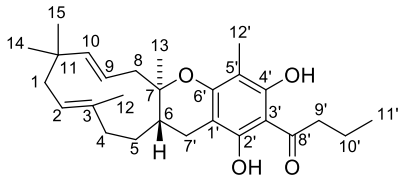

2.75: drychampone B
revised structure

Assignment	Isolated sample ^{1}H NMR, 500 MHz, $CDCl_3$, (J, Hz)[28]	Synthetic sample ^{1}H NMR, 600 MHz, $CDCl_3$, (J, Hz)	Isolated sample ^{13}C NMR, 125 MHz, $CDCl_3$, (J, Hz)[28]	Synthetic sample ^{13}C NMR, 150 MHz, $CDCl_3$, (J, Hz)
1	1.74, dd (12.5, 4.2) 2.17, t (12.5)	1.77, dd (12.9, 4.4) 2.19, t (12.4)	41.6	41.5
2	5.00, dd, (8.7, 4.2)	5.03, m	123.3	123.2
3			136.8	136.7
4	1.84 2.10, m	1.89 – 1.82, overlapped 2.16 – 2.09, m	38.0	37.9
5	1.16, m 1.28, m	1.21– 1.15, m 1.34, m	30.6	30.5
6	1.83	1.89 – 1.82, overlapped	34.8	34.8
7			82.3	82.2
8	2.35, m 2.56, d (14.5)	2.37, ddd (14.5, 7.1, 3.0) 2.60, d (14.5)	43.0	42.9
9	5.15, m	5.18–5.14, m	120.3	120.2
10	5.14, d (16.2)	5.18–5.14, m	143.1	143.1
11			38.4	38.4
12	1.61, s	1.63, s	17.4	17.3
13	1.12, s	1.14, s	20.1	20.1
14	1.00, s	1.02, s	24.4	24.4
15	1.04, s	1.06, s	30.4	30.4
1′			99.5	99.5
2′			154.8	154.7
3′			105.9	105.8
4′			162.9	162.8
5′			101.5	101.5
6′			157.6	157.5
7′	2.05 2.90, dd (16.8, 5.2)	2,07, overlapped 2.92, dd (16.1, 5.7)	23.9	23.9
8′			206.5	206.4
9′	2.99, td (7.5, 3.0)	3.00, td (7.4, 3.8)	46.8	46.7
10′	1.67, m	1.70, q (7.4)	19.0	19.0
11′	0.95, t (7.5)	0.97, t (7.4)	14.3	14.2
12′	2.04, s	2.07, s	7.3	7.2

2.11.3 CD spectra

Figure 2.101: CD spectrum of synthetic littordial C (**2.61**)

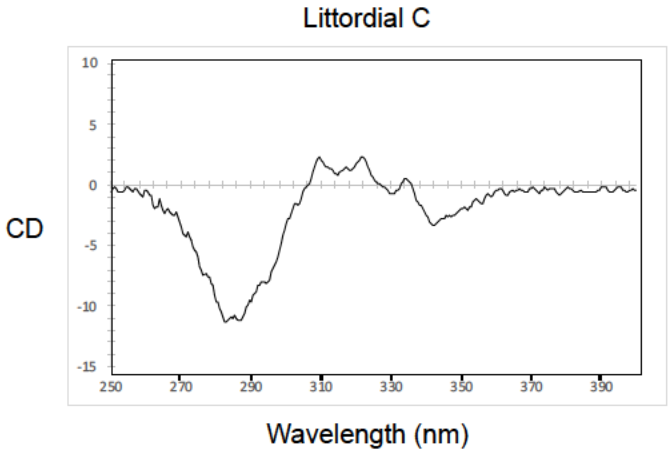

Figure 2.102: CD spectrum of synthetic littordial E (**2.65**)

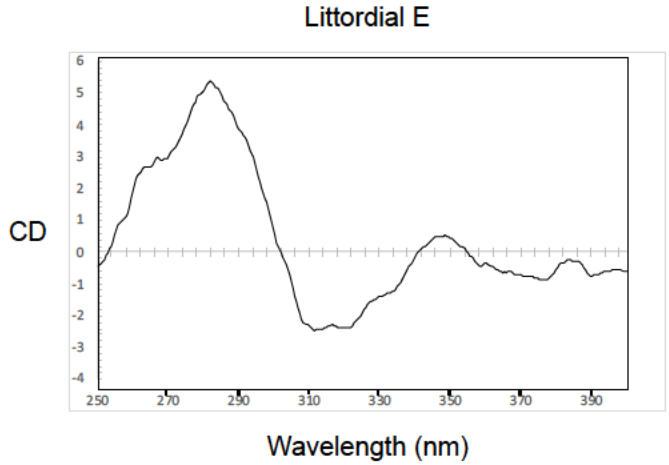

Figure 2.103: CD spectrum of synthetic littordial F (**2.66**)

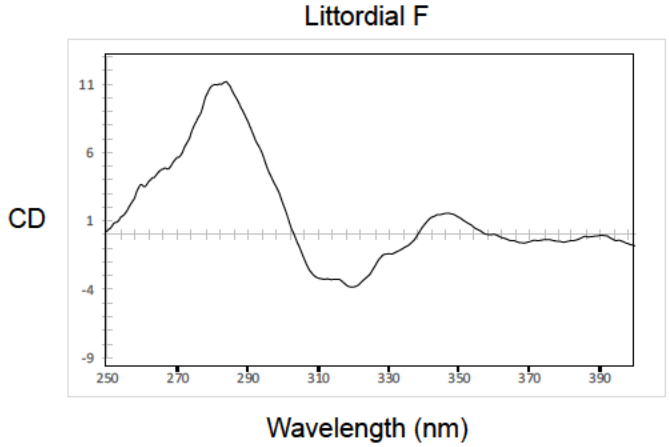

2.11.4 Single crystal X-ray data

A single crystal of littordial C was mounted in paratone-N oil on a MiteGen crystal mount and the data was collected on an X-ray diffraction at 150(2) K on an Oxford X-calibur single crystal diffractometer using Mo Kα radiation. The data set was corrected for absorption using a multi-scan method, and the structures solved by direct methods using SHELXS-97[32] and refined by full-matrix least squares on F2 by SHELXL-2015,[33] interfaced through the programs X-Seed[34] and Olex2.[35] Except as otherwise indicated, all non-hydrogen atoms were refined anisotropically and hydrogen atoms were included as invariants at geometrically estimated positions. The table below provides the crystal data and structure refinement details for littordial C.

Table 2.2: Crystal data and structure refinement for littordial C (**2.61**)

Compound	littordial C
Empirical formula	$C_{29}H_{40}O_5$
Formula weight	468.61
Temperature/K	149.9(3)
Crystal system	tetragonal
Space group	$P4_12_12$
a/Å	11.13120(10)
b/Å	11.13120(10)
c/Å	41.3856(7)
α/°	90
β/°	90
γ/°	90
Volume/Å^3	5127.83(13)
Z	8
ρ_{calc}g/cm^3	1.214
μ/mm^{-1}	0.081
F(000)	2032.0
Crystal size/mm^3	0.28 × 0.253 × 0.049
Radiation	MoKα (λ = 0.71073)
2Θ range for data collection/°	6.504 to 58.868
Index ranges	$-15 \leq h \leq 15$, $-15 \leq k \leq 15$, $-56 \leq l \leq 57$
Reflections collected	183383
Independent reflections	6837 [R_{int} = 0.0878, R_{sigma} = 0.0419]
Data/restraints/parameters	6837/0/316
Goodness-of-fit on F^2	1.061
Final R indexes [I>=2σ (I)]	R_1 = 0.0522, wR_2 = 0.1013
Final R indexes [all data]	R_1 = 0.0738, wR_2 = 0.1076
Largest diff. peak/hole / e Å^{-3}	0.30/-0.20
Flack parameter	0.3(3)

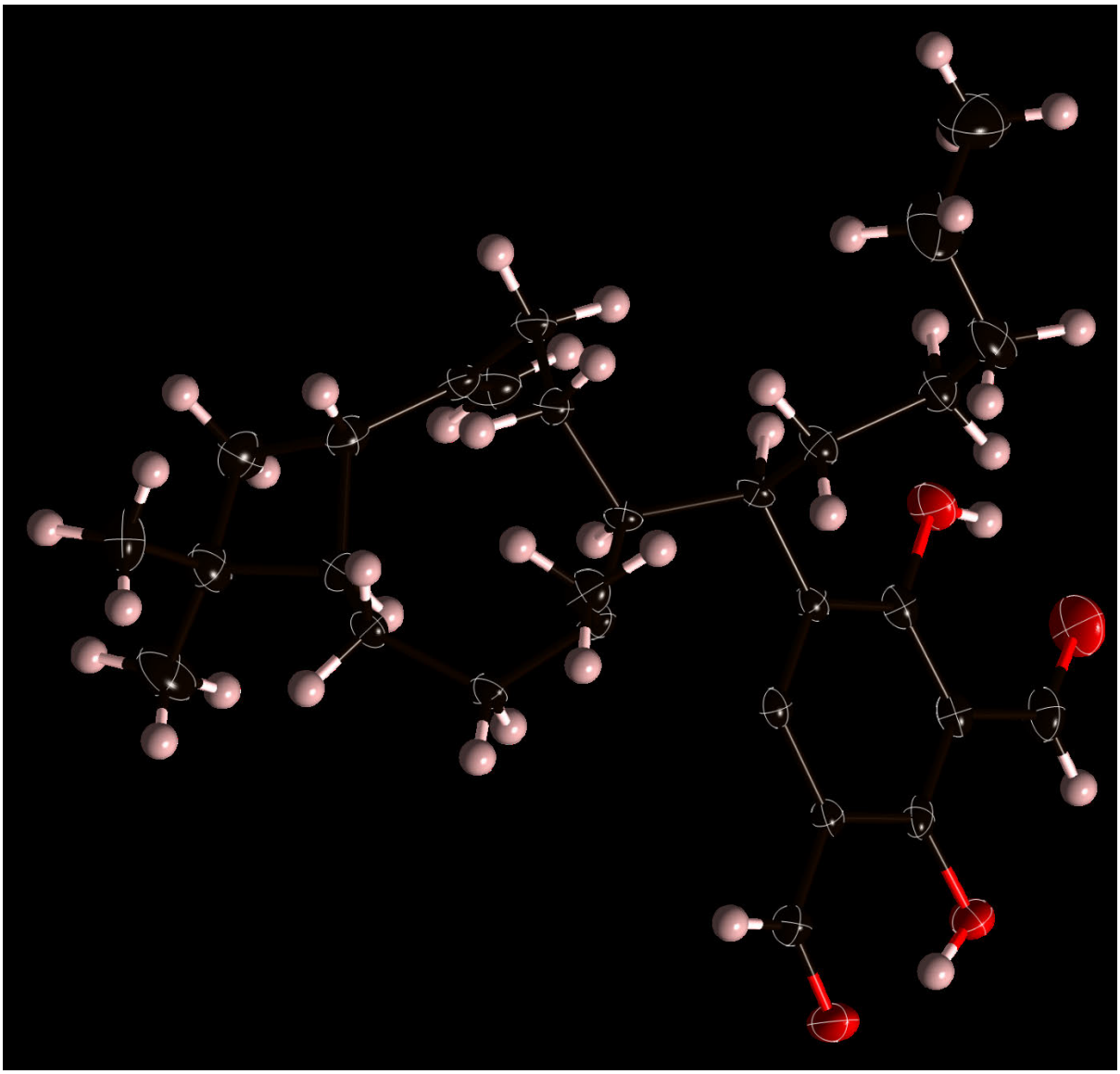

Figure 2.104: A perspective view of one selected molecule of the asymmetric unit of Littordial C (**2.61**), with all non-hydrogen atoms represented by ellipsoids at the 50% probability level (Carbon, black; Hydrogen, white; Oxygen, red).

2.11.5 Computational data

Calculations were carried out with density functional theory (DFT) using Gaussian 16 (revision A.03). Geometries were optimised in the gas phase at the M06-2X/6-31+G(d) level.[36] Stable ground states and transition states were identified by the number of imaginary vibrational frequencies. Zero-point energies and thermal corrections. The transition states were shown to connect reactants and products using intrinsic reaction coordinate calculations.[37] Single-point energy calculations of the optimised geometries were carried out in the gas phase at the M06-2X/6-311+G(d,p) level and in toluene solvent using the SMD continuum solvent model[38] using parameters adapted for hexafluoroisopropanol,[39] at the M06-2X/6-311+G(d,p) level. The optimised geometries are given below in Cartesian coordinates and the energies given in units of Hartree. The Gibbs free energy in solution at 298.15 K was calculated as $G_{soln} = E_{M06\text{-}2X/6\text{-}311+G(d,p),sol.} + TCG_{M06\text{-}2X/6\text{-}31+G(d)} + k_B T \ln(c k_B T/p)$. *TCG* is the thermal correction to the free energy. The final term is a correction to account for the difference in translational entropy resulting from the change in concentration from ideal gas-phase species at pressure p = 1 atm to ideal solution-phase species at concentration c = 1 mol/L at temperature T and is equal to 7.93 kJ/mol at 298.15 K.

Table 2.3: Calculated free energies of starting materials and products. [a]Relative free energy refers to the comparison of isomers for ground state structures, and activation barriers for transition state structures.

Structure	E(M06-2X/6-31+G(d))/a.u.	TCG/a.u.	E(M06-2X/6-311+G(d,p))/a.u.	E(M06-2X/6-311+G(d,p), smd=HFIP)/a.u.	G(M06-2X/6-311+G(d,p), smd=HFIP, kBTln(ckBT/p)/kJ.mol^{-1}	Relative free energy (kJ.mol^{-1})[a]
caryophyllene-*αα*	-585 7257137	0 319369	-585 8701592	-585 8837733	-1537391 4	0 2
caryophyllene-*βα*	-585 7243348	0 318311	-585 8688689	-585 8828104	-1537391 7	0 0
caryophyllene-*ββ*	-585 7241116	0 318325	-585 8685618	-585 8824629	-1537390 7	0 9
caryophyllene-*αβ*	-585 7176052	0 31845	-585 8620886	-585 8758407	-1537373 0	18 7
***E*-o-QM**	-840 2913633	0 181864	-840 517878	-840 5314837	-2206330 0	0 0
***Z*-o-QM**	-840 2928995	0 182755	-840 5197473	-840 5319208	-2206328 8	1 2
caryophyllene- *αα*-E-oQM-DA-endo-TS	-1426 013502	0 526059	-1426 384883	-1426 415368	-3743664 5	57 0
caryophyllene- *αα*-E-oQM-DA-exo-TS	-1426 005817	0 527022	-1426 377629	-1426 408544	-3743644 0	77 4
caryophyllene- *αα*-Z-oQM-DA-endo-TS	-1426 013397	0 525987	-1426 385137	-1426 415652	-3743665 4	54 8
caryophyllene- *αα*-Z-oQM-DA-exo-TS	-1426 010993	0 525416	-1426 383138	-1426 41439	-3743663 6	56 6
caryophyllene-*βα*-E-oQM-DA-endo-TS	-1426 014362	0 524671	-1426 385792	-1426 416022	-3743669 8	51 8
caryophyllene-*βα*-E-oQM-DA-exo-TS	-1426 009367	0 52547	-1426 380946	-1426 4119	-3743656 9	64 8
caryophyllene-*βα*-Z-oQM-DA-endo-TS	-1426 01598	0 526132	-1426 387605	-1426 417901	-3743670 9	49 6
caryophyllene-*βα*-Z-oQM-DA-exo-TS	-1426 011766	0 526119	-1426 383722	-1426 415246	-3743664 0	56 5
caryophyllene-*ββ*-E-oQM-DA-endo-TS	-1426 013817	0 525369	-1426 385293	-1426 414933	-3743665 1	55 6
caryophyllene-*ββ*-E-oQM-DA-exo-TS	-1426 008401	0 525517	-1426 379909	-1426 411371	-3743655 4	65 3
caryophyllene-*ββ*-Z-oQM-DA-endo-TS	-1426 013723	0 525687	-1426 385407	-1426 414787	-3743663 9	55 6
caryophyllene-*ββ* -Z-oQM-DA-exo-TS	-1426 014931	0 523749	-1426 38694	-1426 418456	-3743678 6	40 9
littordial A *α*	-1426 090088	0 534693	-1426 458849	-1426 480928	-3743813 9	0 0
littordial A *β*	-1426 089845	0 53431	-1426 45846	-1426 480299	-3743813 3	0 6
littordial B *α*	-1426 087814	0 534646	-1426 455989	-1426 477299	-3743804 5	16 1
littordial B *β*	-1426 092068	0 534246	-1426 46053	-1426 483029	-3743820 6	0 0
littordial F *α*	-1426 089128	0 534153	-1426 457787	-1426 479869	-3743812 5	5 6
littordial F *β*	-1426 091118	0 533955	-1426 459633	-1426 481796	-3743818 1	0 0
littordial Z *α*	-1426 055952	0 535309	-1426 45999	-1426 481311	-3743813 3	6 8
littordial Z *β*	-1426 058801	0 53523	-1426 462887	-1426 483839	-3743820 1	0 0
littordial C *α*	-1504 637837	0 589259	-1505 062961	-1505 086141	-3950048 6	17 2
littordial C *β*	-1504 641707	0 588419	-1505 067514	-1505 091867	-3950065 9	0 0
littordial E *α*	-1504 676253	0 587463	-1505 064759	-1505 088862	-3950060 5	6 0
littordial E *β*	-1504 678204	0 587124	-1505 066487	-1505 090796	-3950066 5	0 0

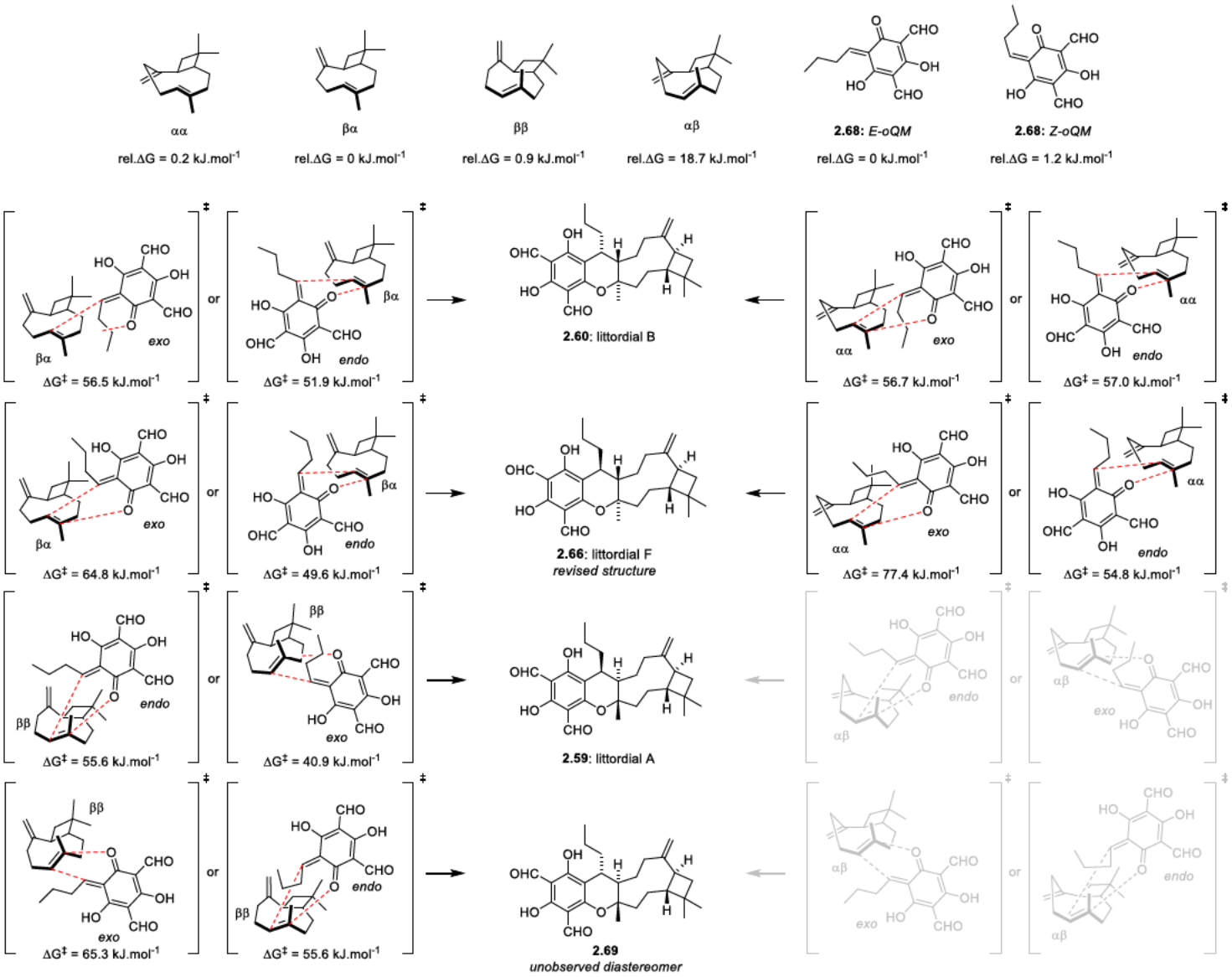

Figure 2.105: Calculated cycloaddition pathways in the synthesis of littordials A, B, F and an unobserved diastereomer

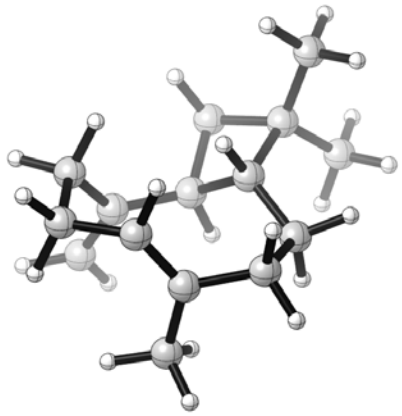

caryophyllene-$\alpha\alpha$
$E_{(M06\text{-}2X/6\text{-}31+G(d))}$: -585.7257137
$TCG_{(M06\text{-}2X/6\text{-}31+G(d))}$: 0.319369
$E_{(M06\text{-}2X/6\text{-}311+G(d,p))}$: -585.8701592
$E_{(M06\text{-}2X/6\text{-}311+G(d,p),\ smd=HFIP)}$: -585.8837733
Imaginary frequencies: none

C 2.35765800 1.28920400 -1.27276900
H 2.75047400 2.24433300 -1.64359300
H 1.60131300 0.94806400 -1.99172900
H 3.16746900 0.55706500 -1.27840400
C 1.75202400 1.48368400 0.09197200
C 2.00209500 0.72477700 1.16689500
H 1.48650900 0.99305700 2.09185500
C 0.61554400 2.47146500 0.16406200
H 0.44692100 2.76399100 1.20764200
H 0.82340500 3.38593000 -0.40608700
C -0.67678900 1.80794600 -0.37586600
H -0.64372100 1.76121100 -1.47302300
H -1.52680800 2.45745900 -0.12391500
C -0.93160000 0.40743700 0.18316800
H -0.58765100 0.35821400 1.22583200
C -0.44091400 -0.86235600 -0.57765700
H -0.55666300 -0.67585300 -1.65374400
C -2.37367500 -0.18484000 0.14935000
C -1.72081500 -1.57264600 -0.06539000
H -1.53510900 -2.07596600 0.89197400
H -2.21006300 -2.27453300 -0.74988300
C -3.18432300 0.24956700 -1.07140300
H -4.09662400 -0.35403400 -1.14837500
H -2.62542400 0.12830900 -2.00581300
H -3.48563400 1.30114700 -0.99547900
C -3.19056700 0.00443200 1.41882000
H -3.43782800 1.06345800 1.56961800
H -2.63609400 -0.34122300 2.29891400
H -4.13310000 -0.55488400 1.36995200
C 0.88279200 -1.56453900 -0.38038600
C 1.48818800 -2.13057100 -1.43033200
H 1.08834400 -2.04013700 -2.43782900
H 2.40837900 -2.70128600 -1.31822500

C 2.64341200 -0.63079000 1.19322500
H 3.14617600 -0.81271700 2.15024700
H 3.38697100 -0.75649500 0.39954400
C 1.52051400 -1.68181400 0.99361500
H 0.76654200 -1.55379500 1.78211700
H 1.94095900 -2.68705700 1.11458000

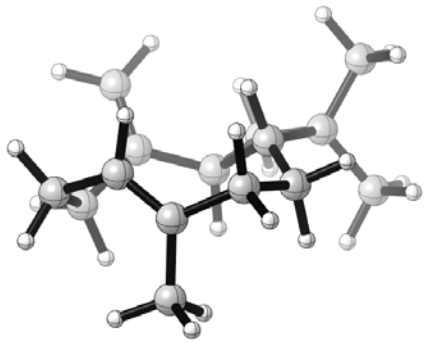

caryophyllene-βα
$E_{(M06\text{-}2X/6\text{-}31+G(d))}$: -585.7243348
$TCG_{(M06\text{-}2X/6\text{-}31+G(d))}$: 0.318311
$E_{(M06\text{-}2X/6\text{-}311+G(d,p))}$: -585.8688689
$E_{(M06\text{-}2X/6\text{-}311+G(d,p),\ smd=HFIP)}$: -585.8828104
Imaginary frequencies: none

C 2.23843300 -1.84841800 1.08026600
H 2.44383000 -2.92553500 1.10085400
H 1.42938800 -1.66586100 1.80056400
H 3.12871200 -1.32670800 1.44095100
C 1.84581800 -1.41663600 -0.30945700
C 2.30204900 -0.30592400 -0.89676800
H 1.93275200 -0.07688600 -1.89649100
C 0.72789700 -2.19037100 -0.95508100
H 0.69214700 -1.96709400 -2.02855800
H 0.87160000 -3.27395200 -0.84745800
C -0.61531800 -1.79571000 -0.31369800
H -0.62501000 -2.11121000 0.73825500
H -1.41508500 -2.36887500 -0.80582900
C -0.98657200 -0.31483900 -0.40198700
H -0.83899400 0.04546400 -1.43182200
C -0.41950300 0.77493100 0.58201000
H -0.15699900 0.29257600 1.53342500
C -2.42837900 0.05739900 0.06962300
C -1.85149100 1.36108500 0.66445700
H -1.98447500 2.20945000 -0.01309200
H -2.20430800 1.65277200 1.66011500
C -2.96781400 -0.85303400 1.17244000
H -3.88991500 -0.42533400 1.58404500
H -2.25579000 -0.95979800 1.99904700

H -3.20161800 -1.85592400 0.79626200
C -3.45669800 0.21133400 -1.04175300
H -3.66495200 -0.75558700 -1.51812800
H -3.09669000 0.89872200 -1.81588200
H -4.40406000 0.60417600 -0.65217000
C 0.70344000 1.71434600 0.18062200
C 0.52132200 2.70648700 -0.69723500
H -0.42914600 2.89075800 -1.19041600
H 1.33973900 3.37058800 -0.96784700
C 3.04931100 0.79965300 -0.19930800
H 3.40649400 1.52590900 -0.93681100
H 3.93130900 0.43632700 0.34243900
C 2.08536500 1.50406900 0.78643900
H 2.50993100 2.46745800 1.09317800
H 1.99398500 0.89232300 1.69195400

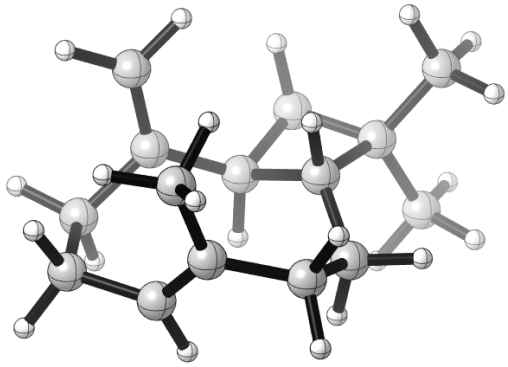

caryophyllene-ββ
$E_{(M06\text{-}2X/6\text{-}31+G(d))}$: -585.7241116
$TCG_{(M06\text{-}2X/6\text{-}31+G(d))}$: 0.318325
$E_{(M06\text{-}2X/6\text{-}311+G(d,p))}$: -585.8685618
$E_{(M06\text{-}2X/6\text{-}311+G(d,p),\ smd=HFIP)}$: -585.8824629
Imaginary frequencies: none

C 2.28618300 1.31135500 1.52130700
H 1.48707700 0.96083400 2.18829600
H 2.60516600 2.29431800 1.89072100
H 3.12621900 0.62167000 1.61889000
C 1.77099000 1.43817900 0.11204500
C 2.15626900 0.67358200 -0.91603800
H 1.69532700 0.86333200 -1.88937500
C 0.63205500 2.42681800 -0.06774800
H 0.43011900 2.91474200 0.89422300
H 0.90506200 3.22612600 -0.76861300
C -0.65448200 1.73201400 -0.55279000
H -0.58963200 1.54223200 -1.63268200
H -1.49611300 2.42689600 -0.41786900
C -0.98002200 0.41824900 0.15880800

H -0.72720600 0.49356200 1.22820100
C -0.44734100 -0.95049300 -0.38083600
H -0.38239300 -0.88116100 -1.47438100
C -2.42975500 -0.14349600 0.03902600
C -1.81606600 -1.56297900 0.01165200
H -1.77837100 -2.00468300 1.01342400
H -2.25447100 -2.29089500 -0.68035400
C -3.10281200 0.19210700 -1.29216700
H -4.02425100 -0.39287200 -1.39872300
H -2.46112100 -0.04084800 -2.14957500
H -3.37230100 1.25315200 -1.35219200
C -3.35888600 0.18333300 1.19862000
H -3.58280700 1.25772700 1.22850400
H -2.90403100 -0.09389200 2.15664900
H -4.31093700 -0.35407100 1.10658600
C 0.81736100 -1.59943400 0.14501200
C 0.93446800 -1.97934300 1.42077100
H 0.13966800 -1.82525400 2.14781900
H 1.84338400 -2.44975400 1.78983100
C 2.94897400 -0.59707200 -0.82693000
H 3.54157700 -0.62839500 0.09173000
H 3.64612000 -0.70025100 -1.66722700
C 1.97079800 -1.79974600 -0.82389200
H 2.52479400 -2.71031400 -0.56793200
H 1.57271600 -1.94063600 -1.83698900

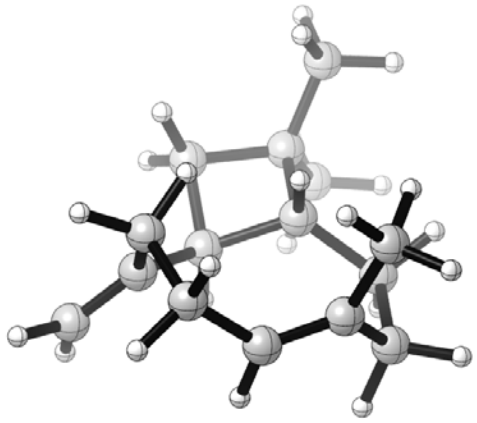

caryophyllene-αβ
$E_{(M06\text{-}2X/6\text{-}31+G(d))}$: -585.7176052
$TCG_{(M06\text{-}2X/6\text{-}31+G(d))}$: 0.31845
$E_{(M06\text{-}2X/6\text{-}311+G(d,p))}$: -585.8620886
$E_{(M06\text{-}2X/6\text{-}311+G(d,p),\ smd=HFIP)}$: -585.8758407
Imaginary frequencies: none

C -1.73996400 -2.33628400 1.04352000
H -0.71621200 -2.50586700 1.40323500
H -2.18377400 -3.32756400 0.88594200

H -2.30201100 -1.83816800 1.83790500
C -1.74144900 -1.56122200 -0.24618700
C -2.35062200 -0.38715600 -0.44019900
H -2.25410800 0.05259300 -1.43319700
C -0.78877500 -2.03383900 -1.31423600
H -0.82239800 -3.12177300 -1.45627400
H -1.06881000 -1.57348300 -2.26761700
C 0.66480500 -1.61010100 -0.95062900
H 1.22543800 -1.45975600 -1.88141100
H 1.16524100 -2.44026900 -0.43052500
C 0.82148600 -0.38276000 -0.04710600
H 0.30867600 -0.57197500 0.90404600
C 0.51235200 1.08665200 -0.47509000
H 0.74342600 1.21985200 -1.53977400
C 2.27288600 0.06028600 0.31466400
C 1.73930600 1.50865100 0.38068200
H 1.42707300 1.77545400 1.39846100
H 2.37193300 2.30952100 -0.01817500
C 3.27244000 -0.11061700 -0.82784400
H 4.20912600 0.40435300 -0.58307600
H 2.89856300 0.30906800 -1.76866800
H 3.50576800 -1.16807300 -1.00033100
C 2.83584400 -0.52496000 1.60217200
H 3.01872300 -1.60227900 1.49673500
H 2.13992100 -0.37939300 2.43666200
H 3.78813700 -0.04964600 1.86830700
C -0.76602600 1.83911100 -0.16065100
C -1.11132700 2.89396700 -0.90623200
H -0.54168100 3.18145000 -1.78719200
H -1.97449600 3.50828400 -0.65783200
C -2.84110800 0.57632900 0.60047600
H -3.27519400 0.08437700 1.47697100
H -3.61090500 1.23210400 0.17828100
C -1.62220100 1.44114900 1.03215000
H -1.02486700 0.86685300 1.75116900
H -1.97345300 2.33909800 1.55341500

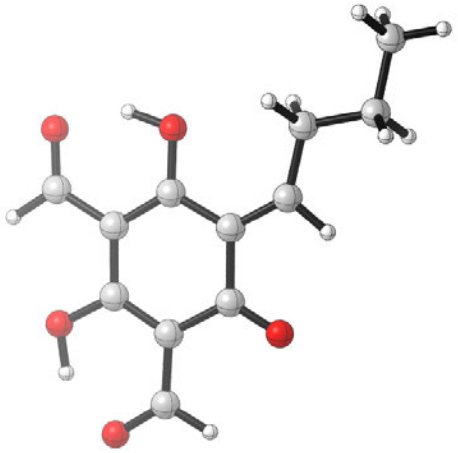

E-*o*-QM
$E_{(M06\text{-}2X/6\text{-}31+G(d))}$: -840.2913633
$TCG_{(M06\text{-}2X/6\text{-}31+G(d))}$: 0.181864
$E_{(M06\text{-}2X/6\text{-}311+G(d,p))}$: -840.517878
$E_{(M06\text{-}2X/6\text{-}311+G(d,p),\ smd=HFIP)}$: -840.5314837
Imaginary frequencies: none

C 0.56465800 -0.47515600 -0.00004700
C 1.85161500 -0.89313600 0.00000100
C 0.16593600 0.92499200 -0.00007100
C -1.17421000 1.30597100 -0.00000500
C -2.19185700 0.28435700 0.00000200
C -1.89334400 -1.07534500 0.00003500
C -0.51022100 -1.53526200 -0.00003700
C -2.96671500 -2.04114200 0.00001700
H -2.67722900 -3.10102900 -0.00004900
C -1.52622100 2.71034600 0.00005500
H -2.59427900 2.96529300 0.00014900
O -4.16290300 -1.72652600 0.00003400
O -0.68124100 3.61104800 0.00002100
O -0.21190700 -2.72226500 -0.00009800
O 1.12544300 1.82265600 -0.00016000
H 0.69271000 2.73025200 -0.00013500
O -3.43741300 0.71494700 0.00006400
H -4.03454500 -0.09420300 0.00007200
C 5.64921100 -0.15432200 0.00004300
H 5.69975900 0.49017000 0.88452900
H 6.53566600 -0.79478000 0.00034500
C 4.36696300 -0.98190500 0.00009700
H 4.34668100 -1.63777900 0.87951000
H 4.34669500 -1.63789600 -0.87923300
C 3.11875500 -0.09900200 0.00002300
H 3.12285400 0.57484400 -0.86794900
H 3.12279700 0.57491500 0.86792900
H 5.70000100 0.48966900 -0.88479000
H 1.95563200 -1.98071600 0.00006700

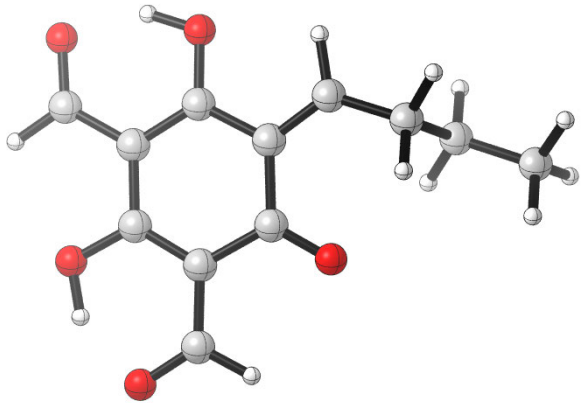

Z-*o*-QM

$E_{(M06\text{-}2X/6\text{-}31+G(d))}$: -840.2928995

$TCG_{(M06\text{-}2X/6\text{-}31+G(d))}$: 0.182755

$E_{(M06\text{-}2X/6\text{-}311+G(d,p))}$: -840.5197473

$E_{(M06\text{-}2X/6\text{-}311+G(d,p),\ smd=HFIP)}$: -840.5319208

Imaginary frequencies: none

C 0.62238900 -0.58613400 -0.23360500
C 1.79886200 -1.21294200 -0.48361900
C -0.58017000 -1.40277300 -0.06997000
C -1.84416100 -0.83468800 0.05463700
C -1.96659000 0.60106300 0.03909200
C -0.86612900 1.44614100 -0.07287400
C 0.48633400 0.90635500 -0.16341400
C -1.06193300 2.87659500 -0.05859700
H -0.15992800 3.49934200 -0.13418300
C -3.01190700 -1.68243900 0.19334600
H -3.98780300 -1.18727200 0.28545900
O -2.17482400 3.40888900 0.03045200
O -2.94548000 -2.91432100 0.20957300
O 1.47576100 1.63142800 -0.18071300
O -0.41903500 -2.70703900 -0.06019300
H -1.32300600 -3.12847200 0.04341100
O -3.19151300 1.07579400 0.14628700
H -3.12750400 2.07881700 0.12723700
C 5.18762500 0.34674200 0.45925700
H 5.08145000 1.30174700 -0.06561100
H 5.67729300 0.54082000 1.41815600
C 3.82301500 -0.30479600 0.66472800
H 3.17412700 0.35884300 1.24424200
H 3.93057500 -1.23978100 1.22792100
C 3.13864400 -0.59430800 -0.68993200
H 3.04842600 0.34821000 -1.23540600
H 3.76458200 -1.28641900 -1.26402900
H 1.75797100 -2.30125800 -0.51152300
H 5.84866100 -0.29548600 -0.13321300

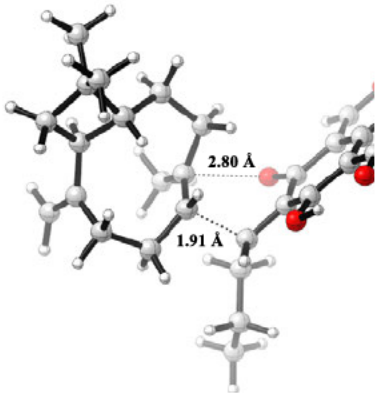

caryophyllene-*αα*-*Z*-oQM-DA-*exo*-TS

$E_{(M06\text{-}2X/6\text{-}31+G(d))}$: -1426.010993
$TCG_{(M06\text{-}2X/6\text{-}31+G(d))}$: 0.525416
$E_{(M06\text{-}2X/6\text{-}311+G(d,p))}$: -1426.383138
$E_{(M06\text{-}2X/6\text{-}311+G(d,p),\ smd=HFIP)}$: -1426.41439
Imaginary frequencies: 1

C 1.31560700 1.42367800 -2.00839200
H 2.01837500 0.85653800 -2.63221300
H 1.80013300 2.35108700 -1.70732500
H 0.42860700 1.63565100 -2.61617400
C 0.88344000 0.57424700 -0.86320500
C 0.83654500 0.98577300 0.47377600
H 0.67632000 0.16245100 1.17327800
C 0.53270000 -0.84571000 -1.15293700
H -0.16454500 -1.19842800 -0.38134800
H 0.04023400 -0.93505000 -2.12422600
C 1.80940100 -1.73710000 -1.13836600
H 2.27833200 -1.68754200 -2.12891300
H 1.47796100 -2.77349100 -1.00513300
C 2.85489300 -1.38589500 -0.08365900
H 2.36728600 -1.14010200 0.86697000
C 3.93416100 -0.32002800 -0.43833500
H 4.12171300 -0.35501000 -1.51952800
C 3.99736800 -2.40517600 0.22535200
C 4.97785700 -1.20831500 0.28911500
H 5.14630100 -0.87013700 1.31791300
H 5.94649200 -1.32125300 -0.20800400
C 4.31303800 -3.34830500 -0.93189400
H 5.23972000 -3.89488000 -0.72580600
H 4.44664200 -2.81157300 -1.87791900
H 3.51551500 -4.08676700 -1.07217200
C 3.82756300 -3.17974200 1.52408600
H 2.98566600 -3.87936200 1.46175800
H 3.63931800 -2.49785100 2.36128000
H 4.73011400 -3.75647700 1.75635600
C 3.87354800 1.12445700 -0.00718500
C 4.48484000 2.06702000 -0.72823400
H 4.97187400 1.83889600 -1.67266300
H 4.52757600 3.10108100 -0.39302700

C 1.75246300 2.05151700 1.04409300
H 1.34372800 2.39766200 2.00003700
H 1.81002900 2.92458900 0.38469700
C 3.17400800 1.50154600 1.28251100
H 3.11885500 0.64230000 1.96294700
H 3.75351500 2.27334400 1.79935200
C -1.91080500 0.65054300 0.37047900
C -0.94028800 1.67045600 0.64076700
C -2.36886800 -0.19730600 1.39297000
C -3.33021800 -1.21252500 1.14680400
C -3.79694300 -1.39471200 -0.18472900
C -3.29460100 -0.63394900 -1.24925200
C -2.27911600 0.37558200 -1.00943500
C -3.75501800 -0.88082600 -2.58829600
H -3.30524900 -0.25718200 -3.37579200
C -3.79533000 -2.04429400 2.22296000
H -4.54238700 -2.81013000 1.97026400
O -4.60621100 -1.72882500 -2.88519100
O -3.39911400 -1.94332100 3.39107400
O -1.67212900 0.95417600 -1.93279900
O -1.88022100 -0.03232800 2.62000800
H -2.33330500 -0.70417000 3.20760400
O -4.70976700 -2.33442800 -0.39086800
H -4.90469500 -2.33633500 -1.37223400
H -0.79672500 1.79980400 1.71548000
C -1.00568500 3.00639500 -0.09671200
H -1.89033800 3.00970900 -0.73801600
H -0.15992400 3.14065800 -0.77865000
C -1.05862500 4.18273800 0.88123800
H -1.92985600 4.06639000 1.53769200
H -0.17603100 4.16500100 1.53337600
C -1.13109100 5.52009900 0.15095500
H -2.01310500 5.56378400 -0.49556000
H -0.24862400 5.66695300 -0.48172300
H -1.18506600 6.35664200 0.85279400

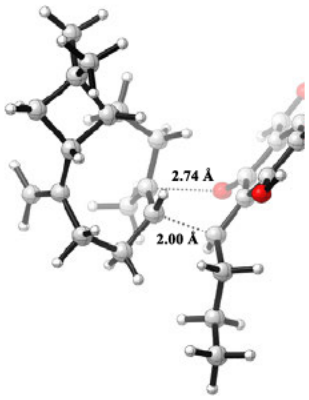

caryophyllene-*αα*-*E*-oQM-DA-*exo*-TS
$E_{(M06\text{-}2X/6\text{-}31+G(d))}$: -1426.005817
$TCG_{(M06\text{-}2X/6\text{-}31+G(d))}$: 0.527022
$E_{(M06\text{-}2X/6\text{-}311+G(d,p))}$: -1426.377629
$E_{(M06\text{-}2X/6\text{-}311+G(d,p),\ smd=HFIP)}$: -1426.408544
Imaginary frequencies: 1

C 1.08562800 1.06382000 -2.81595500
H 0.65747200 2.06048400 -2.96078000
H 0.65008600 0.39443600 -3.55879400
H 2.16867500 1.13338000 -2.98393100
C 0.82298400 0.55470400 -1.43466200
C 0.84486100 1.38615000 -0.31484200
H 0.80040400 0.86669800 0.64707900
C 0.60538400 -0.90435600 -1.25119700
H -0.07774000 -1.07096700 -0.40441600
H 0.14987000 -1.33421700 -2.14722700
C 1.93158000 -1.65067400 -0.94997000
H 2.66872300 -1.42431000 -1.73331400
H 1.69101500 -2.71491900 -1.04866800
C 2.51886100 -1.42027300 0.44005500
H 1.69725200 -1.33554500 1.16512000
C 3.63399900 -0.31272000 0.60255000
H 3.59833100 0.01407700 1.64785700
C 3.60980200 -2.46742500 0.86267700
C 4.68956300 -1.42795200 0.48345000
H 5.57364300 -1.34622300 1.12525500
H 5.01796000 -1.57501200 -0.55125500
C 3.67869100 -3.79307300 0.11615100
H 4.56255600 -4.35252100 0.44492900
H 3.76128800 -3.65362500 -0.96663800
H 2.79829900 -4.41626100 0.31596100
C 3.56058200 -2.72533800 2.36830400
H 2.67364200 -3.31453500 2.62916500
H 3.52344100 -1.79426500 2.94436900
H 4.44653700 -3.28399500 2.69198200
C 3.73165200 0.92998600 -0.24804600
C 4.37543300 0.96015800 -1.41975300
H 4.84579500 0.08253200 -1.85375500
H 4.46382000 1.88561600 -1.98654500

C 1.75930100 2.59507400 -0.31268500
H 1.35628100 3.42412500 0.27361600
H 1.91223300 2.96423500 -1.33208400
C 3.11546500 2.20355100 0.31190500
H 3.81040700 3.04007600 0.17509600
H 2.97182700 2.08813400 1.39325000
C -1.88614200 0.78510000 -0.08237100
C -1.07719700 1.95047300 -0.24591300
H -1.11962000 2.31059600 -1.27443100
C -2.24287500 0.22741800 1.15901400
C -3.07499300 -0.91889600 1.25476700
C -3.50557100 -1.54703000 0.05183300
C -3.09847900 -1.08692000 -1.20731300
C -2.23168700 0.07500500 -1.31205100
C -3.51830700 -1.77496900 -2.39990700
H -3.15785700 -1.36171800 -3.35353600
C -3.43926100 -1.45042200 2.54124900
H -4.09061500 -2.33553300 2.54882400
O -4.24645900 -2.77684200 -2.40038000
O -3.05791900 -0.96692300 3.61664400
O -1.73900200 0.45172700 -2.39404800
C -1.07331000 3.06931500 0.78717200
H -0.25629800 2.95842700 1.51001800
H -1.98405500 2.97537800 1.38730700
O -1.76560800 0.78798200 2.26810900
H -2.13179800 0.27604400 3.04587500
O -4.29020700 -2.61203300 0.17026700
H -4.48293100 -2.94472200 -0.75093300
C -1.04998500 4.45158900 0.12908800
H -1.97838700 4.58191700 -0.44127900
H -0.23575600 4.51391600 -0.60386700
C -0.91074500 5.56966100 1.15900200
H -1.72207000 5.52775300 1.89379000
H -0.93564100 6.55555400 0.68590600
H 0.03537700 5.48195100 1.70601100

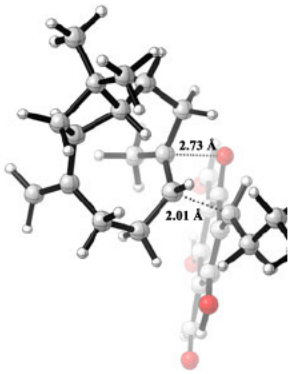

caryophyllene-*αα*-*E*-oQM-DA-*endo*-TS

$E_{(M06\text{-}2X/6\text{-}31+G(d))}$: -1426.013502
$TCG_{(M06\text{-}2X/6\text{-}31+G(d))}$: 0.526059
$E_{(M06\text{-}2X/6\text{-}311+G(d,p))}$: -1426.384883
$E_{(M06\text{-}2X/6\text{-}311+G(d,p),\ smd=HFIP)}$: -1426.415368
Imaginary frequencies: 1

C -2.01585300 0.68175000 -0.51080000
C -0.90921300 1.31576000 -1.14623000
C -2.81421600 -0.24024100 -1.22205000
C -3.94563700 -0.86021700 -0.63623600
C -4.25121400 -0.56468500 0.72359300
C -3.45718700 0.29845700 1.48916600
C -2.28533200 0.93317900 0.90348600
C -3.78544700 0.54717500 2.86867000
H -3.11868600 1.23208100 3.41257900
C -4.76374000 -1.76330100 -1.40288800
H -5.63329400 -2.20207500 -0.89392900
O -4.75568400 0.04267400 3.45037000
O -4.53580500 -2.06133400 -2.58338700
O -1.49124100 1.61611000 1.57722200
O -2.50087100 -0.50595200 -2.48792900
H -3.18180400 -1.14830900 -2.83973300
O -5.31896800 -1.15561300 1.24545500
H -5.38884200 -0.85963800 2.19699200
C 0.19322100 -0.77935700 1.37848600
H 0.05267500 -0.43951500 2.40634700
H 0.81178100 -1.68522300 1.36819300
H -0.77985100 -1.07041200 0.96042900
C 0.83035500 0.27592000 0.54102600
C 0.78206200 0.24404800 -0.84335400
H 1.43113100 0.96551900 -1.34015900
C 1.67456500 1.30001600 1.22072400
H 1.88142500 2.13318000 0.53860000
H 1.17191800 1.69098100 2.11114500
C 3.02616600 0.63907600 1.60434700
H 2.87202600 -0.04866900 2.44605700
H 3.68456100 1.43766000 1.96991600
C 3.70612900 -0.09860000 0.44964400
H 3.46427200 0.39432600 -0.50296400

C 3.55225800 -1.64148700 0.28621500
H 3.54419800 -2.08711300 1.28932100
C 5.25193900 -0.29994500 0.46925600
C 5.01098900 -1.65380600 -0.24184300
H 5.03483900 -1.54047200 -1.33286100
H 5.63481400 -2.50731600 0.04373800
C 5.82165900 -0.49583000 1.87402000
H 6.85977200 -0.84166700 1.80971800
H 5.26008000 -1.23766900 2.45224700
H 5.81919500 0.44307400 2.43984900
C 6.05781700 0.74531700 -0.28756800
H 6.00028600 1.72045400 0.21318400
H 5.68425600 0.86712200 -1.31066700
H 7.11561500 0.46208800 -0.34466600
C 2.50481700 -2.35078500 -0.53949100
C 2.08880900 -3.56684900 -0.16782400
H 2.42998500 -4.03006400 0.75536900
H 1.39384000 -4.14178100 -0.77621000
C 0.60250800 -1.02890800 -1.63984200
H 0.19697500 -0.79509400 -2.62960900
H -0.11039400 -1.70751800 -1.15793600
C 1.96460700 -1.73905600 -1.81822000
H 2.68570000 -1.02616700 -2.24172400
H 1.83653500 -2.53205900 -2.56293500
H -0.84208200 1.06997700 -2.20768200
C -0.54773700 2.76019400 -0.85506200
H -1.50286800 3.30457500 -0.91374100
H -0.21847900 2.88764500 0.17721000
C 0.42955200 3.39734700 -1.84307700
H 0.10532400 3.19104900 -2.87197600
H 1.43028000 2.95859700 -1.73908100
C 0.53251900 4.90669600 -1.62689600
H 1.24459800 5.36224300 -2.32116400
H 0.86350000 5.13194000 -0.60695300
H -0.43911200 5.38996900 -1.77426300

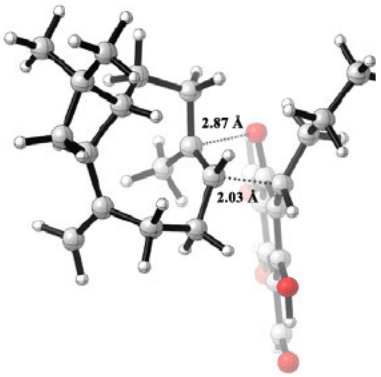

caryophyllene-*αα*-*Z*-oQM-DA-*endo*-TS

$E_{(M06\text{-}2X/6\text{-}31+G(d))}$: -1426.013397

$TCG_{(M06\text{-}2X/6\text{-}31+G(d))}$: 0.525987

$E_{(M06\text{-}2X/6\text{-}311+G(d,p))}$: -1426.385137

$E_{(M06\text{-}2X/6\text{-}311+G(d,p),\ smd=HFIP)}$: -1426.415652

Imaginary frequencies: 1

C 2.00117600 0.59474200 -0.61086900
C 0.86238900 1.32708600 -1.04770400
H 0.53327100 0.97746700 -2.02613100
C 2.86868700 0.98562500 0.42798700
C 3.99719900 0.20695000 0.78819200
C 4.22578000 -1.02077600 0.10209800
C 3.36610200 -1.47758700 -0.90463900
C 2.21024800 -0.68519300 -1.29089400
C 3.62092400 -2.73501900 -1.55839400
H 2.90659800 -3.03114500 -2.34067200
C 4.88092100 0.64428700 1.83783300
H 5.73880000 -0.00244000 2.06901900
O 4.57805000 -3.47289100 -1.28862500
O 4.71973000 1.69256200 2.47744700
O 1.38100100 -1.07306000 -2.13711800
C 0.69958300 2.82561100 -0.87013700
H 0.41384300 3.09368300 0.15153000
H 1.69728400 3.26528100 -1.00140400
O 2.61775000 2.12131400 1.07417700
H 3.34004100 2.24690500 1.75437400
O 5.28786800 -1.72871200 0.46805500
H 5.30306000 -2.55565700 -0.09107700
C -0.26630200 -1.85128800 0.06856600
H -0.15658900 -2.68187400 -0.63120800
H -0.90968000 -2.15307200 0.90513500
H 0.71527000 -1.61997200 0.50357000
C -0.84277700 -0.65139600 -0.60330500
C -0.74090400 0.62027100 -0.05449900
H -1.39742800 1.35927200 -0.51630600
C -1.69096000 -0.84945100 -1.81267900
H -1.80332500 0.10223700 -2.34732900
H -1.23456200 -1.57451200 -2.49269400
C -3.09397600 -1.33833200 -1.36211100

H -3.02855800 -2.38736300 -1.04460700
H -3.74326600 -1.32131300 -2.24710700
C -3.72628300 -0.50321800 -0.24747800
H -3.41764800 0.54723100 -0.34255400
C -3.60978500 -0.94449100 1.24365000
H -3.67645000 -2.03971600 1.27404500
C -5.27613500 -0.49752000 -0.07706400
C -5.03454400 -0.36524300 1.44635900
H -4.99071400 0.68748700 1.75231600
H -5.69930700 -0.90898200 2.12585200
C -5.93189500 -1.83224300 -0.43024200
H -6.97517600 -1.83509700 -0.09412800
H -5.42873800 -2.68264900 0.04261500
H -5.93150900 -2.00184000 -1.51329900
C -6.00557500 0.64780400 -0.76343700
H -5.94896200 0.54838000 -1.85514000
H -5.56946600 1.61483400 -0.48809300
H -7.06602200 0.66286800 -0.48478500
C -2.53839600 -0.52599500 2.22360000
C -2.19123400 -1.36257900 3.20848200
H -2.60641200 -2.36550000 3.27936700
H -1.48091700 -1.07134100 3.97942400
C -0.52898700 0.84671000 1.42415800
H -0.03512800 1.80696300 1.60088300
H 0.11788900 0.07527500 1.85575300
C -1.89289700 0.84552900 2.15465300
H -2.56211700 1.56531600 1.66265700
H -1.73421300 1.21270700 3.17434500
C -0.26141500 3.44895500 -1.88310100
H -1.25774800 2.99455300 -1.79714200
H 0.09183600 3.22557200 -2.89762700
C -0.37811500 4.96053300 -1.69741900
H -1.05538900 5.40184400 -2.43428500
H 0.59878900 5.44362500 -1.80662600
H -0.75953700 5.20463000 -0.69982000

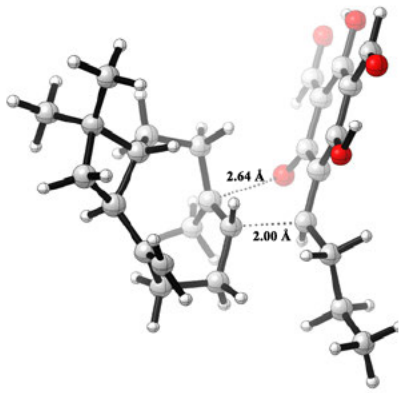

caryophyllene-$\beta\alpha$-*E*-oQM-DA-*exo*-TS

$E_{(M06\text{-}2X/6\text{-}31+G(d))}$: -1426.009367
$TCG_{(M06\text{-}2X/6\text{-}31+G(d))}$: 0.52547
$E_{(M06\text{-}2X/6\text{-}311+G(d,p))}$: -1426.380946
$E_{(M06\text{-}2X/6\text{-}311+G(d,p),\ smd=HFIP)}$: -1426.4119
Imaginary frequencies: 1

C 0.91605500 0.51642100 -3.10911800
H 0.31895000 -0.15708700 -3.72565400
H 1.97750100 0.36989300 -3.35807000
H 0.65382600 1.54614400 -3.36661800
C 0.69326100 0.23749500 -1.65854600
C 0.88943200 1.19838400 -0.66774400
H 0.94160800 0.80163300 0.34835500
C 0.40404700 -1.16196300 -1.24603700
H -0.17141000 -1.15881300 -0.30856900
H -0.18622700 -1.67453200 -2.01135500
C 1.71867600 -1.94797000 -1.00877900
H 2.30682200 -1.96659800 -1.93654200
H 1.41625200 -2.98700300 -0.82127600
C 2.59274700 -1.49689300 0.15874000
H 1.96329100 -1.14515400 0.98990800
C 3.80256200 -0.50685300 0.00436200
H 4.24536700 -0.66949800 -0.98848700
C 3.59474800 -2.54613600 0.73247800
C 4.55378400 -1.37300600 1.03814200
H 4.40255100 -1.01109600 2.05992900
H 5.62448700 -1.53119900 0.87104100
C 4.17699700 -3.47606700 -0.33253800
H 5.01785200 -4.03773300 0.09048500
H 4.55122600 -2.92785600 -1.20439100
H 3.43596100 -4.20334100 -0.68366600
C 3.08892700 -3.35208500 1.91968800
H 2.27819100 -4.02747900 1.61774900
H 2.70542200 -2.69520500 2.70805300
H 3.89094500 -3.96548300 2.34771900
C 3.67238000 0.98186400 0.21872800
C 3.88299600 1.56939700 1.40063200
H 4.14990800 1.01635200 2.29504500
H 3.79811500 2.64898800 1.50980800

C 1.84276400 2.34869000 -0.92152600
H 1.77335500 3.07702000 -0.10814400
H 1.59939600 2.87570400 -1.85143400
C 3.29471900 1.83364000 -0.98411300
H 3.96787100 2.69627000 -1.05060700
H 3.43705100 1.25377100 -1.90323100
C -1.83569200 0.86081600 -0.09716900
C -0.94687600 1.93637600 -0.40151800
H -1.05630300 2.25121000 -1.44033200
C -2.15523900 0.41829000 1.20213300
C -3.07285700 -0.64096700 1.42701900
C -3.62855400 -1.31188600 0.30113900
C -3.26117900 -0.97933400 -1.00878600
C -2.31145700 0.09405700 -1.24416900
C -3.80691400 -1.71022900 -2.12255600
H -3.47194900 -1.39727400 -3.12263100
C -3.40181500 -1.04932900 2.76800500
H -4.12476300 -1.86996500 2.87559800
O -4.61345000 -2.64288000 -2.00869500
O -2.91581400 -0.53027300 3.78219000
O -1.84670900 0.34436700 -2.37575100
C -0.72757900 3.08912500 0.56929600
H 0.13895000 2.91377300 1.21856000
H -1.58121300 3.11687900 1.25389100
O -1.56459200 1.00540900 2.23904200
H -1.92192000 0.58102500 3.07148300
O -4.49127800 -2.29243400 0.54277700
H -4.76624900 -2.67218900 -0.33805000
C -0.62306100 4.44102400 -0.14093200
H -1.57372400 4.64283200 -0.65079000
H 0.14150600 4.40802700 -0.92515100
C -0.31004100 5.56927200 0.83894100
H -1.06939800 5.62639100 1.62639900
H -0.27438300 6.53930200 0.33466300
H 0.65890200 5.40597100 1.32516500

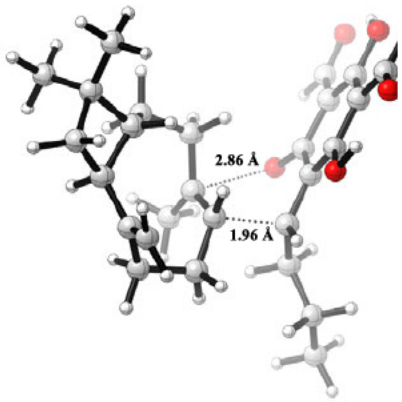

caryophyllene-*βα-Z*-oQM-DA-*exo*-TS
$E_{(M06\text{-}2X/6\text{-}31+G(d))}$: -1426.011766
$TCG_{(M06\text{-}2X/6\text{-}31+G(d))}$: 0.526119
$E_{(M06\text{-}2X/6\text{-}311+G(d,p))}$: -1426.383722
$E_{(M06\text{-}2X/6\text{-}311+G(d,p),\ smd=HFIP)}$: -1426.415246
Imaginary frequencies: 1

C 0.87169600 1.84001800 -2.43376200
H -0.10686800 1.89833100 -2.92866500
H 1.57157100 1.39326000 -3.15185100
H 1.21615000 2.84598200 -2.18899400
C 0.73295800 0.94585400 -1.24913000
C 0.79892900 1.38188200 0.06839700
H 0.88801000 0.57972800 0.80300300
C 0.60282200 -0.51380900 -1.50829700
H 0.02872200 -0.98257800 -0.69614400
H 0.07588300 -0.69185100 -2.45044200
C 2.00130600 -1.17621800 -1.57545700
H 2.57069500 -0.74015400 -2.40779500
H 1.82393500 -2.22520100 -1.84846500
C 2.84900000 -1.16163400 -0.30592200
H 2.21251100 -1.31092800 0.57930000
C 3.89950100 -0.03814400 0.02202200
H 4.30264000 0.33571000 -0.92976400
C 4.01424800 -2.19782400 -0.24248600
C 4.82228600 -1.15379200 0.56011100
H 4.69084300 -1.30958200 1.63507600
H 5.89168500 -1.06047700 0.34320100
C 4.66140700 -2.47167300 -1.60055900
H 5.58941100 -3.03688200 -1.45636900
H 4.91709400 -1.54851800 -2.13292400
H 4.00826200 -3.06648900 -2.24933900
C 3.68665800 -3.50621100 0.46165200
H 2.96023400 -4.09137800 -0.11668000
H 3.26003100 -3.32409300 1.45408800
H 4.58630400 -4.12100000 0.58548500
C 3.58277200 1.15164400 0.89869900
C 3.74727300 1.14218700 2.22504900
H 4.10491100 0.27553200 2.77069600
H 3.52465400 2.02554500 2.82040400

C 1.55667100 2.63316900 0.45704900
H 1.37859900 2.84310900 1.51817400
H 1.21608100 3.51007900 -0.10495000
C 3.06340000 2.41526300 0.22630000
H 3.61133300 3.28624000 0.60378000
H 3.25206600 2.36306800 -0.85380400
C -1.85551100 0.54058300 0.36116300
C -1.08800700 1.73896900 0.47844600
C -1.99503300 -0.32972100 1.45960700
C -2.76493600 -1.51759000 1.38137000
C -3.36401700 -1.85124000 0.13315800
C -3.17944500 -1.06256400 -1.01092700
C -2.36134000 0.13849000 -0.94512100
C -3.76545900 -1.45890800 -2.26426400
H -3.57218200 -0.79894500 -3.12285000
C -2.92301200 -2.36351700 2.53536400
H -3.54455100 -3.26184100 2.41383900
O -4.45891800 -2.47426600 -2.41401000
O -2.39991600 -2.12931200 3.63324800
O -2.02847200 0.78425900 -1.95874900
O -1.38545100 -0.00659800 2.59834600
H -1.60846000 -0.71013900 3.27135000
O -4.09050500 -2.96182900 0.08762800
H -4.42121400 -3.06454400 -0.84879000
H -0.79785800 1.93530000 1.51264500
C -1.50108500 3.00511900 -0.26216400
H -2.45159700 2.81929300 -0.77008000
H -0.79880300 3.26515700 -1.06103100
C -1.64044100 4.18601300 0.70357000
H -2.36446500 3.92645900 1.48668700
H -0.68417900 4.36455100 1.21321800
C -2.08838400 5.45607100 -0.01549500
H -3.05278500 5.30421600 -0.51187100
H -1.36223600 5.74773200 -0.78306000
H -2.19587300 6.29277200 0.68098300

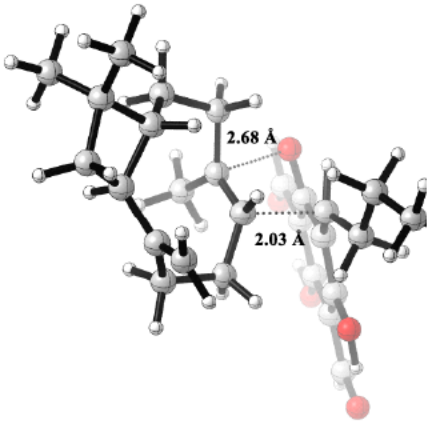

caryophyllene-*βα-E*-oQM-DA-*endo*-TS

$E_{(M06\text{-}2X/6\text{-}31+G(d))}$: -1426.014362
$TCG_{(M06\text{-}2X/6\text{-}31+G(d))}$: 0.524671
$E_{(M06\text{-}2X/6\text{-}311+G(d,p))}$: -1426.385792
$E_{(M06\text{-}2X/6\text{-}311+G(d,p),\ smd=HFIP)}$: -1426.416022
Imaginary frequencies: 1

C 0.13030100 -1.95992600 -0.68821800
H 0.01562700 -2.92585500 -0.19265900
H 0.75878500 -2.09042600 -1.58044000
H -0.85346500 -1.62480100 -1.04187400
C 0.74286300 -0.94723000 0.22212400
C 0.65144100 0.40926600 -0.03631400
H 1.37352200 1.01548400 0.51006700
C 1.61307900 -1.42186600 1.33518900
H 1.72918500 -0.63056600 2.08711100
H 1.16018500 -2.29044800 1.82261700
C 3.00538800 -1.79495500 0.77766400
H 2.89749400 -2.60632700 0.04498700
H 3.58441400 -2.21353100 1.61247600
C 3.81766500 -0.65170900 0.17126100
H 3.73581200 0.24493200 0.80583800
C 3.68709400 -0.20252200 -1.33075200
H 3.39861700 -1.07718800 -1.92966900
C 5.32950900 -0.93757100 -0.08824700
C 5.22736100 -0.05280700 -1.35051900
H 5.53976900 0.97479800 -1.14275900
H 5.74226700 -0.40042700 -2.25248500
C 5.61892400 -2.39213500 -0.45935300
H 6.65138200 -2.48082100 -0.81675100
H 4.96140400 -2.75275500 -1.25863400
H 5.50489800 -3.06210400 0.40061600
C 6.27933700 -0.46885100 1.00418200
H 6.14399200 -1.05767500 1.92052800
H 6.10654300 0.58487800 1.25050800
H 7.32434600 -0.57697900 0.68951000
C 2.83808500 0.97866200 -1.75524300
C 3.22441800 2.24603400 -1.57442400
H 4.16688000 2.51486400 -1.10661900

H 2.59370800 3.07264700 -1.89571900
C 0.31000500 0.93696900 -1.40996500
H 0.11971900 2.01276800 -1.35023600
H -0.60594600 0.47761500 -1.79911400
C 1.48341100 0.69294500 -2.38687000
H 1.34237300 1.32675400 -3.26929100
H 1.45771800 -0.34308600 -2.74107200
C -2.03988600 0.40555600 0.70203200
C -0.84422500 0.97045900 1.21903400
C -2.94919000 1.06753000 -0.14977400
C -4.12427600 0.43229200 -0.62214900
C -4.36010800 -0.92538000 -0.25855800
C -3.46108800 -1.64465500 0.53809300
C -2.25692100 -1.00259000 1.03869200
C -3.72418200 -3.02278900 0.86279000
H -2.97741000 -3.52596900 1.49452100
C -5.04921400 1.14357400 -1.46763200
H -5.94401000 0.59778700 -1.79781000
O -4.72195000 -3.64542900 0.47589900
O -4.88294500 2.31540500 -1.83096100
O -1.39284400 -1.61587400 1.69582900
O -2.68819700 2.32143600 -0.50574100
H -3.44096200 2.63440300 -1.08465600
O -5.46787400 -1.49108200 -0.72270400
H -5.48239700 -2.43387900 -0.39483100
H -0.46796800 0.38939700 2.06058300
C -0.59012900 2.45858900 1.35418500
H -1.53497100 2.90413800 1.69476800
H -0.39693300 2.93123700 0.38669900
C 0.51451400 2.79843100 2.35522100
H 0.26484000 2.36050100 3.33008700
H 1.46634600 2.34613200 2.04600200
C 0.70137300 4.30769300 2.49800900
H 1.48227000 4.54553300 3.22606100
H -0.22579700 4.78722700 2.82994500
H 0.98495400 4.75800500 1.54038600

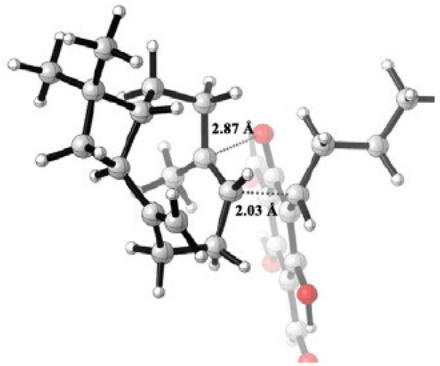

caryophyllene-*βα-Z*-oQM-DA-*endo*-TS

$E_{(M06\text{-}2X/6\text{-}31+G(d))}$: -1426.01598
$TCG_{(M06\text{-}2X/6\text{-}31+G(d))}$: 0.526132
$E_{(M06\text{-}2X/6\text{-}311+G(d,p))}$: -1426.387605
$E_{(M06\text{-}2X/6\text{-}311+G(d,p),\ smd=HFIP)}$: -1426.417901
Imaginary frequencies: 1

C -1.20696500 1.76938400 -1.93742100
H -0.51336400 1.53505800 -2.75014000
H -1.11498400 2.82351000 -1.67402500
H -2.23214600 1.59578300 -2.29507100
C -0.94766700 0.84412500 -0.79819400
C -0.83180200 1.25775100 0.53216400
H -0.82302600 0.43695100 1.25368000
C -0.80508300 -0.60678200 -1.10599800
H -0.80833600 -0.75770000 -2.18949500
H 0.18243300 -0.92683500 -0.73267500
C -1.86583400 -1.50571100 -0.42931800
H -1.60621900 -1.65773700 0.62547600
H -1.79122600 -2.49180300 -0.90487300
C -3.30053100 -0.99937700 -0.52696700
H -3.46825600 -0.50345100 -1.49511500
C -3.88122900 -0.09378900 0.60367400
H -3.44363700 -0.42354700 1.55360900
C -4.47959800 -1.99020700 -0.28370700
C -5.23337400 -0.81999800 0.39648700
H -5.86588600 -0.28267400 -0.31768800
H -5.82061700 -1.04462300 1.29226200
C -4.14146400 -3.09396900 0.71840200
H -5.05147000 -3.64110900 0.98840600
H -3.70759000 -2.69842100 1.64324000
H -3.43283300 -3.81468600 0.29568700
C -5.10745500 -2.58304800 -1.53560400
H -4.40686100 -3.26024500 -2.03926500
H -5.38867000 -1.79804100 -2.24598800
H -6.00808500 -3.15756100 -1.29077000
C -3.81327000 1.41436800 0.53081900
C -4.46289400 2.10755200 -0.40737300
H -5.06789600 1.62297800 -1.16994700
H -4.41664400 3.19332800 -0.44412200
C -1.55335000 2.48846200 1.05232700

H -1.64561700 3.24555300 0.26905200
H -0.98223600 2.94156700 1.87150000
C -2.96368400 2.13404300 1.56281400
H -3.45473300 3.06474800 1.86645100
H -2.87212800 1.51537500 2.46332600
C 1.84475300 0.48167400 0.35797900
C 1.03760300 1.63574800 0.64477800
C 2.19139100 -0.40078300 1.39875000
C 3.05735300 -1.50608200 1.19355400
C 3.54995000 -1.74184600 -0.12016100
C 3.16301300 -0.94041800 -1.20321800
C 2.24651900 0.17430600 -1.01259100
C 3.64967600 -1.24125600 -2.52214900
H 3.29460800 -0.58394100 -3.32959900
C 3.41691300 -2.35700000 2.29389700
H 4.10319600 -3.18753100 2.07556200
O 4.42561600 -2.17093100 -2.78170800
O 2.99849900 -2.20205200 3.44955500
O 1.76670500 0.81119100 -1.97002500
O 1.69230700 -0.17343600 2.61177000
H 2.06720400 -0.87904400 3.21812800
O 4.37249600 -2.76778100 -0.29013400
H 4.60158900 -2.79503300 -1.26476200
H 0.94504600 1.78213400 1.72294500
C 1.30550300 2.94602600 -0.07387900
H 0.57213000 3.69845300 0.23884900
H 1.24312600 2.81798200 -1.15439000
C 2.70868400 3.45292500 0.29396800
H 3.45030500 2.72720900 -0.05750600
H 2.80954300 3.49986000 1.38632000
C 2.99198300 4.82381300 -0.31434300
H 2.92906400 4.78448400 -1.40673300
H 3.99341600 5.17345800 -0.04720600
H 2.27097900 5.57013600 0.03706600

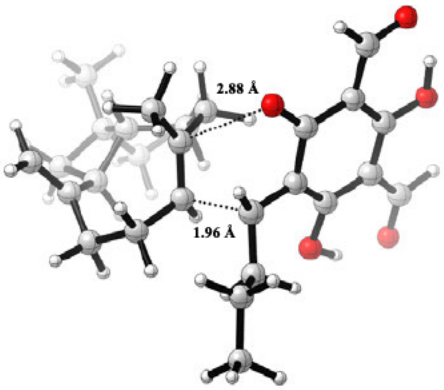

caryophyllene-*ββ*-*E*-oQM-DA-*exo*-TS
$E_{(M06\text{-}2X/6\text{-}31+G(d))}$: -1426.008401
$TCG_{(M06\text{-}2X/6\text{-}31+G(d))}$: 0.525517
$E_{(M06\text{-}2X/6\text{-}311+G(d,p))}$: -1426.379909
$E_{(M06\text{-}2X/6\text{-}311+G(d,p),\ smd=HFIP)}$: -1426.411371
Imaginary frequencies: 1

C -1.11181400 0.71539900 -2.71055200
H -2.19661400 0.75281800 -2.88772000
H -0.66356400 -0.02008100 -3.37896600
H -0.69451900 1.69671500 -2.95266700
C -0.86948900 0.34532400 -1.28350500
C -0.87800200 1.29781100 -0.25778400
H -0.87465800 0.88847600 0.75573200
C -0.59255800 -1.07859100 -0.95524100
H -0.62951300 -1.68114500 -1.86816700
H 0.44827200 -1.12533400 -0.58383100
C -1.49717700 -1.69377300 0.13080800
H -1.21096700 -1.31606200 1.12062900
H -1.28786800 -2.77147900 0.14530800
C -2.98638900 -1.46957600 -0.09846400
H -3.21868200 -1.54869400 -1.17235000
C -3.67691500 -0.19152700 0.46894500
H -3.18895100 0.06688800 1.41714700
C -4.01598700 -2.33355400 0.68938800
C -4.91559600 -1.07530600 0.76444300
H -5.63126800 -1.04253700 -0.06416400
H -5.44776800 -0.88716600 1.70306300
C -3.51907500 -2.74867400 2.07397700
H -4.34548000 -3.17978300 2.65072400
H -3.12447000 -1.90096400 2.64523200
H -2.72892200 -3.50542300 2.00662900
C -4.57466800 -3.53466900 -0.05864500
H -3.79874800 -4.29552500 -0.21187200
H -4.96072200 -3.24216500 -1.04176100
H -5.39347700 -4.00113000 0.50217400
C -3.83709100 1.06368100 -0.35912200
C -4.55033300 1.07901200 -1.48936000
H -5.03589200 0.18707700 -1.87985700
H -4.67246100 1.99119300 -2.06966200

C -1.73328600 2.54469200 -0.41668000
H -1.79923400 2.82679700 -1.47222600
H -1.30614300 3.39760600 0.11513600
C -3.15810600 2.32415600 0.14037700
H -3.75905600 3.20141600 -0.12378000
H -3.10413600 2.29562800 1.23624000
C 1.87516600 0.70096300 -0.09264800
C 1.00748700 1.83205000 -0.23678600
H 1.03245500 2.19969200 -1.26431400
C 2.25640200 0.14535700 1.14328300
C 3.19517800 -0.91541100 1.23345800
C 3.71544800 -1.46300100 0.02612300
C 3.28582200 -1.01777100 -1.23054700
C 2.29883500 0.04672100 -1.33142500
C 3.79623800 -1.63164800 -2.42885300
H 3.40851200 -1.23958800 -3.38049200
C 3.57499000 -1.44546400 2.51546500
H 4.30991100 -2.26251200 2.51974300
O 4.62883000 -2.54839900 -2.43456800
O 3.11884900 -1.03197200 3.59128100
O 1.77765400 0.38077400 -2.41197300
C 1.04046000 2.95567200 0.80218800
H 1.90527800 2.79844200 1.45212200
H 0.17594900 2.92505600 1.47575700
O 1.69631500 0.62459900 2.25217600
H 2.09142400 0.12894300 3.02710100
O 4.60428000 -2.44325600 0.13832400
H 4.84962500 -2.73060500 -0.78585400
C 1.16510800 4.32967400 0.13733500
H 2.11281400 4.36610000 -0.41472100
H 0.37457800 4.46724100 -0.61125200
C 1.11459200 5.46104300 1.16110800
H 1.90485700 5.34625300 1.91087000
H 0.15434700 5.46711700 1.69002000
H 1.24224800 6.43722000 0.68439100

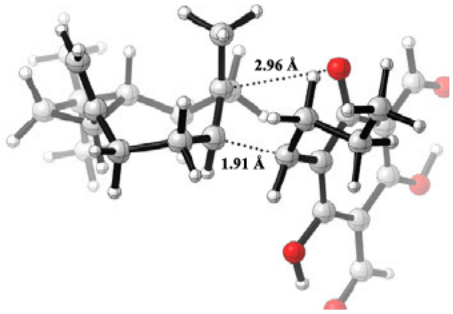

caryophyllene-*ββ*-*Z*-oQM-DA-*exo*-TS

$E_{(M06\text{-}2X/6\text{-}31+G(d))}$: -1426.014931
$TCG_{(M06\text{-}2X/6\text{-}31+G(d))}$: 0.523749
$E_{(M06\text{-}2X/6\text{-}311+G(d,p))}$: -1426.38694
$E_{(M06\text{-}2X/6\text{-}311+G(d,p),\ smd=HFIP)}$: -1426.418456
Imaginary frequencies: 1

C -1.20696500 1.76938400 -1.93742100
H -0.51336400 1.53505800 -2.75014000
H -1.11498400 2.82351000 -1.67402500
H -2.23214600 1.59578300 -2.29507100
C -0.94766700 0.84412500 -0.79819400
C -0.83180200 1.25775100 0.53216400
H -0.82302600 0.43695100 1.25368000
C -0.80508300 -0.60678200 -1.10599800
H -0.80833600 -0.75770000 -2.18949500
H 0.18243300 -0.92683500 -0.73267500
C -1.86583400 -1.50571100 -0.42931800
H -1.60621900 -1.65773700 0.62547600
H -1.79122600 -2.49180300 -0.90487300
C -3.30053100 -0.99937700 -0.52696700
H -3.46825600 -0.50345100 -1.49511500
C -3.88122900 -0.09378900 0.60367400
H -3.44363700 -0.42354700 1.55360900
C -4.47959800 -1.99020700 -0.28370700
C -5.23337400 -0.81999800 0.39648700
H -5.86588600 -0.28267400 -0.31768800
H -5.82061700 -1.04462300 1.29226200
C -4.14146400 -3.09396900 0.71840200
H -5.05147000 -3.64110900 0.98840600
H -3.70759000 -2.69842100 1.64324000
H -3.43283300 -3.81468600 0.29568700
C -5.10745500 -2.58304800 -1.53560400
H -4.40686100 -3.26024500 -2.03926500
H -5.38867000 -1.79804100 -2.24598800
H -6.00808500 -3.15756100 -1.29077000
C -3.81327000 1.41436800 0.53081900
C -4.46289400 2.10755200 -0.40737300
H -5.06789600 1.62297800 -1.16994700
H -4.41664400 3.19332800 -0.44412200
C -1.55335000 2.48846200 1.05232700
H -1.64561700 3.24555300 0.26905200

H -0.98223600 2.94156700 1.87150000
C -2.96368400 2.13404300 1.56281400
H -3.45473300 3.06474800 1.86645100
H -2.87212800 1.51537500 2.46332600
C 1.84475300 0.48167400 0.35797900
C 1.03760300 1.63574800 0.64477800
C 2.19139100 -0.40078300 1.39875000
C 3.05735300 -1.50608200 1.19355400
C 3.54995000 -1.74184600 -0.12016100
C 3.16301300 -0.94041800 -1.20321800
C 2.24651900 0.17430600 -1.01259100
C 3.64967600 -1.24125600 -2.52214900
H 3.29460800 -0.58394100 -3.32959900
C 3.41691300 -2.35700000 2.29389700
H 4.10319600 -3.18753100 2.07556200
O 4.42561600 -2.17093100 -2.78170800
O 2.99849900 -2.20205200 3.44955500
O 1.76670500 0.81119100 -1.97002500
O 1.69230700 -0.17343600 2.61177000
H 2.06720400 -0.87904400 3.21812800
O 4.37249600 -2.76778100 -0.29013400
H 4.60158900 -2.79503300 -1.26476200
H 0.94504600 1.78213400 1.72294500
C 1.30550300 2.94602600 -0.07387900
H 0.57213000 3.69845300 0.23884900
H 1.24312600 2.81798200 -1.15439000
C 2.70868400 3.45292500 0.29396800
H 3.45030500 2.72720900 -0.05750600
H 2.80954300 3.49986000 1.38632000
C 2.99198300 4.82381300 -0.31434300
H 2.92906400 4.78448400 -1.40673300
H 3.99341600 5.17345800 -0.04720600
H 2.27097900 5.57013600 0.03706600

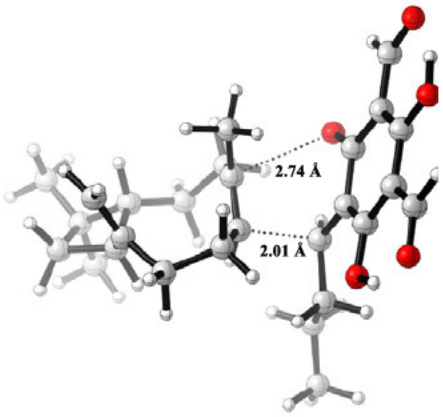

caryophyllene-*ββ*-*E*-oQM-DA-*endo*-TS

$E_{(M06\text{-}2X/6\text{-}31+G(d))}$: -1426.013817

$TCG_{(M06\text{-}2X/6\text{-}31+G(d))}$: 0.525369

$E_{(M06\text{-}2X/6\text{-}311+G(d,p))}$: -1426.385293

$E_{(M06\text{-}2X/6\text{-}311+G(d,p),\ smd=HFIP)}$: -1426.414933

Imaginary frequencies: 1

C 0.11617700 -1.96284700 0.55061200
H 0.71237600 -2.15363600 1.45540500
H 0.00756000 -2.88865500 -0.01552100
H -0.87594700 -1.63476700 0.88720900
C 0.79235900 -0.90605900 -0.25615100
C 0.70211600 0.43189900 0.10527800
H 1.42371300 1.08724000 -0.38275900
C 1.63253300 -1.31810300 -1.43091000
H 1.68500700 -2.41157600 -1.45673200
H 1.10597000 -1.02397300 -2.35085000
C 3.05623000 -0.73395400 -1.41622500
H 3.03952300 0.32957800 -1.68967400
H 3.62247100 -1.23750200 -2.21151900
C 3.79801400 -0.91151100 -0.09283900
H 3.55515900 -1.89421300 0.34180200
C 3.70433800 0.16407100 1.03828800
H 3.60805700 1.15129400 0.56809000
C 5.34680500 -0.73966100 -0.07680100
C 5.20135000 -0.11140800 1.33004900
H 5.31888500 -0.86081200 2.11994800
H 5.82932500 0.75459700 1.56565500
C 5.84928500 0.28500200 -1.09383300
H 6.90598600 0.50709400 -0.90507900
H 5.29783300 1.23040900 -1.03631400
H 5.76579300 -0.09192000 -2.11982900
C 6.15152800 -2.02689300 -0.17654600
H 6.03753700 -2.48358000 -1.16807900
H 5.82167800 -2.75653400 0.57166100
H 7.21981600 -1.83706500 -0.01709800
C 2.70183800 0.05525800 2.16894700
C 2.71630000 -0.97128900 3.02479000
H 3.43511200 -1.78405800 2.94400100

H 2.00091500 -1.03622100 3.84179200
C 0.36019200 0.84281900 1.52220300
H -0.18277500 0.04134700 2.03095000
H -0.29152400 1.72223500 1.54308800
C 1.65736100 1.14931200 2.30233500
H 1.40243800 1.29855100 3.35704000
H 2.07455100 2.09758000 1.93765100
C -1.99811200 0.46571500 -0.63485800
C -0.79129800 1.06787500 -1.08470500
C -2.92184100 1.05832000 0.25169500
C -4.11857200 0.40075500 0.62942200
C -4.36799000 -0.90833000 0.12366300
C -3.46435000 -1.55770700 -0.72556600
C -2.23579500 -0.89338200 -1.12880000
C -3.74526800 -2.88848600 -1.19925400
H -2.99345700 -3.33828500 -1.86420300
C -5.05336400 1.04097900 1.51888100
H -5.96301800 0.48015900 1.77458200
O -4.76353800 -3.52675200 -0.90122200
O -4.88023000 2.16982300 1.99795800
O -1.37485300 -1.44895700 -1.83805400
O -2.65824800 2.27107700 0.73069600
H -3.42350700 2.53621800 1.31854000
O -5.49532700 -1.49741600 0.50355200
H -5.51881400 -2.40037300 0.07786900
H -0.41663900 0.56734600 -1.97808100
C -0.54129400 2.56494200 -1.09379600
H -0.29576500 2.94529300 -0.09639900
H -1.49536600 3.04571400 -1.34621000
C 0.51985300 2.98720300 -2.11066600
H 0.20609800 2.66462100 -3.11138200
H 1.47108000 2.47614400 -1.90765800
C 0.74570600 4.49769200 -2.10088200
H 1.49297100 4.79422900 -2.84256500
H 1.09295700 4.83543500 -1.11816300
H -0.18303400 5.03260700 -2.32661000

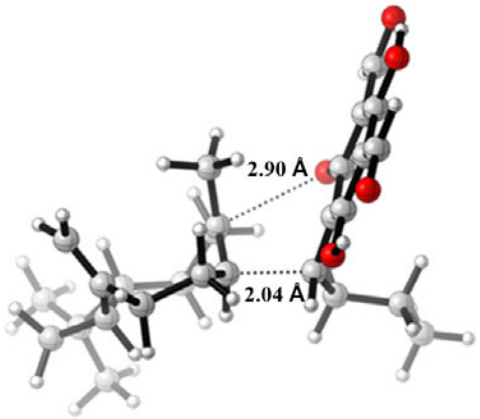

caryophyllene-*ββ*-*Z*-oQM-DA-*endo*-TS
$E_{(M06\text{-}2X/6\text{-}31+G(d))}$: -1426.013723
$TCG_{(M06\text{-}2X/6\text{-}31+G(d))}$: 0.525687
$E_{(M06\text{-}2X/6\text{-}311+G(d,p))}$: -1426.385407
$E_{(M06\text{-}2X/6\text{-}311+G(d,p),\ smd=HFIP)}$: -1426.414787
Imaginary frequencies: 1

C -0.14447900 -0.69084400 1.69600800
H -0.72088900 -1.58695900 1.96752300
H 0.02285800 -0.08698900 2.58906600
H 0.82368500 -1.03897000 1.31307200
C -0.89672200 0.07127600 0.65748400
C -0.88072800 -0.34841400 -0.66454400
H -1.56870600 0.16471500 -1.33692100
C -1.69978300 1.25722700 1.11542800
H -1.81632800 1.17739400 2.20313100
H -1.10130600 2.16430000 0.95775100
C -3.08888300 1.38852200 0.47786600
H -3.01033200 1.63005000 -0.59067300
H -3.58316700 2.25126400 0.94527900
C -3.96228200 0.15311900 0.67980400
H -3.80805900 -0.23699500 1.69827400
C -3.91078200 -1.04866800 -0.31207500
H -3.74750100 -0.65755400 -1.32392600
C -5.49639000 0.24837000 0.42954200
C -5.43558700 -1.21210300 -0.08239200
H -5.63670500 -1.92850300 0.72164800
H -6.04697700 -1.47138500 -0.95343700
C -5.86114800 1.22075900 -0.69182800
H -6.91912800 1.10686100 -0.95499600
H -5.27376100 1.04521000 -1.60014700
H -5.70344700 2.26148400 -0.38511100
C -6.35033100 0.51171600 1.66079700
H -6.17941700 1.52498100 2.04642600
H -6.11647800 -0.19894700 2.46155800
H -7.41773600 0.41941600 1.42672600
C -2.99066000 -2.22972100 -0.08423600
C -3.05039000 -2.96551600 1.02980100
H -3.75072300 -2.74374600 1.83269000
H -2.39749700 -3.82290800 1.17779600

C -0.64011700 -1.80254900 -1.02565300
H -0.03631300 -2.28919500 -0.25412100
H -0.08100100 -1.89758400 -1.96101700
C -1.98748900 -2.55044100 -1.17518100
H -1.78106900 -3.62588800 -1.19436200
H -2.42572000 -2.29456700 -2.14835300
C 1.92575100 0.29659500 -0.60051500
C 0.76836000 0.62561800 -1.35853100
C 2.77581700 -0.75165300 -1.02455600
C 3.96198800 -1.08444800 -0.32689800
C 4.27953600 -0.35549100 0.85600200
C 3.44458600 0.65492700 1.34845000
C 2.21076600 0.99371300 0.65386400
C 3.78956400 1.34679900 2.56321300
H 3.08786700 2.12460400 2.89785200
C 4.82509000 -2.13135000 -0.80899900
H 5.73592500 -2.33358400 -0.22845600
O 4.81064200 1.11399000 3.22444600
O 4.59084100 -2.79897900 -1.82557900
O 1.38520400 1.79885800 1.12264700
O 2.45633500 -1.41912900 -2.12989700
H 3.17369200 -2.09782500 -2.29198700
O 5.40031800 -0.68443600 1.48510800
H 5.47360300 -0.09815000 2.29105900
H 0.69717400 0.04496500 -2.27844900
C 0.30021900 2.05042400 -1.55012500
H 0.07367300 2.53463500 -0.60141100
H -0.60349200 2.05098000 -2.17293300
C 1.39702900 2.86394400 -2.25746500
H 1.72208100 2.34089700 -3.16618700
H 2.26897500 2.92231100 -1.59652000
C 0.90891100 4.26766600 -2.60784300
H 0.59790000 4.80682900 -1.70655500
H 0.05236200 4.22956400 -3.29014600
H 1.69815000 4.85000500 -3.09244300

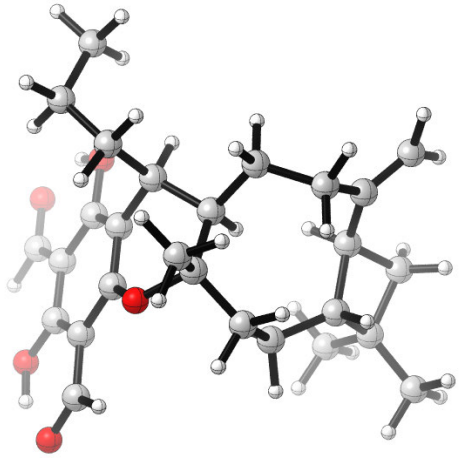

2.59 Littordial A – *α*
$E_{(M06\text{-}2X/6\text{-}31+G(d))}$: -1426.090088
$TCG_{(M06\text{-}2X/6\text{-}31+G(d))}$: 0.534693
$E_{(M06\text{-}2X/6\text{-}311+G(d,p))}$: -1426.458849
$E_{(M06\text{-}2X/6\text{-}311+G(d,p),\ smd=HFIP)}$: -1426.480928
Imaginary frequencies: none

C -1.57589600 0.56454700 -0.00455600
C -0.72946500 1.80269400 0.09630000
C -2.45476700 0.29187100 -1.05947800
C -3.24942200 -0.88611500 -1.08760100
C -3.12993800 -1.80752800 -0.02788900
C -2.23001300 -1.57409600 1.03400400
C -1.46595500 -0.37636400 1.01030600
C -2.06915700 -2.55173600 2.09114500
H -1.32391300 -2.32559500 2.86796400
C -4.16285500 -1.13900700 -2.18633000
H -4.74878200 -2.06813800 -2.14000200
O -2.71115200 -3.60195200 2.14990100
O -4.30313800 -0.37530400 -3.14216000
O -0.64935500 -0.16659100 2.05419400
C -1.42787900 2.88845000 0.93755300
H -1.76272800 2.44473500 1.88303400
H -0.70841600 3.68073900 1.18808800
O -2.53374200 1.18605900 -2.04473400
H -3.19350300 0.85980600 -2.70868700
O -3.87928600 -2.90834100 -0.06607200
H -3.66602100 -3.45313200 0.73423300
C 0.61359600 0.58082300 1.93244300
C 0.66691300 1.35081900 0.59186600
C 1.69111600 -0.51401500 2.08057700
H 2.63261400 -0.05389900 2.39874300
H 1.36003200 -1.12335300 2.92989700
C 1.94474900 -1.41887200 0.86340300
H 2.11012100 -2.44159900 1.22916700
H 1.04519400 -1.47804300 0.23365700
C 3.16928000 -1.05675900 0.02206000
H 4.02280000 -0.89328600 0.69923900

C 3.19643900 0.06729800 -1.05728900
H 2.21756000 0.12626900 -1.55109400
C 3.62598900 -2.06052100 -1.07958200
C 4.11593800 -0.84535200 -1.90315800
H 5.17168300 -0.62798200 -1.70444800
H 3.94986000 -0.87289700 -2.98543000
C 2.45715300 -2.76639200 -1.76661600
H 2.81580300 -3.30128100 -2.65371400
H 1.68293800 -2.06344500 -2.09480800
H 1.98553900 -3.49945800 -1.10158000
C 4.68098700 -3.07173300 -0.65457200
H 4.26858100 -3.78852000 0.06702400
H 5.53791000 -2.57402900 -0.18729400
H 5.04811500 -3.64147600 -1.51679500
C 3.67049600 1.45829400 -0.70662500
C 4.53272100 2.09792700 -1.50361800
H 4.91715800 1.64195200 -2.41237900
H 4.88005300 3.10240900 -1.27512600
C 1.67729100 2.50657900 0.55849300
H 1.48223500 3.08603500 -0.35432300
H 1.49338000 3.19007600 1.39517100
C 3.16882300 2.12441000 0.55861000
H 3.74698400 3.04335700 0.70616300
H 3.39476500 1.48459900 1.42003800
H 1.64542200 1.92548400 3.27821300
C 0.65765800 1.46669400 3.17454100
H -0.09050800 2.26031700 3.14433500
H 0.47384400 0.85044900 4.05987000
H -0.57686000 2.19639700 -0.91544800
H 0.97808300 0.62652200 -0.16238700
C -2.63425200 3.52652700 0.23963000
H -3.14127500 4.17644100 0.96314000
H -3.35659800 2.74705900 -0.03369700
C -2.26535000 4.34431100 -0.99750300
H -1.51172700 5.10284700 -0.75263800
H -3.14261800 4.86215100 -1.39747900
H -1.86953100 3.71100800 -1.79636100

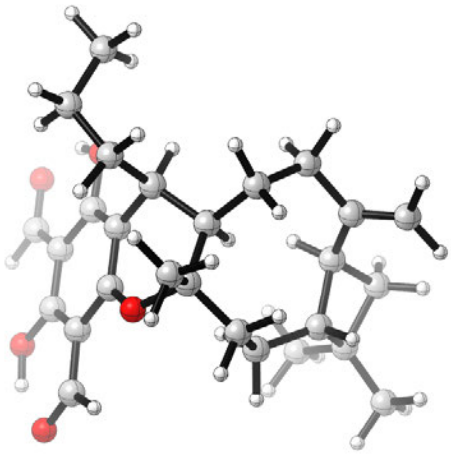

2.59 Littordial A – β
$E_{(M06\text{-}2X/6\text{-}31+G(d))}$: -1426.089845
$TCG_{(M06\text{-}2X/6\text{-}31+G(d))}$: 0.53431
$E_{(M06\text{-}2X/6\text{-}311+G(d,p))}$: -1426.45846
$E_{(M06\text{-}2X/6\text{-}311+G(d,p),\ smd=HFIP)}$: -1426.480299
Imaginary frequencies: none

C -1.55617400 0.52715000 0.04260000
C -0.79301300 1.82280600 0.12497100
C -2.43900600 0.20540300 -0.99547800
C -3.15407800 -1.02198600 -1.02246500
C -2.94805500 -1.94542900 0.02195900
C -2.03975800 -1.66513200 1.06482700
C -1.35578900 -0.41871500 1.04305000
C -1.78551100 -2.64663700 2.10068500
H -1.03514800 -2.38519000 2.86090700
C -4.07141100 -1.32347400 -2.10528200
H -4.59364900 -2.28979000 -2.05782400
O -2.35574500 -3.73775500 2.15772900
O -4.28159500 -0.56105200 -3.04947100
O -0.52138500 -0.19016100 2.07036000
C -1.56359600 2.86007900 0.96532900
H -1.91315300 2.38067300 1.88730400
H -0.89136900 3.67682300 1.26337600
O -2.59547800 1.10091300 -1.97083300
H -3.24572200 0.73718300 -2.62487300
O -3.62318800 -3.09303000 -0.01403800
H -3.35332400 -3.63286200 0.77268100
C 0.63057400 0.71119500 1.96246900
C 0.62351900 1.44395000 0.61324200
C 1.86378800 -0.20111900 2.07967500
H 2.75448600 0.44067100 2.11651900
H 1.79878700 -0.69310200 3.05703700
C 2.03059200 -1.25575000 0.96582700
H 2.24306000 -2.22829500 1.43003600
H 1.08676000 -1.39530100 0.42005300
C 3.16684600 -0.96428600 -0.00939600
H 4.07260700 -0.72658300 0.56935200

C 3.07274700 0.09983900 -1.15048600
H 2.06769400 0.08546900 -1.58760600
C 3.55840000 -2.02336400 -1.07832700
C 3.97024300 -0.84183900 -1.99236600
H 5.03253400 -0.60285200 -1.87823900
H 3.73540500 -0.91932000 -3.05929100
C 2.35402600 -2.77935800 -1.63903600
H 2.65278100 -3.36064900 -2.51911600
H 1.54568000 -2.10562800 -1.94562200
H 1.94470600 -3.47785800 -0.89937500
C 4.65692700 -2.99666300 -0.67635200
H 4.30761300 -3.68164400 0.10669600
H 5.53451500 -2.46348300 -0.29344900
H 4.97588400 -3.60425900 -1.53191700
C 3.48660900 1.53097500 -0.88378100
C 4.76582200 1.86079500 -0.67560300
H 5.56616500 1.12546600 -0.69525000
H 5.05835400 2.88815800 -0.47328900
C 1.64183100 2.59514000 0.52579000
H 2.38127800 2.53800300 1.33247700
H 1.12737200 3.55563200 0.64985400
C 2.41230700 2.60026400 -0.80927700
H 1.70159900 2.47731200 -1.63931400
H 2.88400600 3.58000800 -0.93933200
H 1.47112600 2.19494100 3.30107600
C 0.55518100 1.60737500 3.19627700
H -0.29142900 2.29278900 3.16032100
H 0.45164600 0.97987500 4.08668100
H -0.67528100 2.22013100 -0.89104400
H 0.93907000 0.69104200 -0.11185600
C -2.77412300 3.46190200 0.24226700
H -3.31753100 4.09031400 0.95830000
H -3.46334300 2.66065400 -0.05152500
C -2.40644800 4.29823800 -0.98270500
H -1.66903700 5.06807000 -0.72335300
H -3.28844400 4.80429000 -1.38725400
H -1.99127600 3.67985200 -1.78359900

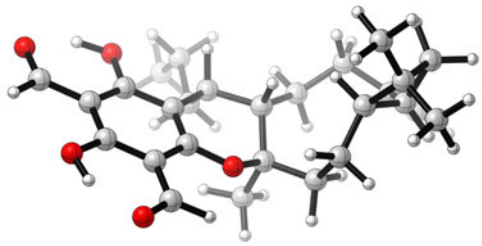

2.60 Littordial B – α
$E_{(M06\text{-}2X/6\text{-}31+G(d))}$: -1426.087814
$TCG_{(M06\text{-}2X/6\text{-}31+G(d))}$: 0.534646
$E_{(M06\text{-}2X/6\text{-}311+G(d,p))}$: -1426.455989
$E_{(M06\text{-}2X/6\text{-}311+G(d,p),\ smd=HFIP)}$: -1426.477299
Imaginary frequencies: none

C 1.82085600 0.31592200 -0.10276300
C 0.87782200 1.49261000 -0.22291700
C 3.08921700 0.35641400 -0.70593300
C 3.99157200 -0.73676400 -0.67243700
C 3.59222300 -1.91526700 -0.01067400
C 2.32935300 -1.99556800 0.60756400
C 1.46753400 -0.86216700 0.54546200
C 1.93174700 -3.20475800 1.30078400
H 0.94131200 -3.20558700 1.77784600
C 5.28962000 -0.64962400 -1.31319600
H 5.93507600 -1.53718100 -1.24821900
O 2.64276700 -4.20895200 1.37679300
O 5.68590400 0.35166000 -1.91157800
O 0.27783300 -1.02310100 1.14279000
O 3.42046400 1.48258000 -1.33526300
H 4.33001100 1.36963000 -1.71594700
O 4.44317000 -2.93892300 0.01432500
H 4.01519100 -3.68053000 0.51549200
C -0.55977800 0.13796000 1.39960800
C -0.55938100 1.02822300 0.13450200
C -1.91785400 -0.48080000 1.76871600
H -1.77170300 -0.96777200 2.74033300
H -2.63396600 0.33384300 1.93995300
C -2.51919100 -1.52269400 0.80894300
H -1.74077800 -2.22765500 0.49085300
H -3.24958800 -2.10418200 1.38641400
C -3.22941800 -0.91899400 -0.38887000
H -2.50620800 -0.46730600 -1.07546700
C -4.35379600 0.10297800 -0.12513200
H -4.95338200 -0.23006500 0.73204900
C -4.21336800 -1.72735200 -1.28832900
C -5.02182000 -0.40850200 -1.43008000
H -4.68787400 0.17087800 -2.29970400
H -6.11505500 -0.47241300 -1.43927600
C -4.99830200 -2.79736300 -0.53320400
H -5.80372400 -3.18754900 -1.16631900
H -5.45601500 -2.41039200 0.38388500
H -4.35125500 -3.63857600 -0.25700900
C -3.61976800 -2.30749900 -2.56392500
H -2.92413000 -3.12475900 -2.33574400
H -3.07121600 -1.54324300 -3.12643400
H -4.40491700 -2.70835000 -3.21638700
C -4.03949100 1.56317500 0.04453800
C -4.80192100 2.33876200 0.82334100

H -5.64346100 1.93244400 1.37951300
H -4.61275700 3.40507900 0.92804600
C -1.53913700 2.22744200 0.17431900
H -1.81681800 2.47372200 1.20699800
H -0.99406400 3.10055600 -0.19535900
C -2.83954400 2.15214000 -0.66908300
H -3.09479700 3.17982700 -0.94898900
H -2.63883000 1.62249900 -1.60976100
C 1.39234600 2.76374100 0.51745600
H 2.33895600 2.53399000 1.02342300
H 0.69008500 3.05859600 1.30660100
C 1.61728400 3.96327300 -0.40596500
H 2.32268500 3.67576900 -1.19260600
H 0.67640700 4.22413500 -0.91002500
C 2.14305900 5.17887400 0.35355900
H 3.09984900 4.95110300 0.83661500
H 1.44096700 5.49011900 1.13586100
H 2.30037500 6.03135400 -0.31423700
H 0.84623800 1.75634000 -1.29058900
H -0.55286100 1.72131100 2.89849800
C 0.02361700 0.82936600 2.63522300
H 1.06383200 1.12461400 2.47764600
H -0.00825000 0.13897800 3.48276700
H -0.85131000 0.36350600 -0.68629800

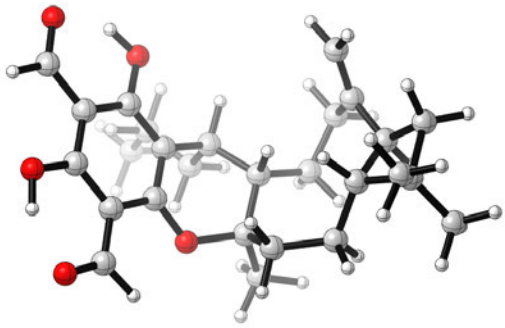

2.60 Littordial B – *β*

$E_{(M06\text{-}2X/6\text{-}31+G(d))}$: -1426.092068
$TCG_{(M06\text{-}2X/6\text{-}31+G(d))}$: 0.534246
$E_{(M06\text{-}2X/6\text{-}311+G(d,p))}$: -1426.46053
$E_{(M06\text{-}2X/6\text{-}311+G(d,p),\ smd=HFIP)}$: -1426.483029
Imaginary frequencies: none

C -1.64561300 0.38414100 0.08910100
C -0.76543000 1.57917900 -0.15852300
C -2.51779700 0.25148600 1.17678000
C -3.35632800 -0.88668100 1.32504400
C -3.29586500 -1.90592700 0.35326100
C -2.41136800 -1.80703100 -0.74224400
C -1.60108500 -0.64630700 -0.83849500
C -2.31797700 -2.87704300 -1.71524800
H -1.58473500 -2.74887400 -2.52510300
C -4.26128000 -0.99935100 2.45477700
H -4.88125600 -1.90598100 2.50445600

O -3.00388900 -3.89953000 -1.66876300
O -4.35870700 -0.14370600 3.33455200
O -0.80209100 -0.54105900 -1.91715100
O -2.55222700 1.24158800 2.06702600
H -3.21252000 1.00751700 2.76723300
O -4.08791300 -2.96677400 0.50587400
H -3.91660700 -3.58830500 -0.24671200
C 0.53803000 0.04240100 -1.77406600
C 0.61394800 1.02101900 -0.57965500
C 1.44661400 -1.17943600 -1.54922100
H 1.00835700 -1.76049400 -0.72448700
H 1.35748700 -1.80205900 -2.44856200
C 2.94262300 -0.96553800 -1.24475600
H 3.43149100 -1.90734000 -1.52852900
H 3.38034500 -0.20957900 -1.91121700
C 3.34456700 -0.70448700 0.21428600
H 2.57910000 -1.12195700 0.88606000
C 3.76429800 0.68995900 0.80235400
H 4.29677800 1.25296800 0.02311900
C 4.72621100 -1.25571700 0.68562900
C 4.79711100 -0.06356500 1.66768900
H 4.38904900 -0.33799800 2.64547700
H 5.76928100 0.41965600 1.81165000
C 5.81538900 -1.15574700 -0.38297900
H 6.79660200 -1.33088100 0.07349800
H 5.84186500 -0.16853100 -0.85788900
H 5.67986400 -1.90482600 -1.17154100
C 4.70429200 -2.65184100 1.28969400
H 4.45488200 -3.40296100 0.52885300
H 3.96043300 -2.72265600 2.09101200
H 5.68279900 -2.91565700 1.70910900
C 2.74199300 1.59642400 1.44437500
C 2.31997800 1.44908100 2.70344100
H 2.71308600 0.68423000 3.36674500
H 1.55345000 2.10036200 3.11595700
C 1.68367800 2.10215900 -0.78002600
H 1.31517400 2.90605400 -1.42614000
H 2.54487600 1.67456700 -1.30288700
C 2.18215300 2.67989500 0.55028700
H 2.97373200 3.41132100 0.33469100
H 1.38346200 3.22195000 1.06954200
C -1.42772100 2.54960400 -1.15383500
H -1.66511600 2.01708600 -2.08491600
H -0.72311100 3.35077000 -1.41457400
C -2.70485800 3.18726100 -0.60477300
H -3.43907800 2.40353400 -0.38012300
H -2.48227200 3.68007600 0.35030700
C -3.31069800 4.19087900 -1.58374300
H -3.56137300 3.70784000 -2.53501300
H -2.60826700 5.00427900 -1.79871100
H -4.22635200 4.63661600 -1.18355000
H -0.63049200 2.10829600 0.79321800
H 1.84419000 0.93888600 -3.26314300
C 0.79030300 0.67783600 -3.13730300
H 0.19209900 1.58194100 -3.27669100
H 0.52117000 -0.03997700 -3.91782000
H 0.92920800 0.42006400 0.28327600

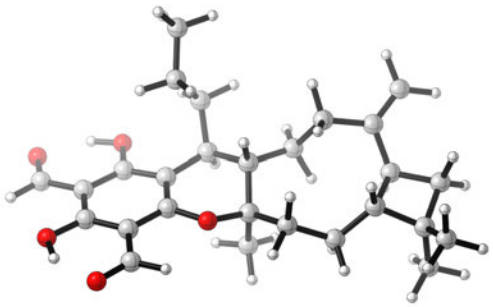

2.66 Littordial F – α
$E_{(M06\text{-}2X/6\text{-}31+G(d))}$: -1426.089128
$TCG_{(M06\text{-}2X/6\text{-}31+G(d))}$: 0.534153
$E_{(M06\text{-}2X/6\text{-}311+G(d,p))}$: -1426.457787
$E_{(M06\text{-}2X/6\text{-}311+G(d,p),\ smd=HFIP)}$: -1426.479869
Imaginary frequencies: none

C -2.12727700 0.31903900 -0.40886800
C -0.97649900 1.27877800 -0.64479400
C -3.44994400 0.65907200 -0.74588100
C -4.55844100 -0.16990500 -0.43395300
C -4.32029800 -1.39665700 0.21708500
C -3.00508100 -1.80309800 0.51298000
C -1.93185400 -0.93386500 0.16626900
C -2.76081400 -3.09212200 1.13005300
H -1.71299600 -3.36936700 1.31200900
C -5.90904600 0.23098400 -0.77994800
H -6.71716300 -0.45908400 -0.49849500
O -3.66011300 -3.87107400 1.45227300
O -6.17925900 1.28375100 -1.35969300
O -0.70405400 -1.41699700 0.42656300
C -1.23399500 2.68278500 -0.04070900
H -0.27108500 3.21032700 0.00435000
H -1.87273800 3.26286300 -0.71161300
O -3.64109700 1.81679000 -1.37486600
H -4.61355600 1.92538600 -1.54062300
O -5.36777300 -2.16095400 0.51876800
H -5.02901600 -2.98805500 0.94938500
C 0.42649400 -0.81390800 -0.27019500
C 0.32206400 0.70167700 -0.05050700
C 1.62820600 -1.47983900 0.43522000
H 1.74654900 -1.02565500 1.42719100
H 1.28724700 -2.50427900 0.62110100
C 2.99701000 -1.56810300 -0.28832800
H 2.88146300 -1.42318500 -1.36958700
H 3.33565100 -2.60683500 -0.17917400
C 4.15006000 -0.69674900 0.22177700
H 4.07406600 -0.58629900 1.31436900
C 4.51823900 0.68490000 -0.39449900
H 4.27792600 0.66719800 -1.46722400
C 5.60562600 -1.16444600 -0.10341700
C 6.00731700 0.32815800 -0.19871900
H 6.37713600 0.70770400 0.76084000
H 6.70902500 0.60711900 -0.99195300
C 5.73184700 -1.85431400 -1.46217500

H 6.79100900 -1.96247300 -1.72342800
H 5.25062000 -1.28234300 -2.26354200
H 5.28877500 -2.85680700 -1.45014300
C 6.28467100 -1.99402400 0.97647500
H 5.79965300 -2.97341100 1.07933600
H 6.23883300 -1.48944000 1.94778700
H 7.33984200 -2.16865100 0.73357900
C 3.95915200 1.93938500 0.22275000
C 4.70430800 3.02769600 0.42847800
H 5.75979100 3.05221600 0.16833700
H 4.28258500 3.92982100 0.86427900
C 1.58264300 1.43525400 -0.53867100
H 2.13050000 0.78837700 -1.23082100
H 1.31422400 2.32198900 -1.12412900
C 2.50892100 1.85211200 0.61661400
H 2.16316900 2.79756800 1.05261300
H 2.43061700 1.10003000 1.41381900
H -0.83924700 1.40410300 -1.73029800
C -1.85678900 2.68359900 1.35667500
H -1.31769000 1.99224300 2.01848400
H -2.88729800 2.31276300 1.30000800
C -1.85490700 4.08269500 1.97041300
H -0.83186500 4.45689000 2.09183000
H -2.39348300 4.78906700 1.32885000
H 1.05537600 -0.69912900 -2.35759600
C 0.32647700 -1.22945700 -1.73935900
H 0.50913900 -2.30445400 -1.83702000
H -0.66702200 -1.01135400 -2.14025900
H 0.25407800 0.82510400 1.04082000
H -2.33429600 4.09004100 2.95395400

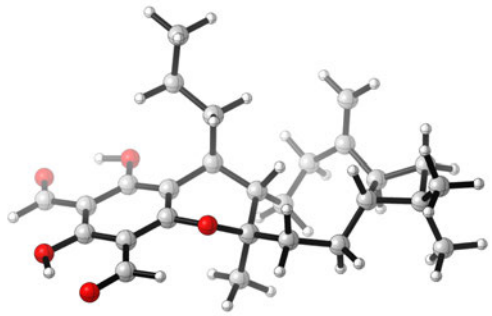

2.66 Littordial F – β

$E_{(M06\text{-}2X/6\text{-}31+G(d))}$: -1426.091118
$TCG_{(M06\text{-}2X/6\text{-}31+G(d))}$: 0.533955
$E_{(M06\text{-}2X/6\text{-}311+G(d,p))}$: -1426.459633
$E_{(M06\text{-}2X/6\text{-}311+G(d,p),\ smd=HFIP)}$: -1426.481796
Imaginary frequencies: none

C -1.85863000 0.37162300 -0.17516000
C -0.58329500 1.17428600 -0.14315700
C -3.08955700 0.89102100 -0.60261300
C -4.29599600 0.14930700 -0.48005000
C -4.24680500 -1.14380000 0.07823800
C -3.01606700 -1.70661700 0.47902000

C -1.84833200 -0.91982300 0.32635100
C -2.95351500 -3.06109400 0.99247500
H -1.95697200 -3.44800800 1.25191500
C -5.56161400 0.71289900 -0.91665500
H -6.45491300 0.08594900 -0.78352800
O -3.94545500 -3.77569700 1.14256600
O -5.67013100 1.83275100 -1.41576500
O -0.66719500 -1.46935900 0.68172400
C -0.43867300 1.90218400 1.21126300
H -0.35877400 1.14457200 2.00574500
H 0.52138700 2.43892700 1.19848900
O -3.09894800 2.11838100 -1.11908300
H -4.03044000 2.34592400 -1.36755000
O -5.38738200 -1.82272900 0.19579700
H -5.17751700 -2.71096100 0.58145700
C 0.42701300 -1.22590500 -0.26406300
C 0.67551900 0.29238900 -0.39783800
C 1.60148500 -1.93726500 0.41584300
H 1.63544100 -1.58170100 1.45411800
H 1.33660900 -3.00104500 0.46213000
C 3.00804500 -1.80734800 -0.19882400
H 2.97879100 -1.91976400 -1.29128600
H 3.56101300 -2.68617400 0.15907000
C 3.85360200 -0.58931500 0.19970000
H 3.51846500 -0.21421800 1.17863500
C 4.12384000 0.66407100 -0.70745000
H 4.17246900 0.33610800 -1.75510900
C 5.39870400 -0.79180900 0.28211800
C 5.55342600 0.69131200 -0.12533300
H 5.62397200 1.33250700 0.75872800
H 6.36447400 0.94745400 -0.81523800
C 5.94728400 -1.72126400 -0.80111800
H 7.03957000 -1.63635800 -0.84034000
H 5.55951600 -1.47416600 -1.79576800
H 5.70488700 -2.77036400 -0.59661600
C 5.93596700 -1.19558400 1.64703300
H 5.60254800 -2.20667700 1.91490400
H 5.58887900 -0.50775100 2.42608000
H 7.03276000 -1.19410400 1.65536600
C 3.23982800 1.88404500 -0.62028700
C 3.40216200 2.83895100 0.30023400
H 4.20412900 2.81869200 1.03191800
H 2.72743200 3.69047500 0.34603100
C 1.33678800 0.65697500 -1.73443600
H 2.02411100 -0.13281300 -2.05298200
H 0.57192500 0.73235700 -2.51796300
C 2.12737300 1.96619600 -1.64313800
H 2.56526500 2.17925400 -2.62858500
H 1.46359400 2.80650500 -1.40396900
H -0.64686700 1.93914600 -0.92704300
C -1.55608000 2.88539400 1.54911500
H -2.51339900 2.35324000 1.61695600
H -1.66437400 3.60956900 0.73201700
C -1.28672400 3.61547000 2.86415800
H -1.19933400 2.90628800 3.69513300
H -0.35105000 4.18386700 2.81333400
H 0.88524900 -1.98871900 -2.25530100
C 0.03702000 -1.92348200 -1.56968000
H -0.29522300 -2.94209400 -1.34381700

H -0.77350000 -1.40014000 -2.08641500
H 1.38808400 0.54433800 0.39832300
H -2.09194500 4.31619600 3.10477000

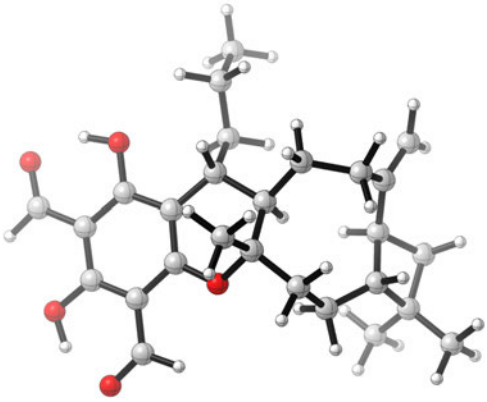

Unobserved diastereomer 2.69 Littoridal Z – *α*
$E_{(M06\text{-}2X/6\text{-}31+G(d))}$: -1426.055952
$TCG_{(M06\text{-}2X/6\text{-}31+G(d))}$: 0.535309
$E_{(M06\text{-}2X/6\text{-}311+G(d,p))}$: -1426.45999
$E_{(M06\text{-}2X/6\text{-}311+G(d,p),\ smd=HFIP)}$: -1426.481311
Imaginary frequencies: none

C -3.13620000 0.73850000 -0.11300000
C -2.51980000 -1.98870000 0.00970000
C -1.83760000 0.37150000 0.28340000
C -4.11970000 -0.21340000 -0.48680000
C -3.79110000 -1.58160000 -0.43810000
C -1.57890000 -0.98980000 0.38340000
C -5.43950000 0.21540000 -0.90570000
H -6.14730000 -0.57740000 -1.18880000
C -2.20720000 -3.39920000 0.11500000
H -1.21170000 -3.66090000 0.50240000
O -4.71370000 -2.46620000 -0.80290000
H -4.31900000 -3.37060000 -0.68660000
O -3.42870000 2.03500000 -0.13420000
H -4.37100000 2.12890000 -0.43860000
O -0.40570000 -1.45720000 0.83660000
C -0.78250000 1.41260000 0.59640000
H -1.09880000 1.95250000 1.50340000
C 0.58940000 0.75170000 0.88800000
C 0.43850000 -0.58270000 1.63630000
O -2.99050000 -4.29460000 -0.20230000
O -5.79050000 1.39390000 -0.95590000
C 1.72290000 -1.41350000 1.76640000
H 2.41140000 -0.90870000 2.45100000
H 1.41580000 -2.33390000 2.27660000
C -0.22310000 -0.43490000 3.00690000
H -1.16170000 0.12350000 2.94510000
H 0.44120000 0.08120000 3.70480000
C 3.00460000 1.67150000 1.51150000
H 3.42290000 2.52820000 2.05140000
C 3.55290000 1.67740000 0.10300000
C 3.50050000 0.39690000 -0.69580000
H 2.60250000 0.38380000 -1.32760000

C 3.63220000 -0.97060000 0.02310000
C 4.72370000 0.00760000 -1.56040000
H 5.64800000 0.39110000 -1.11530000
H 4.70080000 0.26750000 -2.62340000
C 4.47760000 -1.47540000 -1.18870000
C 5.70050000 -2.30810000 -0.83470000
H 6.32600000 -1.79420000 -0.09710000
H 6.31350000 -2.50400000 -1.72200000
H 5.40450000 -3.27670000 -0.41360000
C 3.64110000 -2.18240000 -2.25400000
H 2.76250000 -1.59670000 -2.54530000
H 3.29270000 -3.16090000 -1.90490000
H 4.24520000 -2.34350000 -3.15370000
C 4.08210000 2.78370000 -0.42180000
H 4.13440000 3.71250000 0.14020000
H 4.48370000 2.79790000 -1.43190000
C 2.42200000 -1.79680000 0.44670000
H 1.67870000 -1.81310000 -0.35990000
H 4.31620000 -0.85600000 0.87730000
C -0.62190000 2.46560000 -0.54090000
H 0.41460000 2.44060000 -0.90730000
H -1.25200000 2.18910000 -1.39260000
C -0.95710000 3.89890000 -0.12750000
H -0.30230000 4.20700000 0.69860000
H -1.98070000 3.92670000 0.25770000
C -0.80620000 4.87550000 -1.29030000
H 0.21660000 4.86470000 -1.68280000
H -1.48080000 4.60750000 -2.11030000
H -0.43980000 -1.42680000 3.41310000
H 2.76940000 -2.83370000 0.54630000
C 1.47430000 1.79630000 1.59310000
H 1.23070000 2.77110000 1.15750000
H 1.17550000 1.86180000 2.64720000
H 1.02390000 0.49840000 -0.08590000
H 3.35710000 0.77990000 2.03830000
H -1.03880000 5.90000000 -0.98630000

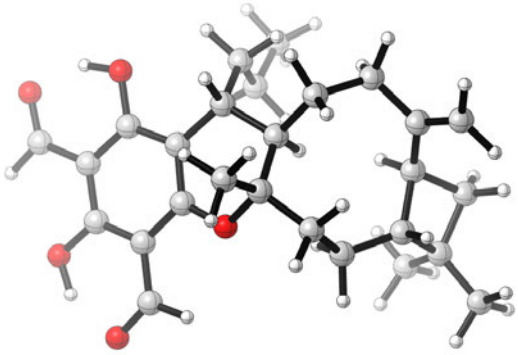

Unobserved diastereomer 2.69 Littoridal Z – *β*

$E_{(M06\text{-}2X/6\text{-}31+G(d))}$: -1426.058801

$TCG_{(M06\text{-}2X/6\text{-}31+G(d))}$: 0.53523

$E_{(M06\text{-}2X/6\text{-}311+G(d,p))}$: -1426.462887

$E_{(M06\text{-}2X/6\text{-}311+G(d,p),\ smd=HFIP)}$: -1426.483839

Imaginary frequencies: none

C 3.20480000 -0.92600000 0.07880000
C 2.57530000 1.80180000 0.12020000
C 1.89460000 -0.55660000 0.43990000
C 4.18780000 0.02230000 -0.30840000
C 3.85290000 1.38980000 -0.30150000
C 1.63280000 0.80820000 0.50570000
C 5.51810000 -0.40730000 -0.69110000
H 6.22340000 0.38310000 -0.98630000
C 2.25510000 3.21330000 0.18430000
H 1.25370000 3.48110000 0.55110000
O 4.77610000 2.26850000 -0.67800000
H 4.37590000 3.17390000 -0.59000000
O 3.51700000 -2.21750000 0.10610000
H 4.46620000 -2.30690000 -0.17960000
O 0.45820000 1.29120000 0.93640000
C 0.82950000 -1.58570000 0.77020000
H 1.10910000 -2.06780000 1.71920000
C -0.55270000 -0.91970000 0.97340000
C -0.42690000 0.43040000 1.69780000
O 3.03920000 4.10320000 -0.14700000
O 5.88140000 -1.58340000 -0.69890000
C -1.73740000 1.22680000 1.73000000
H -2.49650000 0.62810000 2.24730000
H -1.55640000 2.10360000 2.36110000
C 0.15990000 0.29300000 3.10210000
H 1.14140000 -0.18950000 3.07620000
H -0.49850000 -0.30110000 3.74180000
C -2.66090000 -2.48000000 0.81230000
H -2.25370000 -2.81010000 -0.15330000
C -3.81140000 -1.52750000 0.57390000
C -3.63150000 -0.45480000 -0.47110000
H -2.74630000 -0.68010000 -1.07770000
C -3.58470000 1.03450000 -0.03250000
C -4.78770000 -0.06030000 -1.42400000
H -5.76250000 -0.18780000 -0.94200000
H -4.80950000 -0.54190000 -2.40650000
C -4.31180000 1.41410000 -1.35370000
C -5.38980000 2.48050000 -1.23540000
H -6.09750000 2.23650000 -0.43570000
H -5.95400000 2.57570000 -2.17040000
H -4.94880000 3.45930000 -1.01090000
C -3.34800000 1.75070000 -2.49010000
H -2.57000000 0.98900000 -2.61320000
H -2.85100000 2.71150000 -2.31400000
H -3.89380000 1.82350000 -3.43730000
C -4.92760000 -1.62030000 1.29930000
H -5.04830000 -2.38790000 2.05870000
H -5.76190000 -0.93630000 1.16480000
C -2.26460000 1.68040000 0.34980000
H -1.51350000 1.48140000 -0.42390000
H -4.30310000 1.15510000 0.79180000
C 0.71440000 -2.71210000 -0.28260000
H 1.58120000 -3.37110000 -0.20750000
H -0.15820000 -3.32510000 -0.02340000
C 0.58490000 -2.23800000 -1.72990000
H 1.50370000 -1.71730000 -2.02540000
H -0.22730000 -1.50460000 -1.82810000

C 0.32820000 -3.40510000 -2.68050000
H 1.13360000 -4.14390000 -2.61400000
H -0.60970000 -3.91390000 -2.43120000
H 0.27630000 1.28290000 3.55140000
H -2.39760000 2.76950000 0.35730000
C -1.52430000 -1.89860000 1.67930000
H -0.93870000 -2.73670000 2.07660000
H -1.99080000 -1.42670000 2.55100000
H -0.94590000 -0.67850000 -0.02130000
H -3.04440000 -3.37290000 1.31760000
H 0.26310000 -3.07080000 -3.71960000

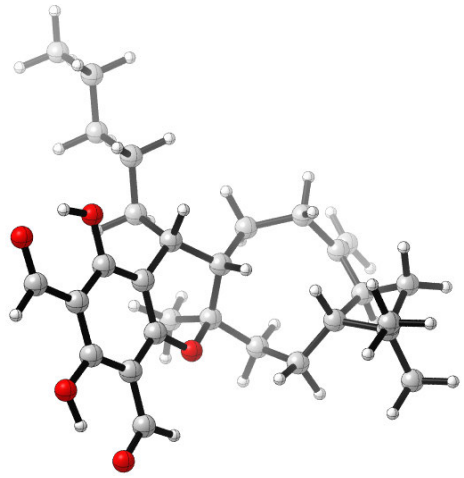

2.61 Littoridial C – α
$E_{(M06\text{-}2X/6\text{-}31+G(d))}$: -1504.637837
$TCG_{(M06\text{-}2X/6\text{-}31+G(d))}$: 0.589259
$E_{(M06\text{-}2X/6\text{-}311+G(d,p))}$: -1505.062961
$E_{(M06\text{-}2X/6\text{-}311+G(d,p),\ smd=HFIP)}$: -1505.086141
Imaginary frequencies: none

C 2.72398800 -1.06764800 -0.68279100
C 1.20279800 -3.03698100 0.59571200
C 1.51087700 -0.68515900 -0.08676700
C 3.20187200 -2.40197800 -0.65850300
C 2.42318700 -3.38418600 -0.01566400
C 0.77407600 -1.68059700 0.54260200
C 4.45864300 -2.74625300 -1.29278400
H 4.76674300 -3.80059400 -1.23602200
C 0.41981600 -4.04993500 1.27314200
H -0.51502500 -3.72044600 1.74972400
O 2.87530200 -4.63397100 0.00143400
H 2.20933900 -5.18330900 0.49368500
O 3.42449200 -0.11644100 -1.29392100
H 4.24412100 -0.53784400 -1.66709000
O -0.40600900 -1.43749900 1.13145100
C 1.02009900 0.74067400 -0.20060100
H 1.08830700 1.00696300 -1.26508700

C -0.49248400 0.78730900 0.14640000
H -0.98782900 0.27103200 -0.68317400
C -0.80264600 -0.06579000 1.39924000
O 0.75009300 -5.23443200 1.33859200
O 5.17320000 -1.93100200 -1.87543200
C -0.02744100 0.37555400 2.64358100
H -0.27249000 1.40547200 2.91844200
H 1.05159500 0.30601500 2.48724200
H -0.29203200 -0.27465300 3.48159800
C -2.29192100 -0.19490300 1.75761600
H -2.69324900 0.81032000 1.93946400
H -2.32319100 -0.71686600 2.72099800
C -1.00472900 2.24809100 0.20174400
H -0.19762400 2.88500900 -0.17093500
H -1.17238100 2.56586700 1.23826600
C -2.26086900 2.62746200 -0.62478300
H -2.15971300 3.68653800 -0.88332600
H -2.25491900 2.08107800 -1.57650700
C -3.58272400 2.45767900 0.09585900
C -4.37808500 1.20097400 -0.11744100
H -5.06276000 1.06909000 0.72966000
C -3.66267500 -0.13389200 -0.40465400
C -5.16763100 0.97427500 -1.43410000
H -4.64632300 1.41893500 -2.29003500
H -6.21610200 1.28699000 -1.45072500
C -4.85764400 -0.54349700 -1.31793700
C -4.49138000 -1.26872100 -2.60409000
H -3.71312500 -0.72721800 -3.15300700
H -5.36241900 -1.36757500 -3.26196500
H -4.11676600 -2.27702900 -2.39126100
C -5.96218700 -1.29511000 -0.57969700
H -6.26297600 -0.79178800 0.34534100
H -5.64001100 -2.31009700 -0.32043600
H -6.85004900 -1.37758900 -1.21629500
C -4.01814900 3.40931800 0.92500000
H -3.46936600 4.33715700 1.06806700
H -4.94177500 3.29545000 1.48618800
C -3.19922300 -0.96191300 0.77944000
H -2.69417600 -1.87687600 0.44780200
H -2.82773200 0.06453600 -1.08430000
H -4.08381800 -1.28071500 1.34509400
C 1.92735700 1.75825900 0.55483500
H 1.36006100 2.26585900 1.34379700
H 2.73686100 1.21841700 1.06112000
C 2.54905900 2.81696200 -0.35749100
H 1.75556000 3.38547200 -0.86436400
H 3.12003500 2.31343800 -1.14573000
C 3.45328800 3.78667100 0.39897700
H 4.25136900 3.22161100 0.90065700
H 2.87928600 4.28027800 1.19650400
C 4.07920900 4.84929600 -0.50242900

H 3.28147200 5.41241100 -1.00401400
H 4.65219100 4.35436200 -1.29674800
C 4.98408800 5.81045400 0.26409400
H 4.42368200 6.33482100 1.04549000
H 5.80347100 5.27035200 0.75005400
H 5.42370000 6.56339500 -0.39623400

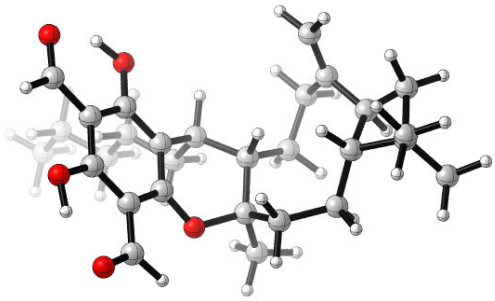

2.61 Littoridial C – β
$E_{(M06\text{-}2X/6\text{-}31+G(d))}$: -1504.641707
$TCG_{(M06\text{-}2X/6\text{-}31+G(d))}$: 0.588419
$E_{(M06\text{-}2X/6\text{-}311+G(d,p))}$: -1505.067514
$E_{(M06\text{-}2X/6\text{-}311+G(d,p),\ smd=HFIP)}$: -1505.091867
Imaginary frequencies: none

C 2.01497300 0.90328500 1.29467800
C 1.44755200 2.54152100 -0.92309800
C 1.28000300 0.37130900 0.22828900
C 2.48608600 2.24378100 1.27531100
C 2.20030300 3.05116000 0.15667100
C 1.00672600 1.19653900 -0.85132000
C 3.25526500 2.76840800 2.38810300
H 3.59037900 3.81296800 2.30632700
C 1.11691300 3.38959400 -2.04961900
H 0.50016700 2.93875900 -2.84177900
O 2.64801200 4.30401400 0.15217800
H 2.34783600 4.72395300 -0.69560700
O 2.27801700 0.10637300 2.32644800
H 2.80555800 0.62898300 2.98433800
O 0.34102200 0.70874100 -1.91582400
C 0.78488000 -1.04760200 0.15931200
H 0.74287300 -1.44579400 1.18064700
C -0.66547800 -0.97600700 -0.37297900
H -1.19180800 -0.36905600 0.37490200
C -0.78679700 -0.20533900 -1.70766500
O 1.48116900 4.56080200 -2.15041100
O 3.53899900 2.11206500 3.38871600
C -0.75947600 -1.08255900 -2.95487800
H -1.68670600 -1.65098600 -3.05889400
H 0.07630000 -1.78604600 -2.93225700
H -0.65050300 -0.44205700 -3.83437700

C -2.01409600 0.72331400 -1.70417000
H -2.03379100 1.21268700 -2.68576300
H -1.81663600 1.51476500 -0.96704600
C -1.37411000 -2.33573800 -0.41809400
H -0.74925400 -3.08792400 -0.91037400
H -2.27923900 -2.25864800 -1.02845300
C -1.78799500 -2.82169000 0.97583900
H -2.32009600 -3.77646100 0.86489000
H -0.90980500 -3.01876800 1.60056500
C -2.69616600 -1.82294000 1.65548100
C -3.88363500 -1.36776800 0.84266800
H -4.17064700 -2.17041300 0.14998300
C -3.83464300 -0.01504000 0.04879500
C -5.15190200 -0.83297300 1.54055300
H -4.91399900 -0.30817500 2.47056000
H -5.95353700 -1.55223800 1.73419600
C -5.34866600 0.16777600 0.37854400
C -5.77574000 1.58102600 0.74350300
H -5.14982500 1.98633000 1.54558200
H -6.81837600 1.60351900 1.08084600
H -5.69205100 2.24976000 -0.12222200
C -6.27327200 -0.40772600 -0.69398600
H -5.98021200 -1.41961100 -0.99429900
H -6.28849000 0.21881300 -1.59250200
H -7.29792600 -0.45892900 -0.30948300
C -2.42286100 -1.35527800 2.87400700
H -1.53531600 -1.67822500 3.41108800
H -3.06218700 -0.64116700 3.38377700
C -3.40923400 0.13423900 -1.41883400
H -4.11956100 0.84101200 -1.86788200
H -3.27568600 0.70150700 0.66856800
H -3.56370800 -0.80543900 -1.96625400
C 1.75200900 -1.92378600 -0.65686800
H 1.31807400 -2.92178900 -0.80213300
H 1.88751500 -1.48578100 -1.65466200
C 3.11864600 -2.08024100 0.01012500
H 2.98524400 -2.46626100 1.02973500
H 3.59066200 -1.09492300 0.11819200
C 4.05127100 -3.00252900 -0.77196500
H 4.17423800 -2.61665700 -1.79394700
H 3.58679600 -3.99386500 -0.87313400
C 5.42533200 -3.15483100 -0.12240900
H 5.30031800 -3.53619800 0.89906600
H 5.88940500 -2.16507200 -0.02578800
C 6.34743600 -4.08191600 -0.91006300
H 5.91393300 -5.08418000 -0.99432100
H 6.50646300 -3.70345600 -1.92542100
H 7.32589900 -4.17883700 -0.43111400

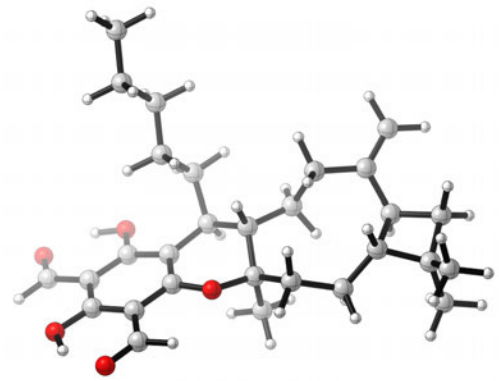

2.65 Littordial E - α
$E_{(M06\text{-}2X/6\text{-}31+G(d))}$: -1504.676253
$TCG_{(M06\text{-}2X/6\text{-}31+G(d))}$: 0.587463
$E_{(M06\text{-}2X/6\text{-}311+G(d,p))}$: -1505.064759
$E_{(M06\text{-}2X/6\text{-}311+G(d,p),\ smd=HFIP)}$: -1505.088862
Imaginary frequencies: none

C -1.92325500 -0.36494200 -0.67953800
C -0.84940600 0.59904800 -1.14660900
C -3.25022400 -0.26455700 -1.13509300
C -4.29794400 -1.07782000 -0.63105700
C -3.98963400 -2.04406100 0.34715800
C -2.66204300 -2.21984600 0.78212500
C -1.65113900 -1.38085900 0.23283000
C -2.34058800 -3.25438700 1.74564200
H -1.28407200 -3.36489600 2.02758900
C -5.65750700 -0.92455200 -1.11326100
H -6.41680300 -1.58460400 -0.67025500
O -3.18492100 -3.99716600 2.25035100
O -5.98628100 -0.10755000 -1.97465000
O -0.40188700 -1.64761300 0.65353500
C -1.26014000 2.08330400 -0.97060200
H -0.35014000 2.69410600 -1.04846100
H -1.90840200 2.38789500 -1.79586500
O -3.50677500 0.64617300 -2.07170500
H -4.47465200 0.60789300 -2.28759900
O -4.98154000 -2.79299800 0.82427600
H -4.59583200 -3.42945000 1.48034000
C 0.70802800 -1.15587600 -0.15510500
C 0.46079400 0.34232700 -0.37883000
C 1.92346200 -1.47431800 0.74289900
H 1.94884800 -0.74970100 1.56665900
H 1.66372000 -2.43335700 1.20446700
C 3.33152500 -1.62680300 0.11113800
H 3.26204000 -1.80262700 -0.96941100
H 3.75310800 -2.55457400 0.51978700
C 4.37523100 -0.53786500 0.38325100
H 4.23073200 -0.13262400 1.39646400
C 4.65448000 0.64393100 -0.59137700
H 4.47441100 0.30150700 -1.62054100
C 5.88135400 -0.93203000 0.24448000
C 6.15630700 0.50530500 -0.26239400
H 6.43993000 1.17449600 0.55813400

H 6.87250000 0.61706600 -1.08337800
C 6.14017000 -1.96077300 -0.85682200
H 7.21733100 -2.03389800 -1.04687000
H 5.65578400 -1.68745400 -1.80106600
H 5.78487400 -2.95764900 -0.57148000
C 6.57118300 -1.35227600 1.53401600
H 6.16939700 -2.30634400 1.89918600
H 6.42898200 -0.60185300 2.31939200
H 7.64919100 -1.48223400 1.37929600
C 3.95620700 1.96009600 -0.37299000
C 4.59198200 3.13013500 -0.46685200
H 5.65377400 3.18416200 -0.69486900
H 4.07076600 4.07244300 -0.31855400
C 1.67691500 1.03006600 -1.02205600
H 2.31586600 0.27220600 -1.48583800
H 1.36364800 1.68505800 -1.84308700
C 2.49994500 1.84503600 -0.00962200
H 2.05047800 2.83620000 0.12862400
H 2.44451700 1.34440300 0.96685000
H -0.66581600 0.42943500 -2.21913100
C -1.95662100 2.40848900 0.35197800
H -1.40834400 1.96775800 1.19745700
H -2.95563700 1.95268300 0.36526600
C -2.09317900 3.91396300 0.57542800
H -1.09269400 4.37050800 0.60568400
H -2.61020800 4.36302300 -0.28502100
H 1.43498000 -1.56978200 -2.17167400
C 0.72412700 -1.97546100 -1.44718400
H 1.00666200 -3.01054800 -1.22969500
H -0.26180300 -1.98012300 -1.91966100
H 0.32423900 0.75993700 0.63006600
C -2.84656000 4.26649000 1.85694700
H -2.33517200 3.80822800 2.71420700
H -3.84864600 3.81922800 1.82029700
C -2.96366300 5.77390800 2.07350000
H -3.50744800 6.00770600 2.99397900
H -3.49479300 6.24769400 1.24034500
H -1.97291300 6.23727100 2.14190500

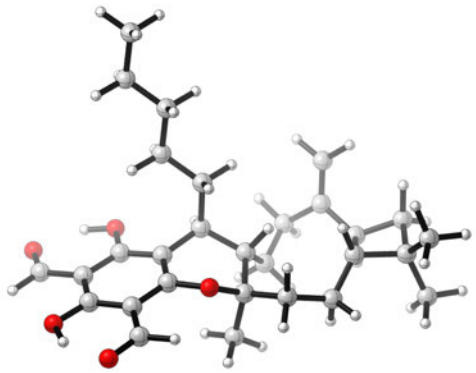

2.65 Littordial E – *β*
$E_{(M06\text{-}2X/6\text{-}31+G(d))}$: -1504.678204
$TCG_{(M06\text{-}2X/6\text{-}31+G(d))}$: 0.587124
$E_{(M06\text{-}2X/6\text{-}311+G(d,p))}$: -1505.066487
$E_{(M06\text{-}2X/6\text{-}311+G(d,p),\ smd=HFIP)}$: -1505.090796
Imaginary frequencies: none

C -1.85863000 0.37162300 -0.17516000
C -0.58329500 1.17428600 -0.14315700
C -3.08955700 0.89102100 -0.60261300
C -4.29599600 0.14930700 -0.48005000
C -4.24680500 -1.14380000 0.07823800
C -3.01606700 -1.70661700 0.47902000
C -1.84833200 -0.91982300 0.32635100
C -2.95351500 -3.06109400 0.99247500
H -1.95697200 -3.44800800 1.25191500
C -5.56161400 0.71289900 -0.91665500
H -6.45491300 0.08594900 -0.78352800
O -3.94545500 -3.77569700 1.14256600
O -5.67013100 1.83275100 -1.41576500
O -0.66719500 -1.46935900 0.68172400
C -0.43867300 1.90218400 1.21126300
H -0.35877400 1.14457200 2.00574500
H 0.52138700 2.43892700 1.19848900
O -3.09894800 2.11838100 -1.11908300
H -4.03044000 2.34592400 -1.36755000
O -5.38738200 -1.82272900 0.19579700
H -5.17751700 -2.71096100 0.58145700
C 0.42701300 -1.22590500 -0.26406300
C 0.67551900 0.29238900 -0.39783800
C 1.60148500 -1.93726500 0.41584300
H 1.63544100 -1.58170100 1.45411800
H 1.33660900 -3.00104500 0.46213000
C 3.00804500 -1.80734800 -0.19882400
H 2.97879100 -1.91976400 -1.29128600
H 3.56101300 -2.68617400 0.15907000
C 3.85360200 -0.58931500 0.19970000
H 3.51846500 -0.21421800 1.17863500
C 4.12384000 0.66407100 -0.70745000
H 4.17246900 0.33610800 -1.75510900
C 5.39870400 -0.79180900 0.28211800
C 5.55342600 0.69131200 -0.12533300
H 5.62397200 1.33250700 0.75872800
H 6.36447400 0.94745400 -0.81523800
C 5.94728400 -1.72126400 -0.80111800
H 7.03957000 -1.63635800 -0.84034000

H 5.55951600 -1.47416600 -1.79576800
H 5.70488700 -2.77036400 -0.59661600
C 5.93596700 -1.19558400 1.64703300
H 5.60254800 -2.20667700 1.91490400
H 5.58887900 -0.50775100 2.42608000
H 7.03276000 -1.19410400 1.65536600
C 3.23982800 1.88404500 -0.62028700
C 3.40216200 2.83895100 0.30023400
H 4.20412900 2.81869200 1.03191800
H 2.72743200 3.69047500 0.34603100
C 1.33678800 0.65697500 -1.73443600
H 2.02411100 -0.13281300 -2.05298200
H 0.57192500 0.73235700 -2.51796300
C 2.12737300 1.96619600 -1.64313800
H 2.56526500 2.17925400 -2.62858500
H 1.46359400 2.80650500 -1.40396900
H -0.64686700 1.93914600 -0.92704300
C -1.55608000 2.88539400 1.54911500
H -2.51339900 2.35324000 1.61695600
H -1.66437400 3.60956900 0.73201700
C -1.28672400 3.61547000 2.86415800
H -1.19933400 2.90628800 3.69513300
H -0.35105000 4.18386700 2.81333400
H 0.88524900 -1.98871900 -2.25530100
C 0.03702000 -1.92348200 -1.56968000
H -0.29522300 -2.94209400 -1.34381700
H -0.77350000 -1.40014000 -2.08641500
H 1.38808400 0.54433800 0.39832300
H -2.09194500 4.31619600 3.10477000